EPS PROGRAMME

GRAS Level 1 Product Generation Function Specification

EUMETSAT
Am Kavalleriesand 31, Postfach D-64297 Darmstadt, Germany
Tel: +49 6151 807345* Fax: +49 6151 807538

The Copyright of this document is the property of EUMETSAT. It is supplied in confidence and shall not be reproduced, copied or communicated to any third party without written permission from EUMETSAT.

©2004 EUMETSAT

Document Change Record

Issue/Revision	Date	DCN No.	Section	Change information
Draft F	23/7/99		All	Addressed CGSRR RIDs
Issue 3, Draft A	15/11/00	DCN.SYS.DCN.024	All	Document rewritten
Issue 4, Rev 0	1/6/01	DCN.SYS.DCN.024		List of Mathematical symbols added
			Section 1.8	AD9 and AD10 changed to RD12 and RD13, respectively
			Section 1.8	AD11 removed
			Section 1.9	Added RD 11
			Section 2.1	Instrument mode description added
			Section 3.1.1	Level 0 processing description updated
			Section 3.1.2	Level 1a processing description updated
			Section 3.1.3	Level 1b processing description updated
			Section 3.1.4	Section added
			Section 4.1	Requirements GRAS-Sec.4.1-10, GRAS-Sec.4.1-50, and GRAS-Sec.4.1-60 modified
				Requirements GRAS-Sec.4.1-110, GRAS-Sec.4.1-120, GRAS-Sec.4.1-130, GRAS-Sec.4.1-140, GRAS-Sec.4.1-150, GRAS-Sec.4.1-160 added

				Requirement GRAS-Sec.4.1-170 added
			Section 4.2	Requirement GRAS-Sec.4.2-30 removed Requirements GRAS-Sec.4.2-50 to GRAS-Sec.4.2-170 removed
			Section 4.3	Requirements GRAS-Sec.4.3-40, GRAS-Sec.4.3-50, GRAS-Sec.4.3-60, GRAS-Sec.4.3-90, GRAS-Sec.4.3-100, GRAS-Sec.4.3-120, GRAS-Sec.4.3-160, GRAS-Sec.4.3-170, GRAS-Sec.4.3-140 and GRAS-Sec.4.3-150 removed Requirement GRAS-Sec.4.3-5, GRAS-Sec.4.3-75, GRAS-Sec.4.3-77, and GRAS-Sec.4.3-220 added Requirements GRAS-Sec.4.3-230 to 4.3-340 added Requirements GRAS-Sec.4.3-10, GRAS-Sec.4.3-30, GRAS-Sec.4.3-110, GRAS-Sec.4.3-130, GRAS-Sec.4.3-180, GRAS-Sec.4.3-190, and GRAS-Sec.4.3-210 modified
			Section 4.4	Requirements GRAS-Sec.4.4-105, GRAS-Sec.4.4-322, GRAS-Sec.4.4-325, GRAS-Sec.4.4-365, GRAS-Sec.4.4-420, GRAS-Sec.4.4-430, GRAS-Sec.4.4-440, GRAS-Sec.4.4-450, GRAS-Sec.4.4-460, and GRAS-Sec.4.4-470 added

				Requirements GRAS-Sec.4.4-110, GRAS-Sec.4.4-140, GRAS-Sec.4.4-160, GRAS-Sec.4.4-190, GRAS-Sec.4.4-200, GRAS-Sec.4.4-210, GRAS-Sec.4.4-220, and GRAS-Sec.4.4-230 removed
				Requirements GRAS-Sec.4.4-80, GRAS-Sec.4.4-180, GRAS-Sec.4.4-230, GRAS-Sec.4.4-240, GRAS-Sec.4.4-310, GRAS-Sec.4.4-330, GRAS-Sec.4.4-360, GRAS-Sec.4.4-380, GRAS-Sec.4.4-390, GRAS-Sec.4.4-400, and GRAS-Sec.4.4-410 modified
			Section 4.5	Section added
			Section 4.6	Section added
			Section 6.1	Section has been updated
			Section 6.2.1	Section added and the old Section 6.1.1 has been included into the new section
			Section 6.2.2	Section name changed and contents updated to include only linear interpolation algorithm
			Section 6.2.3	Section added
			Section 6.3	Section added
			Section 6.5.1	Section structure has been modified
			Section 6.4	Clarification of the Level 0 processing added
			Section 6.5	Section restructured

			Section 6.5.11	Added a reference to RD 4
			Section 6.5.1.3	Added a reference to RD 11
			Section 6.5.2	Section added
			Section 6.5.3	Section modified to support measurement correction in the IMT time frame
			Section 6.5.3.2	Description of the incidence angle algorithm added
			Section 6.6.1	Section added
			Section 6.4.7	Section removed
			Section 6.5.4	Section changed to 6.6.3.1
			Section 6.5.8	Section moved to 6.6.4.5
			Section 6.6	Section restructured
			Section 6.6.2	Section added
			Section 6.6.3	Section added with functionality from old Sections 6.5.4, and 6.5.5 included
			Section 6.6.4	Section added with sections 6.5.6, 6.5.8, 6.5.9, 6.5.10, and 6.5.11 included into this section for GO processing
			Section 6.6.3.5	Section updated
			Section 6.6.5	Section added with old Section 6.5.7 included into the new section

			Section 6.6.6	Section added with old sections 6.5.12, and 6.5.13 included
			Section 6.6.6.2	Section added
			Section 6.6.6.4	Section added
			Section 6.7	Section deleted
Issue 5	15/1/02		Section 6.5.3.1	Section Unit transformations removed
			Section 6.3.3.1	Section Unit transformation has been removed
			Section 6.3.3.2	Section updated
			Section 6.3.3.3	Section updated
			Section 6.3.3.4	Section updated
			Section 6.3.3.5	Section updated
			Section 6.5.3.7	Section Satellite attitude correction removed
			Section 6.6.4	Section added
			Section 6.5.3.7	Section Satellite attitude correction has been removed
			Section 6.6	Section updated and moved (In Issue 4 this section was Section 6.2)
			Section 6.7	Section moved (In Issue 4 this section was Section 6.3)
Issue 6	15/1/02		Section 1.3	Section updated
			Section 1.6	AD5 removed, AD10 and AD11 added
			Section 1.7	RD4, and RD11 removed, RD16 - RD20 added
			Section 2	Section updated

			Section 3	Figures 3.1 - 3.4 updated
			Section 4.1	Section updated
			Section 4.3	Section updated
			Section 4.4	Section updated
			Section 4.5	Section updated
			Section 4.6	Section updated
			Section 5.1	Section updated to contain full, concise description of the GRAS level 1 data processing
			Section 5.3	Section updated
			Section 5.4	Section updated
			Section 5.6	Section updated to include detailed descriptions fiducial station incidence angle determination, atmosphere models, filtering functions, and pseudorange calculation for C/A and P code
			Section 5.7	Section updated
Issue 6 Rev 1	15/6/02	EUM.EPS.SYS.DCR.02.113	Section 1.7	New reference document RD21 added
			Section 2.2.1	Section updated
			Section 3	Sections 3.2 and 3.3 added
			Section 4.1	Requirements GRAS-Sec.4.1-10, GRAS-Sec.4.1-20, GRAS-Sec.4.1-40, GRAS-Sec.4.1-50, GRAS-Sec.4.1-60, GRAS-Sec.4.1-100, GRAS-Sec.4.1-110 modified
			Section 4.1	Requirements GRAS-Sec.4.1-85, GRAS-Sec.4.1-87, GRAS-Sec.4.1-200 added

			Section 4.3	Requirements GRAS-Sec.4.3-5, GRAS-Sec.4.3-30, GRAS-Sec.4.3-75, GRAS-Sec.4.3-135, GRAS-Sec.4.3-250, GRAS-Sec.4.3-340 modified
			Section 4.3	Requirements GRAS-Sec.4.3-10, GRAS-Sec.4.3-80, GRAS-Sec.4.3-110, GRAS-Sec.4.3-180, GRAS-Sec.4.3-190, GRAS-Sec.4.3-200, GRAS-Sec.4.3-210, GRAS-Sec.4.3-220, GRAS-Sec.4.3-280, GRAS-Sec.4.3-290, GRAS-Sec.4.3-300, GRAS-Sec.4.3-310 removed
			Section 4.4	Requirements GRAS-Sec.4.4-90, GRAS-Sec.4.4-260, GRAS-Sec.4.4-270, GRAS-Sec.4.4-322, GRAS-Sec.4.4-450, GRAS-Sec.4.4-460, GRAS-Sec.4.4-470 modified
			Section 4.4	Requirements GRAS-Sec.4.4-120, GRAS-Sec.4.4-130, GRAS-Sec.4.4-150, GRAS-Sec.4.4-170, GRAS-Sec.4.4-240, GRAS-Sec.4.4-250, GRAS-Sec.4.4-280, GRAS-Sec.4.4-290, GRAS-Sec.4.4-300, 320, GRAS-Sec.4.4-330, GRAS-Sec.4.4-340, GRAS-Sec.4.4-350, GRAS-Sec.4.4-360, GRAS-Sec.4.4-365, GRAS-Sec.4.4-370, GRAS-Sec.4.4-380, GRAS-Sec.4.4-390, GRAS-Sec.4.4-400, GRAS-Sec.4.4-410, GRAS-Sec.4.4-430 removed
			Section 4.4	Requirement GRAS-Sec.4.4-323 added
			Section 4.5	Requirement GRAS-Sec.4.5-40 modified

			Section 4.6	Requirement GRAS-Sec.4.6-10, GRAS-Sec.4.6-40, GRAS-Sec.4.6-90, GRAS-Sec.4.6-100, GRAS-Sec.4.6-140, 160, GRAS-Sec.4.6-170, GRAS-Sec.4.6-190, GRAS-Sec.4.6-290, GRAS-Sec.4.6-300, GRAS-Sec.4.6-310, GRAS-Sec.4.6-320, GRAS-Sec.4.6-340, GRAS-Sec.4.6-350, GRAS-Sec.4.6-390, GRAS-Sec.4.6-410 modified
			Section 4.6	Requirement GRAS-Sec.4.6-20, GRAS-Sec.4.6-80, GRAS-Sec.4.6-110, GRAS-Sec.4.6-120, GRAS-Sec.4.6-200, GRAS-Sec.4.6-210, GRAS-Sec.4.6-220, GRAS-Sec.4.6-230, GRAS-Sec.4.6-240, GRAS-Sec.4.6-250, GRAS-Sec.4.6-260, GRAS-Sec.4.6-270, GRAS-Sec.4.6-280, GRAS-Sec.4.6-370, GRAS-Sec.4.6-400 removed
			Section 4.6	Requirement GRAS-Sec.4.6-342, GRAS-Sec.4.6-345, GRAS-Sec.4.6-420 added
			Section 5	Old section 5 split into Section 5 Mathematical Formulation of the Algorithm and new section 6: Referece Functions
			Section 5.1	Section updated
			Section 5.2	Section updated
			Section 5.3	Section updated
			Section 5.4	Section updated
			Section 6.1	Section updated
			Section 6.2	Section updated

			Section 6.3	Section updated
			Section 6.4	Section updated
Issue 6 Rev 2	21/3/03	EUM.EPS.SYS.DCR.03.075		The list of mathematical symbols has been updated.
			Section 1.4	The list of definions has been updated.
			Section 1.6	AD6, AD12, AD13, and AD14 have been removed. Reference numbers of AD7 and AD8 have been corrected.
			Section 1.7	RD13 has been removed.
			Section 3.1.2	Description has been updated to show that pseudorange generation is not part of level 1a processing.
			Section 3.1.3	Smoothing of the level 1b products has been removed from the description. Radio Holographic has been replaced by Wave Optics (WO).
			Section 3.2	References to the use of pseudoranges has been removed.
			Section 5.2	Pseudorange generation has been removed from the block diagram in Figure 5.1.
			Section 5.2.1.2	Setting of the GRAS ID field in MDR-1As and MDR-1B has been clarified.
			Section 5.2.2	The reference to the section with the carrier phase correction functions has been corrected. The description of the pseudorange correction has been replaced by a description of code phase correction.

			Section 5.3	Level 1b product smoothing has been removed from the block diagram in Figure 5.2.
			Section 5.3.3.1	The description of the function has been revised to include two different clock offset product types from the POD.
			Section 5.3.3.2	The definition of the interpolation method to be used for the Metop COM position vectors has been clarified. Notation of the Equation 6.13 has been corrected.
			Section 5.3.3.3	The Shapiro correction for pseudorange has been changed to Shapiro correction for code phase.
			Section 5.3.3.4	An error has been corrected in the DD2 formulation.
			Section 5.3.3.5	The style of index *n* in step 2) of the unwrapping algorithm has been corrected to italic. The unit of the complete unwrapped phase has been corrected. The name of the phase prediction function has been changed to P_ϕ.
			Section 5.3.4.3	Subscript *i* has been added to total bending angle and impact parameter to indicate frequency dependant results.
			Section 5.3.4.7	Use of mean bending bias estimate has been clarified.
			Section 5.3.6.1	The level 1b product smoothing has been removed. Correspondingly also Section 6.2.5.1 has been removed.

			Section 5.4	Appending of the raw sampling mode data into MDR-1A has been clarified.
			Section 6.1.2	Mathematical symbols in Input Parameters have been updated. A provisional an algorithm for removing the Navigation Message has been added to supplement AD11.
			Section 6.1.3	A note "along the orbit arc" has been added to the statement about the orbital position error due to the $t_{rx}^{utc_gras}$ instability.
			Section 6.1.4	The name of the error flag for measurement identification failure has been added to step 6.
			Section 6.1.5	The list of Input Parameters at the beginning of the section has been removed.
			Section 6.1.5.1	The definitions of the origin of the antenna reference point r_{ant}^{arf} and unit vectors $\hat{x}_{ant}^{arf}$, $\hat{y}_{ant}^{arf}$, and $\hat{z}_{ant}^{arf}$ in step 3) have been clarified.
			Section 6.1.5.2	The reception time of the phase measurements has been added into the list of input parameters and the notation of the input parameters has been updated. L2-P1 has been corrected to L1-P1 in the list of output parameters. Equation 6.17 has been corrected to contain sums of the correction terms. $\Delta\phi_{corr}$ has been corrected to $\Delta\phi_{cd}$ in the list of parameters.

			Section 6.1.5.3	Section has been revised to perform group delay correction to code phases instead of pseudoranges. The selection of the characterisation files from the GRAS Characterisation database and setting of the GPS HW DELAY fields in the MDR-1As and MDR-1B have been clarified. Mathematical notation has been updated.
			Section 6.1.5.4	GEU temperature has been added to Equation 6.40 and the mathematical notation has been updated.
			Section 6.1.6	Table 6.4 has been updated to include code phase instead of pseudorange and the names of the quality flags to be set. The setting of the TELEMETY IN RANGE bits string has been clarified. Mathematical notation has been updated.
			Section 6.2.2.2	The mathematical formulation in the section has been revised for consistency with Section 5.3.3.4.
			Section 6.2.2.3	The relativity corrected phase residual has been added into the list of Input Parameters and pseudoranges have been replaced by code phases. Units of the input and output parameters have been added. Estimating the ionosphere delay in step (5) has been revised to use code phase instead of pseudorange.

			Section 6.2.2.4	The relativity corrected phase residual has been added into the list of Input Parameters. Units of the input and output parameters have been added. Setting of the SSD AVAILABILITY flag in Step (2) has been clarified.
			Section 6.2.2.5	The relativity corrected phase residual has been added into the list of Input Parameters and pseudoranges have been replaced by code phases. Units of the input and output parameters have been added.
			Section 6.2.2.6	The relativity corrected phase residual has been added into the list of Input Parameters and pseudoranges have been replaced by code phases. Units of the input and output parameters have been added.
			Section 6.2.2.7	Missing subscript R has been added to the unit vector $\hat{r}_R^{eci}$in Equation 6.74.
			Section 6.2.3.5	The mathematical formulation has been revised to use code phase instead of pseudorange. The notation has been updated for consistency.
			Section 6.2.3.7	Table 6.17 and a rule for selecting bias estimation on/off have been added.
			Section 6.2.4.3	Table 6.19 and description of default CT output values have been added.
			Section 6.2.4.4	Local radius of curvature added to input parameters. Approximate ray height added to output parameters. Default output values added.

			Section 6.2.5.2	Names of the quality flags have been added to Tables 6.20 and 6.21.
			Section 6.2.5.3	The default output values have been added.
			Section 6.3.1.1	The formulation of the Lagrange interpolation has been updated.
			Section 6.3.3.1	Definition of the geocentric latitude has been added as Equation 6.161. Errors in the mathematical formulation in Equations 6.163 - 6.169 have been corrected.
			Section 6.3.3.3	Equation 6.173 has been corrected.
			Section 6.3.7	The mathematical formulations for the pseudorange generation has been removed.
			Section 6.4	All definitions of the occultation table data contents or formats have been removed. The occultation table contents and format are defined in AD4.
Issue 6 Rev 3	10/6/03	EUM.EPS.SYS.DCR.03.086	AppendixA	Mathematical formulation of the Precise Orbit Determination (POD) has been added and the list of reference documents has been updated to include RD22, RD23, and RD24 that are related to the POD formulation.
			Section 5.2.2	A reference to the POD algorithm in Appendix A has been added to the end of the section.
Issue 6 Rev 4	16/7/04	EUM.EPS.SYS.DCR.04.075		The list of mathematical symbols has been removed from the document.

			Section 1.3	SLTH = Straight Line Tangent Height added. SLTH replaces the acronym SLTA that was used in older versions of the document.
			Section 1.4	Definition of the ECI coordinate frame has been clarified. Definition of arctan2 added.
			Section 1.7	References RD25 - RD28 added.
			Section 2.2.1	Section updated.
			Section 4.3	In GRAS-Sec.4.3-75 a definition of the "true latitude" has been added to item 3 and a reference to "PSO angle" has been removed. A reference to AD12 has been replaced with Table 4.1 in item 7.
			Section 4.6	Table 4.1: Accuracy requirements on the GRSA/Metop NRT POD products has been removed. Requirement GRAS-Sec.4.6-30 has been removed. Reference to Table 4.1 has been removed from requirement GRAS-Sec.4.6-310.
			Section 5.2	Figure 5.1 has been updated.
			Section 5.2.1.1	Section has been updated.
			Section 5.2.1.2	Section has been updated.
			Section 5.2.1.3	Section has been updated.
			Section 5.2.2	Mod[2π] has been removed from Equation 5.1 . The notation of the carrier phase has been clarified: ρ is used for phase in radians, ϕ for phase in meters. This change has been applied throughout the document.
			Section 5.3	Figure 5.2 has been updated.

			Section 5.3.3.1	Text updated.
			Section 5.3.3.2	Derivations of the coordinate transform matrixes have been clarified.
			Section 5.3.3.3	Equation 5.17 modified to make the calculation using phase in meters. Notation corrected.
			Section 5.3.3.4	Notation corrected.
			Section 5.3.3.5	Noise filtering has been combined with the cycle slip correction and Table 5.3 has been updated. Consequently old Section 5.3.4.1 has been removed. Equation 5.24 has been updated. Equation 5.26 has been corrected. The use of the atmosphere "law" to convert teh signal to baseband has been clarified.
			Section 5.3.5	Description of the WO retrieval has been updated to include Phase Transform method.
			Section 6.1.1	Links to the quality flags in the PFS have been clarified.
			Section 6.1.2	Notation corrected.
			Section 6.1.4	Typo in the receiver indetification number corrected and the user definable options for the identification number clarified.
			Section 6.1.5.1	In step 3) the derivation of the GPS SRF rotation matrix has been clarified. Equation 6.16 has been updated. Coordinate transform clarified.
			Section 6.1.5.2	Notation corrected.
			Section 6.1.5.4	Notation corrected.

			Section 6.1.6	Product field names for all quality flags have been added into the tables and links to the product fields in PFS have been clarified. Default values for the loss of tracking monitoring have been added. Notation corrected.
			Section 6.2.1	The list of output parameters has been clarified. The product filed names of the low pivot satellite warning flags have been added into the text. The use of a mean elevation angle during a measurement for the cost function calculations has been clarified in all equations.
			Section 6.2.2.1	The notation of the Shapiro delay function has been clarified. The name P_s is now used throughout the document for the function.
			Section 6.2.2.2	Input and output parameters corrected to indicate meters and not radians. Equation 6.54 has been updated and units have been added into the list of symbols for clarification.
			Section 6.2.2.3	Section updated for consistent use of meters as the unit of the carrier phase. Mod[2π] has been removed from Equations 6.55 and 6.58. Statement about the phase re-wrapping has been removed from step (6). Tables 6.11 and 6.12 have been updated.

			Section 6.2.2.4	Section updated for consistent use of meters as the unit of the carrier phase. Tables 6.13 and 6.15 have been updated. Mod[2π] has been removed from Equations 6.61 and 6.69. Statement about the phase re-wrapping has been removed from step (8). Acronym FST has been clarified in step (3).
			Section 6.2.2.6	Equation 6.73 has been added.
			Section 6.2.2.7	List of input and output parameters updated and list of constants removed. Equations 6.77 and 6.82 corrected. Old equation 6.73 for flattening removed. Typos and notation corrected.
			Section 6.2.3.1	Typo corrected.
			Section 6.2.3.2	Equation 6.87 has been removed. Notation in Equation 6.92 has been corrected.
			Section 6.2.3.3	Notation corrected.
			Section 6.2.3.4	The formulation of the geolocation function has been revised. Bending angle, impact parameter, and reference ellipsoid information have been added into the list of input parameters.
			Section 6.2.3.5	Error in the formulation has been corrected.
			Section 6.2.3.6	Table 6.16 has been updated. Filtering parameters have been revised and the extrapolation of the L2 measurements has been clarified.
			Section 6.2.3.7	Integration of the model based bending angle has been clarified. Typos corrected.

			Section 6.2.4.1	Table 6.19 has been updated.
			Section 6.2.4.2	Reference to auxiliary data file has been removed from the end of the section.
			Section 6.2.4.3	Wave Optics (WO) algorithm description completed with the addition of Phase Transform.
			Section 6.2.4.4	Section updated.
			Section 6.2.5.2	Product quality flags clarified.
			Section 6.3.3.1	Calculation of the Equation 6.182 has been clarified. Errors in the formulation corrected. Derivation of θ_{tl} clarified. Links to the quality flags in the PFS clarified.
			Section 6.3.3.3	List of imput parameters corrected. Notation for the eccentricity of the reference ellipsoid corrected to e_e in all equations. Equation 6.200 has been corrected. Error in the list on input arguments corrected. Notation corrected.
			Section 6.3.3.4	A new section has been added to clarify the ECEF to ECI coordinate transform.
			Section 6.3.4	The notation and typos in formulation have been corrected.
			Section 6.3.5.1	The notation and typos in formulation have been corrected.
			Section 6.3.5.3	The correct value for the gas constant for the used formulaiton has been added.
			Section 6.3.6.1	SLTH added into the input parameters.

			Section 6.4 Appendix A	Table 6.26 has been updated. Formulation for the geolocation prediction by using the SLTH values has been clarified. Equations A.1.5-2 and A.1.5-13 have been corrected. Section A.2.5 has been updated.

Contents

1 INTRODUCTION 1

1.1 Purpose and Scope of this Document 1

1.2 A note on terminology 1

1.3 Acronyms 1

1.4 Definitions 3

1.5 Other documents 4

1.6 Applicable Documents 4

1.7 Reference Documents 5

2 SYSTEM CONCEPT 6

2.1 Instrument Description and Rationale 6

2.2 System Concept 8

2.2.1 System Context 8

3 OPERATIONS CONCEPT 10

3.1 Nominal continuous operation 10

3.1.1 Level 0 Processing 10

3.1.2 Level 1a Processing 10

3.1.3 Level 1b Processing 12

3.1.4 Occultation Table Generation 16

3.2 Nominal degraded scenarios 16

3.3 Non-nominal scenarios 19

4 REQUIREMENTS 20

4.1 General Requirements 20

4.2 Level 0 Processing Function 23

4.3 Level 1a Processing Function 23

4.4 Level 1b Processing Function 26

4.5 Occultation Table Generation 27

4.6 GRAS/Metop POD 28

5 MATHEMATICAL FORMULATION OF THE ALGORITHM 31
5.1 Level 0 processing . . . 32
5.2 Level 1a processing . . . 32
5.2.1 Level 1a pre-processing . . . 32
5.2.1.1 Source packet pre-structuring . . . 33
5.2.1.2 Level 1a quality check . . . 34
5.2.1.3 Measurement reassembly . . . 34
5.2.1.4 Measurement identification . . . 35
5.2.2 Instrument corrections . . . 35
5.2.3 Level 1a product quality check . . . 39
5.2.4 Level 1a product formatting . . . 40
5.3 Level 1b processing . . . 40
5.3.1 Pivot satellite and fiducial station selection . . . 40
5.3.2 Occultation isolation . . . 40
5.3.3 Level 1b corrections . . . 42
5.3.3.1 IMT to reference time conversion . . . 42
5.3.3.2 Transmission time determination . . . 43
5.3.3.3 Relativity correction and removal of geometric path . . . 46
5.3.3.4 Clock corrections . . . 47
5.3.3.5 Cycle slip correction and phase unwrapping . . . 49
5.3.3.6 Earth oblateness correction . . . 52
5.3.4 Geometrical optics retrieval . . . 52
5.3.4.1 Doppler calculation . . . 53
5.3.4.2 Total bending angle and impact parameter calculation . . . 53
5.3.4.3 Geolocation . . . 53
5.3.4.4 TEC derivation . . . 53
5.3.4.5 Ionosphere correction . . . 53
5.3.4.6 Total bending angle bias estimation and correction . . . 54
5.3.5 Wave optics retrieval . . . 54
5.3.6 Level 1b post-processing . . . 54
5.3.6.1 Deriving smoothed level 1b products . . . 55
5.3.6.2 Level 1b product quality check . . . 55
5.3.6.3 Product error characteristics estimation . . . 55
5.3.6.4 Level 1b products formatting . . . 55
5.4 Raw sampling mode data processing . . . 55

6 REFERENCE FUNCTIONS 55

6.1 Level 1a processing functions 55

6.1.1 Level 1a quality check parameters 55

6.1.2 Measurement reassembly products 57

6.1.3 Approximation of the measurement time 60

6.1.4 Measurement identification determination 61

6.1.5 Derivation of instrument corrections 63

6.1.5.1 Incidence angle derivation 63

6.1.5.2 Carrier phase correction 67

6.1.5.3 Code phase correction 70

6.1.5.4 Amplitude correction 74

6.1.5.5 USO frequency correction 77

6.1.6 Level 1a product quality check 77

6.2 Level 1b processing functions 85

6.2.1 Pivot satellite and fiducial station selection functions 85

6.2.2 Level 1b corrections 89

6.2.2.1 Relativity correction 89

6.2.2.2 No Differencing (ND) clock correction 90

6.2.2.3 Single Differencing 1 (SD1) clock correction 91

6.2.2.4 Single Differencing 2 (SD2) clock correction 97

6.2.2.5 Double Differencing 1 (DD1) clock correction 106

6.2.2.6 Double Differencing 2 (DD2) clock correction 108

6.2.2.7 Correction for the Earth's oblateness 111

6.2.3 Geometrical optics retrieval functions 113

6.2.3.1 Derivation of the Doppler shifts 113

6.2.3.2 Total bending angle retrieval 114

6.2.3.3 Derivation of the impact parameter 119

6.2.3.4 Geolocation function 119

6.2.3.5 TEC derivation 121

6.2.3.6 Ionosphere correction 122

6.2.3.7 Bending angle bias estimation and correction 123

6.2.4 Wave optics retrieval functions 128

6.2.4.1 Noise filtering 128

6.2.4.2 Back-propagation 129
6.2.4.3 Phase transform 136
6.2.4.4 Ionosphere correction 140
6.2.5 Combining level 1b products 140
6.2.5.1 Derivation of smoothed Level 1b products 140
6.2.5.2 Level 1b products quality check 140
6.2.5.3 Error characteristics estimation 142
6.2.5.4 Level 1b products formatting 142
6.3 General data processing functions 143
6.3.1 Interpolation functions 143
6.3.1.1 Satellite state vector interpolation 143
6.3.1.2 Linear interpolation 143
6.3.1.3 Bi-cubic interpolation for antenna pattern 144
6.3.2 Time conversion functions 144
6.3.2.1 UTC to MJD time format conversion 144
6.3.3 Coordinate frame conversion functions 146
6.3.3.1 Antenna reference frame to ECI transformation 146
6.3.3.2 WGS84 to ITRF97 coordinate transform 155
6.3.3.3 Derivation of geodetic coordinates 156
6.3.3.4 ECEF to ECI coordinate transform 157
6.3.4 Fiducial station incidence angle determination 158
6.3.5 Atmosphere models 159
6.3.5.1 Neutral atmosphere delay mapping function 159
6.3.5.2 Hydrostatic delay model 162
6.3.5.3 Wet delay model 162
6.3.6 Filtering functions 163
6.3.6.1 Adaptive low-pass filter 163
6.3.7 Pseudorange calculations 164
6.3.7.1 C/A code pseudorange 164
6.3.7.2 P code pseudorange 164
6.4 Occultation Table Generation 164

A GRAS/Metop Precise Orbit determination with Square Root Information Filter 169

List of Figures

2.1 The PGE interface facilitates the transfer of instrument and satellite data, along with auxiliary data, and accepts product components for formatting in the CGS. . . . 8

3.1 GRAS data processing elements. 11

3.2 GRAS data processing steps from Level 0 to Level 1b. 12

3.3 GRAS Level 1a data processing functions. 13

3.4 GRAS Level 1b data processing functions. 15

3.5 Principle of single and double differencing techniques. Single differencing (SD) means the calculation of the phase residual difference between the occultation measurement (A) and a reference measurement at a ground station (B). Double Differencing (DD) uses two additional reference measurements. One is between a pivot GPS satellite and the LEO satellite (D) and the other is between a ground station and the pivot GPS satellite (C). 16

5.1 Simplified block diagram of the level 1b data processing functions. 33

5.2 Block diagram of the level 1b data processing. 41

6.1 The occultation geometry for GO solution of the total bending angles. 118

6.2 The principle of bi-cubic interpolation. The data points in the database are marked with circles and the intermediate data points after the first interpolation are marked with crosses. The final desired data point corresponding to the angles φ_g and θ_g is marked with a star. 145

6.3 Coordinate frame definitions onboard Metop spacecraft. 147

6.4 Geometry of the geodetic and geocentric coordinate frames. 152

List of Tables

3.1 GRAS PGF clock differencing modes. 14
4.1 Metop attitude knowledge requirements. 24
5.1 Fallback modes for the clock correction in the case of missing input data. 47
5.2 Default values for the parameters for phase unwrapping and cycle slip correction. . 50
5.3 The default parameters for noise filtering in GO algorithm. 51
6.1 Level 1a quality checks. 57
6.2 Measurement identification parameters and default threshold values. 63
6.3 Generic format of the characterization data records in instrument characterisation database. 70
6.4 Default values for loss of tracking monitoring parameters. 81
6.5 Level 1a product quality check default threshold values. 82
6.6 GRAS telemetry monitoring default threshold values. 83
6.7 Other quality flags for level 1a product quality check. 84
6.8 Quality flags for level 1a products based on external information. 85
6.9 Coefficients for approximated antenna patterns. 89
6.10 Threshold values for cost functions. 89
6.11 The default filtering parameters for phase measurements by GRAS GZA. 93
6.12 The default filtering parameters for the ionosphere compensation. 95
6.13 The default filtering parameters for phase measurements by the fiducial station. . . 99
6.14 The user selectable parameters for the TZD derivation. 103
6.15 The default filtering parameters for ionosphere compensation. 104
6.16 The default parameters for noise filtering in GO algorithm. 123
6.17 Default parameters for the bending angle bias correction model. 124
6.18 Bias estimation parameters and corresponding level 1b product field names. 128
6.19 The default parameters for noise filtering in WO algorithm. 129
6.20 Default values for the phase transform function parameters. 138
6.21 The list of products and the default threshold values for level 1b products quality check. 141
6.22 Threshold values with special conditions for level 1b quality check. 142
6.23 WGS84 reference ellipsoid parameters. 151
6.24 Coefficients for the hydrostatic mapping function. 161
6.25 Coefficients for the wet mapping function. 161
6.26 Default parameters for occultation table generation. 165
6.27 Measurement start and end determination parameters for each GRAS antenna. . . . 167

1 INTRODUCTION

1.1 Purpose and Scope of this Document

The Product Generation Specification (PGS) specifies the requirements for the Metop GRAS instrument Product Generation Function (PGF).

Section 1 of this document is this introduction.

Section 2 of this document provides a short overview of the overall concept of the PGF as a component in a larger system. It also describes the way in which the PGF is expected to be operated.

Section 3 contains the requirements on the PGF.

Section 4 contains the scientific and mathematical algorithm specification that support the requirements.

1.2 A note on terminology

In this document the term “product” is used in two different senses. The first sense is “a piece of information”. Example: Bending angle profile produced by Radioholographic method can be referred to as a product. The second sense is “a collection of records defined by **AD4**”. Example: The GRAS Level 1b product.

1.3 Acronyms

AS	Anti-Spoofing
AGC	Automatic Gain Control
BE	Bias Estimation
BBE	Bending angle Bias Estimation
FBE	Frequency Bias Estimation
CDA	Command & Data Acquisition
CGS	Core Ground Segment
CGSRD	Core Ground Segment Requirements Document
CoM	Center of Mass
DCB	Differential Code Bias
GEU	GRAS Electronic Unit
GID	GRAS Instrument Database

GNSS	Global Navigation Satellite System
GO	Geometrical Optics
GOBS	GRAS On Board Software
GPS	Global Positioning System
GSN	Ground Support Network (service that provides GPS state vectors, clock offset estimates, and ground based measurements from a network of fiducial stations to support clock correction in the GRAS data processing)
ENDP	Extended Navigation Data Packet
FOM	Flight Operations Manual
IGS	International GPS Services for Geodynamics
IMT	Instrument Measurement Time (GRAS clock)
IRD	Interface Requirements Document
ITRF	International Terrestrial Reference Frame
L1	GPS channel 1.57542 GHz
L2	GPS channel 1.2276 GHz
LEO	Low Earth Orbit
LOS	Line of sight
mas	Milli arc second
MCD	Mission Conventions Document
MJD	Modified Julian Date
NWP	Numerical Weather Prediction
PCD	Product Conventions Document
PGE	Product Generation Environment
PGF	Product Generation Function
POD	Precise Orbit Determination
USO	Ultra Stable Oscillator
UTC	Universal Time Coordinated
RFCU	Radio Frequency Conditioning Unit

RH	Radio Holographic
SA	Selective Availability
SLTH	Straight Line Tangent Height
SR	Satellite Reference coordinate frame
SRR	Satellite Relative Reference coordinate frame
SSD	Sounding Support Data
TBC	To be confirmed
TBD	To be defined
TBW	To be written
TOD	True-of-Date coordinate frame
USO	Ultra Stable Oscillator
UTC_{GRAS}	UTC time in the GRAS receiver maintained based on the onboard navigation solution (see **AD10** and **AD11**)
WGS	World Geodetic System
ZPD	Zenith Propagation Delay

1.4 Definitions

C/A code	Coarse Acquisition Code, used in civil navigation applications and to acquire the P code. C/A code has a 1.023 MHz chip rate and a period of 1 ms.
Anti-Spoofing	Encryption of the P code into Y code.
P code	Precision code, used mainly in military applications.
Y code	Encrypted P code. See Anti-Spoofing.
Raw sampling	GRAS has lost or not yet acquired a phase lock on the GPS carrier. In this mode the instrument provides the correlator output data sampled at 1 kHz sampling rate. This mode is also called Open Loop Mode.
ECI	Earth Centered Inertial. Non-rotating (inertial) Mean-of-date J2000 coordinate frame centered in the Earth.
ECEF	Earth Centered, Earth Fixed. Coordinate frame centered in the Earth and rotating with the Earth. ECEF frame used in GRAS data processing is the ITRF frame as specified in AD7.

Reference time	Time frame used by the GRAS GSN to solve GPS state vectors and clock offsets.
Chain	Hardware chain in the GRAS receiver containing the measurement antenna (GVA, GAVA, or GZA), RFCU and GEU.
$\arctan 2$	$-\pi \leq \arctan 2(y, x) \leq \pi$.

1.5 Other documents

The instrument products generation function is a constituent of the CGS. Therefore, unless otherwise specified, all the requirements of the Core Ground Segment Requirements Document (CGSRD) [**AD1**] apply to this product generation function.

In case of conflict between these product generation function requirements and Core Ground Segment Requirements Document (CGSRD) requirements, the latter shall take precedence.

For the definitions used in this document, including the reference frames to be used, see the Mission Conventions Document (MCD) [**AD7**], and the Product Conventions Document [**AD8**].

1.6 Applicable Documents

Following documents are applicable to the Instrument Product generation function:

Ref_No	Name
AD1	EPS Core Ground Segment Requirements Document (EPS/CGS/REQ/95327)
AD2	CGS to Product generation function IRD
AD3	EPS Generic Product Format Specifications (EPS/GGS/SPE/96167)
AD4	GRAS Product Format Specification (EPS/MIS/SPE/97234)
AD5	Removed
AD6	Removed
AD7	EPS Mission Convention Document (EPS/SYS/SPE/990002)
AD8	EPS Product Convention Document (EPS/SYS/TEN/990007)
AD9	EPS Core Ground Segment to GRAS Ground Support Network Interface Requirement Document (EPS/GGS/IRD/980692)
AD10	Measurement Data Interface Control Document (P-GRM-ICD-0008-SE)
AD11	Measurement Data Interpretation and Description (P-GRM-SPC-0036-SE)
AD12	Removed

AD13 Removed

AD14 Removed

1.7 Reference Documents

Ref_No **Name**

RD1 Gorbunov, M.E., and S.V. Sokolovskiy, (1993), Remote sensing of refractivity from space for global observation of atmospheric parameters, Max-Planck-Institut fur Meteorologie Report No. 119, Hamburg.

RD2 Hoeg, P., A. Hauchecorne, G. Kirchengast, S. Syndergaard, B. Belloul, R. Leitinger, W. Rothleitner, (1995), Derivation of Atmospheric Properties Using a Radio Occultation Technique, ESA Contract Report ESTEC/11024/94/NL/CN.

RD3 Fang, P. and Y. Bock, (1996), Scripps Orbit and Permanent Array Center 1995 Report to IGS, in International GPS Service for Geodynamics 1995 Annual Report, Jet Propulsion Laboratory, Pasadena, Ca.

RD4 Removed

RD5 Removed

RD6 Command & Control Interface Control Document (P-GRM-ICD-0007-SE)

RD7 GRAS Characterisation Database Description (P-GRM-REP-0019-SE)

RD8 Meincke, M. D., (2000), Analysis and Definition of Algorithms for Atmospheric Diffraction Effects, Report, April 2000, DMI, Copenhagen, Denmark.

RD9 Syndergaard, S., (1998), Modelling the impact of the Earth's oblateness on the retrieval of temperature and pressure profiles from limb sounding, Journal of Atmospheric and Solar-Terrestrial Physics, Vol 60, No. 2, pp. 171-180.

RD10 Hedin, A. E., (1991) Extension of the MSIS Thermospheric Model into the Middle and Lower Atmosphere, J. Geophys. Res., 96, 1159.

RD11 Removed

RD12 Removed

RD13 Removed

RD14 Boucher, C. and Z. Altamimi, (1996), The ITRF and its relationship to GPS, GPS World Magazine, Vol 7, No. 9.

RD15 Montenbruck, O. and E. Gill, (2000), Satellite Orbits, Springer, ISBN 3-540-67280-X.

RD16 Niell, A.E., (1996), Global mapping functions for the atmosphere delay at radio wavelengths, J. Geophys. Res., 101, 3227-3246.

RD17 Elgered, G., J.L. Davis, T.A. Herring, and I.I. Shapiro, (1991), Geodesy by radio interferometry: Water vapor radiometry for estimation of the wet delay, J. Geophys. Res., 96, 6541-6555.

RD18 Askne, J. and H. Nordius, (1987), Estimation of tropospheric delay for microwaves from surface weather data. Radio Science, 22(3), 379-386.

RD19 Saastamoinen, J., (1972), Atmospheric correction for the troposphere and stratosphere in radio ranging of satellites, in The Use of Artificial Satellite for Geodecy, Geophys. Monogr. Ser., Vol 15, edited by S.W. Henriksen et al., 247-251, AGU, Washington, D.C.

RD20 Ingmann, P. and D. Klaes (ed.), (1998), Report of the GRAS SAG. The GRAS Instrument on Metop. EUMETSAT/ESA.

RD21 GRAS Technical Description (P-GRM-REP-0007-SE)

RD22 GRASPOD TN-01 (GMV-GRASPOD-TN-01)

RD23 GRASPOD Final Report (GMV-GRASPOD-FR-01)

RD24 Bierman, G.J., (1977), Factorization Methods for Discrete Sequential Estimation, the Jet Propulsion Laboratory.

RD25 Jensen, A.S., H-H. B. Lohmann, and, A.S. Nielsen, (2003), Full Spectrum Inversion of radio occultation signals, Radio Science, Vol 38, No 3, 1040.

RD26 Gorbunov, M.E., and K.B. Lauritsen, (2003), Analysis of wave fields by Fourier Integral Operators and its application for radio occultations, Danish Meteorological Institute.

RD27 Ray, R.D., D.J. Steinberg, B.F. Chao, and D.E. Cartwright, (1994), Diurnal and Semidiurnal Variations in the Earth's Rotation Rate Induced by Oceanic Tides, Science, 264, pp. 830-832.

RD28 IERS Technical Note 21, IERS Conventions (1996), Dennis D. McCarthy, U.S. Naval Observatory, July 1996.

2 SYSTEM CONCEPT

2.1 Instrument Description and Rationale

The GRAS (Global Navigation Satellite System Receiver Atmospheric Sounder) will provide radio occultation sounding measurements of the atmosphere in support of the EUMETSAT Polar System mission objectives of operational meteorology and climate monitoring [**RD21**].

Radio occultation is a technique that was originally used to study the atmospheres of Venus, Mars, and the outer planets. In its application to the Earth, a spacecraft emits a radio signal that is received

by a second spacecraft. When this signal passes through the Earths atmosphere, it is refracted by variations in the atmospheres index of refraction, which produces distinctive variations in the amplitude and phase of the received signal. As the motion of the satellites changes the observation geometry the propagation path of the radio waves traverses vertically through the atmosphere. The change of the index of refraction of the atmosphere from the surface level to the altitude of about 100 km causes the phase delay of an L band radio signal to increase by approximately six orders of magnitude. The variation in amplitude and phase of the signal can be used to derive a vertical profile of the geophysical properties of the atmosphere.

GNSS (Global Navigation Positioning System Satellites) satellites are extremely good signal sources for radio occultation observation because they provide a stable signal, global coverage, and their orbits are determined with very high accuracy for geodetic applications. GRAS is designed to monitor only GPS satellites as GPS is currently the only fully operational GNSS system that is also supported by global network of fiducial ground stations.

Radio occultation measurements from the GRAS will be of value as an independent source of information for numerical weather prediction (NWP) models. There is potentially a large benefit to be derived from entering additional independent information into the analysis, as the radio occultation method would provide measurements up to altitudes of 50 km in the Earths atmosphere. With the nominal number of GPS (Global Positioning System) satellites, about 500 measurements are expected per day, nearly equally distributed over the Earths surface. This means a considerable improvement of the coverage of conventional data sparse areas, in particular the oceans and Polar Regions. The world-wide radiosonde network of about 800 stations provides coverage mostly over the densely populated continental areas, usually limited to twice daily. Each radio occultation measurement would represent a virtually instantaneous representation of the atmospheric state, in that such a measurement takes the order of one or two minutes for one profile, compared with a radiosonde ascent of 90 minutes. A radiosonde measurement usually ends between 30 and 10 hPa, i.e. 20-30 km, whereas GRAS occultation measurements allow retrievals up to about 50 km.

The vertical resolution of radio occultation observations is considered to be limited by the vertical diameter of the first order Fresnel zone when Geometrical Optics (GO) approximation is used in data processing. For L band the Fresnel zone diameter changes roughly exponentially from about 0.5 km at the surface level to 1.5 km at 80 km. Wave Optics approximation can potentially increase the vertical resolution beyond the Fresnel zone limit. The temperature measurement accuracy of GRAS is expected to be better than 1 K in the upper troposphere and stratosphere. In the thermosphere and above it the phase delay caused by the neutral atmosphere is equal or smaller than the impact of the ionosphere. So, GRAS observations can not be used to observe neutral atmosphere at these altitudes. In the lower troposphere the temperature measurement accuracy of the GRAS is degraded due to the impact of water vapor on the index of refraction of the atmosphere. Below 5 km the temperature measurement accuracy of GRAS is expected to be 2-5 K depending on the water vapor content.

GRAS has the following operating modes:

STANDBY — Initial mode for the GRAS instrument. The instrument is initialized with almanac data for the GPS satellite constellation before the Navigation mode is entered. No measurements are performed in this mode and no CCSDS packets are transmitted.

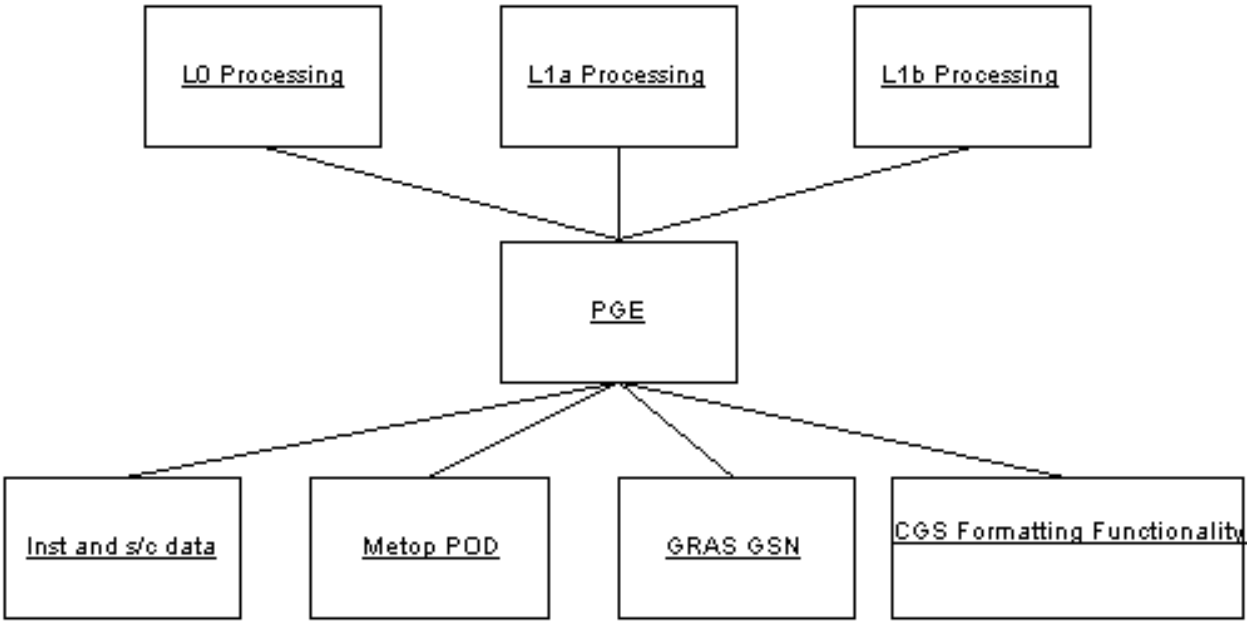

Figure 2.1: The PGE interface facilitates the transfer of instrument and satellite data, along with auxiliary data, and accepts product components for formatting in the CGS.

NAVIGATION — Initially the instrument uses the previously uploaded almanac data and an initial position, velocity, and time to determine which GPS satellites it shall acquire and track. Based on the selected GPS satellites a navigation solution is calculated and the instrument continues to update its current position, velocity, and time based on the GPS satellites in the GPS constellation autonomously. CCSDS packets are transmitted containing ancillary data and measurement data from the zenith antenna chain.

OCCULTATION — In this mode, in addition to the activities performed in Navigation mode, the instrument acquires and tracks GPS satellites on the occultation antenna chains autonomously. CCSDS packets are transmitted containing ancillary data and measurement data from the zenith and occultation antenna chains.

2.2 System Concept

2.2.1 System Context

The PGF interacts with the CGS M&C functionality by means of the PGE.

The PGE provides the means by which the PGF acquires satellite and instrument data down linked via the CDA.

The PGE also provides the means by which data from the GRAS GSN is provided to the PGF.

Furthermore, the PGF acquires information from the GRAS/Metop POD service and the Metop Satellite orbital services via the PGE.

Inputs:

GRAS source packets:	Corresponds to the raw output data provided by the instrument as CCSDS source packets. These packets contain the GRAS measurement data in measurement data packets and house keeping data in ancillary data packets.
Instrument characterisation data:	Contains instrument characterization data to be used for correcting the impact of the instrument and spacecraft hardware on the observation data.
GSN status and configuration data:	Contains characterization of the location and hardware of the fiducial stations of the GRAS GSN, and characterisation data of the currently operational GPS satellites.
GSN products:	Contains products from the GRAS Ground Support Network (GSN).
Flight dynamics information:	Metop manoeuvre information, Metop CoM position vector in the Spacecraft Reference coordinate frame as a function of time.
NWP data:	NWP data about the surface level meteorological parameters at the fiducial stations.

Outputs:

Level 0 data:	Corresponds to the Level 0 products formatted as defined in **AD3**.
Level 1a data:	Corresponds to the Level 1a products formatted as defined **AD4**.
Level 1b data:	Corresponds to the Level 1b products formatted as defined in **AD4**.
Occultation table:	Contains predicted GRAS measurements.
Reporting/Quality Information:	Corresponds to the compiled reporting information produced by the GRAS PGF that are transferred to the reporting function of the CGS. This information includes all quality information required by the Quality Control function of the CGS.

Monitoring Information: Contains all regular monitoring information on the PGF, providing the G/S M&C function with the information on the status of the instrument, data, processing functions, processing platforms, links, etc.

Controls:

G/S Commands: This datastream corresponds to the transfer of commands generated by the G/S and controlling the operation of the GRAS PGF. Note: these influence only the way the processing is done and are not related to any instrument/platform commands.

Services:

Generic PGE services: PGE provides the PGF with all services that are needed for interference free operations.

3 OPERATIONS CONCEPT

This section provides an overview of the functionality implemented by the GRAS processing function. A high level block diagram of the data processing elements is presented in 3.1.

3.1 Nominal continuous operation

This section covers the case of the processor started and running in NRT mode.

The GRAS processing function has to be able to handle data from the GRAS Navigation mode and from the GRAS Occultation mode.

3.1.1 Level 0 Processing

The GRAS instrument was running in occultation mode during the period covered by the dump. The satellite data delivered by the PGE to the PGF contains GRAS CCSDS packets covering several full and some partial occultations, navigation data, ancillary data.

3.1.2 Level 1a Processing

Level 1a processing consists of (see Figure 3.3)

- GRAS measurement data pre-processing,
- Measurement identification,

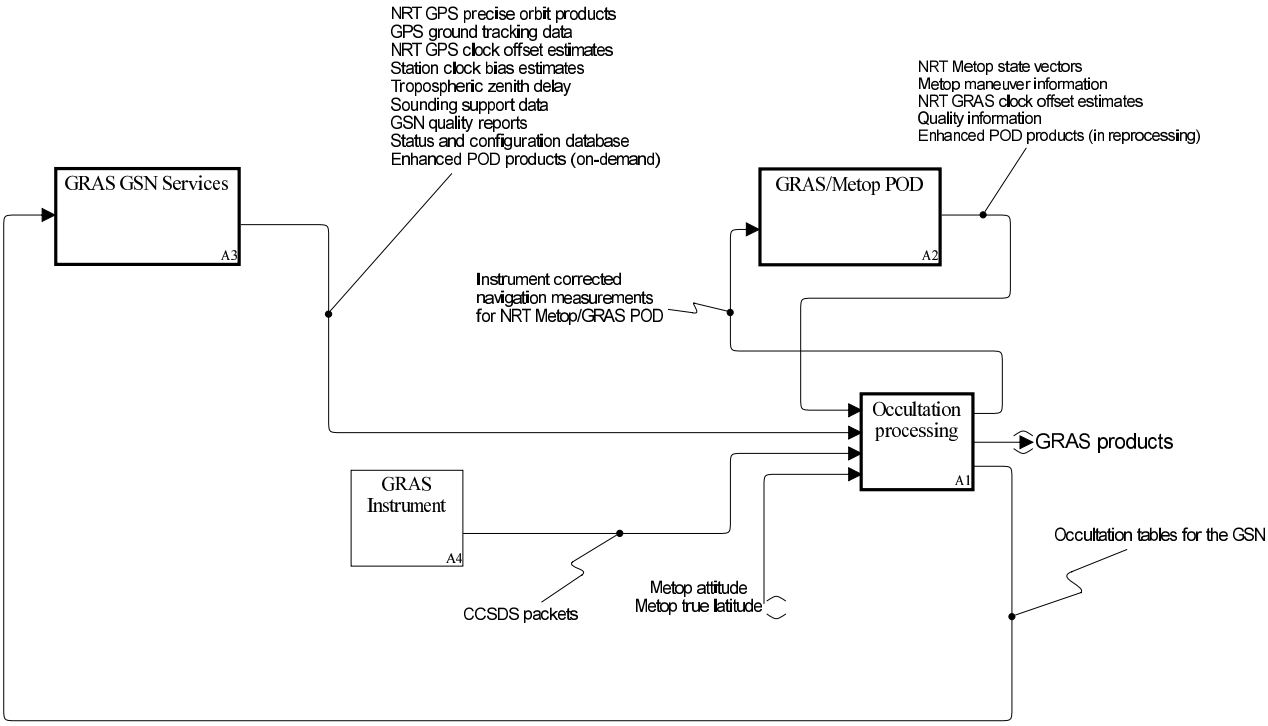

Figure 3.1: GRAS data processing elements.

- Instrument corrections,
- Level 1a products quality check and formatting.

The Level 1a processing function ingests GRAS CCSDS packets. Each CCSDS packet consists of GRAS navigation data and ancillary and measurement data from several occultations. The Level 1a processing function rearranges the GRAS CCSDS packets and pre-processes them to generate complete sequences of raw measurement data. The raw measurement data sequences are reassembled to carrier phase, amplitude, noise, and code phase data.

The Level 1a processing performs the identification of the measured occultations and the navigation data sequences by using the occultation and navigation identification codes from the occultation tables, and the header information in the GRAS navigation, ancillary, and measurement data. The measurement identification includes identification of the antenna and receiving chain (i.e., RFCU and GEU) for each observation.

The Level 1a processing function ingests the GPS Precise Orbit Determination (POD) products provided by the GSN via the PGE. A detailed description of the GSN products and product formats is provided in **RD13.** GPS POD products are used together with the onboard navigation solution included in the GRAS ancillary data to determine the incidence angle of the incoming GPS transmissions in the instrument correction function.

The Level 1a PGF uses the data from the GRAS Instrument Characterization Database to determine the instrument correction parameters to remove the impact of the instrument on the measurement

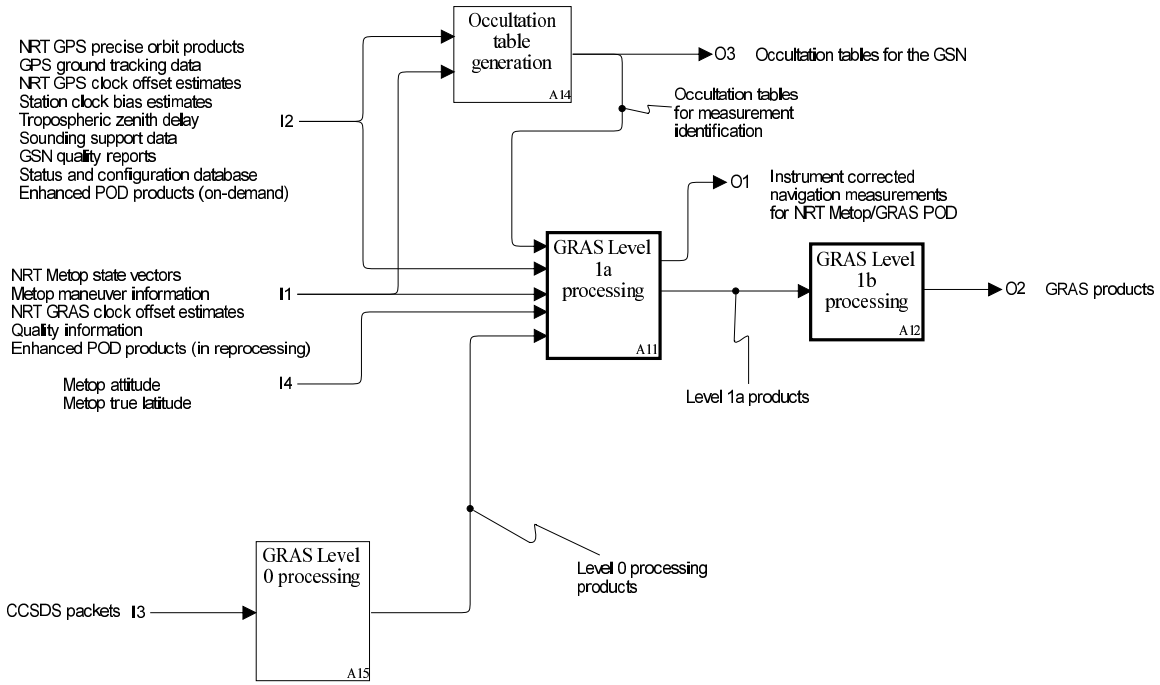

Figure 3.2: GRAS data processing steps from Level 0 to Level 1b.

data. The phase and group delays caused by the receiving antennas, RF components, and electronics are removed, and amplitude measurements are corrected for the variations of the antenna gain pattern and variations in the gain in the RF components and electronics due to temperature variations. All instrument correction functions are user selectable. The contents and the format of the GRAS Instrument Characterization Database is provided in **RD7.** The C/A and P code phase measurements are not converted into pseudoranges in the level 1a processing. However, they are corrected for the Differential Code Bias (DCB) caused by the transmitting GPS satellite and by the receiver. The corrected code phase measurements by the GRAS zenith antenna are provided to the GRAS/Metop NRT POD.

Finally, the Level 1a PGF collects all Level 1a products including the GRAS GSN and GRAS/Metop NRT POD products, performs quality checks, and formats all the products as defined in **AD4**.

3.1.3 Level 1b Processing

The Level 1b processing function calculates the bending angle and the impact parameter from the instrument corrected occultation measurement data.

The Level 1b processing function performs occultation isolation to combine GRAS data for each occultation with the auxiliary data required to retrieve the bending angle profile. The pivot GPS satellite and the fiducial station supporting differencing schemes (for clock correction) have to be selected before all auxiliary data for each occultation can be filtered.

The Level 1b PGF performs several corrections to the measurement data before the actual bending angle retrieval is performed. The phase residual, which is to a good approximation the phase delay introduced by the atmosphere, is calculated by removing the geometrical distance between

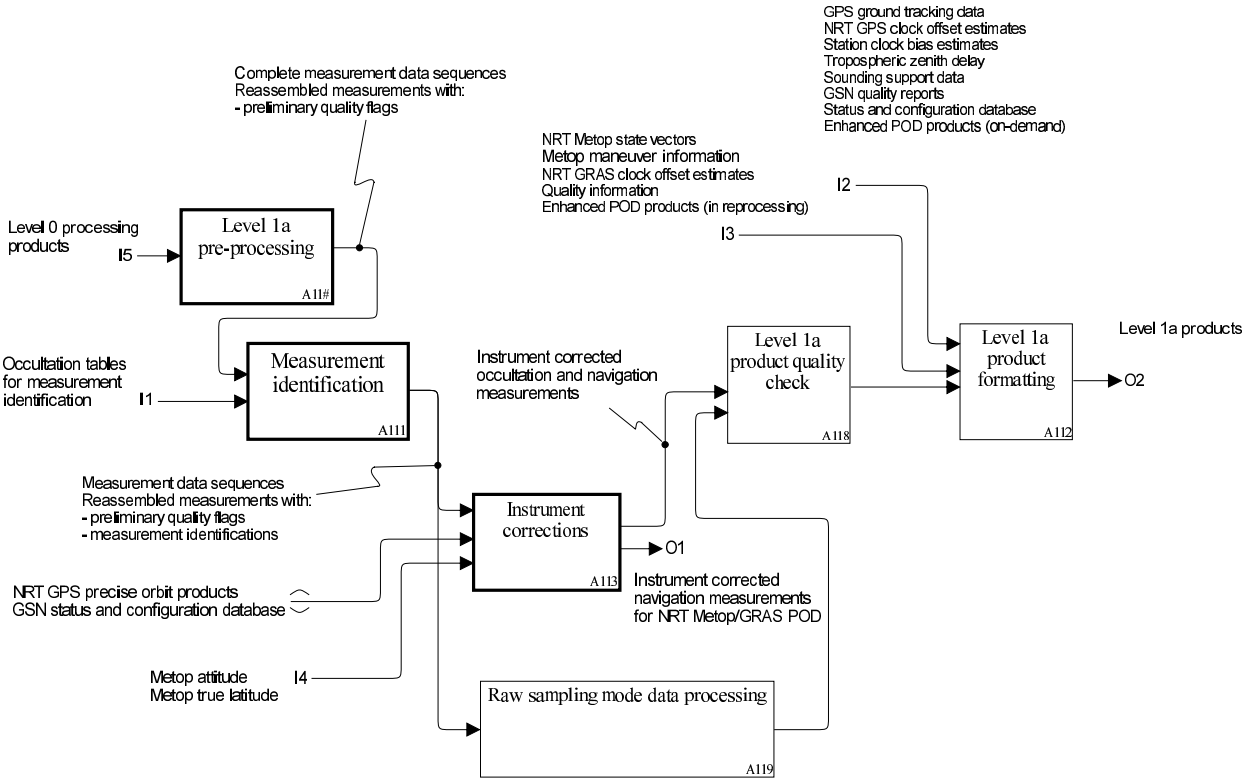

Figure 3.3: GRAS Level 1a data processing functions.

the transmitter and receiver antennas from the measured phase. This requires determination of the true reception and transmission times and interpolation of the satellite state vectors into these times. The corrections for relativistic effects are mostly included into the synchronisation of the measurement time stamps with the reference time provided by the GRAS GSN because the relativistic effects are included in the clock offset estimates calculated in the GPS and GRAS/Metop NRT POD. The only relativistic effect not included in the clock offset estimates is the variation in the apparent velocity of light because of the gravitational field of the Earth (Shapiro effect). This effect is taken into account in the determination of the transmission time and geometric path removal.

After the removal of the geometric path the measured phase residual is still wrapped around 2π. The unwrapping of the phase is in this algorithm combined

After the relativity correction a cycle slip detection and correction function is applied to the phase residual data.

The Level 1b PGF corrects the data provided by the Level 1a function for clock drifts on board the GPS satellite, and, if necessary, the GRAS instrument. The Level 1b processing function obtains, via the PGE, for each of the ground stations supporting differencing the Sounding Support Data (SSD) as defined in **RD13**. GSN also provides an estimate of the Tropospheric Zenith Delay (TZD) for each fiducial station and local surface level meteorological observations (if available). TZD has to be mapped to the elevation of the occulting and pivot GPS satellites by the Level 1b PGF.

More detailed descriptions of the differencing techniques are available in [**RD5**].

Correction technique	Applicability
No differencing (ND)	All clocks in the observation system are considered sufficiently stable and no clock correction is required. Clock biases are removed by using bias estimates from POD.
Single differencing 1 (SD1)	GPS clock is considered stable and only the impact of the GRAS clock instability is corrected for. The differencing is performed between links A and D in Figure 3.5.
Single differencing 2 (SD2)	GRAS clock is considered stable and the impact of the GPS clock instability is corrected for (current baseline scenario). The differencing is performed between links A and B in Figure 3.5.
Double differencing 1 (DD1)	All observation system clock errors are corrected for (GPS, GRAS, fiducial stations). The differencing is performed between all measurement links in Figure 3.5.
Double differencing 2 (DD2)	Similar to DD1, but two ground stations are used. One station tracks the occulting GPS satellite (GPS-1 in Figure 3.5) and the other tracks the pivot satellite (GPS-2 in Figure 3.5). The advantage is that neither station has to have visibility to both GPS satellites. The disadvantage is that the ground station clock errors are not removed.

Table 3.1: GRAS PGF clock differencing modes.

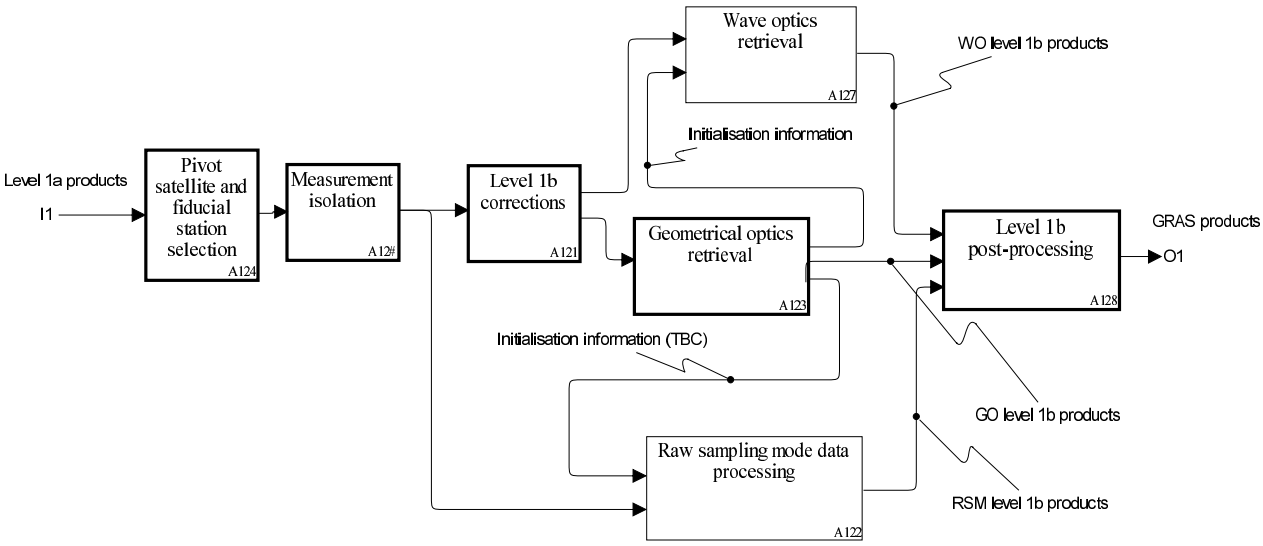

Figure 3.4: GRAS Level 1b data processing functions.

The baseline scenario for the GRAS PGF is clock correction with SD2. DD1 and DD2 are considered as fall-back options in the case that SD2 can not provide good product accuracy. ND and SD1 are optional differencing methods that may be applied depending on the GPS clock characteristics. The PGF must be able to perform any of the clock correction techniques listed in Table 3.1.

In deriving the total bending angle, the Level 1b processing function assumes a locally spherical atmosphere. The errors introduced by this assumption are reduced by applying a correction for the Earth's oblateness. The Level 1b processing function computes correction parameters for this purpose.

The derived phases of the occultation data are corrupted by high-frequency noise. The Level 1b processing function therefore low-pass-filters the derived phase data. The filtering function used in the data processing algorithm is an adaptive bandwidth low pass filter implemented as a Sinc function truncated by a Blackman-Harris window. The filtering function has been modified to handle data with non-linear sampling.

The Level 1b processing function computes the Doppler shift (as a time derivative) for the phase residual observations in the occultation. It retrieves the bending angle as a function of the impact parameter both using Geometrical Optics (GO) approximation and Wave Optics (WO) technique. GO is applied to the whole measured profile and WO to the lower part of the profile to detect and remove impact of atmospheric multipath.

The frequency independent neutral bending angle is computed by correcting for ionospheric dispersion, by applying a linear combination of the bending angles at two frequencies.

Bending angle bias is calculated and a correction is applied if necessary.

The Level 1b processing function also derives the total electron content (TEC) along the ray path.

Error characterization is performed for all Level 1b products.

For the raw sampling mode the Level 1b processing algorithm is to be defined.

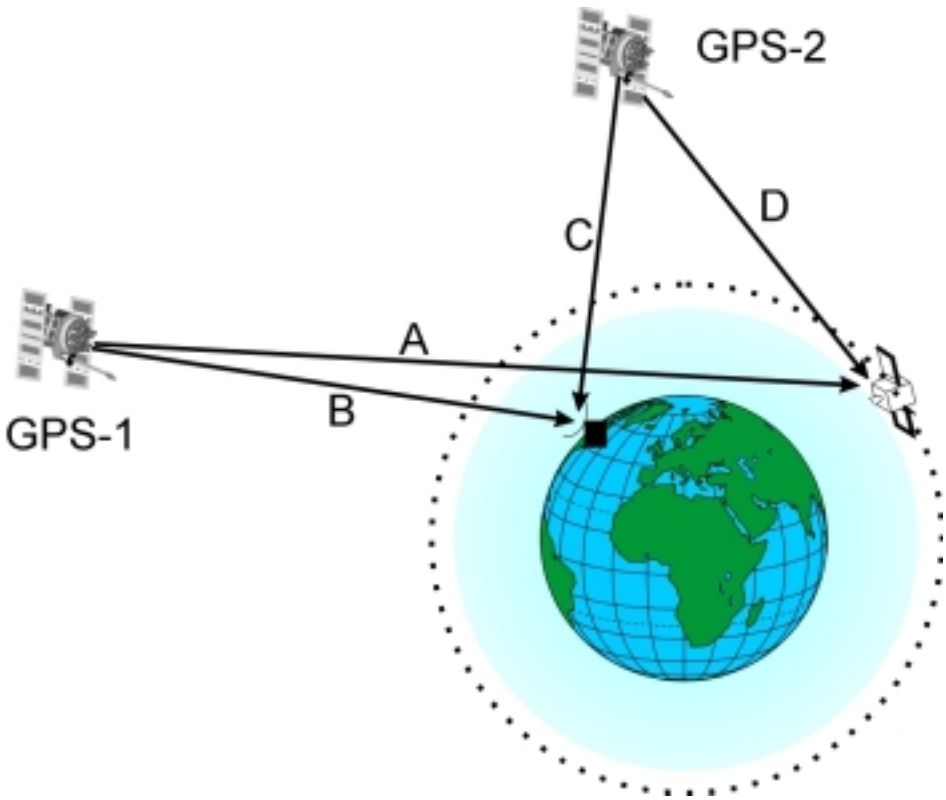

Figure 3.5: Principle of single and double differencing techniques. Single differencing (SD) means the calculation of the phase residual difference between the occultation measurement (A) and a reference measurement at a ground station (B). Double Differencing (DD) uses two additional reference measurements. One is between a pivot GPS satellite and the LEO satellite (D) and the other is between a ground station and the pivot GPS satellite (C).

3.1.4 Occultation Table Generation

Occultation Table Generation function produces a table containing all occultations and navigation measurements theoretically visible for the GRAS receiver for a time period of 24-36 hrs. The table includes the PRN numbers of the occulting GPS satellites and the PRN numbers of the GPS satellites visible for the GZA. An occultation and navigation measurement identification number is applied to each measurement.

Occultation table generation is based on predicted GPS and Metop orbits provided by the GSN and GRAS/Metop POD, respectively.

3.2 Nominal degraded scenarios

The baseline approach for GRAS level 1 data processing is that all measurements are processed and disseminated. The level 1b product quality indicators shall provide the users sufficient information to perform screening of the data at the user level. A measurement is not processed only in the case that the degradation or corruption of the measurement data completely prevents the processing.

The nominal degraded scenarios can be categorised into two classes: 1) degradation of the instrument data, and 2) degradation or missing of the auxiliary data. All degraded scenarios shall cause an error report in the dump processing identifying the error and raise an event of user configurable severity to the CGS via the PGE interface.

The degradation of the instrument data contains at least the following scenarios:

Scenario	Processing strategy
Dual frequency carrier tracking not achieved during an occultation	Measurement is processed as normally as possible. Ionosphere correction and TEC determination are not possible. No L2 products produced. Error flags for all failed product quality tests are set in MDRs.
GRAS USO temperature drift larger that specified threshold	Measurement is processed normally and respective quality flags are set in the MDRs. If this becomes a predominant problem for all or most measurements, the operator may choose to activate USO frequency correction.
Large number of identified cycle slips in occultation measurements	Measurement is processed normally and cycle slip flags are set in MDRs.
No raw sampling mode data for an occultation measurement	As raw sampling mode is activated automatically, this indicates an error by the instrument or a missing measurement sub-packet (possibly an error in pre-structuring function). The closed loop mode data can be processed normally with GO and WO algorithms. Appropriate error flags in the MDRs are set.
No navigation measurement data from the zenith antenna	Occultation measurements can be processed using SD2 and possibly also using ND clock correction options. However, Metop/GRAS NRT POD is not possible. This means that the Metop state vectors would have to be obtained e.g. from FDF. Note: this is potentially a loss of the instrument, because the level 1 product accuracy (depending on the quality of the fallback Metop state vectors) is too low for NWP applications. However, this scenario may still allow off-line processing of level 1 products.
One occultation antenna not functional	The occultation data from the remaining antenna is processed as normally.
Occulting or pivot GPS satellite manoeuvring or eclipting during a measurement	The measurement is processed as normally as possible. Degradation of the phase measurement may reduce the product quality or even prevent the data processing completely. GPS manoeuvre is indicated in the quality flags in the MDRs. Product quality degradation is indicated by the normal product quality flags.
Metop manoeuvring during an occultation measurement	The measurement is processed as normally as possible. Metop manoeuvre and manoeuvre time is indicated in the quality flags in the MDRs. Product quality degradation is indicated by the normal product quality flags.
Onboard navigation solution missing	Degrades level 1b product accuracy as instrument correction for navigation measurements used in POD is not possible.
Other ancillary data missing	Any missing ancillary data shall cause degraded level 1b product accuracy.

The degradation or missing of the auxiliary data contains at least the following scenarios:

Scenario	Processing strategy
TZD data missing	If the TZD estimates are missing, the data processing can be performed using ground based observations or NWP predictions and atmospheric delay models. The algorithm for this scenario is included into the specification in this document.
GPS clock offset data missing	Occultation processing with DD1 or DD2 methods is possible in this case. The prerequisite for this is that the GRAS/Metop POD can be performed (even with degraded accuracy) in this scenario. If GRAS/Metop NRT POD can not be performed, this becomes a non-nominal scenario “Metop POD data missing“ in Section 3.3.
Fiducial station clock offset data missing	Occultation processing can be done using ND, SD1, and DD1 methods.
SSD data missing	Occultation processing can be done using ND, and SD1 methods.
GPS tracking data missing	This scenario may impact only some fallback options of the GRAS/Metop NRT POD. Occultation processing is performed as normally if GRAS/Metop NRT POD can be performed. The impact of this scenario is to be confirmed by the contractor.
Occultation table missing	Impacts the occultation identification function, which has to operate as in the case of unpredicted measurements. Other impact depend on the performance of the GRAS GSN in this scenario. Provisionally the occultation processing can be performed as normally assuming that the GSN inputs are available.
GSN Quality reports missing	Occultation processing as normally. Indirect impact via lack of information of the eclipting or manoeuvring GPS satellites and quality of the fiducial station data. May cause degraded level 1b products.
Metop attitude data missing	Occultation processing can be performed assuming nominal yaw steering mode attitude without mispointing. This may degrade level 1b product accuracy.
Metop clock offset data missing	Occultation processing can be performed using SD1, DD1 and DD2 methods. May cause degraded accuracy in the level 1b products as time synchronisation can only be approximated and relativistic corrections are not performed.

3.3 Non-nominal scenarios

Non-nominal scenarios mean that some vital element of the GRAS measurement system is not functioning. These scenarios normally completely prevent the processing of the data. All non-nominal scenarios shall cause an error report in the dump processing identifying the error and

raise an event of user configurable severity to the CGS via the PGE interface.

The degradation or missing of the auxiliary data contains at least the following scenarios:

Scenario	**Processing strategy**
GPS POD data missing	Neither GRAS/Metop NRT POD or occultation processing is not possible without GPS POD data. Measurements can not be processed.
EOP data missing	GRAS/Metop NRT POD is not possible without GPS EOP data. Measurements can not be processed.
Metop POD data missing	Occultation processing is not possible.

4 REQUIREMENTS

4.1 General Requirements

GRAS-Sec.4.1-10 The PGF shall provide all the functionality required to support the following:

- Reception, acceptance and checking of the input data specified in Section 2.2.1;
- Full online quality control of the products;
- Estimation of the time-varying parameters used by the processing models, including but not limited to the ground station tropospheric correction parameters and the orbit models;
- M&C interfacing functions using the generic PGE services;
- Generation of monitoring information on the observed Instrument and GSN status and the PGF status and its transmission to the PGE services;
- Production of level 0, level 1a, and level 1b products;
- Product formatting (using the corresponding PGE services);
- Detection of abnormal GRAS/Metop POD functionality.

GRAS-Sec.4.1-20 Each function of the PGF shall monitor its performance and raise events of user-configurable severity on the occurrence of :

- Any abnormal instrument behavior being detected;
- Any abnormal GSN behavior being detected;
- Any occurrence and transition to/from a degraded mode of product generation;
- Any non-nominal operation of the function;
- Any occurrence likely to affect the product quality.

Note: Tables of some scenarios causing degraded mode of product generation and non-nominal operation of the GRAS measurement system are provided in Sections 3.2 and 3.3.

GRAS-Sec.4.1-30 All reporting from the PGF shall be performed in accordance with [**AD1**].

GRAS-Sec.4.1-40 All parameters and threshold values defined in the GRAS PGF shall be user definable.

GRAS-Sec.4.1-50 The PGF shall process the level 0 data and produce Level 1a/1b data of a nominal quality for all nominal modes and states of the instrument including the following:

1. Instrument running, time 102 minutes after the end of an in-plane manoeuvre.
2. Instrument running, time 400 minutes after the end of an out of plane manoeuvre.
3. Instrument running, GRAS USO temperature has been stabilised as defined in the GRAS FOM.
4. Instrument running, SSD data from fiducial ground stations and reference data from a pivot GPS satellite available for clock correction.
5. Instrument in raw sampling mode.[1]

GRAS-Sec.4.1-60 The PGF shall process the level 0 data and produce Level 1a/1b data in a degraded manner in the following modes and states of the instrument:

- Instrument running, SSD data from fiducial ground stations not available for clock correction.
- Instrument running, reference data from pivot GPS satellite not available for clock correction.
- Instrument running, data quality from the GSN is degraded;
- Instrument running, one occultation antenna not functional;
- Instrument running, onboard navigation antenna not functional.

GRAS-Sec.4.1-80 The PGF shall produce all GRAS Level 0, Level 1a, and Level 1b products specified in **[AD4]**.

GRAS-Sec.4.1-85 Taken all together, all members of a particular class of variable internal auxiliary data record in a dump shall cover a time period which is continuous and extends at least over the dump.

[1] Raw sampling mode (which generates raw data) implies that the instrument has lost or has not yet acquired phase lock and is possibly receiving multipathed signals. This implies the need to process a large volume of data, to identify signal peaks in a low-SNR regime, and to automatically recognize the onset and termination of raw sampling mode data.

GRAS-Sec.4.1-87 It shall be possible for the user to configure the time interval between the emission of individual members of each separate class of VIADR by the CGS.

Note: This is intended to allow emission of level 1b VIADRs needed by the SAF at the rate at which it needs them.

GRAS-Sec.4.1-90 The PGF shall provide all GRAS Level 0, Level 1a, and Level 1b products in units and data types specified in [**AD4**].

GRAS-Sec.4.1-100 The PGF shall implement all the functionality specified in Sections 5 and 6.

GRAS-Sec.4.1-110 The GRAS PGF shall be able to process any GRAS level 0 product or level 1a product compliant with **AD4**.

GRAS-Sec.4.1-120 The GRAS PGF shall, for each auxiliary dataset which may include and is not limited to precise orbit determination datasets, add unambiguous information to every product generated with that dataset which allows the unambiguous identification of that dataset at any subsequent time.

GRAS-Sec.4.1-130 The GRAS PGF shall support the reception, acceptance and validation of any Auxiliary Data required for Level 0/1a/1b processing.

GRAS-Sec.4.1-140 The GRAS Product Generation Functionality of the EPS CGS shall be able to use the most recent version of any auxiliary dataset that is required to create GRAS products, where auxiliary datasets include and are not limited to precise orbit determination data and GRAS ground support network data.

Example: under this requirement, when the GRAS PGF is in re-processing mode, it shall be able to use restituted precise orbit data covering the time period of its products, if the GRAS/Metop POD functionality has generated restituted precise orbit data by the time the re-processing takes place.

GRAS-Sec.4.1-150 The GRAS PGF shall support the following Operational Modes in compliance with AD1

1. Near-Real Time Mode
2. Backlog Processing Mode
3. Re-processing Mode

GRAS-Sec.4.1-160 The GRAS PGF shall use the generic PGE API as per AD1 to interface with its environment. In particular, the GRAS PGF shall accept at least START/STOP/ABORT commands via the generic PGE API.

GRAS-Sec.4.1-170 The GRAS PGF shall process all data pertaining to occultations that complete before the end of a dump.

Note: This means that auxiliary and measurement data pertaining to the first part of an occultation which began in the previous dump and completed in the dump under consideration must be processed as part of processing the dump.

GRAS-Sec.4.1-180 The GRAS PGF shall make it possible to make a user-selectable set of the input and output data for at least any function defined in Sections 5 and 6 of the PGF available for inspection both within and outside the CGS.

Note: This includes, and is not limited to, the data provided by the GRAS GSN.

GRAS-Sec.4.1-190 In generating level 0, 1a, and 1b data, and all other internal data for all nominal modes and states of the instrument, the GRAS PGF design and its implementation shall not degrade the data quality by introducing errors via processing operations (i.e., word lengths, interpolations, numerical integrations, numerical differentiations, etc).

Note: This shall be taken to mean, inter alia, that the GRAS PGF shall not degrade the data delivered to it.

GRAS-Sec.4.1-200 It shall be possible to monitor the PGF processing for the product quality.

4.2 Level 0 Processing Function

GRAS-Sec.4.2-10 The PGF shall ingest all the GRAS CCSDS packets in the dump via the PGE interface and produce level 0 Products according to **AD3** even in the case of missing, corrupt, or repeated GRAS CCSDS packets.

4.3 Level 1a Processing Function

GRAS-Sec.4.3-3 The Level 1a PGF shall produce Level 1a products using the algorithm specified in Section 5.2.

GRAS-Sec.4.3-5 The Level 1a PGF shall produce Level 1a products in a degraded fashion in the case of missing, corrupt, or repeated auxiliary data.

GRAS-Sec.4.3-20 Level 0 data detected as corrupted shall be identified/flagged by the quality checks as such, allowing the subsequent processing to handle the corrupted data without impacting the processing of the remaining data.

GRAS-Sec.4.3-30 The PGF shall extract and generate information on the data ingested, for the purpose of reporting. These shall include:

- Parameters describing the validity of the received data;
- Completeness information on the received data.

GRAS-Sec.4.3-40 The PGF shall have a user selectable option to display the following in real time using the MMI:

- Parameters describing the validity of the received data;
- Completeness information on the received data.

GRAS-Sec.4.3-70 The PGF Level 1a shall be able to ingest via the PGE interface the Level 0 records.

GRAS-Sec.4.3-75 The Level 1a PGF shall be able to obtain

1. The Metop telemetry data required to process the dump;
2. Metop CoM position vector in spacecraft reference coordinate frame;
3. Metop true latitude defined as the sum of the mean anomaly and the osculating argument of perigee with the accuracy of $0.1°$ at the epochs of the GRAS measurement samples;
4. NWP model field temperature, pressure, and partial pressure of the water vapor for each fiducial station used to support the processing of an occultation measurement at the time of the measurement at the geodetic coordinates of the station;
5. GSN products required to process the dump;
6. GRAS/Metop POD products required to process the dump;
7. All Metop attitude data required to process the dump with the pointing knowledge accuracy as specified in Table 4.1 at the epochs of the GRAS measurement samples.

Table 4.1: Metop attitude knowledge requirements.

Satellite axis	Knowledge requirement
Pitch	$0.17°$
Roll	$0.17°$
Yaw	$0.17°$

GRAS-Sec.4.3-77 The PGF Level 1a shall be able to carry out all the processing specified in Section 6.1.

GRAS-Sec.4.3-85 The PGF Level 1a shall be able to identify the following conditions in the measurement identification and raise events of user configurable severity to the CGS via the PGE interface, as well as including appropriate information in the report of the dump processing:

1. Non-occurence of a forecast measurement;
2. An occurrence of an unforecast measurement;
3. Re-occurrence of a previously identified measurement.

GRAS-Sec.4.3-135 All instrument correction algorithms specified in Section 5.2.2 are user selectable so that any correction can be enabled or disabled.

GRAS-Sec.4.3-220 The Level 1a PGF shall facilitate the subsequent upgrading of Raw Sampling mode data processing functionality at least by providing a well-defined programming interface by which data and commands can be provided to the Raw Sampling mode data processing functionality by the Measurement Identification functionality and received from the Raw Sampling mode data processing functionality by at least the Level 1a Products quality check and Product Formatting functionality.

GRAS-Sec.4.3-230 The Level 1a PGF shall be able to ingest, and extract information from the necessary Metop telemetry data source packets, and add it to the Level 1a product formatted as specified in **AD4**.

GRAS-Sec.4.3-240 The Level 1a PGF shall be able to ingest the NRT GPS orbit time series products from the GRAS GSN.

GRAS-Sec.4.3-250 The Level 1a PGF shall be able to obtain the enhanced GPS POD products from the GRAS GSN.

GRAS-Sec.4.3-260 The Level 1a PGF shall be able to select from the NRT GPS orbit time series the complete orbit arcs that enable processing of all occultations from the Metop data dump.

GRAS-Sec.4.3-270 The Level 1a PGF shall be able to format the NRT GPS orbit time series and reprocessed GPS orbit time series according the GRAS Level 1a product format specified in [**AD4**].

GRAS-Sec.4.3-320 The Level 1a PGF shall be able to obtain the GRAS instrument characterization data and select valid parameters for instrument correction for each occultation in the Metop data dump, correct the measurement data for errors caused by the observation system as explained in Section 5.2.2, and format the instrument characterization data and the measurement data into GRAS level 1a products as specified in [**AD4**].

GRAS-Sec.4.3-330 The PGF shall be able to obtain the required GRAS GSN characterization data and select valid parameters for instrument correction for the entire time period covered by the Metop data dump, correct the GSN

SSD and Ground Tracking Data for errors caused by the GSN observation system, and format the characterization, GSN SSD, and Ground Tracking data into GRAS level 1a products as specified in [**AD4**].

GRAS-Sec.4.3-340 The Level 1a PGF shall be able to obtain the Earth Orientation Parameters (EOP) from the GRAS GSN.

4.4 Level 1b Processing Function

GRAS-Sec.4.4-5 The Level 1b PGF shall produce Level 1b products using the algorithm specified in Section 5.3.

GRAS-Sec.4.4-10 The PGF shall produce bending angle products over the entire globe.

GRAS-Sec.4.4-20 The PGF shall produce bending angle products from all occultations measured by the GRAS receiver (Note: It is assumed that GSN data relevant to the occultations are available).

GRAS-Sec.4.4-30 The PGF shall be able to produce bending angle products from surface to 80 kilometers or from the smallest height that the instrument provide observation data to 80 kilometers.

GRAS-Sec.4.4-40 The PGF shall produce ionosphere corrected bending angle products with an absolute accuracy of better than 1 μrad or 0.4 % (which ever is higher) within the vertical range over which bending angle products are to be generated.

GRAS-Sec.4.4-80 The PGF shall produce all GRAS Level 1b products in the format specified in **[AD4**].

GRAS-Sec.4.4-100 The PGF Level 1b shall be able to process raw sampling mode (i.e., open-loop mode) data as defined in Section 5.4.

GRAS-Sec.4.4-105 The Level 1b PGF shall facilitate the subsequent upgrading of Raw Sampling mode data processing functionality at least by providing a well-defined programming interface by which data and commands can be provided to the Raw Sampling mode data processing functionality at least by the Occultation isolation functionality and by the GO retrieval functionality and and received from the Raw Sampling mode data processing functionality by at least the Level 1b post-processing functionality.

GRAS-Sec.4.4-180 The user shall be able to select for each correction in the PGS whether it is performed in the data processing.

GRAS-Sec.4.4-260 The PGF Level 1b shall detect and correct cycle slips and half cycle slips in the carrier phase measurements for all receiving chains for occultation and navigation antennas for all instrument tracking states.

GRAS-Sec.4.4-270 The PGF Level 1b shall have the capability to limit the cycle slip detection and correction for any occultation data to samples above a user-configurable height limit.

GRAS-Sec.4.4-310 The PGF Level 1b shall be able to use NWP data provided via the PGE interface to compute NRT tropospheric delay estimates for correction of the GSN data.

GRAS-Sec.4.4-322 In cases where sufficient input data is not available to support the clock correction method in force, the PGF shall be able to change automatically to a clock correction method that is supported by the available data as defined in Section 5.3.3.4.

GRAS-Sec.4.4-323 The automatic clock correction change mode can be enabled and disabled by the user.

GRAS-Sec.4.4-325 The choice of which clock correction mode to apply as a default shall be controlled by a user-configurable set of parameters.

GRAS-Sec.4.4-395 The parameters for the smoothing of the bending angle profiles shall be user configurable.

GRAS-Sec.4.4-420 The PGF Level 1b shall be able to process as described in Section 5.3.2 the GSN products and to extract the data related to the identified occultations.

GRAS-Sec.4.4-450 The PGF Level 1b shall maintain the GPS state vector determination accuracy provided by the GSN as defined in **AD13**.

GRAS-Sec.4.4-460 The PGF Level 1b shall maintain the Metop state vector determination accuracy provided by GRAS/Metop POD.

GRAS-Sec.4.4-470 All filtering functions used in the data processing shall be user definable by a set of configurable parameters.

4.5 Occultation Table Generation

GRAS-Sec.4.5-10 The PGF shall be able to generate an occultation table containing all occultations and navigation measurements theoretically visible for GRAS.

GRAS-Sec.4.5-15 The PGF shall generate the occultation table using the algorithm defined in Section 6.4.

GRAS-Sec.4.5-20 The PGF shall be able to generate an occultation table valid for the time period of user definable hours into the future from the time of the table generation.

GRAS-Sec.4.5-30 The occultation table shall contain GPS and Metop orbits that were used in the generation of the table.

GRAS-Sec.4.5-40 The occultation table shall be made available outside the CGS, at least to the GSN and the Calibration and Validation facility.

4.6 GRAS/Metop POD

GRAS-Sec.4.6-10 The output of the NRT GRAS/Metop POD process shall include, as minimum, the products defined in the VIADR-1A-METOP-POD specification in **AD4**.

GRAS-Sec.4.6-40 All Metop state vectors are to be provided in inertial coordinate frame ECI MJD2000 as specified in **AD7**.

GRAS-Sec.4.6-50 All time stamps used in the NRT GRAS/Metop POD products shall be in the same time frame that is used for GRAS GSN POD products.

GRAS-Sec.4.6-60 All clock offset estimates are provided as the epoch-wise offset of the GRAS clock against the reference time provided by the GSN as specified in **AD9**.

GRAS-Sec.4.6-70 The NRT POD process shall provide all specified output products for each POD solution so that the timeliness requirements for processing and dissemination of the GRAS level 1b products can be fulfilled.

GRAS-Sec.4.6-90 The POD shall provide the following items to the monitoring process:

1. Input processing parameters;
2. When supplied to it, invalid input data, clearly flagged as such;
3. When supplied to it, obsolete input data, with epoch indication;
4. Number of actually received data points;
5. Number of culled data points;
6. Minimum number of data points expected to conduct the POD;
7. Non-nominal data processing flag;
8. Processing Time;
9. Deviation of latest POD state vector from previous POD state vector in terms of σ.

GRAS-Sec.4.6-100 The POD shall make the POD, products and the parameters used in making them, available outside the CGS, at least to the Calibration and Validation facility. The list of the products and the parameters includes, but is not limited to:

1. Input processing parameters;
2. When supplied to it, invalid input data, clearly flagged as such;

3. When supplied to it, obsolete input data, with epoch indication;
4. Number of actually received data points;
5. Number of culled data points;
6. Minimum number of data points expected to conduct the POD;
7. Non-nominal data processing flag;
8. Processing Time;
9. Deviation of latest POD state vector from previous POD state vector in terms of σ.
10. Templates containing the process steering parameters (definitions of the variables and file environment, user-selected processing parameters like thresholds and so on).
11. Input data to the NRT POD process
    (a) Data related to the GPS actually used for this run (state vector, clock data);
    (b) Data related to GSN elements involved in this run (ID, coordinates);
    (c) Earth Observation Parameters used;
    (d) Tidal data files.
12. Output data from the NRT POD process.

GRAS-Sec.4.6-130 The GRAS POD shall be able to make a N hours prediction of the Metop orbit for the occultation table generation, where N shall be user-definable and in the range 0 to 36 hours.

GRAS-Sec.4.6-140 It shall be possible to start the Metop orbit prediction process either manually or automatically.

GRAS-Sec.4.6-150 The offline orbit determination on long orbit arcs to calibrate the orbit dynamical parameters

a) Solar radiation pressure with variable reflective area and fix scaling coefficient;

b) Aerodynamic drag with variable frontal area and fix scaling coefficient;

c) One cycle per revolution empirical acceleration with fixed coefficients;

shall be performed periodically, every X days (where X is a real number, user selectable and in the range 0<X<10), to obtain the latest value of the coefficients to be re-used in the short NRT orbit determination arcs.

GRAS-Sec.4.6-160 It must be possible for the operator to change the considered tracking period.

GRAS-Sec.4.6-170 It shall be possible to run the offline calibration process for the orbit dynamical parameters either manually or automatically.

GRAS-Sec.4.6-180 The offline calibration process for the orbit dynamical parameters shall use input data only over time periods that contain no manoeuvres and only over time periods in which the satellite has been in yaw steering mode.

GRAS-Sec.4.6-190 The offline orbit determination process to calibrate the orbit dynamical parameters shall not use input data that has been measured within a user definable period (default = 102 minutes) after the end of an in-plane manoeuvre or within a user definable period (default = 400 minutes) after the end of an out of plane manoeuvre.

GRAS-Sec.4.6-290 The NRT GRAS/Metop POD shall be able to ingest Metop onboard tracking data as produced by the instrument correction function.

GRAS-Sec.4.6-300 The NRT GRAS/Metop POD shall be able to ingest any products necessary for the orbit determination as provided by the GRAS Ground Support Network (GSN). GRAS GSN products are defined in **AD9** and product formats are defined in **AD14**.

GRAS-Sec.4.6-310 The NRT POD shall recover its standard orbit determination accuracy not later than user definable time (default = 102 minutes) after the end of an in-plane manoeuvre and not later than user definable time (default = 400 minutes) after the end of an out of plane manoeuvre.

GRAS-Sec.4.6-320 In case Metop leaves the standard (yaw steering) attitude mode, the above mentioned orbit determination accuracy shall be restored not later than user definable time (default = 400 minutes) following the successful switch on of the yaw steering mode.

GRAS-Sec.4.6-330 In order to check that the NRT POD process is properly working, this process shall output a subset of its normal output to a dedicated screen page and to a report file. The output shall include a s a minimum:

1. Date and Time for POD process start and for POD process end;
2. Current Metop state vector and last Metop state vector;
3. Current and last Solved-for coefficients (e.g. Cd parameters, if relevant);
4. Current state vector covariance matrix.

GRAS-Sec.4.6-340 If one or more elements of the current state vector differ from an element or elements in the past state vector by more than a user-configurable parameter (default value: 4σ) then self explanatory information about the error shall be added to the report of the dump processing, and an event of user configurable severity shall be raised to the CGS via the PGE interface.

GRAS-Sec.4.6-342 The user shall be able to adjust the parameter beyond which state vector differences create an error report and raise events of user configurable severity without interrupting the NRT POD process and have the NRT POD process affected by this action at once.

GRAS-Sec.4.6-345 NRT POD alert messages and audible alarms shall be presented at an operator screen within a user configurable time (default = 3 minutes) after their cause has occurred.

GRAS-Sec.4.6-350 Appropriate guidelines, grouped according to “symptoms”, shall be supplied to allow causes to be identified and remedial action to be taken in case of errors detected in the NRT POD function.

GRAS-Sec.4.6-360 It shall be unnecessary to stop the NRT POD process in case of problems caused by external reasons (for instance bad data).

GRAS-Sec.4.6-380 No corruption of input/output/steering data structures is allowed, even in case the NRT POD process abnormally ends.

GRAS-Sec.4.6-390 The NRT POD process scheduling and monitoring shall issue an alert to the operator and to the log file as soon as the NRT POD process abnormally ends.

GRAS-Sec.4.6-410 The user shall be able to adjust the POD process to reduce the clock offset estimation error to, at a minimum, the clock manufacturer error estimate.

Note: This is intended to minimize the risk that possible errors in the position or velocity estimation may be automatically (and artificially) attributed by the POD process to the clock offset estimates. A reference value for the expected clock errors shall be the clock manufacturer error estimate. Should the POD process consistently attribute errors to the clocks by more than Xσ (default X=4) of the error estimate by the clock manufacturer, it shall be possible for the user to adjust the POD process until the error attributed to the clock decreases below the Xσ level.

GRAS-Sec.4.6-420 The GRAS/Metop NRT POD function shall be able to produce enhanced POD products (as defined in **AD9**) using the enhanced GPS POD products from the GRAS GSN and covering the same time period as the enhanced GPS POD products. The production of enhanced POD products can be performed automatically or manually based on POD system setup by the operator.

5 MATHEMATICAL FORMULATION OF THE ALGORITHM

The mathematical formulation of the GRAS level 1 data processing algorithm is divided into two parts. This section provides a concise description of the complete data processing algorithm. This

description is designed to provide a good overview of the flow of the data processing, order of the data processing steps, and generation of the intermediate data products during the processing. When necessary, a reference to a more detailed mathematical formulation of the individual functions in Section 6 is provided.

It shall be noted that all data processing steps in this section are applied to all GRAS measurement data at L1-C/A, L1-P1 and L2-P2, unless specified otherwise.

Occultation table generation is presented as a separate box detached from the main data processing functions in Figure 5.1. This is because it is a special function in the GRAS data processing system. It is not directly a part of the NRT data processing algorithm and it is performed only once in about 24 hours. The main purpose of this function is to provide the estimated times and locations of all GRAS measurements for the next 24 - 36 hours to the GRAS GSN so that the data transfer between the elements of the measurement system can be made more efficient. The mathematical formulation for the occultation table generation is provided separately in Section 6.4.

5.1 Level 0 processing

The GRAS Level 0 processing is the first step in the GRAS data processing. This function has no mathematically definable algorithm. The purpose is this function is to collect all data from the GRAS instrument from a Metop data dump for archiving. So, the input to this function is the complete data stream from the spacecraft covering one dump.

A special problem related to the archiving is a possibility that one data dump contains measurements at the beginning and at the end of the dump, that are not complete. This happens because the GRAS measurements are split into sub-packets in multiple source packets (as explained in **AD10**). The Level 0 processing together with the archiving functionality shall ensure that when level 0 products are accessed from the archive, it shall be always possible to restore complete measurement sequences for all measurements in the product.

5.2 Level 1a processing

Level 1a processing is the start of the processing of the measurement data. The purpose of the level 1a processing is to prepare the raw measurement data from the instrument for the retrieval of the GRAS level 1b data products and collection of all auxiliary data required for the level 1b processing.

A block diagram of the level 1a processing is presented in Figure 5.1. This diagram presents the general position of each function in the data processing system. The arrows between the function blocks indicate the general direction of data flow. However, this diagram does not present any details of the flow of individual data items between the functions. The detailed data flow can only be determined from the input and output parameter lists of the function descriptions in Section 6.

5.2.1 Level 1a pre-processing

The raw data provided by the GRAS instrument is packeted into measurement and ancillary data packets inside the GRAS CCSDS packets. The level 1a pre-processing functionality handles the

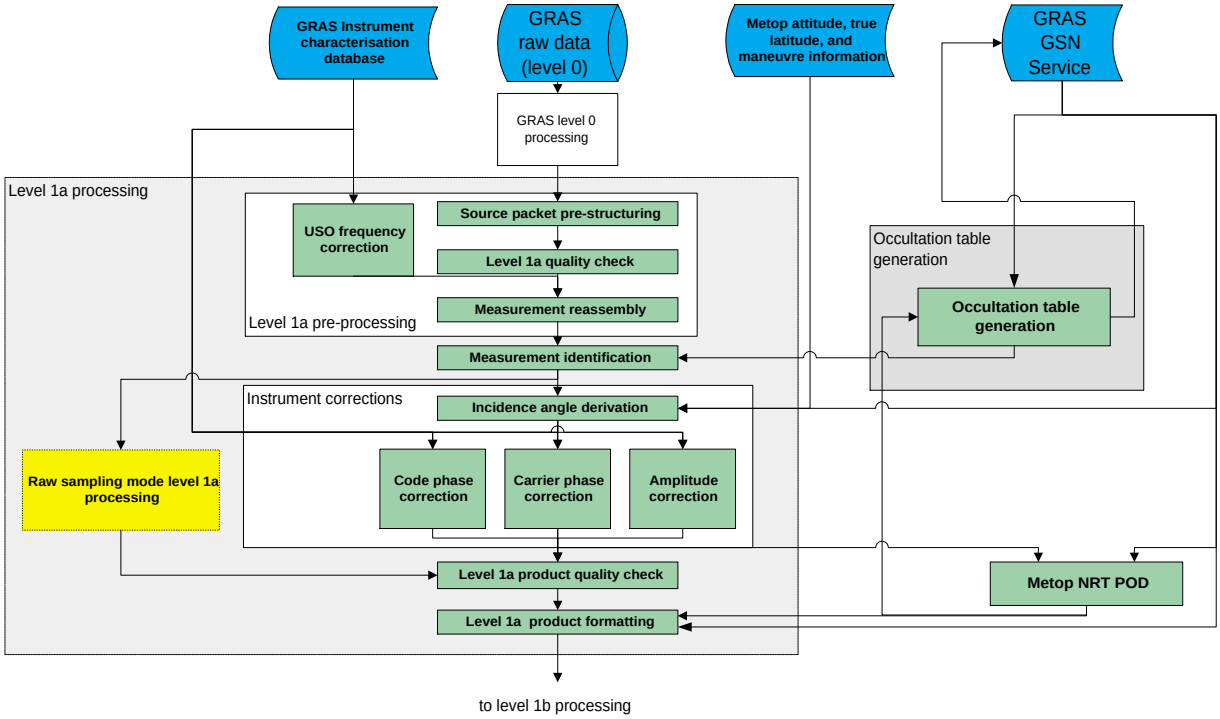

Figure 5.1: Simplified block diagram of the level 1b data processing functions.

restoring of the complete measurement time sequences (in the Source packet pre-structuring function), quality checks the input data (in the Level 1a quality check function), and the reassembly of the raw data into nominal measurement data (Measurement reassembly function).

5.2.1.1 Source packet pre-structuring

The source packet pre-structuring function ingests the raw data in CCSDS packets defined in **AD10**. The raw data produced by GRAS instrument is divided into ancillary and measurement data sub-packets. As described in **AD10** and in **AD11** the measurement sub-packets do not necessarily contain a full occultation or navigation measurement. To restore a complete measurement time sequences the contents of the CCSDS packets must be separated and data from several CCSDS packets must be collected together. The pre-structuring function shall perform the restoration of the complete measurement time sequences. There is no mathematical description of the GRAS source packet pre-structuring algorithm, but some instructions on measurement packet selection and combining are provided in **AD11**.

The pre-structuring function shall provide complete measurement data sequences for the Level 1a quality check function. It shall also provide for each measurement sample the information of which measurement packet type (Single Carrier Frequency, Dual Carrier Frequency, Occultation Raw Sampling) was used in the pre-structuring of the complete measurement data sequence. This is monitoring information that shall be included in the 1B MDRs. In the case when two measurement packet types are generated in parallel (Single Carrier Frequency and Occultation Raw Sampling), also the type of the second packet (i.e., the packet that was not used) is provided.

5.2.1.2 Level 1a quality check

The purpose of the level 1a quality check algorithm is to ensure that the complete measurement time sequences have been restored correctly, no data is missing from the measurement sequences, and that the instrument has not performed non-nominal tracking (e.g. switching tracking between two GPS satellites) during the measurement.

The detailed definitions of the level 1a quality checks are provided in Section 6.1.1.

As part of the level 1a quality check the GRAS_ID shall be set for the MDR-1A-OCCULTATION DATA, or MDR-1A-NAVIGATION DATA, depending on the measurement type. The GRAS_ID shall be set based on the SPACECRAFT_ID in the product MPHR and a user configurable database containing information of which GRAS instrument in onboard which spacecraft.

5.2.1.3 Measurement reassembly

The combined raw measurement data time sequences do not contain data that could directly be used to retrieve GRAS level 1b products. The parameters in the raw data have to be processed with the Measurement reassembly function before next steps of the data processing can be started. The mathematical algorithms for the Measurement reassembly are provided in **AD11**. The input and output parameters of the Measurement reassembly function are listed in Section 6.1.2.

If GRAS USO frequency correction due to the USO temperature variation is enabled in the data processing, this correction has to be performed before the Measurement reassembly. The equation for USO frequency correction is provided in Section 6.1.2.

The products from the Measurement reassembly function contain the “usual” radio occultation measurement products for L1 and L2 channels labeled as:

- Carrier phase;
- Carrier amplitude;
- Code phase;
- Noise estimates;
- Housekeeping information.

Measurement reassembly also converts the time stamps of the measurements from numbers of clock cycles into time in seconds. This enables the identification of the measurements against the predicted measurements in the GRAS Occultation Tables.

The Q_ANA flag in the GRAS level 1a and level 1b products is set based on the Automatic Gain Control Activity Check described in **AD11**.

5.2.1.4 Measurement identification

The measurement identification function compares the predicted measurements in the currently valid Occultation Table to the actual measurements by GRAS. The data items to be compared are:

1. Measured GPS PRN number;
2. Start time of the measurement;
3. End time of the measurement.

Before the start and end time of the measurement can be compared to the predicted start and end time, the IMT (Instrument Measurement Time) time stamps of the measurement have to be synchronised with the time frame that was used in the occultation table generation. For the navigation measurements this is straight forward as the synchronisation of the IMT time stamps with the UTC time estimated in the onboard navigation solution is provided in the Extended Navigation Data Packets **[AD10]**. For the occultation measurements the synchronisation has to be performed using the algorithm presented in Section 6.1.3.

The information for the occultation measurement samples can now be labeled as

$$\left\{ \left(SAT(m), \tau_{rx}^{imt}(m), t_{rx}^{apr}(m) \right) \; ; \; m : 1 \rightarrow N \right\},$$

and for the navigation measurements as

$$\left\{ \left(SAT(k), \tau_{rx}^{imt}(k), t_{rx}^{utc_gras}(k) \right) \; ; \; k : 1 \rightarrow K \right\}.$$

The time stamps at the beginning and at the end of the measurement can now be compared to the predicted measurement start and end time of the GPS satellite identified by the PRN number. This allows verification that the actual measurement and the predicted measurement in the occultation table are the same.

The detailed description of the time stamp comparison procedure, thresholds, and measurement consistency checks are defined in Section 6.1.4.

5.2.2 Instrument corrections

The purpose of the instrument correction function is to remove the impact of the receiver and transmitter hardware from the measurement data. For the impact of the receiver this is based on characterisation measurements by the instrument manufacturer at ground before the launch of the spacecraft. For the transmitter the correction would ideally be based on similar measurements of the transmitter hardware. For GPS satellites the transmitter characterisation data is not available. So, the instrument correction is partly based on empirically determined models of the antenna phase center position and partly on the characterisation data included in the navigation message.

The IMT time used for the time stamping of the measurement samples is directly derived from GRAS USO by counting the number of core clocks in the AGGA. The IMT counter starts running

from zero when the instrument is entering the Navigation mode and is continuously updated when ever the instrument is in Navigation or Occultation mode. The IMT count must be synchronised once with a representation of a coordinate time. This shall be done using the UTC_{GRAS} time as a coordinate time when the instrument enters the Navigation mode. A re-synchronisation of the IMT with the UTC_{GRAS} time shall be a user selectable option.

Let the set of N regenerated phase samples and their corresponding IMT times for a given channel and a particular occultation after the Measurement reassembly function be:

$$\left\{\left(\phi_{reg}(m), \tau_{rx}^{imt}(m)\right) \; ; \; m : 1 \rightarrow N\right\}$$

Note that these IMT times are times stamped at the ADC. (These stamped times are considered to be the IMT time as opposed to the time at the USO - there being a small offset between the two.)

The regenerated phase is given by the following equation:

$$\begin{aligned}\rho_{reg}\left(\tau_{rx}^{imt}\right) = \; & \frac{2\pi f_{gps}\left|\vec{r}_{ant}^{eci}\left(t_{rx}^{ref}\right)-\vec{r}_{tx}^{eci}\left(t_{tx}^{ref}\right)\right|}{c} \\ & +2\pi f_{gps} P_s\left[\vec{r}_{ant}^{eci}\left(t_{rx}^{ref}\right), \vec{r}_{tx}^{eci}\left(t_{tx}^{ref}\right)\right] \\ & +2\pi f_{gps}\left(\Delta t_{gras}\left(t_{rx}^{ref}\right) - \Delta t_{gps}\left(t_{tx}^{ref}\right)\right) \\ & -\rho_{ntrl}\left(\tau_{rx}^{imt}\right) - \rho_{ion}\left(\tau_{rx}^{imt}\right) \\ & +\rho_{inst}\left(\theta_{ant}\left(t_{rx}^{ref}\right), \varphi_{ant}\left(t_{rx}^{ref}\right), T_k\left(t_{rx}^{ref}\right), g_{ana}\left(\tau_{rx}^{imt}\right)\right) \\ & +2\pi N_{cs}\left(\tau_{rx}^{imt}\right) + \rho_{const},\end{aligned} \tag{5.1}$$

where

ρ_{reg} = the regenerated phase at the GRAS antenna reference point;

τ_{rx}^{imt} = the reception time of the GPS transmission in the IMT time frame;

f_{gps} = the frequency of the GPS transmission channel (L1 or L2);

$\vec{r}_{ant}^{eci}$ = the position vector of the GRAS antenna reference point in ECI coordinate frame;

t_{rx}^{ref} = the reception time of the GPS signal in the reference time frame;

$\vec{r}_{tx}^{eci}$ = the position vector of the transmitting GPS satellite antenna reference point in ECI coordinate frame;

t_{tx}^{ref} = the transmission time of the GPS signal in the reference time frame;

P_s = the relativistic correction for the Shapiro effect;

Δt_{gras} = the clock offset of the GRAS receiver;

Δt_{gps} = the clock offset of the transmitter of the measured GPS satellite;

ρ_{ntrl} = the phase delay due to the neutral atmosphere;

ρ_{ion} = the phase delay due to the ionosphere;

ρ_{inst} = the phase delay due to the receiver characteristics;

θ_{ant} = the zenith angle between the local antenna normal to the direction of the incoming ray;

φ_{ant} = the azimuth angle of the incoming GPS transmission at the reception antenna;

T_k = the temperature of the element k in the GRAS receiver chain (k = RFCU, GEU);

N_{cs} = an integer number of cycle slips in the received phase;

ρ_{const} = a constant phase offset due to the phase ambiguity.

In the equation above for the regenerated phase the terms have the following significance. The first and second terms are associated with geometric delay between the transmitter and the receiver; the first term is the normal geometrical distance and the second term is a correction for general relativistic effects due to the Earth's gravitational field. The third term is associated with the clock offset of the transmitter and receiver with respect to reference time. The fourth and fifth terms are the phases associated with the troposphere and the ionosphere, that we wish to recover. The sixth term is an instrument characterisation term depending on the angles of reception in the antenna frame, the reception channel which depends on (a) L1 or L2 frequency, (b) C/A, P or Y code, and (c) the temperatures of various hardware units associated with the given chain (antenna, RFCU, GEU) and the analog gain setting of the receiver. The seventh term is the cycle slip term. This term is deemed to be zero at the start of a setting occultation (when the tracking loop first locks the carrier) and remains zero unless the tracking loop skips one or more cycles between adjacent samples. For a rising occultations, similar considerations apply except the cycle slip term is deemed to be zero at the end of the occultation. The eighth term is a constant phase offset.

Equation 5.1 is equally applicable for occultation and navigation phase measurements by GRAS. In the case of navigation measurements the neutral atmosphere term can be considered zero.

The objective first stage of the processing is to recover the sum of the tropospheric and ionospheric phase from the regenerated phase be eliminating the impact of all other terms.

The purpose of the instrument correction is to remove the impact of the sixth term in Equation 5.1 from the measurement data. This is done using approximate position and timing information from the on-board navigation solutions, that is perfectly adequate for this purpose.

It should be noted that it is possible to perform most carrier phase related calculations in the GRAS data processing by converting the phase data into radians, degrees, or meters. The unit of the data does not impact the accuracy of the bending angle retrieval as long as the units of all data are consistent. However, the unit of the data impacts the formulation of the algorithm. In this document the unit of the phase data is radians in level 1a and meters in level 1b processing (except in cycle slip correction, where the data is temporarily converted to radians). In the mathematical notation the symbol ρ is used for phase data in radians and ϕ for phase data in meters. These units have been selected to ease the mathematical formulation of the algorithm. The implementation of the algorithm may deviate from the unit specification used in this document as long as the consistency

of the input and output data is maintained. The units of the level 1a and level 1b products must follow the specification in **AD4**.

The instrument correction for the occultation carrier phase measurements is performed by subtraction

$$\begin{aligned}\rho_{ic_ch}\left(\tau_{rx}^{imt}\right) &= \rho_{reg_ch}\left(\tau_{rx}^{imt}\right) - \Lambda\left(\theta_{ant}\left(t_{rx}^{apr}\right), \varphi_{ant}\left(t_{rx}^{apr}\right), CH\right) \\ &\quad -\Xi\left(T_{rfcu}\left(t_{rx}^{apr}\right), CH\right) - \Gamma\left(T_{geu}\left(t_{rx}^{apr}\right), g_{ana}\left(t_{rx}^{apr}\right), CH\right), \end{aligned} \tag{5.2}$$

where

ρ_{ic_ch} = the instrument corrected carrier phase for channel ch;

Λ = the function estimating the impact of the antenna phase center on the measured carrier phase;

Ξ = the function estimating the impact of the RFCU phase delay on the measured carrier phase;

Γ = the function estimating the impact of the GEU phase delay on the measured carrier phase;

t_{rx}^{apr} = the reception time of the carrier phase sample approximated using the onboard navigation solution time;

CH = the channel and the code of the received transmission (L1-C/A, L1-P1, L2-P2).

The derivations of the functions Λ, Ξ, and Γ are presented in Section 6.1.5.

The correction for the carrier phase measurements with the navigation antenna GZA is also performed using Equation 5.2. Because the navigation measurements are already time stamped by the UTC_{gras} time, the τ_{rx}^{imt} and t_{rx}^{apr} times are replaced with $t_{rx}^{utc_gras}$.

The instrument correction for the amplitude measurements by the occultation channels is performed by

$$E_{ic_ch}\left(\tau_{rx}^{imt}\right) = E_{reg_ch}\left(\tau_{rx}^{imt}\right) \cdot \Delta E_{inst}\left(\theta_{ant}\left(t_{rx}^{apr}\right), \varphi_{ant}\left(t_{rx}^{apr}\right), T_{rfcu}\left(t_{rx}^{apr}\right), T_{geu}\left(t_{rx}^{apr}\right), g_{ana}\left(t_{rx}^{apr}\right), CH\right), \tag{5.3}$$

where

E_{reg_ch} = the regenerated amplitude from measurement reassembly function at channel ch;

ΔE_{inst} = a function providing an estimate for the total amplitude change caused by the receiver hardware.

The detailed definition of ΔE_{inst} is provided in Section 6.1.5.

For the amplitude measurements by GZA the τ_{rx}^{imt} and t_{rx}^{apr} time stamps in Equation 5.3 are replaced by $t_{rx}^{utc_gras}$.

Finally, instrument correction is to be performed also to the code phase measurements. The instrument corrected code phase measurements are derived from the function

$$CP_{ic_ch}\left(\tau_{rx}^{imt}\right) = \Xi_{cp}\left(CP_{ch}\left(\tau_{rx}^{imt}\right), T_{rfcu_chn}\left(\tau_{rx}^{imt}\right), T_{geu}\left(\tau_{rx}^{imt}\right), g_{ana}\left(\tau_{rx}^{imt}\right), CHN, P_{lo_rfcu}, \Delta t_{dcb}\right), \tag{5.4}$$

where

CP_{ic_ch} = the instrument corrected code phase for code ch (L1-C/A, L1-P1, or L2-P2);

CP_{ch} = the measured code phase for code ch;

T_{rfcu_chn} = the temperature of the RFCU corresponding to the antenna chain CHN;

T_{geu} = the temperature of the GEU;

g_{ana} = the analog gain setting of the GEU;

CHN = the antenna chain indicator;

P_{lo_rfcu} = the LO power feeding the the RFCU during the measurement;

Δt_{dcb} = the Differential Code Bias (DCB) of the measured GPS satellite.

Function 5.4 is called for each GRAS measurement for each code L1-C/A, L1-P1, and L2-P2 to derive the instrument corrected code phases.

The detailed formulation of the function Ξ_{cp} is provided in Section 6.1.5.3.

The instrument corrected navigation measurements (phase, amplitude, code phase) are used by the GRAS/Metop NRT POD function for determination of the Metop orbit and clock offset. The mathematical formulation of the POD algorithm is presented in Appendix A.

5.2.3 Level 1a product quality check

The level 1a product quality check function monitors the quality of the level 1a products and telemetry information. The purpose of this check is to set the appropriate quality flags in the level 1a and level 1b MDRs. No measurements are rejected because of the level 1a quality checks.

One important function of the level 1a quality check is to monitor the tracking status of the instrument using the carrier amplitude. This supports the detection of a transient loss of the carrier tracking in low SNR conditions. This temporary loss of track may not be visible in the tracking status flag or measurement packet type.

Detailed specifications of the Level 1a product quality check input and output parameters, and threshold levels are provided in Section 6.1.6.

The main output of the Level 1a product quality check function are the product quality flags in the level 1a MDRs.

5.2.4 Level 1a product formatting

The Level 1a products contain GRAS measurement data, housekeeping data, and auxiliary data from GRAS/Metop NRT POD function and GRAS GSN. The detailed data contents, data structure in the forms of VIADRs and MDRs, and detailed data format is defined in **AD4**.

There is no mathematical formulation for this function.

5.3 Level 1b processing

Level 1b processing retrieves phase residual, Doppler residual, and total bending angle from the occultation measurement data prepared in level 1a processing.

A block diagram of the level 1b processing is presented in Figure 5.2. This diagram presents the general position of each function in the data processing system. The arrows between the function blocks indicate the general direction of data flow. However, this diagram does not present any details of the flow of individual data items between the functions. The detailed data flow can only be determined from the input and output parameter lists of the function descriptions in Section 6.

5.3.1 Pivot satellite and fiducial station selection

The first function of the level 1b processing is to select the pivot GPS satellite and the fiducial ground station that shall be used to support the clock correction with differencing techniques. The pivot satellite shall be selected from the group of satellites tracked by the GZA over the full time period of the occultation measurement. The fiducial station shall be selected from the sub-net of fiducial stations that have visibility to the occulting and the pivot GPS satellite.

The selection of the fiducial ground station and the pivot GPS satellite for clock differencing is based on calculating a cost function for each provisional station-satellite combination. A different cost function is defined for each differencing technique. The fiducial station, pivot satellite, or the station-satellite combination depending on the differencing mode with the smallest cost function is selected for the occultation data processing. The detailed cost models and selection parameters are provided in Section 6.2.1.

The Pivot satellite and fiducial station selection function shall provide the identifications of the selected satellites and stations for Measurement isolation.

5.3.2 Occultation isolation

The purpose of the occultation isolation function is to collect all auxiliary data required for processing of one occultation from the level 1b VIADRs . Because the sampling rate of the auxiliary data is always 1 Hz or lower, the accuracy of the t_{rx}^{apr} is sufficient for the isolation of the auxiliary data. Thus, as input parameters the Occultation isolation function requires:

- the identification of the occulting GPS;

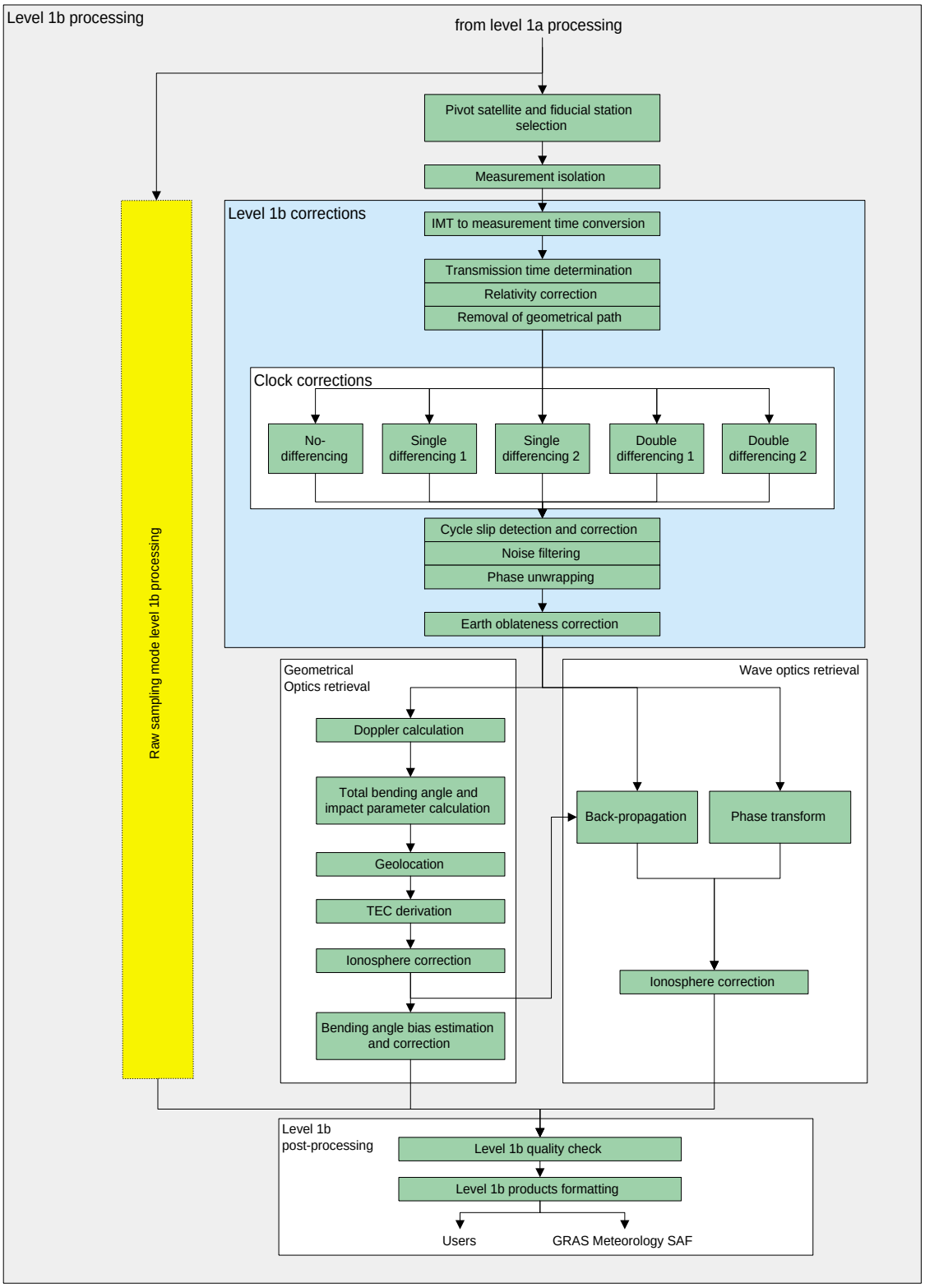

Figure 5.2: Block diagram of the level 1b data processing.

– identification of the pivot GPS;

– identification of the fiducial stations 1 and 2;

– and start and end time stamps of the occultation measurement as t_{rx}^{apr} time.

The GPS and station identifications are produced by the Pivot satellite and fiducial station selection function and the time stamps are generated for each occultation in the Measurement identification function.

There is no mathematical description of the algorithm as the isolation of the auxiliary data only requires comparisons of the GPS satellite and fiducial station identification codes and the time stamps of the data items.

5.3.3 Level 1b corrections

The Occultation isolation function produces complete data sets containing occultation measurement data and auxiliary data required for level 1b product retrieval. The purpose of the correction functions at level 1b is to remove more terms from the measured phase data as expressed in Equation 5.1 in order to derive only the phase residual caused by the neutral atmosphere and ionosphere at frequencies L1 and L2. Level 1b corrections shall also correct or reduce the impact of errors caused by relativistic effects, clock offsets, and Earth oblateness.

5.3.3.1 IMT to reference time conversion

The time stamps of the measurement data in IMT time frame can be converted into reference time frame using the GRAS clock offset estimates produced in the GRAS/Metop NRT POD function. The algorithm to be used in the time conversion depends on the format of the POD output. If the clock offsets are provided as a function, the conversion is performed with iterative inversion of the function. If the offsets are provided as discrete samples, the conversion is performed using interpolation.

If the POD clock offset data is provided as a function, $\Delta t_{gras}\left(t^{ref}\right)$, it allows IMT time to be computed at any reference time as

$$\tau^{imt} = t^{ref} + \Delta t_{gras}\left(t^{ref}\right), \tag{5.5}$$

where

τ^{imt} = time in the IMT time frame;

t^{ref} = time in the reference time frame.

The Equation 5.5 can be solved iteratively to yield the inverse relationship

$$t^{ref} = \tau^{imt} + D_{gras}\left(\tau^{imt}\right), \tag{5.6}$$

where

D_{gras} = the offset between t^{ref} and τ^{imt} as a function of τ^{imt}.

If the POD output is provided as series of discreet values

$$\left\{\left(\Delta t_{gras}(m), t^{ref}(m)\right);\ m:1\rightarrow N\right\}$$

the inverse relationship at the measurement times τ^{imt} can be solved by linear interpolation

$$D_{gras}(\tau^{imt}) = \Delta t_{gras}(t_m^{ref}) + \left[\tau^{imt} - \tau^{imt}\left(t_m^{ref}\right)\right]\frac{\Delta t_{gras}\left(t_{m+1}^{ref}\right) - \Delta t_{gras}\left(t_m^{ref}\right)}{t_{m+1}^{ref} - t_m^{ref}}, \tag{5.7}$$

where $\tau^{imt}\left(t_m^{ref}\right) \leq \tau^{imt} \leq \tau^{imt}\left(t_{m+1}^{ref}\right)$.

If the clock offsets are provided as discrete values, the IMT to reference time conversion function shall include a user selectable option to filter the data before interpolation. The filter options shall include a least squares fit of nth order polynomial to the data and applying a low pass filter as defined in Section 6.3.6.1 with user definable parameters $B(t)$ and $L(t)$.

After the inverse relationship has been solved, the IMT times (stamped at the ADC) may be converted to reference times of arrival at the GRAS antennas using the equation

$$t_{rx}^{ref} = \tau_{rx}^{imt} - \delta_{rx}\left(CH\right) + D_{gras}\left(\tau_{rx}^{imt} - \delta_{rx}\left(CH\right)\right), \tag{5.8}$$

where $\delta_{rx}(CH)$ is a chain dependent delay time between the antenna and the ADC (in the GRAS rest frame). Using this equation we can extend the labeling of the set of N regenerated phase samples for a given channel and a particular occultation as

$$\left\{\left(\rho_{ic_ch}(m), \tau_{rx}^{imt}(m), t_{rx}^{ref}(m)\right);\ m:1\rightarrow N\right\}$$

Note that knowledge of the reference time of reception allows the position of the Metop satellite centre of mass at the reference time of reception to be determined from the POD position data.

5.3.3.2 Transmission time determination

It is now necessary to determine the reference time of transmission to allow the position of the GPS(n) satellite centre of mass to be determined. This is achieved by iterating the equation

$$t_{tx*}^{ref} = t_{rx}^{ref} - \frac{\left|\vec{r}_{ant}^{eci}\left(t_{rx}^{ref}\right) - \vec{r}_{tx}^{eci}\left(t_{tx*}^{ref}\right)\right|}{c} - P_s\left[\vec{r}_{ant}^{eci}\left(t_{rx}^{ref}\right), \vec{r}_{tx}^{eci}\left(t_{tx*}^{ref}\right)\right], \tag{5.9}$$

where

t_{tx*}^{ref} = the estimate of the transmit time;

P_s = the function calculating the delay caused by the Shapiro effect [s];

$\vec{r}_{ant}^{eci}$ = the position vector of the GRAS antenna reference point in ECI coordinate frame;

$\vec{r}_{tx}^{eci}$ = the position vector of the transmitting GPS satellite antenna phase center in ECI coordinate frame.

The function P_s for calculating the Shapiro effect is given in Equation 6.52 in Section 6.2.2.1.

The position vector of the GRAS antenna $\vec{r}_{ant}^{eci}$ is calculated from

$$\vec{r}_{ant}^{eci}\left(t_{rx}^{ref}\right) = \vec{r}_{leo}^{eci}\left(t_{rx}^{ref}\right) + \mathbf{M}_{metop}\left(t_{rx}^{ref}\right)\left[\vec{r}_{ant}^{srf} - \vec{r}_{com}^{srf}\left(t_{rx}^{ref}\right)\right], \tag{5.10}$$

where

$\vec{r}_{leo}^{eci}$ = the position vector of the Metop CoM in the ECI coordinate frame;

$\mathbf{M}_{metop}$ = the rotation matrix from the Metop Satellite Reference Frame (SRF) to ECI;

$\vec{r}_{ant}^{srf}$ = the position vector of the antenna reference point in the SRF coordinate frame;

$\vec{r}_{com}^{srf}$ = the position vector of the Metop CoM in the SRF coordinate frame.

The coordinate transform from Metop SRF to ECI is defined in steps 4) - 6) in Section 6.3.3.1.

The position vector of the Metop CoM in Equation 5.10 shall be interpolated to the observations times t_{rx}^{ref} using the Lagrange interpolation (Section 6.3.1.1).

The position vector of the GPS transmission antenna phase center $\vec{r}_{tx}^{eci}$ is calculated from

$$\vec{r}_{tx}^{eci}\left(t_{tx*}^{ref}\right) = \vec{r}_{gps}^{eci}\left(t_{tx*}^{ref}\right) + \mathbf{M}_{gps}\left(t_{tx*}^{ref}\right) \cdot \vec{r}_{tx}^{srf}, \tag{5.11}$$

where

$\vec{r}_{gps}^{eci}$ = the position vector of the GPS CoM in the ECI coordinate frame;

t_{tx*}^{ref} = the estimate of the transmission time;

$\mathbf{M}_{gps}$ = the rotation matrix from the GPS SRF to ECI;

$\vec{r}_{tx}^{srf}$ = the position vector of the GPS antenna phase center in the GPS SRF frame (assumed to be constant over time).

The rotation matrix $\mathbf{M}_{gps}$is calculated from

$$\mathbf{M}_{gps} = \begin{pmatrix} U_{11} & U_{12} & U_{13} \\ U_{21} & U_{22} & U_{23} \\ U_{31} & U_{32} & U_{33} \end{pmatrix}^{-1}. \tag{5.12}$$

The matrix elements U_{ij} are derived from unit vectors in the local GPS SRF frame as

$$\begin{aligned}
\hat{u}_z &= \frac{-\vec{r}_{gps}^{eci}}{\left|\vec{r}_{gps}^{eci}\right|} \\
&= \frac{-\left(x_{gps}\hat{x}^{eci} + y_{gps}\hat{y}^{eci} + z_{gps}\hat{z}^{eci}\right)}{\sqrt{x_{gps}^2 + y_{gps}^2 + z_{gps}^2}} \\
&= \frac{-x_{gps}}{r_{gps}}\hat{x}^{eci} - \frac{y_{gps}}{r_{gps}}\hat{y}^{eci} - \frac{z_{gps}}{r_{gps}}\hat{z}^{eci} \\
&= U_{31}\hat{x}^{eci} + U_{32}\hat{y}^{eci} + U_{33}\hat{z}^{eci}, \qquad (5.13)
\end{aligned}$$

where

$$r_{gps} = \sqrt{x_{gps}^2 + y_{gps}^2 + z_{gps}^2},$$

$$\begin{aligned}
\hat{u}_y &= \frac{\vec{u}_z \times \vec{r}_{sun}^{eci}}{\left|\vec{u}_z \times \vec{r}_{sun}^{eci}\right|} \\
&= \frac{\left(U_{31}\hat{x}^{eci} + U_{32}\hat{y}^{eci} + U_{31}\hat{z}^{eci}\right) \times \left(x_s\hat{x}^{eci} + y_s\hat{y}^{eci} + z_s\hat{z}^{eci}\right)}{\left|\left(U_{31}\hat{x}^{eci} + U_{32}\hat{y}^{eci} + U_{31}\hat{z}^{eci}\right) \times \left(x_s\hat{x}^{eci} + y_s\hat{y}^{eci} + z_s\hat{z}^{eci}\right)\right|} \\
&= \frac{U_{32}z_s - U_{33}y_s}{u_y}\hat{x}^{eci} + \frac{U_{33}x_s - U_{31}z_s}{u_y}\hat{y}^{eci} + \frac{U_{31}y_s - U_{32}x_s}{u_y}\hat{z}^{eci} \\
&= U_{21}\hat{x}^{eci} + U_{22}\hat{y}^{eci} + U_{23}\hat{z}^{eci}, \qquad (5.14)
\end{aligned}$$

where

$$u_y = \sqrt{\left(U_{32}z_s - U_{33}y_s\right)^2 + \left(U_{33}x_s - U_{31}z_s\right)^2 + \left(U_{31}y_s - U_{32}x_s\right)^2},$$

and

$$\begin{aligned}
\hat{u}_x &= \frac{\hat{u}_y \times \hat{u}_z}{\left|\hat{u}_y \times \hat{u}_z\right|} \\
&= \frac{U_{22}U_{33} - U_{23}U_{32}}{u_x}\hat{x}^{eci} + \frac{U_{23}U_{31} - U_{21}U_{33}}{u_x}\hat{y}^{eci} + \frac{U_{21}U_{32} - U_{22}U_{31}}{u_x}\hat{z}^{eci} \\
&= U_{11}\hat{x}^{eci} + U_{12}\hat{y}^{eci} + U_{13}\hat{z}^{eci} \qquad (5.15)
\end{aligned}$$

where

$$u_x = \sqrt{\left(U_{22}U_{33} - U_{23}U_{32}\right)^2 + \left(U_{23}U_{31} - U_{21}U_{33}\right)^2 + \left(U_{21}U_{32} - U_{22}U_{31}\right)^2}.$$

The sun position vector $\vec{r}_{sun}^{eci}$ in Equation 5.14 is estimated by using a standard algorithm described e.g. in Montenbruck & Gill, Section 3.3.2 or 3.3.3.

The position vector of the antenna phase center in the GPS SRF coordinate frame $\vec{r}_{tx}^{srf}$ is provided for each GPS satellite in the GSN Status and Configuration Database.

When the iteration has converged

$$t_{tx}^{ref} = t_{tx*}^{ref}. \tag{5.16}$$

Using this equation we can, once again, extend the labeling of the set of N regenerated, instrument-corrected phase samples for a given channel and a particular occultation in the following manner:

$$\left\{ \left(\rho_{ic_ch}(m), \tau_{rx}^{imt}(m), t_{rx}^{ref}(m), t_{tx}^{ref}(m) \right) ;\ m : 1 \rightarrow N \right\}$$

5.3.3.3 Relativity correction and removal of geometric path

Having established the reference times of transmission and reception, the geometrical path terms may now be removed from the regenerated phase by subtraction using the GPS and Metop POD data as

$$\begin{aligned} \phi_{atm}\left(t_{rx}^{ref}\right) &= \frac{c}{2\pi f_{gps}} \rho_{ic}\left(t_{rx}^{ref}\right) \\ &- \left| \vec{r}_{ant}^{eci}\left(t_{rx}^{ref}\right) - \vec{r}_{tx}^{eci}\left(t_{tx}^{ref}\right) \right| \\ &- c\Delta t_s \left[\vec{r}_{ant}^{eci}\left(t_{rx}^{ref}\right), \vec{r}_{tx}^{eci}\left(t_{tx}^{ref}\right) \right], \end{aligned} \tag{5.17}$$

where

ϕ_{atm} = the phase residual due to the neutral atmosphere and ionosphere;

f_{gps} = the GPS transmission frequency (L1 or L2).

It is important to note that the satellite state vectors interpolate to the approximate reception and transmission times in the level 1a processing are not valid any more as the more accurate reception times and transmission times have been solved. So, new interpolations of the satellite state vectors are necessary.

The accurate knowledge of the transmission and reception times allows correction of the measured code phases for the error caused by the Shapiro effect as

$$\begin{aligned} CP_{rc_ca}\left(t_{rx}^{ref}\right) &= CP_{ic_ca}\left(t_{rx}^{ref}\right) - 1023 \cdot 10^3 \cdot P_s \left[\vec{r}_{ant}^{eci}\left(t_{rx}^{ref}\right), \vec{r}_{tx}^{eci}\left(t_{tx}^{ref}\right) \right] \\ CP_{rc_p1}\left(t_{rx}^{ref}\right) &= CP_{ic_p1}\left(t_{rx}^{ref}\right) - 10230 \cdot 10^3 \cdot P_s \left[\vec{r}_{ant}^{eci}\left(t_{rx}^{ref}\right), \vec{r}_{tx}^{eci}\left(t_{tx}^{ref}\right) \right] \\ CP_{rc_p2}\left(t_{rx}^{ref}\right) &= CP_{ic_p2}\left(t_{rx}^{ref}\right) - 10230 \cdot 10^3 \cdot P_s \left[\vec{r}_{ant}^{eci}\left(t_{rx}^{ref}\right), \vec{r}_{tx}^{eci}\left(t_{tx}^{ref}\right) \right]. \end{aligned} \tag{5.18}$$

The function P_s for calculating the Shapiro effect is given in Equation 6.52 in Section 6.2.2.1.

Table 5.1: Fallback modes for the clock correction in the case of missing input data.

Fallback mode	Comments
DD2 => DD1	DD2 mode has been selected, but input data from the second fiducial station is missing. As a result DD1 is the only available double differencing mode.
DD1 => SD2	1. DD1 mode has been selected, but reference measurement of the pivot GPS satellite is not available. SD2 is the only available differencing mode. 2. DD1 mode has been selected (or used as a fallback option), but SSD from the fiducial station is missing. SD2 would normally be the fallback option, Missing SSD forces another fallback from SD2 to SD1 (so this case is effectively DD1 => SD1).
SD2 => SD1	SD2 mode has been selected, but SSD from the fiducial station is missing. SD1 is the only available differencing option.
SD1 => ND	SD1 (or any of the higher differing modes) has been selected, but some or all of the reference measurements are missing. Only option is to use ND mode.

5.3.3.4 Clock corrections

The phase residual data after the Removal of the geometrical path function must be corrected for the clock offsets between the transmitter and the receivers. This algorithm includes five different clock correction methods. The clock correction method to be used is user selectable. The processing system shall provide a user selectable option to perform all corrections in parallel and provide the results as an output.

In the case that sufficient data is not available to perform the selected clock correction method, a fallback method shall be applied in the as defined in Table 5.1. It shall be noted that depending of the missing input data, the clock correction mode can “drop” more than one step. The automatic selection of a clock correction fallback mode can be enabled and disabled by the operator. If the automatic fallback selection is disabled and the selected mode can not be performed, self explanatory information about the error is added in the report of the dump processing, and an event of user configurable severity to the CGS via the PGE interface is raised.

The clock correction options from (a) to (e) are listed below:

(a) No Differencing (ND)

$$\phi_{nd}\left(t_{rx}^{ref}\right) = \phi_{atm}\left(t_{rx}^{ref}\right) - 2\pi f_{gps}\left(\Delta t_{gras}\left(t_{rx}^{ref}\right) - \Delta t_{gps}\left(t_{tx}^{ref}\right)\right), \tag{5.19}$$

where

ϕ_{nd} = the phase residual after ND clock correction;

Δt_{gras} = the clock offset estimate for the GRAS instrument from the GRAS/Metop NRT POD;

Δt_{gps} = the clock offset estimate for the occulting GPS satellite from the GRAS GSN products.

The detailed description of the derivation of ϕ_{nd} is provided in Section 6.2.2.2.

(b) Single Differencing 1 (SD1)

$$\phi_{sd1}\left(t_{rx}^{ref}\right) = \phi_{atm}\left(t_{rx}^{ref}\right) - \phi_{res_sd1}\left(t_{rx}^{ref}\right), \tag{5.20}$$

where

ϕ_{sd1} = the phase residual after SD1 clock correction;

ϕ_{res_sd1} = the phase residual from the measurement of the pivot GPS satellite by GRAS.

The detailed description of the derivation of ϕ_{sd1} is provided in Section 6.2.2.3.

(c) Single Differencing 2 (SD2)

$$\phi_{sd2}\left(t_{rx}^{ref}\right) = \phi_{atm}\left(t_{rx}^{ref}\right) - \phi_{res_sd2}\left(t_{rx}^{ref}\right), \tag{5.21}$$

where

ϕ_{sd2} = the phase residual after SD2 clock correction;

ϕ_{res_sd2} = the phase residual from the measurement of the occulting GPS satellite by the fiducial station.

The detailed description of the ϕ_{sd2} algorithm is provided in Section 6.2.2.4.

(d) Double Differencing 1 (DD1)

$$\phi_{dd1}\left(t_{rx}^{imt}\right) = \phi_{atm}\left(t_{rx}^{imt}\right) - \phi_{res_sd2}\left(t_{rx}^{ref}\right) - \phi_{res_pv1}\left(t_{rx}^{ref}\right) + \phi_{res_sd1}\left(t_{rx}^{ref}\right), \tag{5.22}$$

where

ϕ_{dd1} = the phase residual after SD2 clock correction;

ϕ_{res_sd2} = the phase residual from the measurement of the occulting GPS satellite by the fiducial station number 1;

ϕ_{res_pv1} = the phase residual from the measurement of the pivot GPS satellite by the fiducial station number 1;

ϕ_{res_sd1} = the phase residual from the measurement of the pivot GPS satellite by GRAS.

The detailed description of the ϕ_{dd1} algorithm is provided in Section 6.2.2.5.

(e) Double Differencing 2 (DD2)

$$\phi_{dd2}\left(t_{rx}^{imt}\right) = \phi_{atm}\left(t_{rx}^{imt}\right) - \phi_{res_sd2}\left(t_{rx}^{ref}\right) - \phi_{res_pv2}\left(t_{rx}^{ref}\right) + \phi_{res_sd1}\left(t_{rx}^{ref}\right), \tag{5.23}$$

where

ϕ_{dd2} = the phase residual after SD2 clock correction;

ϕ_{res_sd2} = the phase residual from the measurement of the occulting GPS satellite by the fiducial station number 1;

ϕ_{res_pv2} = the phase residual from the measurement of the pivot GPS satellite by the fiducial station number 2;

ϕ_{res_sd1} = the phase residual from the measurement of the pivot GPS satellite by GRAS.

The detailed description of the ϕ_{dd2} algorithm is provided in Section 6.2.2.6.

5.3.3.5 Cycle slip correction and phase unwrapping

Next the cycle slip correction and phase unwrapping are performed. If a cycle slip occurs, generally the phase will jump away from the positive I, zero Q position (i.e. the tracking attractor) and then rapid return to it after a few samples. This occurs because momentarily the superposition of (multipath) signals at the receiver has a spectral characteristic which the loop is unable track. Thus cycle slips can be corrected by predicting the next phase from the previous K phases and at the same time unwrapping the phase. However to facilitate this process it is first useful to remove the expected phase variation from the signal to bring the signal as close to baseband as possible (thereby reducing the number of times the phase wraps around). Thus cycle slip correction and phase unwrapping are performed by applying the following algorithm. First the expected phase variation is removed from the signal and the phase values are converted to radians as

$$\rho_{bbw}(m) = \frac{2\pi f_{gps}}{c}\left[\phi_{cc}(m) - \phi_{law}(m)\right], \tag{5.24}$$

where

ϕ_{bbw} = the high frequency phase component after the expected phase delay has been removed;

ϕ_{cc} = the phase residual after clock correction (cc denotes any of the clock correction techniques ND, SD1, SD2, DD1, or DD2);

ϕ_{law} = the low frequency phase component based on a simple law of the phase residual.

Table 5.2: Default values for the parameters for phase unwrapping and cycle slip correction.

Parameter	Default value
K	10
T_{uw1}	π
T_{uw2}	π

The low frequency phase component ϕ_{law}represents the phase residual as a function of time during an occultation in the case that the measured atmosphere is smooth and ideal. Due to the unique shape of the phase residual, ϕ_{law} can not be expressed by a polynomial function. The approach used in this algorithm is to use a generic "law" that has been derived numerically with a ray-tracing simulation. This law shall be provided as a lookup table in the form $\phi_{law}(t_{offset})$, where t_{offset} is the time offset from the beginning of the measurement. The law must then be fitted to match the shape of the measured phase residual as a function of time by using a least-squares-fit. Finally, the law has to be interpolated to the measurement sampling times.

Then the phase is unwrapped (as necessary) by

1) Unwrap samples 2 to K:

If $|\rho_{bbw}(m) - \rho_{bbw}(m-1)| \geq T_{uw1}$

If $\rho(m) - \rho_{bbw}(m-1) < 0$

Then $\rho_{bbu}(m) = \rho_{bbw}(m) + 2\pi$

If $\rho_{bbw}(m) - \rho_{bbw}(m-1) > 0$

Then $\rho_{bbu}(m) = \rho_{bbw}(m) - 2\pi$

If $|\rho_{bbw}(m) - \rho_{bbw}(m-1)| < T_{uw1}$

Then $\rho_{bbu}(m) = \rho_{bbw}(m)$

2) Unwrap samples K+1 to N

$$\rho_{predicted}(m) = P_\phi \left[\begin{array}{l} \rho_{bbu}(m-1), \rho_{bbu}(m-2), \ldots, \rho_{bbu}(m-K); \\ t_{tx}^{ref}(m), t_{tx}^{ref}(m-1), t_{tx}^{ref}(m-2), \ldots, t_{tx}^{ref}(m-K) \end{array} \right]$$

If $|\rho_{bbw}(m) + 2\pi n - \rho_{predicted}(m)| \geq T_{uw2}$ for all n

Then $\rho_{bbu}(m) = \rho_{predicted}(m)$

If $|\rho_{bbw}(m) + 2\pi n - \rho_{predicted}(m)| < T_{uw2}$ for some n

Then $\rho_{bbu}(m) = \rho_{bbw}(m) + 2\pi n$

The default values for the parameters K, T_{uw1}, and T_{uw2} are provided in Table 5.2. $P_\phi$is a Nth order polynomial fitted in least squares sense to the phase data that is to be unwrapped.

Noise filtering is most effective, when it is applied to the baseband signal. Thus, the noise filtering with a low pass filter is performed before the expected phase variation is added back to the data.

The baseband phase data is low-pass filtered by

Table 5.3: The default parameters for noise filtering in GO algorithm.

Parameter	**Bandwidth range [Hz]**	**SLTH range [km]**	**Polynomial order**
B_{go}	4 - 4	80 - 25	0
	2 - 2	25 - -80	0
Parameter	**Window length range [samples]**	**SLTH range [km]**	**Polynomial order**
L_{go}	40	80 - -80	0

$$\rho_{bbu_lp}(t) = \left\langle \rho_{bbu}\left(t_{rx}^{ref}\right)\right\rangle_{B_{bw_go}\left(t_{rx}^{ref}\right)}, \tag{5.25}$$

where

ρ_{bbu} = the baseband phase residual after cycle slip correction;

ρ_{bbu_lp} = the low-pass filtered phase residual;

B_{bw_go} = the bandwidth of the phase residual filter in GO algorithm.

The filter bandwidth is determined by user definable polynomials $B_{go}\left(t_{rx}^{ref}\right)$ and $L_{go}\left(t_{rx}^{ref}\right)$ as described in the detailed description of the low-pass filter function and filter parameters in Section 6.3.6.1. The default parameters for the polynomials are defined in Table 5.3. The bandwith range column shows the bandwidth parameter B_{go} and window length L_{go} values corresponding to the SLTH values in the SLTH range column. The filtering function shall perform a polynomial fit to generate a polynomial function of the defined order (in the polynomial order column) so that the B_{go} and L_{go} values and the SLTH values match. The range columns can contain more than two values (e.g. bandwidth range 4 - 3 - 2, and corresponding SLTH range 80 - 45 - 20) for higher order polynomials. The order of the polynomials and the coefficients shall be completely user definable.

Finally the subtracted expected phase variation is added to the unwrapped phase and the phase residual is converted into distance in meters as

$$\phi_{uw}(m) = \frac{c}{2\pi f_{gps}}\rho_{bbu}(m) + \phi_{law}(m), \tag{5.26}$$

where

c = the speed of light in vacuum [m/s];

f_{gps} = the transmission frequency of the GPS channel [Hz];

ϕ_{uw} = the complete unwrapped phase residual [m].

The parameters K, T_{uw1}, T_{uw2}, and the function P_ϕ shall be user definable. The parameters T_{uw1}, T_{uw2} can be made adaptive on the basis of the local standard deviation of the phase estimated from the data.

For a setting occultation the phase unwrapping is performed as described above. For a rising occultation the phase unwrapping is performed from the end of the occultation backward in time (i.e. a re-parameterisation $j = N + 1 - m$ is required).

Because in the lower atmosphere the natural phase delay caused by the atmosphere may look like a cycle slip in the defined detection algorithm, the user shall be able to define a height limit for the cycle slip detection and correction algorithm. The detection and correction shall not be performed below the defined height limit. The default lowest height limit for cycle slip correction is SLTH = 0 m.

Thus finally the set of N regenerated, fully corrected phase samples for a given channel and a particular occultation are obtained. These determine the phase variation caused by the atmosphere and ionosphere up to an additive constant over the occultation.

$$\left\{ \left(\phi_{uw_ch}(m), \tau_{rx}^{imt}(m), t_{rx}^{ref}(m), t_{tx}^{ref}(m) \right) ;\ m : 1 \rightarrow N \right\} \tag{5.27}$$

5.3.3.6 Earth oblateness correction

Earth oblateness correction performs a coordinate transform from Earth centered coordinate frame to a new coordinate frame determined by a sphere tangential to the ellipsoid at the location of the measured profile. The radius of the new sphere is the radius of curvature of the Earth ellipsoid in the occultation plane. The Earth oblateness correction is performed to the position vectors of the GPS and Metop satellites so that

$$\vec{r}_i^{sci} = \vec{r}_i^{eci} + \Delta\vec{r}, \tag{5.28}$$

where i denotes any position vector in ECI frame, i.e., $i = gva,\ gava,\ gxa,\ tx,$ and leo.

The derivation of the translation vector $\Delta\vec{r}$ is defined in Section 6.2.2.7.

5.3.4 Geometrical optics retrieval

After the Earth oblateness correction function the level 1b data processing is split into two paths as shown in Figure 5.2. All measurement data is processed with the Geometrical Optics (GO) retrieval algorithm. This algorithm is defined in this section.

Occultation measurement data below a user selectable impact parameter height are also processed with Wave Optics (WO) retrieval algorithm to improve the probability that a good bending angle profile is retrieved even in the atmospheric conditions including atmospheric multipath propagation. The algorithm for WO retrieval is defined in Section 5.3.5.

5.3.4.1 Doppler calculation

Derivative of the filtered phase residual $D_{atm}(m)$ is computed from

$$D_{atm}(m) = \left.\frac{d\phi_{lp}}{dt}\right|_{t=t^{ref}_{rx-der}}, \tag{5.29}$$

where

t^{ref}_{rx-der} = time stamp of the Doppler residuals after derivation.

The detailed form of the Equation 5.29 and the calculation of t^{ref}_{rx-der} is presented in Section 6.2.3.1.

5.3.4.2 Total bending angle and impact parameter calculation

The total bending angle $\alpha_i\left(t^{ref}_{rx}\right)$ corresponding to the Doppler shift caused by the atmosphere is calculated by solving the root of the equation

$$P\left(\vec{v}^{eci}_{ant}, \vec{v}^{eci}_{tx}, \vec{r}^{eci}_{ant}, \vec{r}^{eci}_{tx}, D_{atm}, t^{ref}_{rx}, t^{ref}_{tx}\right) = 0, \tag{5.30}$$

where P is the Doppler equation of a radio occultation measurement. P is Equation 6.84 in Section 6.2.3.2. Section 6.2.3.2 also contains the detailed description of the root solving algorithm.

The length of the impact parameter $|\vec{a}_i\left(t^{ref}_{rx}\right)|$ is solved from the total bending angle by Equation 6.93 defined in Section 6.2.3.3.

5.3.4.3 Geolocation

The location of the bending angle profile is determined with the Geolocation function defined in Section 6.2.3.4. This function produces the geodetic latitude and longitude of the ground projection of the ray perigee for each measurement sample.

5.3.4.4 TEC derivation

The Total Electron Content (TEC) is calculated as defined in Section 6.2.3.5.

5.3.4.5 Ionosphere correction

The frequency independent total bending angle is calculated as

$$\alpha\left(t^{ref}_{rx}\right) = f\left(\alpha_{l1}\left(t^{ref}_{rx}\right), \alpha_{l2}\left(t^{ref}_{rx}\right), a_{l1}\left(t^{ref}_{rx}\right)\right). \tag{5.31}$$

The detailed algorithm for calculating the neutral bending angle is provided in Section 6.2.3.6.

5.3.4.6 Total bending angle bias estimation and correction

The retrieved neutral bending angle may contain detectable bias due to the clock drifts, POD errors, some other error source that was not compensated in the retrieval. Comparison of the bending angle against a reference bending angle based on climatological model can be used to detect and correct for a constant bias in the retrieved profile. The generic equation for the bending angle bias correction is

$$\alpha_{bc}(a_{l1}) = \alpha(a_1) + \Delta\alpha_{model}, \tag{5.32}$$

where

α_{bc} = the bias corrected bending angle;

a_{l1} = the impact parameter at L1;

α = the neutral bending angle with bias;

$\Delta\alpha_{model}$ = model based bending angle estimate.

In practice it is necessary to replace $\Delta\alpha_{model}$ with $\Delta\alpha_{mean}$, which is a mean bias estimate over some height window.

The detailed algorithm for the bending angle bias estimation and correction is provided in Section 6.2.3.7.

5.3.5 Wave optics retrieval

The Wave Optics (WO) retrieval is a bending angle retrieval technique that is used in parallel with the GO retrieval in the lower part of the atmosphere. The purpose of the WO retrieval is to solve a high quality bending angle profile in the atmospheric multipath conditions where the GO retrieval does not work correctly. Two WO retrieval algorithm option are included into the GRAS data processing: Back Propagation (BP) and Phase Transform (PT). The selection of the WO retrieval method shall be user definable.

WO retrieval shall be initialised at a user definable impact height.

The input data for the WO retrieval is basically the same as the input to the GO retrieval algorithm. The output from the WO retrieval is the bending angle as a function of the impact parameter.

The detailed descriptions of the WO retrieval functions are provided in Section 6.2.4.

5.3.6 Level 1b post-processing

The level 1b post processing function performs the final processing steps at level 1b.

5.3.6.1 Deriving smoothed level 1b products

This section has been removed.

5.3.6.2 Level 1b product quality check

The Level 1b product quality check function performs online monitoring of the retrieved level 1b products by comparing them against user definable threshold levels. The quality check function shall set the respective quality flags in the MDR-1B.

The parameters for level 1b quality checks are defined in Section 6.2.5.2.

5.3.6.3 Product error characteristics estimation

The error characterisation for the GRAS level 1b products is to be written.

5.3.6.4 Level 1b products formatting

The level 1b products shall be formatted as defined in **AD4**. There is no mathematical formulation for this functionality.

5.4 Raw sampling mode data processing

The algorithm for the raw sampling mode data processing shall be added at a later stage of the data processing system development. The raw sampling mode measurements are appended to the MDR-1B as defined in **AD4**. The header information is repeated for each sample. The IMT time stamps are synchronised with the UTC-GRAS time and the reference time in the same way as for the close loop mode measurements (Section 5.3.3.1). The L1_PHASE, L1_AMPLITUDE, and L1_CODE_PHASE fields are filled with products from the measurement reassembly function (Section 6.1.2).

6 REFERENCE FUNCTIONS

6.1 Level 1a processing functions

6.1.1 Level 1a quality check parameters

Input Parameters:

1. Complete measurement data sequences;
2. Tracking state data for the duration of the measurements;
3. Measurement packet type for each sub-packet used in the pre-structuring of the measurement data sequence.

Output Parameters:

1. Complete measurement data sequences with quality flags from the level 1a quality check;

The quality check at Level 1a checks the completeness of the measurement data sequences collected by the source packet de-multiplexing function. The quality checks to be performed are listed in 6.1. The respective quality flags are set in the level 1a products as defined in **AD4** based on the results of the quality checks.

The most important check is the completeness of the data sequence. The data produced by GRAS does not provide any direct means to check the completeness of a pre-structured measurement data sequence. Two indirect ways of checking the completeness of the data sequence are:

Measurement time stamps

The measurement time stamps should form a consistent time series. This is checked by using the measurement time stamps equation from **AD10** to calculate the first and the last time stamp of a measurement data package. The time difference between the last time stamp of a packet and the first time stamp of the next packet of the same data sequence should not be more than the threshold value defined in Table 6.1. Longer time difference means that a measurement data packet is missing.

Tracking_state

The measurement time stamp check does not reveal if the first or the last measurement data packet of the sequence is missing. This shall be checked by monitoring the instrument tracking state during a measurement. The instrument tracking state for the observed GPS satellite should go through a cycle of steps from C/A code acquisition (tracking state 1) to the highest tracking state and back to 0. Incomplete tracking state cycle indicates that the measurement data quality is degraded. If any of the tracing states 1 - 3 are missing, it is possible that the first measurement data packet is missing. Missing last measurement data packet is indicated by missing tracking state 0 at the end of the occultation. If none of the measurement data packets contains tracking state 15, the quality of the measurement is degraded because tracking of the L2 signal has not been possible. If tracking state 15 has not been reached during a measurement, L2_NOT_TRACKED flag is set in the corresponding MDRs.

Second check related to the tracking state is the existence of raw sampling mode data packets. Each measurement data sequence should contain one or more raw sampling mode data packet (even an empty one). If no raw sampling mode packets are identified before GRAS has lost C/A code lock, the RS_DATA_MISSING error flag is set, an event of user configurable severity to the CGS via the PGE interface is raised, and the measurement id number and error characterization information is added in the report of the dump processing.

Table 6.1: Level 1a quality checks.

Data	Quality check	Threshold value
GPS satellite PRN number	The number must not change during one occultation measurement.	Not applicable
Measurement chain identification	The identification must not change during a measurement.	Not applicable
Measurement packet time tags	The time tags must form a consistent time series without gaps.	$\frac{1}{s_{rate}}$, where s_{rate} is the sampling rate of the measurement samples
Tracking state	The tracking state must go through the steps of a normal occultation measurement from 1 to 15 and back to 0 [**RD4**].	Not applicable
Completeness of the input data	Availability of all input data packets for each occultation is checked with the GPS satellite PRN number.	Not applicable
Existence of Raw Sampling mode data packet(s)	Each occultation measurement should include one or more Raw Sampling mode data packets.	Not applicable
Automatic gain control activity check	The check is defined in **AD11**.	

If the measurement is detected to be incomplete, the MEASUREMENT_INCOMPLETE flag is set in the corresponding MDRs.

6.1.2 Measurement reassembly products

Input Parameters:

1. Complete measurement sequences of GRAS measurement, and ancillary data
2. USO frequency correction $\Delta f_{uso}(m)$ for each measurement data sample (only if USO frequency correction is selected)

Output Parameters:

1. For occultation measurement sample m
   - IMT time stamp $\tau_{rx}^{imt}(m)$;
   - L1-CA carrier phase $\rho_{ca}(m)$;
   - L1-P1 carrier phase $\rho_{p1}(m)$;
   - L2-P2 carrier phase $\rho_{p2}(m)$;
   - L1-CA amplitude $E_{reg_ca}(m)$;

- L1-P1 amplitude $E_{reg_p1}(m)$;
- L2-P2 amplitude $E_{reg_p2}(m)$;
- L1-CA code phase $CP_{ca}(m)$;
- L1-P1 code phase $CP_{p1}(m)$;
- L2-P2 code phase $CP_{p2}(m)$;

2. For navigation measurement sample k

   - IMT time stamp $\tau_{rx}^{imt}(k)$;
   - OBT time stamp $t_{rx}^{obt}(k)$;
   - UTC_{GRAS} time stamp $t_{rx}^{utc_gras}(k)$;
   - L1-CA carrier phase $\rho_{ca}(k)$;
   - L1-P1 carrier phase $\rho_{p1}(k)$;
   - L2-P2 carrier phase $\rho_{p2}(k)$;
   - L1-CA amplitude $E_{reg_ca}(k)$;
   - L1-P1 amplitude $E_{reg_p1}(k)$;
   - L2-P2 amplitude $E_{reg_p2}(k)$;
   - L1-CA code phase $CP_{ca1}(k)$;
   - L1-P1 code phase $CP_{p1}(k)$;
   - L2-P2 code phase $CP_{p2}(k)$;

3. Receiver noise estimate

   - L1 $N_0^{l1}(\tau^{imt})$;
   - L2 $N_0^{l2}(\tau^{imt})$;

4. Gain setting and histogram

   - $HIST(\tau^{imt})$;
   - $g_{ana}(\tau^{imt})$;
   - $DIG(\tau^{imt})$;

5. Tracking state

   - $TS(\tau^{imt})$;

6. Onboard navigation solution

   - $NSM(\tau^{imt})$;
   - $POS_X(\tau^{imt})$;

- $POS_Y\,(\tau^{imt})$;
- $POS_Z\,(\tau^{imt})$;
- $VEL_X\,(\tau^{imt})$;
- $VEL_Y\,(\tau^{imt})$;
- $VEL_Z\,(\tau^{imt})$;

7. Navigation data frame
   - $NDF_BITS\,(\tau^{imt})$;
8. GPS Ephemeris data
   - Data format and contents specified in **AD10**.

The output of the measurement reassembly function depends on whether the input measurement sequence is occultation or navigation measurements. Occultation measurements shall produce a set of measurement data with m samples and with $\tau_{rx}^{imt}(m)$ as the only time stamp of the data samples. The output of the navigation measurement sequence is k data samples. The time stamps in the Extended Navigation Data packet can be used to synchronise the navigation measurement samples with the UTC_{GRAS} time t^{utc_gras} and OBT time t^{obt}. Detailed descriptions of UTC_{GRAS} and OBT times are provided in **AD10** and **AD11**.

In the case that the USO frequency correction is selected, the temperature corrected USO frequency must be used in the measurement reassembly. In this case the corrected USO frequency for the measurement sample m is

$$f_{uso_ic}(m) = f_{uso} + \Delta f_{uso}(m), \tag{6.1}$$

where

f_{uso} = the nominal USO frequency;

Δf_{uso} = the USO frequency correction interpolated from the instrument characterisation database as defined in Section 6.1.5.5.

The Issue 4 of **AD11** does not include an algorithm for removing the navigation message from the carrier phase measurements. A provisional algorithm for removing the navigation message from the carrier phase measurements is provided here to supplement **AD11**:

For the C/A and P2 codes, all samples with a negative I-component are rotated π radians before determining the angle. For the P1 code, all samples with negative Q-component are rotated π radians before determining the angle. Mathematically this can be described as

$$\begin{aligned} I_{C/A} &= \left|I_{samp,C/A}\right| \text{ and } Q_{C/A} = sign\left(I_{samp,C/A}\right) \cdot Q_{samp,C/A} \\ I_{P2} &= \left|I_{samp,P2}\right| \text{ and } Q_{P2} = sign\left(I_{samp,P2}\right) \cdot Q_{samp,P2} \\ Q_{P1} &= \left|Q_{samp,P1}\right| \text{ and } I_{P1} = sign\left(Q_{samp,P1}\right) \cdot I_{samp,P1}, \end{aligned} \tag{6.2}$$

where I_{samp} and Q_{samp} are the sampled I and Q values. $I_{C/A,P1,P2}$ and $Q_{C/A,P1,P2}$ are the values used for residual phase evaluation.

6.1.3 Approximation of the measurement time

Input Parameters:

1. For each Extended Navigation Data Packet k
   - Time of the navigation solution in IMT time frame $\tau_{rx}^{imt}(k)$;
   - Time of the navigation solution in UTC_{GRAS} time frame $t_{rx}^{utc_gras}(k)$;
2. For each occultation measurement sample m
   - Time of the measurement sample $\tau_{rx}^{imt}(m)$.

Output Parameters:

1. For each occultation measurement sample m
   - Approximated time of the measurement sample in UTC_{GRAS} time frame $t_{rx}^{apr}(m)$.

The position vectors in the Extended Navigation Data Packet (ENDP) in the GRAS Ancillary data contains position and velocity vectors of the GRAS based on the onboard navigation solution. The navigation solution is produced for each navigation measurement with the GZA antenna. So, the ENDPs provide labeling of the onboard navigation solutions and GZA measurement reception times as

$$\left\{ \left(\vec{r}_{leo}^{wgs84}(k), \vec{v}_{leo}^{wgs84}(k), \tau_{rx}^{imt}(k), t_{rx}^{utc_gras}(k), t_{rx}^{obt}(k) \right) ;\ k : 1 \rightarrow K \right\} . \tag{6.3}$$

This provides a way to synchronize the IMT time stamps and the UTC_{GRAS} time with limited accuracy. The limited accuracy is caused by the instability of the $t_{rx}^{utc_gras}$ time from the onboard navigation solution. However, the orbital position error along the orbit arc caused by a timing error due to the $t_{rx}^{utc_gras}$ instability is less than 1 cm, so its impact on the incidence angle estimate is negligible.

The ENDPs are generated at the rate of 1 Hz. So, the time stamps for each occultation measurement have to be derived using interpolation. Because $t^{utc_gras}(k)$ and $\tau^{imt}(k)$ for the ENDP k are automatically synchronized, a reception time $t_{rx}^{apr}(m)$ can be estimated for each occultation measurement m by linear interpolation

$$t_{rx}^{apr}(m) = t^{utc_gras}(k) + \frac{t^{utc_gras}(k+1) - t^{utc_gras}(k)}{\tau^{imt}(k+1) - \tau^{imt}(k)} \left[\tau_{rx}^{imt}(m) - \tau^{imt}(k) \right] , \tag{6.4}$$

where

m = index of the occultation measurement sample $(\tau^{imt}(k) \leq \tau_{rx}^{imt}(m) \leq \tau^{imt}(k+1))$;

k = index of the ENDP;

$t_{rx}^{apr}(m)$ = time stamp of the occultation measurement m in UTC_{GRAS} time;

$t^{utc_gras}(k)$ = time stamp of the ENDP k in UTC_{GRAS} time;

$\tau^{imt}(k)$ = time stamp of the ENDP k in IMT time;

$\tau_{rx}^{imt}(m)$ = time stamp of the occultation measurement m in IMT time.

Because navigation measurements are automatically synchronized with the navigation solutions, $t^{utc_gras}(k)$ time stamps can directly be used for instrument corrections for navigation measurements.

For instrument correction calculations the $t^{utc_gras}(k)$ and $t_{rx}^{apr}(m)$ time stamps are converted to MJD format with the algorithm described in Section 6.3.2.1.

6.1.4 Measurement identification determination

Input Parameters:

1. For occultation measurement sample m
   - IMT time stamp $\tau_{rx}^{imt}(m)$;
   - GPS satellite PRN number $SAT(m)$;
2. For navigation measurement sample k
   - IMT time stamp $\tau_{rx}^{imt}(k)$;
   - UTC_{GRAS} time stamp $t_{rx}^{utc_gras}(k)$;
   - GPS satellite PRN number $SAT(m)$;
3. Occultation table covering the time period of the measurement time;
4. GSN quality information of the GPS satellites and fiducial stations.

Output Parameters:

1. For each occultation measurement
   - Measurement identification occ_{id}
   - Predicted occultation measurement start time $t_{start_pred}^{mjd}$;
   - Predicted occultation measurement end time $t_{end_pred}^{mjd}$;
   - Predicted occultation geolocation λ_{g_pred}, φ_{g_pred}, h_{slta_pred};
   - The approximated UTC_{GRAS} time of the occultation measurement sample m as $t_{rx}^{apr}(m)$;
2. For each navigation measurement

- Measurement identification nav_{id};
- Predicted navigation measurement start time $t^{mjd}_{start_pred}$;
- Predicted navigation measurement end time $t^{mjd}_{end_pred}$;

Algorithm

Because the geometry of the observation does not allow the same GPS satellite to occult twice during a short period of time, the satellite PRN number is normally a reliable identification of a measurement. The start time and the end time of the occultation are only roughly estimated in the occultation and they can only be used to support the identification.

The rules in the measurement identification are:

1. Search the occultation table for the PRN number of the measured GPS satellite;
2. Calculate the time differences between the predicted start and and the actual start time of the measurement and predicted end and actual end time of the measurement. If the actual times and the predicted times do not differ more than a user definable threshold (defaults defined in Table 6.2), the test is successful.
3. If step 2 is OK, then assign an identification number to the measurement;
4. If step 2 is not OK, continue search and repeat the start and end time test each time when the correct GPS PRN number is found.
5. If the actual measurement does not match any of the predicted measurements, the possible reasons for this are:
   - This measurement has been predicted, but either the approximated start and end time or the time stamps in the measurement data contain significant errors. This shall cause an error message to be produced as defined in the step number 6;
   - This measurement has not been predicted, i.e., the occultation table generation algorithm is not correct. This shall cause an error message to be produced as defined in the step number 6.
6. If the measurement identification against the occultation table fails, the ID_FAILED flag in the MDR-1A-OCCULTATION DATA or in the MDR-1A-NAVIGATION DATA is set, an event of user configurable severity to the CGS via the PGE interface is raised, and the measurement id number and self explanatory error characterization information is added in the report of the dump processing. If the identification failed for an occultation measurement, the ID_FAILED flag shall also be set for the corresponding MDR-1B record. An identification shall be generated to the non-predicted measurement and the measurement data shall be processed as normally as possible.

The measurement identification number for GRAS observations is:

MMM_GGG_YYYY_DDD_NNNN

where

Table 6.2: Measurement identification parameters and default threshold values.

Parameter	Threshold value
Δt_{start}	$\leq$30 s
Δt_{end}	$\leq$30 s
GPS PRN	Not applicable

MMM = the measurement type, i.e., OCC or NAV;

GGG = the receiver identification number;

YYYY = the year of the measurement;

DDD = the day of the year;

NNNN = the sequential number of the measurement of that type of the day.

The measurement identification number format shall be user definable so that the user can select in which order the fields identified above shall appear in the identification.

Non-predicted occultations will be numbered with XXXX.

6.1.5 Derivation of instrument corrections

This section contains mathematical description of the functions that are used to correct the measurement data for errors caused by the transmitter and receiver hardware.

6.1.5.1 Incidence angle derivation

Input Parameters:

1. GPS CoM position vector $\vec{r}_{gps}^{eci}(t^{ref})$ in ECI frame
2. GPS CoM velocity vector $\vec{v}_{gps}^{eci}(t^{ref})$ in ECI frame
3. Metop position vector in WGS84 coordinate frame $\vec{r}_{leo}^{wgs84}(k)$, $\tau_{rx}^{imt}(k)$, $t_{rx}^{utc_gras}(k)$
4. Metop velocity vector in WGS84 coordinate frame $\vec{v}_{leo}^{wgs84}(k)$, $\tau_{rx}^{imt}(k)$, $t_{rx}^{utc_gras}(k)$
5. Time stamps of the carrier phase and code phase measurements for GVA, GAVA $\tau_{rx}^{imt}(m)$
6. Time stamps of the carrier and code phase measurements for GZA $\tau_{rx}^{imt}(k)$
7. Antenna reference point position vectors $\vec{p}_{ant}^{srf}$ in Satellite Reference (SR) frame for GVA, GAVA, and GZA
8. Metop Center of Mass (CoM) $\vec{r}_{com}^{srf}$ in SR frame
9. GPS antenna phase center characterization from the GSN Status and Configuration Database

Output Parameters:

1. Incidence angles $\theta_{ant}^{eci}(m)$ and $\varphi_{ant}^{eci}(m)$ for GVA and GAVA
2. Time stamps of the occultation measurements $t_{rx}^{utc_gras}(m)$ in UTC_{GRAS} time frame
3. Incidence angles $\theta_{gza}^{eci}(k)$ and $\varphi_{gza}^{eci}(k)$ for GZA
4. Time stamps of the navigation measurements $t_{rx}^{utc_gras}(k)$ in UTC_{GRAS} time frame

Algorithm

This function derives the incidence angle of the incoming signal of the occulting GPS satellite. The incidence angle is used to derive the instrument correction parameters for carrier phase and amplitude correction.

The incidence angle of the incoming ray is estimated through the following steps:

1) Interpolation of the Metop orbit

The Metop position and velocity vector $\vec{r}_{leo}^{wgs84}(k)$ and $\vec{v}_{leo}^{wgs84}(k)$ in ENDP are in the WGS84(G873) coordinate frame. Because the difference between ITRF97 coordinate frame and WGS84(G873) coordinate frame is worldwide less than 10 cm, these two frames can be considered to be the same for the purpose of the incidence angle estimation. However, a user definable option is to apply the WGS84 to ITRF coordinate transform specified in Section 6.3.3.2 to all input coordinates as a part of the instrument correction algorithm. So, the starting status of the Metop state vectors in ECEF coordinate frame before interpolation is labeling as

$$\left\{ \left(\vec{r}_{leo}^{itrf97}(k), \vec{v}_{leo}^{itrf97}(k), \tau_{rx}^{imt}(k), t_{rx}^{utc_gras}(k) \right) ;\ k : 1 \rightarrow K \right\} . \tag{6.5}$$

The transformation of the Metop position and velocity vectors from the ITRF frame to the Mean-of-Date J2000.0 ECI frame is performed using the transform defined in Section 6.3.3.4. This produces extended labeling as

$$\left\{ \left(\vec{r}_{leo}^{eci}(k), \vec{v}_{leo}^{eci}(k), \vec{r}_{leo}^{itrf97}(k), \vec{v}_{leo}^{itrf97}(k), \tau_{rx}^{imt}(k), t_{rx}^{utc_gras}(k) \right) ;\ k : 1 \rightarrow K \right\} . \tag{6.6}$$

The Metop position and velocity vectors in the ECI coordinate frame are interpolated to the $t_{rx}^{apr}(m)$ times of the occultation samples using linear interpolation (Equation 6.166) for each position and velocity vector component. The produced set of Metop state vectors is labeled as

$$\left\{ \left(\vec{r}_{leo}^{eci}(m), \vec{v}_{leo}^{eci}(m), t_{rx}^{apr}(m) \right) ;\ m : 1 \rightarrow N \right\} . \tag{6.7}$$

The interpolated position and velocity vectors $\vec{r}_{leo}^{eci}$ and $\vec{v}_{leo}^{eci}$ are copied into the POS_METOP_OBN and VEL_METOP_OBN fields in the MDR-1A-OCCULTATION DATA or MDR-1A-NAVIGATION DATA, depending on the measurement type.

2) Interpolation of the GPS orbit

The position vectors of the GPS satellites $\vec{r}_{gps}(t^{ref})$ are provided by the GRAS GSN in Mean-of-Date J2000.0 ECI coordinate frame. All time stamps of the GSN POD products are in Modified Julian Date (MJD).

The state vectors or the GPS satellites are needed at the time of the transmission. For the incidence angle estimation it is sufficient to approximate the traveling time of the signal by using constant time delays of $\Delta t_{t_occ} = 0.1\,s$ for occulting GPS satellites and $\Delta t_{t_nav} = 0.08\,s$ for navigation. The first order approximations of the GPS transmission times are then estimated for occultation measurements as

$$t_{tx}^{apr} = t_{rx}^{apr} - \Delta t_{t_occ}, \tag{6.8}$$

and for navigation measurements as

$$t_{tx}^{utc_gras} = t_{rx}^{utc_gras} - \Delta t_{t_nav}. \tag{6.9}$$

The interpolation of the GPS position vectors is performed using the Lagrange interpolation algorithm described in 6.3.1.1 for occultation and navigation measurement times to expand the labeled data sets as

$$\left\{ \left(\vec{r}_{gps}^{eci}(m), \vec{r}_{leo}^{eci}(m), \vec{v}_{leo}^{eci}(m), t_{tx}^{apr}(m), t_{rx}^{apr}(m) \right) ;\ m : 1 \rightarrow N \right\}, \tag{6.10}$$

and

$$\left\{ \left(\vec{r}_{gps}^{eci}(k), \vec{r}_{leo}^{eci}(k), \vec{v}_{leo}^{eci}(k), \vec{r}_{leo}^{itrf97}(k), \vec{v}_{leo}^{itrf97}(k), \tau_{rx}^{imt}(k), t_{tx}^{apr}(k), t_{rx}^{utc_gras}(k) \right) ;\ k : 1 \rightarrow K \right\}. \tag{6.11}$$

3) Incidence angle estimation

A unit vector $\hat{r}_{ray}^{eci}$ pointing to the direction of the incoming GPS signal is calculated geometrically using the position of the GRAS antenna reference point and the transmitting GPS antenna phase center. The calculation is performed in the ECI coordinate frame.

After the steps 1-3 described above the GPS and Metop position vectors and Metop velocity vectors are already in the ECI coordinate frame and the sampling times are synchronized with the measurement sampling times taking into account the signal time of travel.

The antenna reference point $\vec{r}_{ant}^{arf}$ is at the origin of the the local Antenna Reference (AR) frame defined by the unit vectors $\hat{x}_{ant}$, $\hat{y}_{ant}$, and $\hat{z}_{ant}$, i.e.,

$$\vec{r}_{ant}^{arf} = 0 \cdot \hat{x}_{ant} + 0 \cdot \hat{y}_{ant} + 0 \cdot \hat{z}_{ant}. \tag{6.12}$$

The position vector $\hat{r}_{ant}^{arf}$ shall be transformed into the ECI frame by using the algorithm defined in Section 6.3.3.1 to get the position vector $\vec{r}_{ant}^{eci}$ in ECI frame. Subscript ant is used is used here to denote the antenna that the incidence angle is derived for, i.e., GVA, GAVA, or GZA.

The GRAS GSN provides via the GSN Status and Configuration Database a correction for the location of the GPS transmitting antenna phase center in respect to the GPS CoM. A generic format for the GPS antenna phase center taking into account the correction is

$$\vec{r}_{tx}^{eci} = \vec{r}_{gps}^{eci} + \mathbf{M_{gps}}\vec{p}_{tx}^{grf}, \tag{6.13}$$

where

$\vec{r}_{tx}$ = position vector of the GPS transmission antenna phase center in ECI frame;

$\vec{r}_{gps}$ = position vector of the GPS CoM;

$\mathbf{M_{gps}}$ = rotation matrix for the GPS satellite reference frame to ECI frame;

$\vec{p}_{tx}$ = position vector of the antenna phase center in the local GPS satellite reference frame.

$\vec{r}_{gps}$ has been used here as a generic notation for the observed GPS satellite. In the case of GVA and GAVA it stands for the occulting GPS satellites and for GZA it stands for the GPS satellites observed for navigation. The calculation of the $\mathbf{M_{gps}}$ matrix is defined in Equation 5.12 in Section 5.3.3.2. Vector $\vec{p}_{tx}^{grf}$ is provided in the GSN Status and Configuration Database.

When all vectors are in the same ECI coordinate frame, the unit vector pointing from the antenna reference point to the direction of the incoming ray can be derived as

$$\hat{r}_{ray}^{eci} = \frac{\vec{r}_{tx-}^{eci}\,\vec{r}_{ant}^{eci}}{\left|\vec{r}_{tx-}^{eci}\,\vec{r}_{ant}^{eci}\right|}. \tag{6.14}$$

All antenna coordinate frames are oriented in the same way so that the $\hat{x}_{ant}$, $\hat{y}_{ant}$, and $\hat{z}_{ant}$ point approximately to the directions of the $\hat{x}_s$, $\hat{y}_s$, and $\hat{z}_s$ (difference is caused by the antenna misalignment). This means that the definition of the angles characterizing the antenna gain pattern in the Instrument Database is the same for all antenna independent of the direction that the antenna radiating surface plane is pointing.

The angle θ_{ant}^{eci} used in the antenna gain pattern characterization in the Instrument Database is be derived from

$$\theta_{ant}^{eci} = \arccos \frac{\hat{r}_{ray}^{eci} \cdot \hat{z}_{ant}^{eci}}{\left|\hat{r}_{ray}^{eci}\right| \left|\hat{z}_{ant}^{eci}\right|}, \tag{6.15}$$

where

θ_{ant}^{eci} = the zenith angle (angle between the antenna normal and the direction of the incoming ray) of the ray;

$\hat{z}_{ant}^{eci}$ = a unit vector normal to the antenna radiating surface plane at the antenna reference point.

The unit vector $\hat{z}_{ant}^{eci}$ is derived by transforming the unit vector $\hat{z}_{ant}^{arf}$ in the local antenna coordinate frame into ECI frame using the algorithm defined in Section 6.3.3.1.

The azimuth angle φ_{ant} used in the gain pattern characterization can be derived from

$$\varphi_{ant}^{eci} = \arctan 2\left(\hat{r}_{ray}^{eci} \cdot \hat{y}_{ant}^{eci}, \hat{r}_{ray}^{eci} \cdot \hat{x}_{ant}^{eci}\right), \tag{6.16}$$

where

$\hat{y}_{ant}^{eci}$ = the unit vector $\hat{y}_{ant}^{srf}$ in the local antenna coordinate frame transformed into ECI frame;

$\hat{x}_{ant}^{eci}$ = the unit vector $\hat{x}_{ant}^{arf}$ in the local antenna coordinate frame transformed into ECI frame.

6.1.5.2 Carrier phase correction

Input Parameters:

1. Incidence angle for GVA, GAVA, or GZA
   - zenith angle $\theta_{ant}^{eci}(m)$, $t_{rx}^{time}(m)$ [deg];
   - azimuth angle $\varphi_{ant}^{eci}(m)$, $t_{rx}^{time}(m)$ [deg];
2. RFCU temperature for the receiving chain $T_{rfcu_chn}(t^{obt})$ [°C];
3. GEU temperature $T_{geu}(t^{obt})$ [°C];
4. GEU analog gain setting $g_{ana}(\tau^{imt})$.
5. Reception times of the carrier phase samples $t_{rx}^{time}(m)$

Output Parameters:

1. Antenna phase correction for measurement samples
   - L1-CA $\Lambda_{ant_ca}(m)$ [rad];
   - L1-P1 $\Lambda_{ant_p1}(m)$ [rad];
   - L2-P2 $\Lambda_{ant_p2}(m)$ [rad].
2. RFCU phase correction for measurement samples
   - L1-CA $\Xi_{rfcu_ca}(m)$ [rad];

- L1-P1 $\Xi_{rfcu_p1}(m)$ [rad];
- L2-P2 $\Xi_{rfcu_p2}(m)$ [rad].

3. GEU phase correction for measurement samples

   - L1-CA $\Gamma_{geu_ca}(m)$ [rad];
   - L1-P1 $\Gamma_{geu_p1}(m)$ [rad];
   - L2-P2 $\Gamma_{geu_p2}(m)$ [rad].

4. Total phase correction for measurement samples

   - L1-CA $\Delta\rho_{ca}(m)$ [rad];
   - L1-P1 $\Delta\rho_{p1}(m)$ [rad];
   - L2-P2 $\Delta\rho_{p2}(m)$ [rad].

Algorithm

The total carrier phase correction due to the receiver hardware is the sum of three terms as

$$\begin{aligned}\Delta\rho_{cd}(t_{rx}) &= \Lambda\left(\theta_{ant}\left(t_{rx}^{time}\right), \varphi\left(t_{rx}^{time}\right), CHN, CH\right) \\ &\quad +\Xi\left(T_{rfcu}\left(t_{rx}^{time}\right), CHN, CH\right) \\ &\quad +\Gamma\left(T_{geu}\left(t_{rx}^{time}\right), g_{ana}\left(t_{rx}^{time}\right), CHN, CH\right),\end{aligned} \tag{6.17}$$

where

$\Delta\rho_{cd}$ = the total instrument correction to the measured phase for code cd (=C/A, P1, or P2) [rad];

Λ = the impact of the antenna phase center on the measured carrier phase [rad];

Ξ = the impact of the RFCU phase delay on the measured carrier phase [rad];

Γ = the impact of the GEU phase delay on the measured carrier phase [rad];

t_{rx}^{time} = the reception time of the carrier phase sample. For occultation measurements t_{rx}^{time} is t_{rx}^{apr} and for navigation measurements t_{rx}^{time} is $t_{rx}^{utc_gras}$ [s];

CH = the channel and the code of the received transmission (L1-C/A, L1-P1, L2-P2).

Estimation of antenna impact

The impact of the receiving antenna on the measured phase has been mapped into the Instrument Characterisation database for each antenna as a function of the azimuth and zenith angles φ_{ant}^{eci} and θ_{ant}^{eci} of the incoming ray. The database contains phase correction terms both for RHCP and LHCP signals. For GRAS instrument correction LHCP is ignored because the direct GPS transmission is always RHCP.

The quadratic phase correction term is interpolated from the values in the database using the bi-cubic interpolation algorithm defined in Section 6.3.1.3. This provides a data set that can be labeled for the measurements as

$$\left\{ \left(\varphi_{ant}^{eci}(m), \theta_{ant}^{eci}(m), \Delta\rho_{ant_I_ch}^{rhcp}(m), \Delta\rho_{ant_Q_ch}^{rhcp}(m), t_{rx}^{time}(m) \right) ;\ m : 1 \rightarrow N \right\} . \tag{6.18}$$

where ch denotes codes L1-C/A, L1-P1, and L2-P2.

The carrier phase correction in for the measured phase sample m is derived then from the I and Q components of the correction term as

$$\Lambda_{ant_ch}(m) = \arctan \frac{\Delta\rho_{ant_ch_Q}^{rhcp}(m)}{\Delta\rho_{ant_ch_I}^{rhcp}(m)} . \tag{6.19}$$

Estimation of RFCU impact

The impact of the RFCU on the measured phase is characterised in the Instrument Database as a function of the RFCU temperature. Each RFCU has its own characterisation file. The correct characterisations file for the L1-C/A, L1-P1, and L2-P2 phase measurements for the RFCU that was part of the measurement chain shall be identified using the GRAS chain identification CHN in the measurement data packet.

The RFCU temperature data in the temperature data packet is time stamped with OBT_{32} time. The time stamps of the temperature data have to be interpolated to $t_{rx}^{time}(m)$ times of the observations using time synchronization in the ENDPs and Equation 6.4. This provides a data set labeled as

$$\left\{ \left(T_{rfcu}(m), t_{rx}^{time}(m), CHN, CH \right) ;\ m : 1 \rightarrow N \right\} . \tag{6.20}$$

The subscript $rfcu$ denotes the identification of the RFCU unit for the measurement chain.

The generic format of the data records in the instrument characterisation database is presented in Table 6.3. The RFCU phase delay correction shall be derived using linear interpolation for each measurement sample to generate data set

$$\left\{ \left(\Xi_{rfcu_ch}(m), T_{rfcu}(m), t_{rx}^{time}(m), CHN, CH \right) ;\ m : 1 \rightarrow N \right\} , \tag{6.21}$$

Ξ_{rfcu_ch} = the RFCU phase correction for the code ch (= L1-C/A, L1-P1, and L2-P2) [rad].

Table 6.3: Generic format of the characterization data records in instrument characterisation database.

Data record	
x_1	y_1
x_2	y_2
...	...
x_N	y_N

Estimation of GEU impact

The carrier phase correction for the impact of the GEU is derived in a very similar way as the impact of the RFCU. The only difference is that the phase delay caused by the GEU depends also on the GEU analog gain setting. On the other hand, there is only one GEU unit onboard each Metop satellite. So, the identification of the correct GEU is directly based on the Metop satellite identification. The correct GEU characterisation file is then found by using the measurement chain (velocity, anti-velocity, or zenith), and analog gain setting from the Gain Setting Packet. This provides a data set for occultation measurements labeled as

$$\left\{ \left(g_{ana}(m), t_{rx}^{time}(m), CH, Metop_{id} \right) ;\ m : 1 \rightarrow N \right\} . \tag{6.22}$$

The GEU phase delay correction is derived using linear interpolation for each measurement sample to generate data sets for occultation measurement samples as

$$\left\{ \left(\Gamma_{geu_ch}(m), g_{ana}(m), t_{rx}^{time}(m), CH, Metop_{id} \right) ;\ m : 1 \rightarrow N \right\} , \tag{6.23}$$

where

Γ_{geu_ch} = the GEU phase correction for the code ch (= L1-C/A, L1-P1, and L2-P2) [rad].

6.1.5.3 Code phase correction

Input Parameters:

1. Code phase measurements
   - L1-CA code phase $CP_{ca}\left(\tau_{rx}^{imt}\right)$ [chips];
   - L1-P1 code phase $CP_{p1}\left(\tau_{rx}^{imt}\right)$ [chips];
   - L2-P2 code phase $CP_{p2}\left(\tau_{rx}^{imt}\right)$ [chips];
2. RFCU temperature $T_{rfcu_ch}\left(t^{obt}\right)$ [°C];
3. GEU temperature $T_{geu}\left(t^{obt}\right)$ [°C];

4. GEU analog gain setting $g_{ana}\left(\tau^{imt}\right)$;
5. Receiving antenna chain identification information CH;
6. LO power feeding the RFCU during the measurement;
7. GPS Differential Code Bias (DCB) correction term for the measured GPS satellite Δt_{dcb}.

Output Parameters:

1. RFCU code phase correction
   - L1-CA Δcp_{rfcu_ca} [chips];
   - L1-P1 Δcp_{rfcu_p1} [chips];
   - L2-P2 Δcp_{rfcu_p2} [chips];
2. GEU code phase correction
   - L1-CA Δcp_{geu_ca} [chips];
   - L1-P1 Δcp_{geu_p1} [chips];
   - L2-P2 Δcp_{geu_p2} [chips];
3. GPS differential code bias Δt_{dcb};
4. Instrument corrected code phases
   - L1-CA CP_{ic_ca} [chips];
   - L1-P1 CP_{ic_p1} [chips];
   - L2-P2 CP_{ic_p2} [chips].

Algorithm

The code phases for the C/A, P1, and P2 codes are derived as part of the measurement reassembly (see Section 6.1.2). The produced data set is labeled as

$$\left\{\left(CP_{ca}(m), CP_{p1}(m), CP_{p2}(m), \tau_{rx}^{imt}(m), CHN\right);\ m:1\rightarrow N\right\}, \tag{6.24}$$

where CHN (Channel Identification in **AD10**) tells which antenna chain was performing the code phase measurement.

The code phase correction data are stored in files in the GRAS Characterisation Database. The file naming convention for the database files is described in **RD7**. The naming convention shows that the RFCU characterisation files are identified based on the RFCU serial number, GPS code, and LO power feeding the RFCU during the measurements. The GEU characterisation files are identified based on the GEU chain, GPS code, and the analogue IF-attenuation value. The GRAS

data processing system must be able to provide all necessary information for correctly identifying the RFCU and GEU units using the SPACECRAFT_ID in the product MPHR. This can be accomplished e.g. by including in the system a user configurable lookup table that contains the serial numbers of each RFCU and GEU for each GRAS instrument onboard each Metop spacecraft.

After the RFCU serial number has been correctly identified, the remaining selection criteria for the RFCU characterisation files are the GPS code, and LO power feeding the RFCU during the measurements. Because the correction is applied for all measured code phases, the GPS code shall have values C/A, P1, and P2. The default value for the LO power is 14 dBm[2].

The identification of the GEU code phase correction data files are based on the GEU chain, GPS code, and the analogue IF-attenuation value. The GEU chain is directly identified from the CHN value: 0 - 7 = Zenith, 8 - 9 = Velocity, and 10 - 11 = Anti-Velocity. The GPS code shall have values C/A, P1, and P2. The analogue IF-attenuation is the absolute value of the analog gain setting that was valid during the measurement. Because it is possible that the analog gain setting has been changed by the Automatic Gain Control (AGC) during a measurement, the code phase correction function shall be able to select and apply different GEU code phase correction data files at different samples in the measurement depending on what analog gain setting value is valid for the particular sample.

The RFCU and GEU temperature data in the temperature data packet are time stamped with OBT_{32} time so that the temperature data set can be expressed as

$$\left\{ \left(T_{rfcu_gava}(n), T_{rfcu_gva}(n), T_{rfcu_gza}(n), T_{geu}(n), t^{obt}(n) \right) ;\ n : 1 \rightarrow M \right\} . \tag{6.25}$$

The t^{obt}time stamps of the temperature data have to be converted to τ^{imt}times by linear interpolation

$$\tau^{imt}(n) = \tau_k^{imt} + \frac{\tau_{k+1}^{imt} - \tau_k^{imt}}{t_{k+1}^{obt} - t_k^{obt}} \left(t^{obt}(n) - t_k^{obt} \right) , \tag{6.26}$$

where τ_k^{imt}, τ_{k+1}^{imt}, t_k^{obt}, and t_{k+1}^{obt} are time stamps from the ENDPs so that $t_k^{obt} \leq t^{obt}(m) < t_{k+1}^{obt}$.

The temperature data set can now be expanded as

$$\left\{ \left(T_{rfcu_gava}(n), T_{rfcu_gva}(n), T_{rfcu_gza}(n), T_{geu}(n), t^{obt}(n), \tau^{imt}(n) \right) ;\ n : 1 \rightarrow M \right\} . \tag{6.27}$$

The RFCU and GEU temperature data shall be interpolated with linear interpolation to the code phase measurement times $\tau_{rx}^{imt}(m)$. This allows the expansion of the data set 6.24 as

$$\left\{ \left(T_{rfcu}(m), T_{geu}(m), CP_{ca}(m), CP_{p1}(m), CP_{p2}(m), \tau_{rx}^{imt}(m), CHN \right) ;\ m : 1 \rightarrow N \right\} , \tag{6.28}$$

[2] All available sample databases have characterisation files only for 14 dBm. However, it may be possible that other power levels exist and that the power level can be either selected by a MCMD or that the automatically adjusted power level can be derived from the telemetry. This shall be clarified later. The code phase correction function shall be able to use the LO power in the input parameters in the characterisation file selection.

where T_{rfcu} corresponds to the temperature of the RFCU for the GRAS antenna chain identified by CHN.

The group delay corrections for each $T_{rfcu}(m)$ and $T_{geu}(m)$ sample shall be derived by using linear interpolation and the RFCU and GEU code phase correction data files selected from the GRAS Characterisation Database. This allows us to write a group delay correction data set as

$$\{(\Delta t_{rfcu_ca}(m), \Delta t_{rfcu_p1}(m), \Delta t_{rfcu_p2}(m), \Delta t_{geu_ca}(m), \Delta t_{geu_p1}(m), \Delta t_{geu_p2}(m))\,;\ m : 1 \rightarrow N\}\,. \tag{6.29}$$

The RFCU code phase corrections are calculated from 6.29 as

$$\begin{aligned} \Delta cp_{rfcu_ca}(m) &= 1023 \cdot 10^3 \cdot \Delta t_{rfcu_ca}(m) \\ \Delta cp_{rfcu_p1}(m) &= 10230 \cdot 10^3 \cdot \Delta t_{rfcu_p1}(m) \\ \Delta cp_{rfcu_p2}(m) &= 10230 \cdot 10^3 \cdot \Delta t_{rfcu_p2}(m). \end{aligned} \tag{6.30}$$

Similarly the GEU code phase corrections are calculated as

$$\begin{aligned} \Delta cp_{geu_ca}(m) &= 1023 \cdot 10^3 \cdot \Delta t_{geu_ca}(m) \\ \Delta cp_{geu_p1}(m) &= 10230 \cdot 10^3 \cdot \Delta t_{geu_p1}(m) \\ \Delta cp_{geu_p2}(m) &= 10230 \cdot 10^3 \cdot \Delta t_{geu_p2}(m). \end{aligned} \tag{6.31}$$

A user selectable option is to perform a correction of the measured code phases for the impact of the GPS transmitter group delay. This correction shall use the Differential Code Bias (DCB) estimate Δt_{dcb} provided by the GRAS GSN for each GPS satellite. $\Delta t_{dcb}$for the measured GPS satellite shall be copied into the GPS_HW_DELAY field in the MDR-1A-OCCULTATION DATA, or MDR-1A-NAVIGATION DATA, depending on the measurement type. Δt_{dcb} for the occulting GPS satellite shall also be copied into the OCC_GPS_HW_DELAY field in the MDR-1B. $\Delta t_{dcb}$for the selected pivot GPS satellite shall be copied into the PIV_GPS_HW_DELAY field in the MDR-1B.

The GPS hardware corrections are calculated as

$$\begin{aligned} \Delta cp_{gps_ca} &= \frac{-f_2^2}{(f_1^2 - f_2^2)} 1023 \cdot 10^3 \cdot \Delta t_{dcb} \\ \Delta cp_{gps_p1} &= \frac{-f_2^2}{(f_1^2 - f_2^2)} 10230 \cdot 10^3 \cdot \Delta t_{dcb}. \end{aligned} \tag{6.32}$$

The code phase correction for L2-P2 Δcp_{gps_p2} is 0.

The instrument corrected code phases are calculated by subtracting the corrections from the measured code phase as

$$
\begin{aligned}
CP_{ic_ca}(m) &= CP_{ca}(m) - \Delta cp_{rfcu_ca}(m) - \Delta cp_{geu_ca}(m) - \Delta cp_{gps_ca} \\
CP_{ic_p1}(m) &= CP_{p1}(m) - \Delta cp_{rfcu_p1}(m) - \Delta cp_{geu_p1}(m) - \Delta cp_{gps_p1} \\
CP_{ic_p2}(m) &= CP_{p2}(m) - \Delta cp_{rfcu_p2}(m) - \Delta cp_{geu_p2}(m) - \Delta cp_{gps_p2}.
\end{aligned} \tag{6.33}
$$

6.1.5.4 Amplitude correction

Input Parameters:

1. Incidence angle for GVA, GAVA or GZA
   - zenith angle $\theta_{ant}^{eci}(m)$, $t_{rx}^{time}(m)$ [deg];
   - azimuth angle $\varphi_{ant}^{eci}(m)$, $t_{rx}^{time}(m)$ [deg];
2. RFCU temperature for the receiving chain $T_{rfcu_ch}(t^{obt})$ [°C];
3. GEU temperature $T_{geu}(t^{obt})$ [°C];
4. GEU analog gain setting $g_{ana}(\tau^{imt})$.

Output Parameters:

1. Antenna amplitude corrections
   - L1-CA $\Delta E_{ant_ca}(m)$;
   - L1-P1 $\Delta E_{ant_p1}(m)$:
   - L2-P2 $\Delta E_{ant_p2}(m)$.
2. RFCU amplitude corrections
   - L1-CA $\Delta E_{rfcu_ca}(m)$;
   - L1-P1 $\Delta E_{rfcu_p1}(m)$:
   - L2-P2 $\Delta E_{rfcu_p2}(m)$.
3. GEU amplitude corrections
   - L1-CA $\Delta E_{geu_ca}(m)$;
   - L1-P1 $\Delta E_{geu_p1}(m)$:
   - L2-P2 $\Delta E_{geu_p2}(m)$.
4. Total amplitude correction for measurement samples
   - L1-CA $\Delta E_{ca}(m)$;
   - L1-P1 $\Delta E_{p1}(m)$:
   - L2-P2 $\Delta E_{p2}(m)$.

Algorithm

The total amplitude correction is the product of three terms as

$$\begin{aligned}\Delta E_{inst} &= \Delta E_{ant}\left(\theta_{ant}\left(t_{rx}^{time}\right), \varphi_{ant}\left(t_{rx}^{time}\right), CH, CHN\right) \\ &\cdot \Delta E_{rfcu}\left(T_{rfcu}\left(t_{rx}^{time}\right), CH, CHN\right) \\ &\cdot \Delta E_{geu}\left(T_{geu}\left(t_{rx}^{time}\right), g_{ana}\left(t_{rx}^{time}\right), CH, CHN\right),\end{aligned} \tag{6.34}$$

where

ΔE_{inst} = total amplitude correction for code CH (= L1-C/A, L1-P, L2-C/A, L2-P) and chain CHN;

ΔE_{ant} = the amplitude correction due to the complex antenna pattern;

ΔE_{rfcu} = the amplitude correction due to the RFCU;

ΔE_{geu} = the amplitude correction due to the GEU;

t_{rx}^{time} = the reception time of the code phase. For navigation measurements $time = utc_gras$ and for occultation measurements $time = apr$ [s].

Estimation of antenna impact

The receiving antenna gain pattern is provided in the instrument characterisation database as a function of the angles θ_{ant} and φ_{ant} for each of the GRAS antenna and for codes C/A, P1, and P2. The correct antenna characterisation files are selected based on the GRAS chain identification.

The quadratic correction term for the amplitude is the same that is used for carrier phase correction in Section 6.1.5.2. So, the bi-cubic interpolation algorithm defined in Section 6.3.1.3 can be used to derive a data set that can be labeled for the measurement m as

$$\left\{\left(\varphi_{ant}^{eci}(m), \theta_{ant}^{eci}(m), \Delta\phi_{ant_I_ch}^{rhcp}(m), \Delta\phi_{ant_Q_ch}^{rhcp}(m), t_{rx}^{time}(m)\right);\ m : 1 \rightarrow N\right\}. \tag{6.35}$$

where ch denotes codes L1-C/A, L1-P1, and L2-P2.

The amplitude correction for antenna ant and code ch is derived from the interpolated antenna gain pattern characterization by

$$\Delta E_{ant}(m) = \sqrt{\left(\Delta\phi_{ant_I_ch}^{rhcp}(m)\right)^2 + \left(\Delta\phi_{ant_Q_ch}^{rhcp}(m)\right)^2}. \tag{6.36}$$

Estimation of RFCU impact

The impact of the RFCU on the measured amplitude is characterised in the Instrument Database as a function of the RFCU temperature. Each RFCU has its own characterisation file. The correct characterisations file for the code L1-C/A, L1-P1, and L2-P2 amplitude measurements for the RFCU that was part of the measurement chain shall be identified using the GRAS chain CHN identification in the measurement data packet.

The RFCU temperature data in the temperature data packet is time stamped with OBT_{32} time. The time stamps of the temperature data have to be interpolated to $t_{rx}^{time}(m)$ times of the observations using time synchronization in the ENDPs and Equation 6.4. This provides a data set labeled as

$$\left\{\left(T_{rfcu}(m), t_{rx}^{time}(m), CH, CHN\right);\ m : 1 \rightarrow N\right\}. \tag{6.37}$$

The generic format of the data records in the instrument characterisation database is presented in Table 6.3. The RFCU amplitude correction shall be derived using linear interpolation for each measurement sample m and converting the dB value from the database to a real number to generate data set

$$\left\{\left(\Delta E_{rfcu}(m), T_{rfcu}(m), t_{rx}^{time}(m), CH, CHN\right);\ m : 1 \rightarrow N\right\}, \tag{6.38}$$

where

ΔE_{rfcu} = the RFCU amplitude correction.

Estimation of GEU impact

The amplitude correction for the impact of the GEU is derived identifying the correct GEU characterisation file using the GPS code CH, the measurement chain CHN (velocity, anti-velocity, or zenith), and analog gain setting from the Gain Setting Packet. This provides a data set for occultation measurements labeled as

$$\left\{\left(g_{ana}(m), t_{rx}^{time}(m), CH, CHN\right);\ m : 1 \rightarrow N\right\}. \tag{6.39}$$

The GEU amplitude correction is derived using linear interpolation for each measurement sample m and converting the dB value from the database to a real number to generate data sets for occultation measurement samples as

$$\left\{\left(\Delta E_{geu}(m), T_{geu}(m), g_{ana}(m), t_{rx}^{time}(m), CH, CHN\right);\ m : 1 \rightarrow N\right\}, \tag{6.40}$$

where

ΔE_{geu} = the GEU amplitude correction.

6.1.5.5 USO frequency correction

Input Parameters:

1. USO frequency $f_{uso}(m)$, $t_{rx}^{utc_gras}(m)$
2. USO temperature $T_{uso}(t^{obt})$

Output Parameters:

1. USO frequency $f_{uso}(m)$
2. USO temperature correction $\Delta f_{uso}(m)$

Algorithm

The USO external thermistor temperature measurements from the temperature and voltage data packet are interpolated to the $t_{rx}^{utc_gras}(m)$ times of the measurement samples using linear interpolation (Equation 6.4) and synchronization in the ENDPs. This allows the linear interpolation of the USO frequency corrections from the USO frequency stability data record in the GID.

The USO frequency correction is performed using the results of the interpolation as

$$f_{uso}(m) = f_{uso}(m) + \Delta f_{uso}(m). \tag{6.41}$$

The USO frequency correction derived with Equation 6.41 is applied also to the navigation measurements when $t_{rx}^{utc_gras}(m) = t_{rx}^{utc_gras}(k)$.

6.1.6 Level 1a product quality check

Input Parameters:

1. For occultation measurement sample m
   - IMT time stamp $\tau_{rx}^{imt}(m)$;
   - L1-CA carrier phase $\rho_{ic_ca}(m)$;
   - L1-P1 carrier phase $\rho_{ic_p1}(m)$;
   - L2-P2 carrier phase $\rho_{ic_p2}(m)$;
   - L1-CA amplitude $E_{ic_ca}(m)$;
   - L1-P1 amplitude $E_{ic_p1}(m)$;
   - L2-P2 amplitude $E_{ic_p2}(m)$;
   - L1-CA code phase $CP_{ic_ca1}(m)$;

- L1-P1 code phase $CP_{ic_p1}(m)$;
- L2-P2 code phase $CP_{ic_p2}(m)$;

2. For navigation measurement sample k

   - IMT time stamp $\tau_{rx}^{imt}(k)$;
   - OBT time stamp $t_{rx}^{obt}(k)$;
   - UTC_{GRAS} time stamp $t_{rx}^{utc_gras}(k)$;
   - L1-CA carrier phase $\rho_{ic_ca}(k)$;
   - L1-P1 carrier phase $\rho_{ic_p1}(k)$;
   - L2-P2 carrier phase $\rho_{ic_p2}(k)$;
   - L1-CA amplitude $E_{ic_ca}(k)$;
   - L1-P1 amplitude $E_{ic_p1}(k)$;
   - L2-P2 amplitude $E_{ic_p2}(k)$;
   - L1-CA code phase $CP_{ic_ca1}(k)$;
   - L1-P1 code phase $CP_{ic_p1}(k)$;
   - L2-P2 code phase $CP_{ic_p2}(k)$;

3. Receiver noise estimate

   - L1 $N_0^{l1}(\tau^{imt})$;
   - L2 $N_0^{l2}(\tau^{imt})$;

4. Gain setting and histogram

   - $HIST(\tau^{imt})$;
   - $g_{ana}(\tau^{imt})$;
   - $DIG(\tau^{imt})$;

5. Tracking state

   - $TS(\tau^{imt})$;

6. Onboard navigation solution

   - $NSM(\tau^{imt})$;
   - $POS_X(\tau^{imt})$;
   - $POS_Y(\tau^{imt})$;
   - $POS_Z(\tau^{imt})$;
   - $VEL_X(\tau^{imt})$;

- $VEL_Y\,(\tau^{imt})$;
- $VEL_Z\,(\tau^{imt})$;

7. Navigation data frame
   - $NDF_BITS\,(\tau^{imt})$;
8. GPS Ephemeris data
   - Data format and contents specified in **AD10**.
9. USO oven temperature $T_{uso}(m)$
10. Metop maneuver information

Output Parameters:

1. Quality flags for each checked parameter

Algorithm

The level 1a products to be checked and the threshold values are listed in the tables below. The products listed in Table 6.5 must be within the specified threshold range. If the products are outside the threshold, the corresponding quality flag (as listed in the table) in the level 1a and level 1b products shall be set.

The threshold values for monitoring the GRAS telemetry parameters are specified in Table 6.6. All values in the table shall be user adjustable. If any of the monitored parameters is outside the specified threshold range, the corresponding bit shall be set in the TELEMETRY_IN_RANGE bit string in MDR-1As and in MDR-1B. Each bit in the bit string has a name that is identical with the telemetry parameter listed in Table 6.6.

Table 6.7 specifies special quality checks with variable types of error criteria. The Metop manoeuvre flag is based on information requested via PGE. This flag is set for all occultation measurements that are even partially overlapping with a manoeuvre or that are within a user definable time period after the end of an in-plane or out of plane manoeuvre. The default time periods after the manoeuvres are defined in the Table 6.7. GPS navigation data health flag and GPS signal health bit string are directly copied from the GRAS Ephemeris Data Packet. Onboard navigation solution method is copied from the Extended Navigation Data Packet.

The LOCAL_MULTIPATH flag is set to indicate high probability of local multipath for a measurement with the respective antenna in the case that the incidence angle of the incoming ray is inside the specified zenith angle and azimuth range in Table 6.7. The LOCAL_MULTIPATH_SOURCE bit string is set to indicate the potential multipath source as defined in the table.

The quality flags set by the tests specified in Table 6.8 are based on external data. The SA flag is set for the products when the information from the GRAS GSN says that SA has been activated for

the measured GPS satellite. The user shall have an option to set this flag manually for all products or to products based on a specified list of GPS satellites.

The quality flags SA_FLAG, GPS_MANOEUVRE, and GPS_ECLIPTING are set for the measured GPS satellite based on the information provided by the GRAS GSN. The EOP_STATUS flag is set based on whether the EOP parameters used in the data processing are predicted or determined.

If any of the quality tests cause an error flag to be set in the level 1a products, the self explanatory information in the report of the dump processing is added, and an event of user configurable severity to the CGS via the PGE interface is raised.

A special task for the Level 1a quality check is to monitor the amplitude of the tracked signal. If the mean amplitude over a short time is very low or it drops temporarily significantly below the mean amplitude level before and after the dropped level, it is probable that the receiver has temporarily lost track of the signal. If the loss of track is very short, it may not be detectable in the instrument tracking state data or in the measurement packet type.

The amplitude to be monitored is the magnitude of the complex amplitude signal as

$$V_J^{IN}(m) = \sqrt{V_{I_J}^{IN}(m)^2 + V_{Q_J}^{IN}(m)^2}, \tag{6.42}$$

where

$V_{I_J}^{IN}$ = the I signal amplitude corrected for the receiver gain changes calculated as explained in **AD11**;

$V_{Q_J}^{IN}$ = the Q signal amplitude corrected for the receiver gain changes calculated as explained in **AD11**;

J = denotes the GPS code C/A, P1, and P2.

The monitoring is performed by calculating a mean amplitude over $2M$ samples as

$$\bar{V}_J^{IN}(m) = \frac{1}{2M+1} \sum_{i=-M}^{M} V_J^{IN}(m-i). \tag{6.43}$$

A probable loss of signal tracking is indicated if any of the following tests is true:

1. The mean amplitude drops below a user definable threshold value $\bar{V}_{min_J}^{IN}$;
2. The mean amplitude drops X dB below the average mean amplitude level before and after the amplitude drop (X is a user definable value and the average is calculated over user definable number of samples);
3. The mean amplitude drop between two consecutive samples exceeds a user definable threshold $\Delta\bar{V}_{max_J}^{IN}$.

Table 6.4: Default values for loss of tracking monitoring parameters.

Parameter	Default value
M	10
$V^{IN}_{min_J}$	amplitude thresholds in Table 6.5
X	2 dBV
$\Delta V^{IN}_{max_J}$	2 dBV

Default values for the parameters for the loss of tracking are provided in Table 6.4.

When a loss of tracking is detected in a measurement with the tests described above, the time of the loss of tracking is added into the corresponding MDRs (see Table 6.5) and the cumulative count of low amplitude counter for the measurement is incremented.

The METOP_MANOEUVRE quality flag in the corresponding MDRs is set based on the manoeuvre information acquired by the PPF. If the manoeuvre has taken place within the user definable threshold time limit, the flag is set to indicate that the MDR is impacted by a manoeuvre. The default time limit for in-plane manoeuvre is 120 min and for out-of-plane manoeuvre 400 minutes.

Table 6.5: Level 1a product quality check default threshold values.

Parameter	**Default threshold value**		**Quality flag**
	GVA, GAVA	GZA	
Carrier amplitude			
L1-C/A	-75 dBV	-68 dBV	L1_CA_AMP_LOW L1_CA_AMP_LOW_TIME
L1-P1	-87 dBV	-75 dBV	L1_P1_AMP_LOW L1_P1_AMP_LOW_TIME
L2-P2	-87 dBV	-75 dBV	L2_P2_AMP_LOW L2_P2_AMP_LOW_TIME
Receiver noise estimate			
L1-C/A	48 dB/Hz	40 dB/Hz	L1_CA_NOISE_FLAG
L1-P1	42 dB/Hz	35 dB/Hz	L1_P1_NOISE_FLAG
L2-P2	35 dB/Hz	20 dB/Hz	L2_P2_NOISE_FLAG
Code phase			
L1-C/A	0$\leq CP_{ic_ca} \leq$1 024	0$\leq CP_{ic_ca} \leq$1 024	L1_CA_PSEUDORANGE_FLAG
L1-P1	0$\leq CP_{ic_p1} \leq$10 229 999	0$\leq CP_{ic_p1} \leq$10 229 999	L1_P1_PSEUDORANGE_FLAG
L2-P2	0$\leq CP_{ic_p2} \leq$10 229 999	0$\leq CP_{ic_p2} \leq$10 229 999	L2_P2_PSEUDORANGE_FLAG
USO oven temperature	$-20°C \leq T_{uso} \leq 60°C$		USO_TEMP_NOMINAL (only in MDR-1B)
USO oven temperature change	$\Delta T_{uso} \leq 0.03°C$ in 60 s		USO_TEMP_DRIFT_NOMINAL (only in MDR-1B)
Instrument stable	(USO oven relay on) and (USO_TIM $\geq$ 2 weeks)		INSTRUMENT_STABLE

Table 6.6: GRAS telemetry monitoring default threshold values.

Telemetry	Default threshold value
ENDP Position X [cm]	$-7.8 \cdot 10^8 \leq pos_x \leq +7.8 \cdot 10^8$
ENDP Position Y [cm]	$-7.8 \cdot 10^8 <\leq pos_y \leq +7.8 \cdot 10^8$
ENDP Position Z [cm]	$-7.8 \cdot 10^8 \leq pos_z \leq +7.8 \cdot 10^8$
ENDP Velocity X [cm/s]	$-7.5 \cdot 10^5 \leq pos_vx \leq +7.5 \cdot 10^5$
ENDP Velocity Y [cm/s]	$-7.5 \cdot 10^5 \leq pos_vy \leq +7.5 \cdot 10^5$
ENDP Velocity Z [cm/s]	$-7.5 \cdot 10^5 \leq pos_vz \leq +7.5 \cdot 10^5$
Zenith antenna thermistor	$-55° \leq t_{gza} \leq +94°$
Velocity antenna thermistor	$-108° \leq t_{gva} \leq +65°$
Anti-velocity antenna thermistor	$-108° \leq t_{gava} \leq +77°$
Zenith RFCU thermistor	$-30° \leq t_{rfcu_gza} \leq +55°$
Velocity RFCU thermistor	$-30° \leq t_{rfcu_gva} \leq +55°$
Anti-velocity RFCU thermistor	$-30° \leq t_{rfcu_gava} \leq +55°$
GEU thermistor	$-27° \leq t_{geu} \leq +64°$
ISAC thermistor	$-27° \leq t_{isac} \leq +64°$
USO internal thermistor	$+74° \leq t_{uso_in} \leq +85°$
USO external thermistor	$+74° \leq t_{uso_out} \leq +85°$
DBU power voltage	$5.771\,V \leq V_{dbu} \leq 6.295\,V$
Thermistor supply voltage	$9.5\,V \leq V_{tsv} \leq 10.5\,V$
FG thermistor	$-27° \leq t_{fgt} \leq +62°$
USO ground	$-0.062\,V \leq V_{usog} \leq +0.062\,V$
Digital 5 V	$+4.814\,V \leq V_{d5v} \leq +5.292\,V$

Table 6.7: Other quality flags for level 1a product quality check.

Quality flag	**Nominal value**	**Threshold value**	**Product field**
Metop manoeuvre	no manoeuvre	Manoeuvre during measurement or shortly before the measurement	METOP_MANOEUVRE_FLAG
Time after the end of an in-plane manoeuvre	Not applicable	$\Delta t_{inplane} \leq 102$ min	METOP_MANOEUVRE
Time after the end of and out of plane manoeuvre	Not applicable	$\Delta t_{outplane} \leq 400$ min	METOP_MANOEUVRE
Metop steering mode	Yaw steering mode	Any other steering mode	METOP_STEERING_MODE
GPS navigation data health flag	all navigation data OK	Some or all navigation data bad	GPS_NAV_HEALTH
GPS signal health information (SH flag in the Ephemeris Data Packet)	all signals OK	Detailed list of error codes in **RD11**	GPS_SH
Onboard navigation solution method (NSM flag in the ENDP)	Kalman filter solution	Detailed list of other codes in **RD11**	ONBOARD_NAV_SOLUTION
Local multipath (GZA)	Not applicable	$50° \leq \theta_{gza} \leq 90°$ $320° \leq \varphi_{gza} \leq 330°$	LOCAL_MULTIPATH_SOURCE (solar panel)
Local multipath (GAVA)	Not applicable	$-22° \leq \theta_{gava} \leq -35°$ $60° \leq \varphi_{gava} \leq 85°$	LOCAL_MULTIPATH_SOURCE (ASCAT ANT RA)
Local multipath (GAVA)	Not applicable	$-35 \leq \theta_{gava} \leq -50°$ $10° \leq \varphi_{gava} \leq 80°$	LOCAL_MULTIPATH_SOURCE (ASCAT ANT RF)

Table 6.8: Quality flags for level 1a products based on external information.

Quality flag	Triggering threshold	Error source
SA_FLAG (Selective Availability)	Quality information provided by GSN says that SA is active for the measured GPS at the time of the measurement. Flag can also be set manually by operator for all specified GPS satellites.	SA activated for some or all GPS satellites for limited geographical regions or globally.

6.2 Level 1b processing functions

6.2.1 Pivot satellite and fiducial station selection functions

Input Parameters:

1. Occulting GPS identification GPS_{id_occ}
2. Occulting GPS antenna phase center position vector $\vec{r}^{eci}_{tx}(t^{ref}_{rx})$
3. Occulting GPS antenna phase center velocity vector $\vec{v}^{eci}_{tx}(t^{ref}_{rx})$
4. Identifications of all provisional pivot GPS satellites $GPS_{id_piv_k}$
5. Position vectors of all provisional pivot GPS satellite antenna phase centers $\vec{r}^{eci}_{tx_k}(t^{ref}_{rx})$
6. Velocity vectors of all provisional pivot GPS satellite antenna phase center $\vec{v}^{eci}_{tx_k}(t^{ref}_{rx})$
7. Position vector of Metop receiving antenna phase center $\vec{r}^{eci}_{ant}\left(t^{ref}_{rx}\right)$
8. Velocity vector of Metop receiving antenna phase center $\vec{v}^{eci}_{ant}\left(t^{ref}_{rx}\right)$
9. Antenna phase center position vectors in ITRF coordinate frame for all provisional reference fiducial stations $\vec{r}^{itrf}_{fs_n}$;
10. SNR measurement data for all provisional reference fiducial stations for L1 $SNR^{l1}_{fs_n}$ and L2 $SNR^{l2}_{fs_n}$;
11. Earth model id $Earth_{id}$

Output Parameters:

1. Pivot GPS id for SD1, DD1 and DD2
2. GSN station id for SD2 and DD1
3. Second GSN station id for DD2

Algorithm

Single Differencing 1 (SD1)

Because no ground based data is used in the SD1 mode, the cost function for this mode is based on the elevation of the provisional pivot GPS satellite as

$$C_{sd1} = \frac{\pi}{2} - \bar{\epsilon}_{gza}, \tag{6.44}$$

where $\bar{\epsilon}_{gza}$ is the mean elevation of the GPS satellite from Equation 6.15. The mean elevation is calculated from the sum of all elevations during the time period of the occultation measurement as

$$\bar{\epsilon}_{gza} = \frac{1}{N}\sum_{i=1}^{N}\epsilon_i. \tag{6.45}$$

The cost function is calculated for all GPS satellites tracked by GRAS with the GZA that are not flagged bad for the time of the occultation in the GSN quality information.

The GPS satellite with the smallest C_{sd1} value is selected as the pivot satellite for SD1 mode.

If $\bar{\epsilon}_{gza}$ of the selected GPS satellite is lower than the threshold value defined in Table 6.10, the LOW_PIV_GZA_SD1 warning flag in the MDR-1B product record is set, event of user configurable severity to the CGS via the PGE interface is raised, and the measurement id number and error characterization information is added in the report of the dump processing.

Single Differencing 2 (SD2)

SD2 mode does not require a pivot satellite, so the cost function is based on the elevation of the incoming ray calculated for the occulting GPS satellite as

$$C_{sd2} = \frac{\pi}{2} - \bar{\epsilon}_{occ}, \tag{6.46}$$

where $\bar{\epsilon}_{occ}$ is the mean elevation of the GPS satellite. The elevation angles of the incoming rays are calculated with Equation 6.206. The mean elevation angle is calculated from the sum of all elevations angles during the occultation measurement using the formula in Equation 6.45.

The cost function is calculated for all fiducial stations provisionally capable of supporting SD2 mode for the occultation. The pre-selection of the fiducial stations has been performed by the GSN. The cost function is not calculated for any fiducial station that is flagged bad for the time of the occultation in the GSN quality information even if SSD from such a station is available.

The fiducial station with the smallest C_{sd2} value is selected as the reference station for SD2 mode. If two or more stations share the same smallest C_{sd2} value, the station with the highest average SNR is selected.

If $\bar{\epsilon}_{occ}$ of the occulting GPS satellite from the selected fiducial station is lower than the threshold value defined in Table 6.10, the LOW_OCC_FID_SD2 warning flag in the MDR-1B product record

is set , event of user configurable severity to the CGS via the PGE interface is raised, and the measurement id number and error characterization information is added in the report of the dump processing.

Double Differencing 1 (DD1)

DD1 mode requires both a reference fiducial station and a pivot satellite. Because the elevation angles of the incoming ray from the occulting GPS and the pivot PGS to the fiducial station and the incidence angle of the pivot satellite to the GZA have to be considered, the cost function for DD1 mode is more complex than for the SD modes.

The attenuation of the incoming signal due to the antenna gain pattern and the atmosphere has been selected as the basis for the cost function. The justification for this is that the SNR of the incoming signal determines the phase noise level of the measured carrier phase.

The cost function for DD1 is

$$C_{dd1} = \frac{1}{f_{gza}(\bar{\epsilon}_{gza}) \cdot f_{fid}(\bar{\epsilon}_{piv}) \cdot f_{fid}(\bar{\epsilon}_{occ}) \cdot f_{atm}(\bar{\epsilon}_{piv}) \cdot f_{atm}(\bar{\epsilon}_{occ})}, \tag{6.47}$$

where

$\bar{\epsilon}_{gza}$ = the mean elevation angle of the pivot GPS satellite (see Equation 6.15) [rad];

$\bar{\epsilon}_{piv}$ = the mean elevation of the pivot satellite at the fiducial station from Equation 6.15 [rad];

$\bar{\epsilon}_{occ}$ = the mean elevation of the occulting GPS satellite at the fiducial station from Equation 6.15 [rad].

The mean elevation angles are calculated from the sum of the elevations angles during the occultation measurement using the formula in Equation 6.45.

The function f_{gza} is an approximation of the normalised GRAS GZA antenna gain pattern as

$$f_{gza}(\bar{\epsilon}) = a_{gza}(\frac{\pi}{2} - \bar{\epsilon})^2 + b_{gza}(\frac{\pi}{2} - \bar{\epsilon}) + c_{gza}, \tag{6.48}$$

where coefficients a_{gza}, b_{gza}, and c_{gza} are listed in Table 6.9.

The approximation of the normalised fiducial station antenna gain pattern f_{fid} is

$$f_{fid}(\bar{\epsilon}) = a_{fid}(\frac{\pi}{2} - \bar{\epsilon})^2 + b_{fid}(\frac{\pi}{2} - \bar{\epsilon}) + c_{fid}, \tag{6.49}$$

where the coefficients a_{fid}, b_{fid}, and c_{fid} are listed in Table 6.9.

The normalised dry atmosphere attenuation f_{atm} is given by

$$f_{atm}(\bar{\epsilon}) = \frac{1}{\sin \bar{\epsilon}}. \tag{6.50}$$

The cost function is calculated for all provisional fiducial station - pivot satellites pairs. The pair with the lowest cost function is selected for the occultation processing with the DD1 mode. If two or more pairs share the same smallest C_{dd1} value, the pair with the highest average SNR for the SSD during the occultation is selected.

If for the selected station or the pivot satellite $\bar{\epsilon}_{gza}$, $\bar{\epsilon}_{piv}$, or $\bar{\epsilon}_{occ}$ is smaller than the threshold value defined in Table 6.10, the respective warning flag LOW_PIV_GZA_DD1, LOW_PIV_FID_DD1, or LOW_OCC_FID_DD1 in the MDR-1B product record is set, event of user configurable severity to the CGS via the PGE interface is raised, and the measurement id number and error characterization information is added in the report of the dump processing.

Double Differencing 2 (DD2)

In the DD2 mode the group of potential fiducial stations is larger as the second station does not have to have visibility to the occulting GPS satellite. So, all fiducial stations providing SSD from the occulting GPS satellite during the whole occultation are candidates for the fiducial station 1. All fiducial stations providing SSD from any of the GPS satellite tracked by the GZA during the whole occultation are candidates for the fiducial station 2.

The cost function for DD2 is

$$C_{dd2} = \frac{1}{f_{gza}(\bar{\epsilon}_{gza}) \cdot f_{fid1}(\bar{\epsilon}_{occ}) \cdot f_{fid2}(\bar{\epsilon}_{piv}) \cdot f_{atm}(\bar{\epsilon}_{piv}) \cdot f_{atm}(\bar{\epsilon}_{occ})}, \tag{6.51}$$

where

$\bar{\epsilon}_{gza}$ = the mean elevation angle of the pivot GPS satellite (see Equation 6.15) [rad];

$\bar{\epsilon}_{occ}$ = the mean elevation of the occulting GPS satellite at the fiducial station 1 from Equation 6.15 [rad];

$\bar{\epsilon}_{piv}$ = the mean elevation of the pivot satellite at the fiducial station 2 from Equation 6.15 [rad].

The mean elevation angles are calculated from the sum of the elevations angles during the occultation measurement using the formula in Equation 6.45.

The cost function is calculated for all provisional station 1 - station 2 - pivot satellite triplets. The triplet with the lowest cost function is selected for the occultation processing with DD2 mode. If two or more triplets share the same smallest C_{dd2} value, the triplet with the highest average SNR for the SSD during the occultation is selected.

If for the selected stations or the pivot satellite $\bar{\epsilon}_{gza}$, $\bar{\epsilon}_{piv}$, or $\bar{\epsilon}_{occ}$ is smaller than the threshold value defined in Table 6.10, the respective warning flag LOW_PIV_GZA_DD2, LOW_PIV_FID_DD2, or LOW_OCC_FID_DD2 in the MDR-1B product record is set, event of user configurable severity to the CGS via the PGE interface is raised, and the measurement id number and error characterization information is added in the report of the dump processing.

Table 6.9: Coefficients for approximated antenna patterns.

	a	b	c
f_{gza}	-0.00000005092044	-0.00011775552894	1.00578881224659
f_{fid}	-0.00000000778357	-0.00013000147824	1.00005341636642

Table 6.10: Threshold values for cost functions.

Elevation	Threshold value
ϵ_{gza}	$20°$
ϵ_{occ}	$20°$
ϵ_{piv}	$20°$

6.2.2 Level 1b corrections

6.2.2.1 Relativity correction

Input Parameters:

1. Position vectors of the occulting GPS satellite $\vec{r}_{gps}^{eci}\left(t_{tx}^{ref}\right)$
2. Position vector of Metop $\vec{r}_{leo}^{eci}\left(t_{rx}^{ref}\right)$

Output Parameter:

1. Estimated Shapiro delay $\Delta t_s\left(t_{rx}^{ref}\right)$

The relativity correction is performed to combine the phase observations and the POD products in a fashion compatible with special and general relativity. This algorithm assumes a non-rotating ECI coordinate frame.

The total Shapiro effect for the traveling time of the GPS transmission to a LEO orbit is calculated from

$$\begin{aligned}\Delta t_s\left(t_{rx}^{ref}\right) = P_s(\vec{r}_1,\vec{r}_2) &= \frac{2GM_e}{c^3} ln\left[\frac{|\vec{r}_1| + \sqrt{|\vec{r}_1|^2 - r_0^2}}{r_0}\right] \\ &+ \frac{2GM_e}{c^3} ln\left[\frac{|\vec{r}_2| + \sqrt{|\vec{r}_2|^2 - r_0^2}}{r_0}\right] \\ &+ \frac{GM_e}{c^3}\sqrt{\frac{|\vec{r}_1| - r_0}{|\vec{r}_1| + r_0}} \\ &+ \frac{GM_e}{c^3}\sqrt{\frac{|\vec{r}_2| - r_0}{|\vec{r}_2| + r_0}},\end{aligned} \tag{6.52}$$

where

$$r_0 = |\vec{r}_1|\sqrt{1 - \frac{\left(|\vec{r}_1|^2 - \vec{r}_1\cdot\vec{r}_2\right)^2}{|\vec{r}_1|^2\left(|\vec{r}_1|^2 + |\vec{r}_2|^2 - 2\vec{r}_1\cdot\vec{r}_2\right)}}, \tag{6.53}$$

and

$\vec{r}_1$ = the position vector of the GPS CoM, i.e., $\vec{r}_1 = \vec{r}_{gps}^{\,eci}\left(t_{tx}^{ref}\right)$ [m];

$\vec{r}_2$ = the position vector of the Metop CoM, i.e., $\vec{r}_2 = \vec{r}_{leo}^{\,eci}\left(t_{rx}^{ref}\right)$ [m];

r_0 = the radius of the ray perigee;

GM_e = the Earth's gravitational constant (= 3.986004415·10^{14}) [m^3/s^2].

6.2.2.2 No Differencing (ND) clock correction

Input Parameter:

1. GPS and GRAS clock offset estimates $\Delta t_{gras}\left(t^{ref}\right)$ and $\Delta t_{gps}\left(t^{ref}\right)$ [s];
2. Relativity corrected phase residual measurements $\phi_{atm}(t_{rx}^{ref})$ [m].

Output Parameter:

1. Clock corrected phase residuals $\phi_{nd}(t_{rx}^{ref})$ [m].

The data processing with ND is feasible only in the case when the errors in the transmitter and receiver clocks are either extremely small or when they can be estimated with a very good accuracy in the POD processing. In such a case the clock correction algorithm for the GRAS occultation data becomes straight forward.

The first processing step in ND clock correction is the interpolation of the clock offset estimates to the phase residual measurement times t_{rx}^{ref}. If the GRAS clock offset estimate, the measured GPS satellite clock offset estimate, or both are provided as functions, the interpolation shall be performed by using the functions. If any of the clock offsets are provided as discreet clock offset samples, linear interpolation shall be used to derive the clock offsets at the measurement times.

The clock corrected phase residual samples are calculated by subtracting the excess phase caused by the clock offsets from the observed phase as

$$\phi_{nd}(t_{rx}^{ref}) = \phi_{atm}(t_{rx}^{ref}) - c\left(\Delta t_{gras}(t_{rx}^{ref}) - \Delta t_{gps}(t_{tx}^{ref})\right), \tag{6.54}$$

where

ϕ_{nd} = the clock corrected phase residual [m];

ϕ_{atm} = the relativity corrected phase residual including the clock errors [m];

c = the speed of light in vacuum [m/s];

Δt_{gras} = GRAS clock offset estimate from the GRAS/Metop NRT POD [s];

Δt_{gps} = clock offset estimate for the occulting GPS satellite from the GRAS GSN [s].

The ND clock correction is performed for all measured carrier phases L1-C/A, L1-P2, and L2-P2.

6.2.2.3 Single Differencing 1 (SD1) clock correction

Input Parameter:

1. Relativity corrected phase residual measurements $\phi_{atm}(t_{rx}^{ref})$ [m];
2. GRAS GZA phase measurements $\phi_{reg_gza}\left(\tau_{rx_gza}^{imt}\right)$ [m];
3. Metop CoM position vector in ECI coordinate frame $\vec{r}_{leo}^{eci}\left(t_{rx_gza}^{ref}\right)$ [m];
4. Position vector of the Metop CoM in SRF coordinate frame $\vec{r}_{com}^{srf}\left(t_{rx_gza}^{ref}\right)$ [m];
5. Position vector of the pivot GPS satellite CoM in ECI frame $\vec{r}_{gps}^{eci}\left(t_{rx_gza}^{ref}\right)$ [m];
6. Position vector of the pivot GPS antenna phase center in the local GPS satellite reference frame $\vec{p}_{tx}\left(t_{rx_gza}^{ref}\right)$ [m];
7. GRAS clock offset from the GRAS/Metop NRT POD $\Delta t_{gras}\left(t^{ref}\right)$ [s];
8. Pivot GPS clock offset from the GRAS/Metop NRT POD $\Delta t_{gps_pv}\left(t^{ref}\right)$ [s];
9. Occulting GPS clock offset from the GRAS/Metop NRT POD $\Delta t_{gps}\left(t^{ref}\right)$ [s];
10. Code phase measurements $CP_{rc_p1}\left(t_{rx_gza}^{ref}\right)$ and $CP_{rc_p2}\left(t_{rx_gza}^{ref}\right)$ [chips];

Output Parameters:

1. SD1 corrected phase residual $\phi_{sd1}\left(t_{rx}^{ref}\right)$ [m];
2. Interpolated reference measurements $\phi_{res_gza}\left(t_{rx}^{ref}\right)$ [m];
3. Interpolated occulting GPS clock offset estimates $\Delta t_{gps}\left(t_{rx}^{ref}\right)$ [s];
4. Interpolated pivot GPS clock offset estimates $\Delta t_{gps_pv}\left(t_{rx}^{ref}\right)$ [s];

Algorithm:

Let the set of N regenerated phase samples and their corresponding IMT times for a given GRAS GZA chain be:

$$\left\{\left(\phi_{reg_gza}(k), \tau_{rx_gza}^{imt}(k)\right)\ ;\ k:1\rightarrow N\right\}$$

The regenerated phase in meters measured by the GRAS GZA is given by

$$\begin{aligned}\phi_{reg_gza}\left(\tau_{rx_gza}^{imt}\right) = \ & \left|\vec{r}_{gza}^{eci}\left(t_{rx_gza}^{ref}\right) - \vec{r}_{tx_pv}^{eci}\left(t_{tx_gza}^{ref}\right)\right| \\ & + cP_s\left[\vec{r}_{gza}^{eci}\left(t_{rx_gza}^{ref}\right), \vec{r}_{tx_pv}^{eci}\left(t_{tx_gza}^{ref}\right)\right] \\ & + c\left(\Delta t_{gras}\left(t_{rx_fs}^{ref}\right) - \Delta t_{gps_pv}\left(t_{tx_fs}^{ref}\right)\right) \\ & - \phi_{ion_gza}\left(\tau_{rx_fs}^{imt}\right) \\ & + N_{cs_gza}\left(\tau_{rx}^{imt}\right) + \phi_{const_gza},\end{aligned} \tag{6.55}$$

where

ϕ_{reg_gza} = the regenerated phase at the GRAS GZA reference point [m];

$\tau_{rx_gza}^{imt}$ = the reception time of the pivot GPS transmission in the IMT time frame [s];

c = the speed of light in vacuum [m/s];

$\vec{r}_{gza}^{eci}$ = the position vector of the GRAS GZA reference point in ECI coordinate frame [m];

$t_{rx_gza}^{ref}$ = the reception time of the pivot GPS signal in the reference time frame [s];

$\vec{r}_{tx_gza}^{eci}$ = the position vector of the pivot GPS satellite antenna reference point in ECI coordinate frame [m];

$t_{tx_gza}^{ref}$ = the transmission time of the pivot GPS signal in the reference time frame [s];

P_s = the relativistic correction function for the Shapiro effect for the GZA antenna [s];

Δt_{gras} = the clock offset of the GRAS receiver [s];

Δt_{gps_pv} = the clock offset of the pivot GPS transmitter [s];

ϕ_{ion_gza} = the phase delay due to the ionosphere [m];

N_{cs_gza} = the number of cycle slips in the received phase;

ϕ_{const_gza} = a constant phase offset due to the phase ambiguity [m].

Equation 6.55 assumes that the instrument impact has been corrected in the level 1a processing and that the impact of the neutral atmosphere to the GRAS GZA measurements is negligible.

(1) Filtering of the phase measurements

The GZA phase measurements shall be filtered using the filtering algorithm defined in Section 6.2.4.1. The filter parameters are user definable. The default values for the filtering parameters are listed in Table 6.11. The bandwith range column shows the bandwidth parameter B_{go} and window length L_{go} values. In the case of the GZA measurements the SLTH value is not an applicable parameter for the filtering polynomial. In this case the filter bandwidth and window length are fitted over the elevation angle of the measurement.

Table 6.11: The default filtering parameters for phase measurements by GRAS GZA.

Parameter	**Bandwidth range [Hz]**	**Elevation range [km]**	**Polynomial order**
B_{go}	4 - 4	0 - 90	0
Parameter	**Window length range [samples]**	**Elevation range [km]**	**Polynomial order**
L_{go}	4 - 4	0 - 90	0

(2) IMT to reference time conversion

The time stamps in reference time frame are computed for the IMT time stamps of the GZA measurements using Equations 5.5 - 5.8. The phase samples and time stamps for the measurement can now be labeled as

$$\left\{ \left(\phi_{reg_gza}(k), \tau^{imt}_{rx_gza}(k), t^{ref}_{rx_gza}(k) \right) \; ; \; k : 1 \rightarrow N \right\}$$

(3) Transmission time determination

The transmission time of the signal measured by GZA is determined by iterating the Equation 5.9. In this case the Shapiro effect $P_s(\vec{r}_1, \vec{r}_2)$ must be calculated for the pivot GPS satellite. This is done by using $r_0 = |\vec{r}^{\,eci}_2| = |\vec{r}^{\,eci}_{gza}|$. The detailed equation for calculating the Shapiro effect is given as Equation 6.52 in Section 6.2.2.1.

The position vectors of the GRAS GZA and GPS antenna phase centers are calculated by applying Equations 5.10 and 6.13, respectively.

The labeling of the measurement samples can now be extended as

$$\left\{ \left(\phi_{reg_gza}(k), \tau^{imt}_{rx_gza}(k), t^{ref}_{rx_gza}(k), t^{ref}_{tx_gza}(k) \right) \; ; \; k : 1 \rightarrow N \right\}$$

(4) Geometrical path length determination

Having established the reference times of transmission and reception, the geometrical path terms for the regenerated phase can now be determined as

$$\begin{aligned} \phi_{gp_gza}\left(t^{ref}_{rx_gza}\right) &= \left| \vec{r}^{\,eci}_{gza}\left(t^{ref}_{rx_gza}\right) - \vec{r}^{\,eci}_{tx}\left(t^{ref}_{tx_gza}\right) \right| \\ &\quad + c\, P_s \left[\vec{r}^{\,eci}_{gza}\left(t^{ref}_{rx_fs}\right), \vec{r}^{\,eci}_{tx}\left(t^{ref}_{tx_gza}\right) \right], \end{aligned}$$

where

ϕ_{gp_gza} = the phase delay due to the geometrical path length including Shapiro effect change-bar [m];

$\vec{r}^{\,eci}_{tx}\left(t^{ref}_{tx_gza}\right)$ = the position vector of the phase center of the pivot GPS antenna interpolated to the transmission time $t^{ref}_{tx_gza}$ using the interpolation algorithm defined in Section 6.3.1.1 [m].

The labeling can again be extended as

$$\left\{ \left(\phi_{reg_gza}(k), \phi_{gp_gza}(k), \tau^{imt}_{rx_gza}(k), t^{ref}_{rx_gza}(k), t^{ref}_{tx_gza}(k) \right) \; ; \; k : 1 \rightarrow N \right\}$$

(5) Estimating the ionosphere delay

The GPS carrier phase advance caused by the ionosphere can be estimated from the code phase measurement at L1 and L2. The code phase measurements have to be filtered using the filtering algorithm defined in Section 6.2.4.1. The filter parameters are user definable. The default values for the filter parameters are listed in Table 6.12. The order of the polynomials and the coefficients shall be completely user definable. In the case of the GZA measurements the filter bandwidth and window length are fitted over the elevation angle of the measurement.

The phase delays for measurements at L1 and L2 are estimated as

$$\phi^{l1}_{ion_gza}\left(t^{ref}_{rx_gza}\right) = -c \frac{f_2^2}{f_1^2 - f_2^2} \left(\frac{\left\langle CP_{rc_p1}\left(t^{ref}_{rx_gza}\right)\right\rangle_{B_{sd1}} - \left\langle CP_{rc_p2}\left(t^{ref}_{rx_gza}\right)\right\rangle_{B_{sd1}}}{10230 \cdot 10^3} \right), \quad (6.56)$$

Table 6.12: The default filtering parameters for the ionosphere compensation.

Parameter	Bandwidth range [Hz]	Elevation range [km]	Polynomial order
B_{go}	0.1 - 0.1	0 - 90	0
Parameter	**Window length range [samples]**	**Elevation range [km]**	**Polynomial order**
L_{go}	4 - 4	0 - 90	0

$$\phi^{l2}_{ion_gza}\left(t^{ref}_{rx_gza}\right) = -c\frac{f_1^2}{f_1^2 - f_2^2}\left(\frac{\left\langle CP_{rc_p1}\left(t^{ref}_{rx_gza}\right)\right\rangle_{B_{sd1}} - \left\langle CP_{rc_p2}\left(t^{ref}_{rx_sd1}\right)\right\rangle_{B_{sd1}}}{10230 \cdot 10^3}\right), \quad (6.57)$$

where

$\phi^{l1}_{ion_gza}$ = the phase delay on L1 [m];

$\phi^{l2}_{ion_gza}$ = the phase delay on L2 [m];

c = speed of light in vacuum [m/s];

f_1 = the GPS frequency at L1 [Hz];

f_2 = the GPS frequency at L2 [Hz];

CP_{rc_p1} = the code phase measurement at L1-P1 [chips];

CP_{rc_p2} = the code phase measurement at L2-P2 [chips];

$\langle\rangle_{B_{sd1}}$ = indicates low pass filtering to the cutoff frequency B_{sd1}.

Note that Equations 6.56 and 6.57 are expected to produce normally a negative phase delay, because ionosphere causes a GPS carrier phase advance.

The labeling can again be extended as

$$\left\{\left(\phi_{reg_gza}(k), \phi_{gp_gza}(k), \phi_{ion_gza}(k), \tau^{imt}_{rx_gza}(k), t^{ref}_{rx_gza}(k), t^{ref}_{tx_gza}(k)\right) \; ; \; k : 1 \rightarrow N\right\}.$$

(6) Determining the phase residual

The equation for the phase measurement by GZA can now be written taking into account the compensation for the geometrical path length, and ionosphere as

$$\begin{aligned}\phi_{res_gza}\left(t^{ref}_{rx_gza}\right) &= \phi_{reg_gza}\left(t^{ref}_{rx_gza}\right) - \phi_{gp_gza}\left(t^{ref}_{rx_gza}\right) - \phi_{ion_gza}\left(t^{ref}_{rx_gza}\right) \\ &= c\left(\Delta t_{gras}\left(t^{ref}_{rx_gza}\right) - \Delta t_{gps_pv}\left(t^{ref}_{tx_gza}\right)\right) \\ &\quad + N_{cs}\left(t^{ref}_{tx_gza}\right) + \phi_{const_gza},\end{aligned} \tag{6.58}$$

where

ϕ_{res_gza} = the residual phase measurement by GZA [m].

The labeling can again be extended as

$$\left\{\left(\phi_{reg_gza}(k), \phi_{gp_gza}(k), \phi_{ion_gza}(k), \phi_{res_gza}(k), \tau^{imt}_{rx_gza}(k), t^{ref}_{rx_gza}(k), t^{ref}_{tx_gza}(k)\right) \; ; \; k : 1 \rightarrow N\right\}.$$

(7) Interpolating to the occultation measurement times

The phase residuals by GRAS GZA at the times of the occultation measurements $\phi_{res_gza}\left(t^{ref}_{rx}\right)$ are derived by linear interpolation from the measurements $\phi_{res_gza}\left(t^{ref}_{rx_gza}\right)$ providing a new labeling for the synchronized occultation measurements and the interpolated phase measurements of the pivot satellite as

$$\left\{\left(\phi_{atm}(m), \phi_{res_gza}(m), t^{ref}_{rx}(m)\right) \; ; \; m : 1 \rightarrow M\right\}.$$

(8) Differencing the occultation measurement

The single difference corrected carrier phase can be calculated by subtracting the phase residual from the GZA measurement from step (7) from ϕ_{atm} as

$$\phi_{sd1}\left(t^{ref}_{rx}\right) = \phi_{atm}\left(t^{ref}_{rx}\right) - \phi_{res_gza}\left(t^{ref}_{rx}\right), \tag{6.59}$$

A user selectable option is to subtract the GSN clock offset estimates for the pivot GPS satellite and for the occulting satellite from the SD1 results because they are not removed by SD1 correction. The user can select to remove just the pivot clock offset Δt_{gps_pv} or the occulting GPS clock offset Δt_{gps}, or both. The mathematical formulation for the enhanced SD1 correction with the subtraction is

$$\phi_{sd1} = \phi_{sd1}\left(t^{ref}_{rx}\right) - c\left[\Delta t_{gps_pv}\left(t^{ref}_{rx}\right) - \Delta t_{gps}\left(t^{ref}_{rx}\right)\right], \tag{6.60}$$

where $\phi_{sd1}\left(t^{ref}_{rx}\right)$ is the output from Equation 6.59.

The labeling of the final products from SD1 function can now be written as

$$\left\{ \left(\phi_{sd1}(m), \phi_{atm}(m), \phi_{res_gza}(m), \Delta t_{gps_pv}(m), \Delta t_{gps}(m), t_{rx}^{ref}(m) \right) \; ; m : 1 \rightarrow M \right\},$$

where Δt_{gps_pv} and Δt_{gps} are only provided in the case that they are used in the function.

6.2.2.4 Single Differencing 2 (SD2) clock correction

Input Parameter:

1. Relativity corrected phase residual measurements $\phi_{atm}(t_{rx}^{ref})$ [m];
2. Fiducial ground station phase measurement $\phi_{reg_fs}\left(\tau_{rx_fs}^{fst}\right)$ [m];
3. Metop CoM position vector in ECI coordinate frame $\vec{r}_{leo}^{eci}\left(t_{rx_fs}^{ref}\right)$ [m];
4. Position vector of the Metop CoM in SRF coordinate frame $\vec{r}_{com}^{srf}\left(t_{rx_fs}^{ref}\right)$ [m];
5. Position vector of the occulting GPS satellite CoM in ECI frame $\vec{r}_{gps}^{eci}\left(t_{rx_fs}^{ref}\right)$ [m];
6. Position vector of the occulting GPS antenna phase center in the local GPS satellite reference frame $\vec{p}_{tx}\left(t_{rx_fs}^{ref}\right)$ [m];
7. Position vector of the fiducial station antenna phase center in ECEF coordinate frame $\vec{r}_{fs}^{ecef}$ [m];
8. GRAS clock offset from the GRAS/Metop NRT POD $\Delta t_{gras}\left(t^{ref}\right)$ [s];
9. Fiducial station clock offset from the GSN $\Delta t_{fs}\left(t^{ref}\right)$ [s];
10. Occulting GPS clock offset from the GSN $\Delta t_{gps}\left(t^{ref}\right)$ [s];
11. Pseudorange measurement by the fiducial station at L1 $p_1\left(t_{rx_fs}^{ref}\right)$ and L2 $p_2\left(t_{rx_fs}^{ref}\right)$ [m].

Output Parameters:

1. SD2 corrected phase residual $\phi_{sd2}\left(t_{rx}^{ref}\right)$ [m];
2. Interpolated reference measurement $\phi_{res_fs}\left(t_{rx}^{ref}\right)$ [m];
3. Interpolated occulting GPS clock offset estimate $\Delta t_{gras}\left(t_{rx}^{ref}\right)$ [s];
4. Interpolated fiducial station clock offset estimate $\Delta t_{fs}\left(t_{rx}^{ref}\right)$ [s].

Let the set of N regenerated phase samples and their corresponding local times for a given fiducial station be:

$$\left\{ \left(\phi_{reg_fs}(k), \tau^{fst}_{rx_fs}(k) \right) \; ; \; k : 1 \rightarrow N \right\}$$

The regenerated phase measured by the fiducial station is given by

$$\begin{aligned} \phi_{reg_fs}\left(\tau^{fst}_{rx_fs}\right) = \; & \left| \vec{r}^{\,eci}_{fs}\left(t^{ref}_{rx_fs}\right) - \vec{r}^{\,eci}_{tx}\left(t^{ref}_{tx_fs}\right) \right| \\ & + c\, G_{rel_fs}\left[\vec{r}^{\,eci}_{fs}\left(t^{ref}_{rx_fs}\right), \vec{r}^{\,eci}_{tx}\left(t^{ref}_{tx_fs}\right) \right] \\ & + c\left(\Delta t_{fs}\left(t^{ref}_{rx_fs}\right) - \Delta t_{gps}\left(t^{ref}_{tx_fs}\right) \right) \\ & - \phi_{ntrl_fs}\left(\tau^{ref}_{rx_fs}\right) - \phi_{ion_fs}\left(\tau^{ref}_{rx_fs}\right) \\ & + \phi_{inst_fs}\left(\theta_{fs}\left(t^{ref}_{rx_fs}\right), \varphi_{fs}\left(t^{ref}_{rx_fs}\right) \right) \\ & + \phi_{const_fs}, \end{aligned} \tag{6.61}$$

where

ϕ_{reg_fs} = the regenerated phase at the fiducial station antenna reference point [m];

$\tau^{fst}_{rx_fs}$ = the reception time of the GPS transmission in the local clock time frame of the station [s];

$\vec{r}^{\,eci}_{fs}$ = the position vector of the fiducial station antenna phase center in ECI coordinate frame [m];

$t^{ref}_{rx_fs}$ = the reception time of the GPS signal at the fiducial station in the reference time frame [s];

$\vec{r}^{\,eci}_{tx}$ = the position vector of the transmitting GPS satellite antenna reference point in ECI coordinate frame [m];

$t^{ref}_{tx_fs}$ = the transmission time of the GPS signal recorded at the ground station in the reference time frame [s];

P_s = the relativistic correction function for the Shapiro effect for the fiducial station [s];

Δt_{fs} = the clock offset of the fiducial station receiver [s];

Δt_{gps} = the clock offset of the GPS transmitter [s];

ϕ_{ntrl_fs} = the phase delay due to the neutral atmosphere [m];

Table 6.13: The default filtering parameters for phase measurements by the fiducial station.

Parameter	Bandwidth range [Hz]	Elevation range [km]	Polynomial order
B_{sd2}	4 - 4	0 - 90	0
Parameter	**Window length range [samples]**	**Elevation range [km]**	**Polynomial order**
L_{sd2}	4 - 4	0 - 90	0

ϕ_{ion_fs} = the phase delay due to the ionosphere [m];

ϕ_{inst_fs} = the phase delay due to the receiver characteristics [m];

θ_{fs} = the elevation angle of the incoming GPS transmission at the reception antenna [deg];

φ_{fs} = the azimuth angle of the incoming GPS transmission at the reception antenna [deg];

ϕ_{const_fs} = a constant phase offset due to the phase ambiguity [m].

Equation 6.61 assumes that the cycle slips for the ground based measurements have been detected and corrected by the GRAS GSN.

The phase measurements by the fiducial station have to processed in a similar way as the occultation measurements by GRAS before differencing.

(1) Filtering of the phase measurements

The phase measurements shall be filtered using the filtering algorithm defined in Section 6.2.4.1. The default values for the filter parameters are listed in Table 6.13. In the case of the SSD measurements the filter bandwidth and window length are fitted over the elevation angle of the measurement. The order of the polynomials and the coefficients shall be completely user definable.

(2) Removal of instrument characterisation

This is a user selectable function.

If removal of instrument characterisation term is selected for the SSD (Sounding Support Data), the instrument characterisation data is acquired from the GRAS GSN (Ground Support Network) Status and Configuration Database via PGE. The azimuth and elevation angles of the incoming ray are derived at each epoch of the SSD samples applying the algorithm defined in Section 6.1.5.1.

If instrument correction has been selected for SSD, but instrument characterisation data is not available in the GRAS GSN Status and Configuration Database, or any input information for performing the instrument characterisation is missing, the data processing continued without instrument characterisation, the corresponding bit in SSD_AVAILABILITY bit string is set in the level 1b products (see **AD4**), event of user configurable severity to the CGS via the PGE interface is raised, and the measurement id number and error characterization information is added in the report of the dump processing.

The instrument characterisation term is removed by subtraction

$$\phi_{ic_fs}\left(t_{rx}^{fst}\right) = \phi_{reg_fs}\left(\tau_{rx}^{fst}\right) - \Lambda_{fs}\left(\theta_{fs}\left(t_{rx}^{fst}\right), \varphi_{fs}\left(t_{rx}^{fst}\right), CH\right), \tag{6.62}$$

where

Λ_{fs} = the impact of the antenna phase center on the measured phase [rad];

θ_{fs} = the zenith angle of the incoming ray [deg];

φ_{fs} = the azimuth angle of the incoming ray [deg];

The set of measurements can now be labeled as

$$\left\{\left(\phi_{reg_fs}(k), \phi_{ic_fs}(k), \tau_{rx_fs}^{fst}(k)\right) \; ; \; k : 1 \rightarrow N\right\}$$

(3) Fiducial Station Time (FST) to reference time conversion

The clock offset estimate $\Delta t_{fs}\left(t^{ref}\right)$ provided by the GRAS GSN defines the offset between the local station time used for the measurement data time stamping and the reference time. The SSD data time stamps are converted to reference time as

$$t_{rx_fs}^{ref}(m) = \tau_{rx_fs}^{fst}(m) - \Delta t_{fs}(m), \tag{6.63}$$

where

Δt_{fs} = the clock offset estimate from GSN products interpolated to the time of the SSD sample m [m].

The determination of the time stamps in reference time allows expansion of the labeling as

$$\left\{\left(\phi_{reg_fs}(k), \phi_{ic_fs}(k), \tau_{rx_fs}^{fst}(k), t_{rx_fs}^{ref}(k)\right) \; ; \; k : 1 \rightarrow N\right\}.$$

(4) Transmission time determination

The transmission time of the signal measured by the fiducial station is determined by iterating the equation

$$t_{tx_fs*}^{ref} = t_{rx_fs}^{ref} - \frac{\left|\vec{r}_{fs}^{eci}\left(t_{rx_fs}^{ref}\right) - \vec{r}_{tx}^{eci}\left(t_{tx_fs*}^{ref}\right)\right|}{c} - G_{rel_fs}\left[\vec{r}_{fs}^{eci}\left(t_{rx_fs}^{ref}\right), \vec{r}_{tx}^{eci}\left(t_{tx_fs*}^{ref}\right)\right], \quad (6.64)$$

where

$t_{tx_fs*}^{ref}$ = the estimate of the transmit time of the signal received by the fiducial station [s];

P_s = the function for the relativistic delay caused by the Shapiro effect [s];

$\vec{r}_{fs}^{eci}$ = the position vector of the fiducial station antenna reference point in ECI coordinate frame [s];

$\vec{r}_{tx}^{eci}$ = the position vector of the transmitting GPS satellite antenna phase center in ECI coordinate frame [m].

The function $P_s(\vec{r}_1, \vec{r}_2)$ for calculating the Shapiro effect is given in Equation 6.52 in Section 6.2.2.1. In the case of a fiducial station, the Equation 6.52 is applied by using $r_0 = |\vec{r}_2^{eci}| = |\vec{r}_{fs}^{eci}|$.

The position vector of the fiducial station antenna reference point is provided in ECEF coordinate frame as $\vec{r}_{fs}^{ecef}$ in the GRAS GSN Status and Configuration Database. The ECEF coordinates are transformed into J2000 ECI coordinate frame using the algorithm explained in Section 6.3.3.4 and interpolated to the reception times of the SSD samples to get $\vec{r}_{fs}^{eci}\left(t_{rx_fs}^{ref}\right)$.

The position vector of the GPS transmission antenna phase center $\vec{r}_{tx_fs}^{eci}$ is calculated using Equation 6.13.

When the iteration has converged

$$t_{tx_fs}^{ref} = t_{tx_fs*}^{ref}. \quad (6.65)$$

The labeling of the measurements can now be expanded to include all time stamps as

$$\left\{\left(\phi_{reg_fs}(k), \phi_{ic_fs}(k), \tau_{rx_fs}^{fst}(k), t_{rx_fs}^{ref}(k), t_{tx_fs}^{ref}(k)\right) \; ; \; k : 1 \rightarrow N\right\}.$$

(5) Geometrical path length determination

Having established the reference times of transmission and reception, the geometrical path terms can now be determined as

$$\begin{aligned}\phi_{gp_fs}\left(t^{ref}_{rx_fs}\right) &= \left|\vec{r}^{\,eci}_{fs}\left(t^{ref}_{rx_fs}\right) - \vec{r}^{\,eci}_{tx}\left(t^{ref}_{tx_fs}\right)\right| \\ &\quad + cP_s\left[\vec{r}^{\,eci}_{fs}\left(t^{ref}_{rx_fs}\right), \vec{r}^{\,eci}_{tx}\left(t^{ref}_{tx_fs}\right)\right],\end{aligned}$$

where

ϕ_{gp_fs} = the phase delay due to the geometrical path length including Shapiro effect [rad];

$\vec{r}^{\,eci}_{tx}\left(t^{ref}_{tx_fs}\right)$ = the position vector of the phase center of the occulting GPS antenna interpolated to the transmission time $t^{ref}_{tx_fs}$ using the interpolation algorithm is defined in Section 6.3.1.1 [m].

The labeling of the measurements can now be expanded to

$$\left\{\left(\phi_{reg_fs}(k), \phi_{gp_fs}(k), \phi_{ic_fs}(k), \tau^{fst}_{rx_fs}(k), t^{ref}_{rx_fs}(k), t^{ref}_{tx_fs}(k)\right) \; ; \; k : 1 \rightarrow N\right\}.$$

(6) Estimating the neutral atmosphere delay

The delay caused by the neutral atmosphere is provided by the GRAS GSN as TZD (Tropospheric Zenith Delay) estimate. The user can select in the software setup between two options for using the TZD estimates:

1. The TZD estimate closest to the epoch of the first measurement sample is used for processing all samples;
2. The TZD is interpolated to the time of each measurement sample using the last available TZD estimate before the measurement and the next TZD estimate after the measurement epoch.

If the time between the epoch of the closest available TZD estimate and the epoch of any measurement sample is between user selectable threshold values defined in Table 6.14, the data processing is continued with the available TZD estimates, an appropriate error flag is set in the level 1b products, event of user configurable severity to the CGS via the PGE interface is raised, and the measurement id number and error characterization information is added in the report of the dump processing.

If the closest available TZD estimate is outside the threshold time range defined in Table 6.14 or the TZD uncertainty is larger than a user selectable threshold value defined in Table 6.14, TZD values from the GRAS GSN products are not used in the neutral atmosphere delay estimation. In this case the zenith delay estimate is derived as defined in Section 6.3.5, the corresponding bit in SSD_AVAILABILITY bit string is set in the level 1b products (see **AD4**), and an event of user configurable severity to the CGS via the PGE interface shall be raised. The measurement id number and error characterization information are also added in the report of the dump processing.

Table 6.14: The user selectable parameters for the TZD derivation.

Parameter	Default value
Fixed TZD or linear interpolation between two estimates	fixed
Minimum TZD epoch time distance	15 min
Maximum TZD epoch time distance	120 min
Maximum acceptable TZD uncertainty	1 cm

The elevation of the incoming ray at the fiducial station $\varepsilon_{fs}\left(t^{ref}_{rx_fs}\right)$ is derived as defined in Section 6.3.4.

The delay caused by the neutral atmosphere is calculated by multiplying the TZD with the mapping function as

$$\begin{aligned}\phi_{ntrl_fs}\left(t^{ref}_{rx_fs}\right) &= \Delta L_{tot}\left(t^{ref}_{rx_fs}\right) \\ &= \Delta L^0_h\left(t^{ref}_{rx_fs}\right) m_h\left(t^{ref}_{rx_fs}\right) + \Delta L^0_w\left(t^{ref}_{rx_fs}\right) m_w\left(t^{ref}_{rx_fs}\right),\end{aligned} \tag{6.66}$$

where

$$\Delta L^0_w\left(t^{ref}_{rx_fs}\right) = TZD\left(t^{ref}_{rx_fs}\right) - \Delta L^0_h,$$

and

ϕ_{ntrl_fs} = the delay caused by the neutral atmosphere [rad];

ΔL^0_h = the zenith hydrostatic delay estimated using the algorithm in Section 6.3.5.2 [m];

TZD = the tropospheric zenith delay [m];

m_h = the hydrostatic mapping function defined in Section 6.3.5.1;

m_w = the wet mapping function defined in Section 6.3.5.1.

The labeling of the measurements can again be expanded to

$$\left\{\left(\phi_{reg_fs}(k), \phi_{ntrl_fs}(k), \phi_{gp_fs}(k), \phi_{ic_fs}(k), \tau^{fst}_{rx_fs}(k), t^{ref}_{rx_fs}(k), t^{ref}_{tx_fs}(k)\right) \; ; \; k : 1 \rightarrow N\right\}.$$

Table 6.15: The default filtering parameters for ionosphere compensation.

Parameter	Bandwidth range [Hz]	Elevation range [km]	Polynomial order
B_{ionc}	0.1 - 0.1	0 - 90	0
Parameter	**Window length range [samples]**	**Elevation range [km]**	**Polynomial order**
L_{ionc}	4 - 4	0 - 90	0

(7) Estimating the ionosphere delay

The GPS carrier phase advance caused by the ionosphere can be estimated from the pseudorange measurement at L1 and L2. The pseudorange measurements have to be filtered using the filtering algorithm defined in Section 6.2.4.1. The default values for the filter parameters are listed in Table 6.12. The order of the polynomials and the coefficients shall be completely user definable. In the case of the SSD measurements the filter bandwidth and window length are fitted over the elevation angle of the measurement.

The phase advances for measurements at L1 and L2 are estimated as

$$\phi^{l1}_{ion_fs}\left(t^{ref}_{rx_fs}\right) = -\frac{f_2^2}{f_1^2 - f_2^2}\left(\left\langle p_2\left(t^{ref}_{rx_fs}\right)\right\rangle_{B_{diff}} - \left\langle p_1\left(t^{ref}_{rx_fs}\right)\right\rangle_{B_{diff}}\right), \tag{6.67}$$

$$\phi^{l2}_{ion_fs}\left(t^{ref}_{rx_fs}\right) = -\frac{f_1^2}{f_1^2 - f_2^2}\left(\left\langle p_2\left(t^{ref}_{rx_fs}\right)\right\rangle_{B_{diff}} - \left\langle p_1\left(t^{ref}_{rx_fs}\right)\right\rangle_{B_{diff}}\right), \tag{6.68}$$

where

$\phi^{l1}_{ion_fs}$ = the phase advance on L1 [rad];

$\phi^{l2}_{ion_fs}$ = the phase advance on L2 [rad];

f_1 = the GPS frequency at L1 [Hz];

f_2 = the GPS frequency at L2 [Hz];

p_1 = the pseudorange measurement at L1 [m];

p_2 = the pseudorange measurement at L2 [m];

$\langle\rangle_{B_{diff}}$ = indicates low pass filtering to the cutoff frequency B_{diff}.

(8) Determining the phase residual

The equation for the phase measurement by the fiducial station can now be written taking into account the compensation for the geometrical path length, neutral atmosphere, and ionosphere as

$$\phi_{res_fs}\left(t^{ref}_{rx_fs}\right) = \phi_{ic_fs}\left(t^{ref}_{rx_fs}\right) - \phi_{gp_fs}\left(t^{ref}_{rx_fs}\right) - \phi_{ntrl_fs}\left(t^{ref}_{rx_fs}\right) - \phi_{ion_fs}\left(t^{ref}_{rx_fs}\right), \quad (6.69)$$

where

ϕ_{res_fs} = the residual phase at the fiducial station [m].

The labeling of the measurements can again be expanded to

$$\left\{\left(\phi_{res_fs}(k), \phi_{reg_fs}(k), \phi_{ntrl_fs}(k), \phi_{gp_fs}(k), \phi_{ic_fs}(k), \tau^{fst}_{rx_fs}(k), t^{ref}_{rx_fs}(k), t^{ref}_{tx_fs}(k)\right) \; ; \; k : 1 \rightarrow N\right\}.$$

(9) Interpolating to the occultation measurement times

The phase residuals at the fiducial station at the times of the occultation measurements $\phi_{res_fs}\left(t^{ref}_{rx}\right)$ are derived by linear interpolation from the measurements $\phi_{res_fs}\left(t^{ref}_{rx_fs}\right)$ providing a new labeling for the synchronized occultation measurements and the interpolated phase measurements of the pivot satellite as

$$\left\{\left(\phi_{atm}(m), \phi_{res_fs}(m), t^{ref}_{rx}(m)\right) \; ; \; m : 1 \rightarrow M\right\}.$$

(10) Differencing the occultation measurement

Applying the interpolated phase values from step (9) the equation for the phase residual after SD2 correction can be written as

$$\phi_{sd2}\left(t^{ref}_{rx}\right) = \phi_{atm}\left(t^{ref}_{rx}\right) - \phi_{res_fs}\left(t^{ref}_{rx}\right), \quad (6.70)$$

A user selectable option is to subtract the GRAS clock offset estimate Δt_{gras} derived in the NRT POD and the fiducial ground station clock offset estimate Δt_{fs}provided by the GSN from the SD2 corrected phase residual ϕ_{sd2}. The user can select to remove just the GRAS clock offset or the fiducial clock offset, or both. The mathematical formulation for the enhanced SD1 correction with the subtraction is

$$\phi_{sd2} = \phi_{sd2}\left(t^{ref}_{rx}\right) - c\left[\Delta t_{gras}\left(t^{ref}_{rx}\right) - \Delta t_{fs}\left(t^{ref}_{rx}\right)\right], \quad (6.71)$$

where $\phi_{sd2}\left(t^{ref}_{rx}\right)$ is the output from Equation 6.59.

The labeling of the final products from the SD2 function can now the expanded as

$$\left\{\left(\phi_{sd2}(m), \phi_{atm}(m), \phi_{res_fs}(m), \Delta t_{gras}(m), \Delta t_{fs}(m), t^{ref}_{rx}(m)\right) \; ; \; m : 1 \rightarrow M\right\}.$$

6.2.2.5 Double Differencing 1 (DD1) clock correction

Input Parameter:

1. Relativity corrected phase residual measurements $\phi_{atm}(t_{rx}^{ref})$ [rad];
2. GRAS GZA phase measurements $\phi_{reg_gza}\left(\tau_{rx_gza}^{imt}\right)$ [rad];
3. Fiducial ground station phase measurement $\phi_{reg_fs}\left(\tau_{rx_fs}^{fst}\right)$ [rad];
4. Pivot satellite phase measurement by the fiducial ground station $\phi_{reg_pv}\left(\tau_{rx_fs}^{fst}\right)$ [rad];
5. Metop CoM position vector in ECI coordinate frame $\vec{r}_{leo}^{eci}\left(t_{rx_gza}^{ref}\right)$ [m];
6. Position vector of the Metop CoM in SRF coordinate frame $\vec{r}_{com}^{srf}\left(t_{rx_gza}^{ref}\right)$ [m];
7. Position vector of the occulting GPS satellite CoM in ECI frame $\vec{r}_{gps}^{eci}\left(t_{rx_fs}^{ref}\right)$ [m];
8. Position vector of the occulting GPS antenna phase center in the local GPS satellite reference frame $\vec{p}_{tx}\left(t_{rx_fs}^{ref}\right)$ [m];
9. Position vector of the pivot GPS satellite CoM in ECI frame $\vec{r}_{gps}^{eci}\left(t_{rx_gza}^{ref}\right)$ [m]:
10. Position vector of the pivot GPS antenna phase center in the local GPS satellite reference frame $\vec{p}_{tx}\left(t_{rx_gza}^{ref}\right)$ [m];
11. GRAS clock offset from the GRAS/Metop NRT POD $\Delta t_{gras}\left(t^{ref}\right)$ [s];
12. Pivot GPS clock offset from the GRAS/Metop NRT POD $\Delta t_{gps_pv}\left(t^{ref}\right)$ [s];
13. Occulting GPS clock offset from the GRAS/Metop NRT POD $\Delta t_{gps}\left(t^{ref}\right)$ [s];
14. Fiducial station clock offset from the GRAS/Metop NRT POD $\Delta t_{fs}\left(t^{ref}\right)$ [s];
15. Code phase measurements by GZA at L1-P1 $CP_{rc_p1}\left(t_{rx_gza}^{ref}\right)$ and L2-P2 $CP_{rc_p2}\left(t_{rx_gza}^{ref}\right)$ [chips];
16. Pseudorange measurement by the fiducial station at L1 $p_{1_occ}\left(t_{rx_fs}^{ref}\right)$ and L2 $p_{2_occ}\left(t_{rx_fs}^{ref}\right)$ [m];
17. Pseudorange measurement by the fiducial station at L1 $p_{1_pv}\left(t_{rx_fs}^{ref}\right)$ and L2 $p_{2_pv}\left(t_{rx_fs}^{ref}\right)$ [m];
18. Position vector of the fiducial station antenna phase center in ECEF coordinate frame $\vec{r}_{fs}^{ecef}$ [m].

Output Parameters:

1. DD1 corrected phase residual $\phi_{dd1}\left(t_{rx}^{ref}\right)$ [rad];
2. Interpolated reference measurements $\phi_{res_gza}\left(t_{rx}^{ref}\right)$ [rad];
3. Interpolated reference measurement $\phi_{res_fs}\left(t_{rx}^{ref}\right)$ [rad];
4. Interpolated reference measurement $\phi_{res_pv}\left(t_{rx}^{ref}\right)$ [rad];
5. Interpolated occulting GPS clock offset estimates $\Delta t_{gps}\left(t_{rx}^{ref}\right)$ [s];
6. Interpolated pivot GPS clock offset estimates $\Delta t_{gps_pv}\left(t_{rx}^{ref}\right)$ [s];
7. Interpolated fiducial station clock offset estimate $\Delta t_{fs}\left(t_{rx}^{ref}\right)$ [s].

Constants:

1. GPS transmission frequencies f_{gps} (L1 and L2).

The DD1 correction uses four measurements to differentiate out all clock offset terms from the equations for the regenerated phases. The main task in the DD2 algorithm is to pre-process all reference measurements by the fiducial ground station and GRAS GZA so that they can be interpolated to the times of the occultation measurements.

Using the same labeling of the measurements as in Figure 3.5, the processing of all measurement links are defined below.

(1) Link A: Occultation measurement by GRAS GVA or GAVA

The processing of the occultation data is performed as defined in Section 5.2.2 using DD1 clock offset removal option. The residual phase measurement after step (4) can be labeled as

$$\left\{\left(\phi_{atm}(m), t_{rx}^{ref}(m)\right)\ ;\ m:1\rightarrow M\right\}.$$

(2) Link B: Reference measurement by the fiducial ground station

The processing of the occulting GPS satellite phase data from the fiducial ground station is performed as in the case of SD2 correction as defined in Section 6.2.2.4. Only steps (1) to (9) are performed to generate interpolated data set that allows expansion of the measurement sample labeling as

$$\left\{\left(\phi_{atm}(m), \phi_{res_fs}(m), t_{tx}^{ref}(m)\right)\ ;\ m:1\rightarrow M\right\}.$$

(3) Link D: Measurement of the pivot GPS satellite by GRAS GZA

The processing of the pivot satellite phase data from GRAS GZA is performed as in the case of SD1 correction as defined in Section 6.2.2.3. Only steps (1) to (7) are performed to generate interpolated data set that allows further expansion of the labeling as

$$\left\{ \left(\phi_{atm}(m), \phi_{res_fs}(m), \phi_{res_gza}(m), t_{tx}^{ref}(m) \right) \; ; \; m : 1 \rightarrow M \right\}.$$

(4) Link C: Measurement of the pivot GPS satellite by the fiducial ground station

The processing of the pivot satellite phase data from the fiducial ground station follows the SD2 algorithm defined in Section 6.2.2.4. The differences in the input data in the case of processing pivot satellite phase measurements are:

1. $\vec{r}_{gps}^{eci}$ = the position vector of the pivot GPS satellite CoM;
2. $\vec{p}_{tx}$ = the position vector of the pivot GPS satellite antenna phase center in the local satellite reference frame;
3. Δt_{gps} = the clock offset estimate of the pivot GPS satellite from GRAS/Metop NRT POD.

Obviously the incidence angle for the incoming ray has to be calculated in the case of link C for the pivot satellite and not for the occulting GPS satellite.

The steps (1) to (9) of the SD2 algorithm applied on the pivot satellite measurement allow further expansion of the measurement data labeling as

$$\left\{ \left(\phi_{atm}(m), \phi_{res_fs}(m), \phi_{res_gza}(m), \phi_{res_pv}(m), t_{tx}^{ref}(m) \right) \; ; \; m : 1 \rightarrow M \right\}.$$

(5) Differencing the occultation measurement

The double differencing of the data from the four measurements can now be written as

$$\begin{aligned} \phi_{dd1}\left(t_{rx}^{ref}\right) &= \phi_{atm}\left(t_{rx}^{ref}\right) - \phi_{res_fs}\left(t_{rx}^{ref}\right) - \left(\phi_{res_gza}\left(t_{rx}^{ref}\right) - \phi_{res_pv}\left(t_{rx}^{ref}\right)\right) \\ &= \phi_{atm}\left(t_{rx}^{ref}\right) - \phi_{res_fs}\left(t_{rx}^{ref}\right) - \phi_{res_gza}\left(t_{rx}^{ref}\right) + \phi_{res_pv}\left(t_{rx}^{ref}\right). \end{aligned} \tag{6.72}$$

6.2.2.6 Double Differencing 2 (DD2) clock correction

Input Parameter:

1. Relativity corrected phase residual measurements $\phi_{atm}(t_{rx}^{ref})$ [rad];
2. GRAS GZA phase measurements $\phi_{reg_gza}\left(\tau_{rx_gza}^{imt}\right)$ [rad];

3. Fiducial station 1 phase measurement $\phi_{reg_fs}\left(\tau^{fst}_{rx_fs}\right)$ [rad];
4. Pivot satellite phase measurement by the fiducial station 2 $\phi_{reg_pv}\left(\tau^{fst}_{rx_fs}\right)$ [rad];
5. Metop CoM position vector in ECI coordinate frame $\vec{r}^{eci}_{leo}\left(t^{ref}_{rx_gza}\right)$ [m];
6. Position vector of the Metop CoM in SRF coordinate frame $\vec{r}^{srf}_{com}\left(t^{ref}_{rx_gza}\right)$ [m];
7. Position vector of the occulting GPS satellite CoM in ECI frame $\vec{r}^{eci}_{gps}\left(t^{ref}_{rx_fs}\right)$ [m];
8. Position vector of the occulting GPS antenna phase center in the local GPS satellite reference frame $\vec{p}_{tx}\left(t^{ref}_{rx_fs}\right)$ [m];
9. Position vector of the pivot GPS satellite CoM in ECI frame $\vec{r}^{eci}_{gps}\left(t^{ref}_{rx_gza}\right)$ [m];
10. Position vector of the pivot GPS antenna phase center in the local GPS satellite reference frame $\vec{p}_{tx}\left(t^{ref}_{rx_gza}\right)$ [m];
11. GRAS clock offset from the GRAS/Metop NRT POD $\Delta t_{gras}\left(t^{ref}\right)$ [s];
12. Pivot GPS clock offset from the GRAS/Metop NRT POD $\Delta t_{gps_pv}\left(t^{ref}\right)$ [s];
13. Occulting GPS clock offset from the GRAS/Metop NRT POD $\Delta t_{gps}\left(t^{ref}\right)$ [s];
14. Fiducial station 1 clock offset from the GRAS/Metop NRT POD $\Delta t_{fs1}\left(t^{ref}\right)$ [s];
15. Fiducial station 2 clock offset from the GRAS/Metop NRT POD $\Delta t_{fs2}\left(t^{ref}\right)$ [s];
16. Code phase measurements by GZA at L1-P1 $CP_{rc_p1}\left(t^{ref}_{rx_gza}\right)$ and L2-P2 $CP_{rc_p2}\left(t^{ref}_{rx_gza}\right)$ [chips];
17. Pseudorange measurement by the fiducial station 1 at L1 $p_{1_occ}\left(t^{ref}_{rx_fs}\right)$ and L2 $p_{2_occ}\left(t^{ref}_{rx_fs}\right)$ [m];
18. Pseudorange measurement by the fiducial station 2 at L1 $p_{1_pv}\left(t^{ref}_{rx_fs}\right)$ and L2 $p_{2_pv}\left(t^{ref}_{rx_fs}\right)$ [m];
19. Position vector of the fiducial station 1 antenna phase center in ECEF coordinate frame $\vec{r}^{ecef}_{fs1}$ [m];
20. Position vector of the fiducial station 2 antenna phase center in ECEF coordinate frame $\vec{r}^{ecef}_{fs2}$ [m].

Output Parameters:

1. DD1 corrected phase residual $\phi_{dd1}\left(t_{rx}^{ref}\right)$ [rad];
2. Interpolated reference measurement by GZA $\phi_{res_gza}\left(t_{rx}^{ref}\right)$ [rad];
3. Interpolated reference measurement by fiducial station 1 $\phi_{res_fs}\left(t_{rx}^{ref}\right)$ [rad];
4. Interpolated reference measurement by fiducial station 2 $\phi_{res_pv}\left(t_{rx}^{ref}\right)$ [rad];
5. Interpolated occulting GPS clock offset estimate $\Delta t_{gps}\left(t_{rx}^{ref}\right)$ [s];
6. Interpolated pivot GPS clock offset estimate $\Delta t_{gps_pv}\left(t_{rx}^{ref}\right)$ [s];
7. Interpolated fiducial station 1 clock offset estimate $\Delta t_{fs}\left(t_{rx}^{ref}\right)$ [s];
8. Interpolated fiducial station 2 clock offset estimate $\Delta t_{fs}\left(t_{rx}^{ref}\right)$ [s].

Constants:

1. GPS transmission frequencies f_{gps} (L1 and L2).

The DD2 correction uses four measurements to differentiate out clock offset terms from the equations for the regenerated phases. The difference between DD2 and DD1 is that two fiducial ground stations are used to collect the data. The station 1 measures the occulting GPS satellite and station 2 measures the pivot GPS satellite. This approach may provide some advantage in the selection of the stations and pivot satellite as it allows more freedom in the optimisation of the elevation angles of the incoming rays. However, the penalty from applying DD2 is that the errors caused by the fiducial station clock offsets are not removed from the measurement data.

Formally the treatment of the measurements from links A - D is in the case of DD2 exactly the same as in the case of DD1. The only difference is that in the processing of the link B in the input data the reception antenna phase center position vector is $\vec{r}_{fs1}^{ecef}$ for station 1 and for the link D the position vector is $\vec{r}_{fs2}^{ecef}$ for station 2, respectively.

A user definable option is to use the clock offset estimates Δt_{fs1} and Δt_{fs2} provided by the GRAS GSN to remove the clock offset terms from the phase residual measurement. The user can select to remove either of the fiducial clock offsets, or both. The mathematical formulation for the enhanced SD1 correction with the subtraction is

$$\phi_{dd2} = \phi_{dd2}\left(t_{rx}^{ref}\right) - c\left[\Delta t_{fs1}\left(t_{rx}^{ref}\right) - \Delta t_{fs2}\left(t_{rx}^{ref}\right)\right], \tag{6.73}$$

where $\phi_{dd2}\left(t_{rx}^{ref}\right)$ is the output from DD2 correction without subtraction of the fiducial station clock offsets.

Following the steps (1) to (4) of the DD1 algorithm produces a set of interpolated data samples labeled as

$$\left\{\left(\phi_{atm}(m), \phi_{res_fs}(m), \phi_{res_gza}(m), \phi_{res_pv}(m), t_{tx}^{ref}(m)\right) \; ; \; m : 1 \rightarrow M\right\}.$$

The double differencing of the samples can now be written exactly in the same form as for DD1 as

$$\begin{aligned}\phi_{dd2}\left(t_{rx}^{ref}\right) &= \phi_{atm}\left(t_{rx}^{ref}\right) - \phi_{res_fs}\left(t_{rx}^{ref}\right) - \left(\phi_{res_gza}\left(t_{rx}^{ref}\right) - \phi_{res_pv}\left(t_{rx}^{ref}\right)\right) \\ &= \phi_{atm}\left(t_{rx}^{ref}\right) - \phi_{res_fs}\left(t_{rx}^{ref}\right) - \phi_{res_gza}\left(t_{rx}^{ref}\right) + \phi_{res_pv}\left(t_{rx}^{ref}\right). \end{aligned} \tag{6.74}$$

6.2.2.7 Correction for the Earth's oblateness

Input Parameters:

1. Position vectors of the occulting GPS satellite $\vec{r}_{tx}^{eci}\left(t_{rx}^{ref}\right)$;
2. Position vectors of Metop $\vec{r}_{ant}^{eci}\left(t_{rx}^{ref}\right)$;
3. Reference ellipsoid semimajor axis R_{eq} and flattening f_e.

Output Parameter:

1. Oblateness corrected satellite antenna phase center position vectors $\vec{r}_{tx}^{eci}\left(t_{rx}^{ref}\right)$ and $\vec{r}_{ant}^{eci}\left(t_{rx}^{ref}\right)$;
2. Geocentric radius of the ellipsoid R_g;
3. Radius of the curvature vector $\vec{r}_c^{eci}$;
4. Coordinate system origin translation vector $\Delta\vec{r}^{eci}\left(t_{rx}^{ref}\right)$.

Algorithm:

The coordinates of the occulting GPS satellite and Metop satellite have to be corrected for the error caused by the assumption of spherical atmosphere before calculating the total bending angle [**RD9**]. This correction is done by creating a new spherical atmosphere approximation with the local radius of the curvature of the WGS-84 ellipsoid as the radius of the spherical atmosphere and by moving the origin of the spherical atmosphere to the point that corresponds to this radius and normal to the local curvature of the ellipsoid.

Let the surface of the reference ellipsoid in a Cartesian coordinates to be defined as

$$S(x,y,z) = \sqrt{x^2+y^2+z^2} - R(x,y,z) = 0, \tag{6.75}$$

where

x, y, z = the coordinates of a point on the surface;

$R_g(x,y,z)$ = the geocentric radius of the ellipsoid at the coordinates x, y, z.

R_g can be defined as a function of the co-latitude θ_{co} as

$$R_g = R_{eq}\left(1 - f cos^2\theta_{co}\right), \tag{6.76}$$

where

R_{eq} = the semimajor axis of the reference ellipsoid;

f = the Earth's flattening;

and

$$\theta_{co} = \arcsin\left(\frac{z}{\sqrt{x^2+y^2+z^2}}\right). \tag{6.77}$$

A vector normal to the surface of the ellipsoid at the coordinates (x, y, z) can be estimated to first order in f from

$$\vec{n}_s^{eci} = \hat{r}_R^{eci} - 2 f_e z_{r_R} \begin{pmatrix} x_{r_R} z_{r_R} \\ y_{r_R} z_{r_R} \\ z_{r_R}^2 - 1 \end{pmatrix}, \tag{6.78}$$

where x_{r_R}, y_{r_R}, and z_{r_R} are components of a unit vector $\hat{r}_R^{eci}$ pointing in the direction of the local geocentric radius.

The radius vector of the curvature in the occultation plane $\vec{r}_c^{eci}$ is found from

$$\vec{r}_c^{eci} = \frac{\vec{n}_s^{eci}}{|d\vec{n}_s^{eci}/ds|}. \tag{6.79}$$

The derivative $d\vec{n}_s^{eci}/ds = d\left(\nabla S\right)/ds$ can be calculated from

$$\frac{d\vec{n}_s^{eci}}{d\vec{s}} = \mathbf{J_s}\hat{n}_p, \tag{6.80}$$

where $\hat{n}_p$ is a unit vector parallel to the surface in the occultation plane. As the first order approximation in f , matrix $\mathbf{J_s}$ becomes

$$\mathbf{J_s} = \frac{1}{R_{eq}} \begin{pmatrix} 1 - x_{r_R}^2 - f_e z_{r_R}^2(1 - 7x_{r_R}^2) & -x_{r_R} y_{r_R}(1 - 7 f_e z_{r_R}^2) & -x_{r_R} z_{r_R}(1 + f_e(4 - 7z_{r_R}^2)) \\ -x_{r_R} y_{r_R}(1 - 7 f_e z_{r_R}^2) & 1 - y_{r_R}^2 - f_e z_{r_R}^2(1 - 7y_{r_R}^2) & -y_{r_R} z_{r_R}(1 + f_e(4 - 7z_{r_R}^2)) \\ -x_{r_R} z_{r_R}(1 + f_e(4 - 7z_{r_R}^2)) & -y_{r_R} z_{r_R}(1 + f_e(4 - 7z_{r_R}^2)) & (1 - z_{r_R}^2)(1 + f_e(2 - 7z_{r_R}^2)) \end{pmatrix} \tag{6.81}$$

The unit vector is a vector parallel to the line connecting the two satellites at the moment when the line is tangential to the surface of the ellipsoid.

The origin of the new spherical atmospheric approximation can now be found with a vector sum as

$$\Delta\vec{r}^{eci} = R_g \hat{r}_R^{eci} - \vec{r}_c^{eci} \tag{6.82}$$

The satellite position vectors are transferred to the new coordinate system by translation with the vector $\Delta\vec{r}^{eci}$.

The definition of the location of the origin of the new coordinate system is not unique as the position of the ray perigee and the local curvature or the ellipsoid is slowly changing during the occultation. The time of the coordinate transfer is fixed by using the time and point when the line connecting the two satellites is tangential to the surface of the ellipsoid.

6.2.3 Geometrical optics retrieval functions

The Geometrical Optics (GO) approximation is used to derive the total bending angle in conditions when there is little atmospheric multipath. It is also used to derive initialization parameters for Back Propagation technique that is presented in Section 6.2.4.2.

6.2.3.1 Derivation of the Doppler shifts

Input Parameters:

1. Noise filtered phase residuals $\phi_{lp}(m)$;
2. Reception times of the phase residual samples $t_{rx}^{ref}(m)$.

Output Parameter:

1. Atmospheric Doppler $D_{atm}(m)$;
2. Reception times of the Doppler samples $t_{rx-der}^{ref}(m)$.

Algorithm:

The atmospheric Doppler is calculated from the corrected phase residuals as

$$D_{atm}(m) = \left.\frac{d\phi}{dt}\right|_{t=t_{rxd}^{ref}(m)} = \frac{\phi_{lp}(m+1) - \phi_{lp}(m)}{t_{rx}^{ref}(m+1) - t_{rx}^{ref}(m)}, \tag{6.83}$$

where

$$t_{rx-der}^{ref}(m) = \frac{t_{rx}^{ref}(m+1) - t_{rx}^{ref}(m)}{2},$$

and where $m : 1 \rightarrow N-1$.

6.2.3.2 Total bending angle retrieval

Input Parameters:

1. Atmospheric Doppler residual D_{atm};
2. Position vector of the occulting GPS satellite transmission antenna phase center $\vec{r}_{tx}^{eci}\left(t_{tx}^{ref}\right)$;
3. Position vector of the GRAS receiving antenna phase center $\vec{r}_{ant}^{eci}\left(t_{rx}^{ref}\right)$;
4. Velocity vector of the occulting GPS satellite transmission antenna phase center $\vec{v}_{tx}^{eci}\left(t_{tx}^{ref}\right)$;
5. Velocity vector of the GRAS receiving antenna phase center $\vec{v}_{ant}^{eci}\left(t_{rx}^{ref}\right)$;
6. Radius of the curvature $\vec{r}_{c}^{eci}$.

Output Parameters:

1. Total bending angle $\alpha\left(t_{rx}^{ref}\right)$;
2. The angles of the occultation geometry in geometrical optics approximation $\beta\left(t_{rx}^{ref}\right)$, $\delta\left(t_{rx}^{ref}\right)$, $\gamma\left(t_{rx}^{ref}\right)$, $\Theta\left(t_{rx}^{ref}\right)$ and $\psi\left(t_{rx}^{ref}\right)$.

Constants:

1. GPS transmission frequencies $f_{l1} = 1.57542$ GHz and $f_{l2} =$1.2276 GHz
2. Speed of light in vacuum c

Algorithm:

The Doppler components of the signal received by the GRAS instrument can be formed into the equation

$$\begin{aligned} 0 \;=\; & \frac{\left[\left(\vec{v}_{ant}^{eci}\left(t_{rx}^{ref}\right)-\vec{v}_{tx}^{eci}\left(t_{tx}^{ref}\right)\right)\cdot\left(\vec{r}_{ant}^{eci}\left(t_{rx}^{ref}\right)-\vec{r}_{tx}^{eci}\left(t_{tx}^{ref}\right)\right)\right]}{\left|\vec{r}_{ant}^{eci}\left(t_{rx}^{ref}\right)-\vec{r}_{tx}^{eci}\left(t_{tx}^{ref}\right)\right|} \\ & +\left(\vec{v}_{tx}^{eci}\left(t_{tx}^{ref}\right)\cdot\hat{r}_{2}^{eci}\left(t_{tx}^{ref}\right)+\vec{v}_{ant}^{eci}\left(t_{rx}^{ref}\right)\cdot\hat{r}_{1}^{eci}\left(t_{rx}^{ref}\right)\right) \\ & +D_{atm}\left(t_{rx}^{ref}\right), \end{aligned} \tag{6.84}$$

where

f_{gps} = the transmission frequency of the GPS (for processing of the L1 channel $f_{gps} = f_{l1}$ and for L2 channel $f_{gps} = f_{l2}$) [Hz];

$\vec{r}_{ant}^{eci}$ = the position vector of the phase center of the receiving antenna in ECI coordinate frame [m];

$\vec{r}_{tx}^{eci}$ = the position vector of the phase center of the transmitting antenna in ECI coordinate frame [m];

$\vec{v}_{ant}^{eci}$ = the velocity vector of the phase center of the receiving antenna in ECI coordinate frame [m/s];

$\vec{v}_{tx}^{eci}$ = the velocity vector of the phase center of the transmitting antenna in ECI coordinate frame [m/s];

$\hat{r}_2^{eci}$ = a unit vector parallel to the ray leaving the occulting GPS satellite antenna;

$\hat{r}_1^{eci}$ = a unit vector anti-parallel to the incoming ray at the reception antenna at GRAS instrument.

The position and velocity vectors of the GVA antenna $\left(\vec{r}_{gva}^{eci}, \vec{v}_{gva}^{eci}\right)$ are used for $\vec{r}_{ant}^{eci}$ and $\vec{v}_{ant}^{eci}$ when a rising occultation is processed. The position and velocity vectors of the GAVA antenna $\left(\vec{r}_{gava}^{eci}, \vec{v}_{gava}^{eci}\right)$ are used for $\vec{r}_{ant}^{eci}$ and $\vec{v}_{ant}^{eci}$ in the case of processing of a setting occultation.

We may define a new coordinate basis, which depends on the transmission and reception times as

$$\vec{r}_{con} = \vec{r}_{ant}^{eci}\left(t_{rx}^{ref}\right) - \vec{r}_{tx}^{ref}\left(t_{tx}^{ref}\right)$$

$$\hat{x} = \frac{\vec{r}_{con}}{|\vec{r}_{con}|}$$

$$\hat{z} = -\frac{\left(\vec{r}_{tx}^{eci}\left(t_{tx}^{ref}\right) \times \hat{x}\right)}{\left|\vec{r}_{tx}^{ref}\left(t_{tx}^{ref}\right)\right|} \tag{6.85}$$

$$\hat{y} = \hat{z} \times \hat{x}$$

In this coordinate system the unit vector parallel to the direction the ray leaving transmitting antenna, the unit vector anti-parallel to the direction the ray arrives at the receiving antenna and the cosine of the bending angle are given by the equations

$$\hat{r}_2^{eci}\left(t_{tx}^{ref}\right) = \cos(\delta)\hat{x} + \sin(\delta)\hat{y} \tag{6.86}$$

$$\hat{r}_1^{eci}\left(t_{rx}^{ref}\right) = -\cos(\gamma)\hat{x} + \sin(\gamma)\hat{y} \tag{6.87}$$

and

$$\cos(\alpha) = \cos(\delta + \gamma) = -\hat{r}_1^{eci} \cdot \hat{r}_2^{eci} \tag{6.88}$$

where

δ = the angle between the straight line between the antennas and the ray leaving the transmitter antenna [rad];

γ = the angle between the straight line between the antennas and the incoming ray to the receiver antenna [rad];

α = the total bending angle of the ray path [rad].

The Equation 6.84 may now be re-written with the new coordinates as

$$\begin{aligned} 0 &= \vec{v}_{tx} \cdot \hat{x} \cos(\delta) + \vec{v}_{tx} \cdot \hat{y} \sin(\delta) \\ &\quad -\vec{v}_{ant} \cdot \hat{x} \cos(\gamma) + \vec{v}_{ant} \cdot \hat{y} \sin(\gamma) \\ &\quad + (\vec{v}_{ant} - \vec{v}_{tx}) \cdot \hat{x} \\ &\quad + D_{atm}. \end{aligned} \tag{6.89}$$

This equation has two unknowns, namely δ and γ, and thus can not be solved. It is therefore necessary to impose an equation of constraint relating these two angle. This is done by assuming that the impact parameters for the rays on either side of the atmosphere are equal or, equivalently, that equal amounts of bending occur on either side of the position where the ray direction is normal to a line from the centre of the Earth (the tangent radius). Thus the equation of constraint is

$$\begin{aligned} a &= a_{gps} = a_{leo} \\ &= \vec{r}_{ant}^{\,eci}\left(t_{rx}^{ref}\right) \sin(\gamma + \psi) \\ &= \vec{r}_{tx}^{\,ref}\left(t_{tx}^{ref}\right) \sin(\delta + \beta), \end{aligned} \tag{6.90}$$

where

$$\beta = \pi - \arccos\left(\frac{\hat{x} \cdot \vec{r}_{tx}^{\,eci}\left(t_{tx}^{ref}\right)}{\left|\vec{r}_{tx}^{\,eci}\left(t_{tx}^{ref}\right)\right|}\right),$$

and

$$\psi = \arccos\left(\frac{\hat{x} \cdot \vec{r}_{ant}^{\,eci}\left(t_{rx}^{ref}\right)}{\left|\vec{r}_{ant}^{\,eci}\left(t_{rx}^{ref}\right)\right|}\right).$$

The bending angle may now be solved by Newton's method (or by an alternative optimisation technique). Using Newton's method we iterate the following equations starting with an initial guess for the value of γ_0 with the equations

$$\delta_n = \arcsin\left(\frac{\left|\vec{r}_{ant}^{eci}\left(t_{rx}^{ref}\right)\right|}{\left|\vec{r}_{tx}^{eci}\left(t_{tx}^{ref}\right)\right|}\sin\left(\gamma_n + \psi\right)\right) - \beta \tag{6.91}$$

$$\gamma_{n+1} = \gamma_n - \frac{\Lambda\left(\gamma_n\right)}{\left(\left.\frac{d\Lambda}{d\gamma}\right|_{\gamma=\gamma_n}\right)}.$$

The objective function and its derivative with respect to γ are given by

$$\begin{aligned}\Lambda(\gamma) \quad = \quad & \vec{v}_{tx}\cdot\hat{x}\cos(\delta) + \vec{v}_{tx}\cdot\hat{y}\sin(\delta) \\ & -\vec{v}_{ant}\cdot\hat{x}\cos(\gamma) + \vec{v}_{ant}\cdot\hat{y}\sin(\gamma) \\ & +\left(\vec{v}_{ant} - \vec{v}_{tx}\right)\cdot\hat{x} \\ & +D_{atm}\end{aligned} \tag{6.92}$$

$$\begin{aligned}\frac{d\Lambda}{d\gamma} \quad = \quad & -\vec{v}_{tx}\cdot\hat{x}\sin(\delta)\frac{d\delta}{d\gamma} + \vec{v}_{tx}\cdot\hat{y}\cos(\delta)\frac{d\delta}{d\gamma} \\ & +\vec{v}_{ant}\cdot\hat{x}\sin(\gamma) + \vec{v}_{ant}\cdot\hat{y}\cos(\gamma)\end{aligned}$$

where

$$\frac{d\delta}{d\gamma} = \frac{\frac{\left|\vec{r}_{ant}^{eci}\left(t_{rx}^{ref}\right)\right|}{\left|\vec{r}_{tx}^{eci}\left(t_{tx}^{ref}\right)\right|}\cos\left(\gamma+\psi\right)}{\sqrt{1-\left(\frac{\left|\vec{r}_{ant}^{eci}\left(t_{rx}^{ref}\right)\right|}{\left|\vec{r}_{tx}^{eci}\left(t_{tx}^{ref}\right)\right|}\right)^2\sin^2\left(\gamma+\psi\right)}}$$

After the iteration has converged the total bending angle α can be calculated from γ and δ using Equation 6.88.

The impact parameter is calculated from α using Equation 6.93.

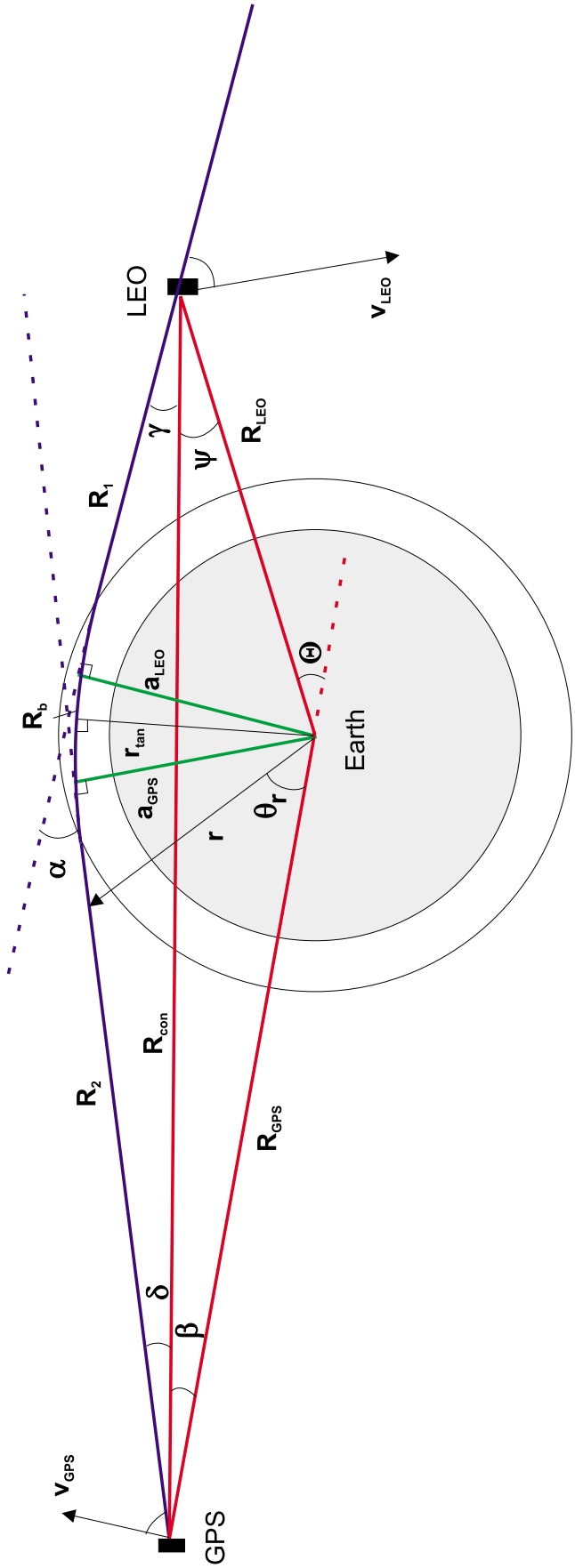

Figure 6.1: The occultation geometry for GO solution of the total bending angles.

6.2.3.3 Derivation of the impact parameter

Input Parameters:

1. Position vector of the phase center of the receiving antenna $\vec{r}_{ant}^{eci}\left(t_{rx}^{ref}\right)$;
2. Corresponding observation geometry angle $\gamma\left(t_{rx}^{ref}\right)$, and $\psi\left(t_{rx}^{ref}\right)$.

Output Parameter:

1. Impact parameter $a\left(t_{rx}^{ref}\right)$.

Algorithm:

The impact parameter is derived using the observation geometry as

$$a\left(t_{rx}^{ref}\right) = \left|\vec{r}_{ant}^{eci}\left(t_{rx}^{ref}\right)\right| \cdot \sin(\gamma\left(t_{rx}^{ref}\right) + \psi\left(t_{rx}^{ref}\right)). \tag{6.93}$$

6.2.3.4 Geolocation function

Input Parameters:

1. Receiving antenna phase center position vector $\vec{r}_{ant}^{eci}\left(t_{rx}^{ref}\right)$;
2. Transmitting antenna phase center position vector $\vec{r}_{tx}^{eci}\left(t_{rx}^{ref}\right)$;
3. Coordinate system translation vector from Earth oblateness correction function $\Delta\vec{r}^{eci}\left(t_{rx}^{ref}\right)$;
4. Corresponding observation geometry angle $\gamma\left(t_{rx}^{ref}\right)$, and $\psi\left(t_{rx}^{ref}\right)$;
5. Bending angle $\alpha\left(t_{rx}^{ref}\right)$;
6. Impact parameter $a\left(t_{rx}^{ref}\right)$;
7. Reference ellipsoid semimajor axis and flattening.

Output Parameter:

1. Geodetic latitude and longitude of the ground projection of the ray perigee $\varphi_p\left(t_{rx}^{ref}\right)$ and $\lambda_p\left(t_{rx}^{ref}\right)$.

Algorithm:

A unit vector pointing from origin of the coordinate frame after oblateness correction $\hat{r}_{tan}^{eci}\left(t_{rx}^{ref}\right)$ (Section 6.2.2.7) to the ray perigee is calculated from

$$\vec{r}_{tan}^{eci}\left(t_{rx}^{ref}\right) = \frac{\sin\left(\gamma\left(t_{rx}^{ref}\right)+\psi\left(t_{rx}^{ref}\right)\right)}{cos\left(\frac{\alpha\left(t_{rx}^{ref}\right)}{2}\right)} \cdot \left[cos\left(\frac{\alpha\left(t_{rx}^{ref}\right)}{2}+\theta_{a1}\left(t_{rx}^{ref}\right)\right)\hat{r}_{rx}^{eci}\left(t_{rx}^{ref}\right)+sin\left(\frac{\alpha\left(t_{rx}^{ref}\right)}{2}+\theta_{a1}\left(t_{rx}^{ref}\right)\right)\hat{r}_{\perp}^{eci}\left(t_{rx}^{ref}\right)\right], \tag{6.94}$$

where

$$\theta_{a1}\left(t_{rx}^{ref}\right) = \arccos\left(\frac{\left|\vec{a}^{eci}\left(t_{rx}^{ref}\right)\right|}{\left|\vec{r}_{rx}^{eci}\left(t_{rx}^{ref}\right)\right|}\right),$$

$$\left(t_{rx}^{ref}\right) = \frac{\vec{r}_{rx}^{eci}\left(t_{rx}^{ref}\right)}{\left|\vec{r}_{rx}^{eci}\left(t_{rx}^{ref}\right)\right|},$$

and

$$\hat{r}_{\perp}^{eci}\left(t_{rx}^{ref}\right) = \frac{\vec{r}_{rx}\left(t_{rx}^{ref}\right)\times\left[\vec{r}_{tx}^{eci}\left(t_{tx}^{ref}\right)\times\vec{r}_{rx}\left(t_{rx}^{ref}\right)\right]}{\left|\vec{r}_{rx}\left(t_{rx}^{ref}\right)\times\left[\vec{r}_{tx}^{eci}\left(t_{tx}^{ref}\right)\times\vec{r}_{rx}\left(t_{rx}^{ref}\right)\right]\right|}.$$

The unit vector point to the direction of the ray perigee is

$$\hat{r}_{tan}^{eci}\left(t_{rx}^{ref}\right) = \frac{\vec{r}_{tan}^{eci}\left(t_{rx}^{ref}\right)}{\left|\vec{r}_{tan}^{eci}\left(t_{rx}^{ref}\right)\right|}. \tag{6.95}$$

The geolocation of the ray perigee is the point where a vector parallel to $\hat{r}_{tan}$ passes through the ellipsoid surface of the Earth model.

Vector $\hat{r}_{tan}^{eci}\left(t_{rx}^{ref}\right)$ from Equation 6.95 can be expressed in the form

$$\hat{r}_{tan}^{eci}\left(t_{rx}^{ref}\right) = a_r\hat{x}+b_r\hat{y}+c_r\hat{z}. \tag{6.96}$$

The length k of the vector parallel to $\hat{r}_{tan}^{eci}\left(t_{rx}^{ref}\right)$ and reaching the surface of the ellipsoid can be found from

$$k = \sqrt{\frac{a_e^2\left(1-f_e\right)^2}{\left(1-f_e\right)^2\left(a_r^2+b_r^2\right)+c_r^2}}, \tag{6.97}$$

where a_r, b_r, and c_r are the coefficients from Equation 6.96.

The position vector of the geolocation of the ray perigee as a function of the reference time are then found from

$$\bar{r}_{geo}^{eci}\left(t_{rx}^{ref}\right) = \Delta\bar{r}^{eci}\left(t_{rx}^{ref}\right) + k\left(t_{rx}^{ref}\right)\hat{r}_{tan}^{eci}\left(t_{rx}^{ref}\right).$$

The geocentric coordinates of the estimated geolocation are transformed into Earth fixed coordinate frame (ITRF) by inverting the ECEF to ECI transform algorithm described in Section 6.3.3.4.

Finally, the geodetic latitude, longitude, and height of the geolocation coordinates are derived using the iterative algorithm defined in Section 6.3.3.3.

6.2.3.5 TEC derivation

Input Parameters:

1. Observed phase residuals $\phi_{uw1}(t)$, $\phi_{uw2}(t)$;
2. Measured code phases $CP_{rc_p1}(t)$, $CP_{rc_p2}(t)$;
3. GPS transmission frequencies f_{L1} and f_{L2};

Output Parameters:

1. TEC as a function of impact parameter $TEC(a)$

Algorithm:

The relative TEC shall be calculated as a linear combination of phase observations at L1 and L2 as

$$TEC_r = \frac{1}{d}\frac{f_{L1}^2 f_{L2}^2}{\left(f_{L1}^2 - f_{L2}^2\right)}(\phi_{uw1} - \phi_{uw2}) + B, \tag{6.98}$$

where

d = a constant corresponding to the square of the plasma frequency divided by the electron density ($= e^2/(4\pi^2\varepsilon_0 m) = 40.3$;

B = the undetermined bias which is constant for a connected arc.

The absolute TEC without bias but with a high noise level shall be calculated from the linear combination of the code phase measurements at L1-P1 and L2-P2 as

$$TEC_a = \frac{1}{d}\frac{f_{L1}^2 f_{L2}^2}{\left(f_{L1}^2 - f_{L2}^2\right)}\left[\frac{c}{10230 \cdot 10^3}\left(CP_{rc_p1} - CP_{rc_p2}\right)\right]. \tag{6.99}$$

In 6.98 and in 6.99 the phase and code phase samples must be interpolated to the same moments of time using the interpolation algorithm presented in 6.3.1.2.

The constant B is solved by a least-squares minimizing of

$$\sum (TEC_a - TEC_r)^2. \tag{6.100}$$

Derivation of the TEC is not performed when the receiver can not track both L1 and L2 phase and code.

The impact parameters corresponding to each TEC estimate are derived by interpolating the impact parameter time series from Equation 6.93 to the times of the TEC estimates.

6.2.3.6 Ionosphere correction

Input Parameters:

1. Total bending angle as a function of the impact parameter $\alpha_i(a_i)$;
2. GPS transmission frequencies f_{L1} and f_{L2}.

Output Parameters:

1. Ionosphere corrected total bending angle as a function of the impact parameter $\alpha(a_1)$.

Neutral bending angle calculation:

The ionosphere corrected bending angle shall be calculated as

$$\alpha(a_1) = \langle \alpha_1(a_1) \rangle_{BW_n} + \left(\frac{f_{L2}^2}{f_{L1}^2 - f_{L2}^2} \left(\langle \alpha_1(a_1) \rangle_{BW_i} - \langle \alpha_2(a_1) \rangle_{BW_i} \right) \right), \tag{6.101}$$

where

α	= the neutral bending angle [rad];
α_k	= the total bending from the phase residual at the GPS channel Lk [rad];
a_1	= the impact parameter from L1 [m];
BW_n	= the observation bandwidth of the neutral atmosphere [Hz];
BW_i	= the observation bandwidth of the ionosphere [Hz].

Table 6.16: The default parameters for noise filtering in GO algorithm.

Parameter	Bandwidth range [Hz]	SLTH range [km]	Polynomial order
B_n	4 - 4	80 - 25	0
B_n	2 - 2	25 - -80	0
B_i	0.1 - 0.1	80 - -80	0
Parameter	**Window length range [samples]**	**SLTH range [km]**	**Polynomial order**
L_n	40	80 - -80	0
L_i	40	80 - -80	0

The total bending angles from L2 shall be interpolated to a_1 heights before applying Equation 6.101 with interpolation technique specified in 6.3.1.2.

The observation bandwidths for α_1 and α_2 are achieved by low-pass filtering the data with the filtering function defined in Section 6.2.4.1. The filtering parameters shall be defined so that the the filter bandwidths meet to the observation bandwidth requirements in **RD20**. The default values for the filtering parameters are listed in Table 6.16.

The bandwith range column shows the bandwidth parameter B_{go} and window length L_{go} values corresponding to the SLTH values in the SLTH range column. The filtering function shall perform a polynomial fit to generate a polynomial function of the defined order (in the polynomial order column) so that the B_{go} and L_{go} values and the SLTH values match. The range columns can contain more than two values (e.g. bandwidth range 4 - 3 - 2, and corresponding SLTH range 80 - 45 - 20) for higher order polynomials. The order of the polynomials and the coefficients shall be completely user definable.

The order of the polynomials and the coefficients shall be completely user definable.

The ionosphere correction using Equation 6.101 is not possible if sounding data from both channels is not available. This situation may happen in the troposphere where the phase lock on L2 channel is lost due to lower SNR ratio. When L2 is not available, the ionospheric correction is performed by first calculating the ionosphere ionosphere correction term

$$\frac{f_{L2}^2}{f_{L1}^2 - f_{L2}^2}\left(\langle\alpha_1(a_1)\rangle_{BW_i} - \langle\alpha_2(a_1)\rangle_{BW_i}\right)$$

for the range where both signals are available. This correction term shall then be extrapolated to the height range when only L1 is available. Any ringing effects caused by the noise in the data at the beginning or at the end of the extrapolated ionosphere correction term must be filtered before the correction is applied.

6.2.3.7 Bending angle bias estimation and correction

Input Parameters:

1. Neutral bending angle as a function of the impact parameter $\alpha(a)$.

Output Parameters:

1. Bias corrected bending angle as a function of the impact parameter $\alpha_{bc}(a)$;
2. Bias estimate $\Delta\alpha_{mean}$;
3. Standard deviation of the bias estimate $\sigma_{\Delta\alpha}$.

Algorithm:

It is expected that at least sometimes the derived bending angles shall contain bias from clock errors, satellite velocity determination errors in POD, and from other sources.

The magnitude of the bias shall be estimated by comparing the derived neutral bending angles to bending angles derived from an atmospheric model at the location and the time of the occultation. The characterization of the atmospheric model and model input parameters shall be used in the bias estimation are presented in Table 6.17. All parameters for the bending bias correction are user definable. If the window half width is set to 0, bias estimation and correction is not performed.

Table 6.17: Default parameters for the bending angle bias correction model.

Parameter	Value
Bias comparison height:	70 km
Bias comparison window half width:	5 km
Atmospheric model:	MSISE90
Model input parameters:	
Profile lat, long, ephemeris	from geolocation
F107A, F107, AP:	default

The MSISE90 model is described in [**RD10**].

The MSISE90 model produces the temperature, and pressure at the selected altitude, location, and solar time. The location of the profile is provided by geolocation function that is described in Section 6.2.3.4.

The reference bending angle from the atmospheric model shall be derived using the inverse of the Abel transform as

$$\alpha_m(a) = -2a \int_a^\infty \frac{1}{n\sqrt{\mu^2 - a^2}} \left(\frac{dn}{d\mu}\right) d\mu, \tag{6.102}$$

where

$$\mu = nr,$$

and

n = the index of refraction at the geocentric radial distance r.

Equation 6.102 can be solved by writing it as

$$\alpha(a) = -2a \int_a^\infty \frac{\frac{d \ln n}{dx}}{\sqrt{x^2 - a^2}} dx. \tag{6.103}$$

Equation 6.103 can be simplified by calculating the bending angle between two consecutive height levels j and $j+1$ and by using approximations

$$\frac{d \ln n}{dx} \approx 10^{-6} \frac{dN}{dx}, \tag{6.104}$$

and

$$\sqrt{(x^2 - a^2)} \approx \sqrt{2a\,(x-a)}. \tag{6.105}$$

The dN/dx term in Equation 6.104 can be written as

$$\frac{dN}{dx} = -k_j N_j e^{-k_j(x - x_j)}, \tag{6.106}$$

where

$$k_j = \frac{\ln\left(\frac{N_j}{N_{j+1}}\right)}{x_{j+1} - x_j}. \tag{6.107}$$

The bending angle between the levels j and $j+1$ can now be written as

$$\Delta\alpha = 10^{-6} k_j N_j e^{k_j(x_j - a)} \sqrt{2a} \int_{x_j}^{x_{j+1}} \frac{e^{-k_j(x-a)}}{\sqrt{x-a}} dx. \tag{6.108}$$

This function can be solved analytically using the “error function” (erf) for calculating exponential integrals. The bending angle between two levels can then be written into the form

$$\Delta\alpha = 10^{-6} \sqrt{2\pi a k_j} N_j e^{k_j(x_j - a)} erf\left(\sqrt{k_j\,(x-a)}\right). \tag{6.109}$$

Because the generic definition of the error function is

$$erf(x) = \frac{2}{\sqrt{\pi}} \int_0^x e^{-t^2} dt,$$

the error function for an integral $\int_{x_j}^{x_{j+1}}$ has to be calculated in two parts, i.e.,

$$erf\,(x) = erf\,(x_{j+1}) - erf\,(x_j)\,. \tag{6.110}$$

If the measured bending angle values do not cover the upmost level of the BBE window, the error function must be calculated by extrapolating the $\sqrt{k_j(x-a)}$ term 100 km above the uppermost layer. This can be done simply by adding 100 km to the x_{j+1}term.

The total bending angle is given by summing the $\Delta\alpha$terms from Equation 6.109 for each level within the bias estimation window.

Calculation of the model based bending angle values requires as input an estimate of the atmosphere refractivity. The refractivity of the neutral atmosphere at height h can be estimated from the equation

$$N(h) = k_1 R_d \rho_m(h) + \left(k_2' \frac{e(h)}{T(h)} + k_3 \frac{e(h)}{T(h)^2} \right) Z_w^{-1}, \tag{6.111}$$

k_1, k_2', k_3 = refractivity coefficients;

R_d = gas constant for dry air;

ρ_m = mass density;

e = partial pressure of the water vapor [mbar];

T = temperature;

Z_w^{-1} = the inverse compressibility of moist air.

Because the bias estimation in the GRAS data processing is performed very high in the atmosphere (h > 60 km), the impact of the humidity on the refractivity is negligible. So, in the GRAS bending bias estimation the refractivity of the neutral atmosphere is calculated from the equation

$$N(h) = k_1 R_d \rho_m(h), \tag{6.112}$$

where

k_1 = 77.604 [$K\,mbar^{-1}$];

R_d = 2.87 [$mbar\,m^3 K^{-1}\,kg^{-1}$];

ρ_m = the total mass density from MSISE90 model [kg/m^3].

The refractivity profile estimated with the MSISE90 model must start well below the lower limit of the bending bias estimation window and continue well above the upper limit of the bending bias estimation window to allow the total bending angle integration as described below.

The integration of the total bending angle requires as an input the product of the refractive index at height $n(h)$ and the corresponding radius $r(h)$. This product is calculated from

$$x_j = \left(1 + 10^{-6} N(h)\right) r(h), \tag{6.113}$$

where r is the sum of the geometric height h, local radius of curvature $|\vec{r}_c^{eci}|$, and the difference between the geoid and the WGS-84 ellipsoid (undulation) r_Δ, i.e.,

$$r(h) = h + \left|\vec{r}_c^{eci}\right| + r_\Delta. \tag{6.114}$$

The undulation at the geolocation of the measurement is calculated by using the EGM96 geoid model [http://cddisa.gsfc.nasa.gov/926/egm96/egm96.html] at the mean geolocation of the measurement.

The total bending angle difference is calculated as

$$\Delta\alpha(a) = \alpha(a) - \alpha_m(a), \tag{6.115}$$

where

α = neutral bending angle derived from the observations;

α_m = bending angle derived from the atmospheric model.

The average bending angle bias shall be estimated as

$$\Delta\alpha_{mean} = \frac{1}{N_s} \sum_{i=1}^{N_s} \Delta\alpha_i(a). \tag{6.116}$$

The average bending angle bias shall be estimated for each sample within the window defined in Table 6.17.

The bending angle bias correction shall be performed, if the average bending angle bias is larger than a user definable threshold (default = 0.5 μrad). The bias corrected bending angle is then calculated by subtracting the average bias from all

$$\alpha_{bc}(a) = \alpha(a) - \Delta\alpha_{mean}. \tag{6.117}$$

The standard deviation of the $\Delta\alpha(a)$ shall be used to monitor the quality of the ionosphere corrected bending angles before bias correction.

If a bias correction is performed, the BE_FLAG in MDR-1B is set and the BE_TYPE flag is set to indicate the bias correction type (default is BBE). The bias correction characteristics are included

Table 6.18: Bias estimation parameters and corresponding level 1b product field names.

Parameter	Field name
Bias estimation and correction activated	BE_FLAG
Bias estimation type (default = BBE)	BE_TYPE
Bias comparison height	BE_HEIGHT
Bias comparison window half width:	BE_WINDOW
Atmospheric model:	BE_MODEL
$\Delta\alpha_{mean}$	BE_BIAS_ESTIMATE

into the Level 1b product as defined in **AD4**. The names of the flag and the corresponding bias estimation parameters are listed in Table 6.18.

All level 1b products impacted by the bias corrected bending angle values must be recalculated after the bias correction.

6.2.4 Wave optics retrieval functions

This section describes the wave optics (WO) algorithm that is used for processing the data in the lower stratosphere and troposphere.

6.2.4.1 Noise filtering

Input Parameters:

1. The measured amplitude and excess phase data for each sample (indicated by the time-dependence t), and for both frequencies $E_{ic_1}(t)$, $\phi_{cc_1}(t)$ and $E_{ic_2}(t)$, $\phi_{cc_2}(t)$ (signal amplitudes in V/V and phases in rad). The excess phase being defined as the measured phase subtracted by the contribution from the direct distance between the satellites. Relativistic corrections corrections and corrections for receiver effects should have been performed.

Output Parameters:

1. Low pass filtered amplitude and excess phase data $E_1(t)$, $\phi_1(t)$ and $E_2(t)$, $\phi_2(t)$.

A user selectable option is to low-pass filter the phase residual and amplitude data before back-propagation.

The phase data is low-pass filtered by

$$\phi_i(t) = \left\langle \phi_{cc_i}\left(t_{rx}^{ref}\right)\right\rangle_{B_{bw_wo}\left(t_{rx}^{ref}\right)}, \tag{6.118}$$

where

Table 6.19: The default parameters for noise filtering in WO algorithm.

Parameter	Bandwidth range [Hz]	SLTH range [km]	Polynomial order
B_{wo}	2 - 2	25 - -80	0
B_{i_wo}	0.1 - 0.1	25 - -80	0
Parameter	**Window length range [samples]**	**SLTH range [km]**	**Polynomial order**
L_{wo}	40	25 - -80	0
L_{i_wo}	40	25 - -80	0

ϕ_{cc_i} = the clock corrected phase residual of the GPS channel i;

ϕ_i = the low-pass filtered phase residual;

B_{bw_wo} = the bandwidth of the phase residual filter in WO algorithm.

The filtering of the amplitude data is defined as

$$E_i(t) = \left\langle E_{ic_i}\left(t_{rx}^{ref}\right)\right\rangle_{B_{bw_wo}\left(t_{rx}^{ref}\right)}, \tag{6.119}$$

where

E_{ic_i} = the instrument corrected amplitude of the GPS channel i;

E_i = the low-pass filtered amplitude;

B_{bw_wo} = the bandwidth of the phase residual filter in WO algorithm.

The filter bandwidth is determined by user definable polynomials $B_{wo}\left(t_{rx}^{ref}\right)$ and $L_{wo}\left(t_{rx}^{ref}\right)$ as described in the detailed description of the low-pass filter function and filter parameters in Section 6.3.6.1. The default parameters for the polynomials are defined in Table 5.3. The order of the polynomials and the coefficients shall be completely user definable.

6.2.4.2 Back-propagation

Diffraction correction with back propagation algorithm shall be used to derive total bending angle in the lower stratosphere and in the troposphere to avoid degradation of the product quality due to atmospheric multipath propagation. This algorithm has been presented in **RD 8**.

Input Parameters:

1. The measured amplitude and excess phase data for each sample (indicated by the time-dependence t), and for both frequencies $E_1(t)$, $\phi_1(t)$ and $E_2(t)$, $\phi_2(t)$ (signal amplitudes in V/V and phases in rad). The excess phase being defined as the measured phase subtracted by the contribution from the direct distance between the satellites. Relativistic corrections corrections and corrections for receiver effects should have been performed;

2. For each sample: The position vector of the GPS satellite ($x_G(t)$, $y_G(t)$, $z_G(t)$) (at the transmission time) and the position vector of the LEO satellite ($x_L(t)$, $y_L(t)$, $z_L(t)$) (at the reception time);

3. From the geometrical optics inversion algorithm the displacement of the center of refractivity from the center of the coordinate system $d\vec{r}$ and the local radius of curvature of the earth $\vec{r}_c^{eci}$;

4. From the geometrical optics inversion algorithm the ionosphere corrected bending angle $\alpha(t)$ and the corresponding impact parameter $a(t)$.

Output Parameter:

1. The back-propagated bending angle as a function of impact parameter for both frequencies $\alpha_{b,i}(\xi_S)$, $a_{b,i}(\xi_S)$;

2. The back-propagated phase residual $\Psi_i(\xi_S)$ and amplitude $A_i(\xi_S)$;

3. The position vector of the GPS satellite ($x_{1,G}(t)$, $y_{1,G}(t)$, $z_{1,G}(t)$) and LEO satellite ($x_{1,L}(t)$, $y_{1,L}(t)$, $z_{1,L}(t)$) in the BP coordinate frame;

4. Center of curvature ξ_R, z_R , $y_{1,R}$;

5. Local radius of curvature R_c.

Constants:

1. The GPS frequencies f_1 and f_2;

2. The speed of light in free space c;

3. The signal wave length in free space defined as $\lambda_1 = c/f_1$ and $\lambda_2 = c/f_2$;

4. The wave number in free space $k_1 = 2\pi/\lambda_1$ and $k_2 = 2\pi/\lambda_2$;

5. The earth's oblateness factor f = 0.0033528.

The derivation of the total bending angle with back-propagation is performed in three phases that are 1) Calculation of a new coordinate system, 2) Calculation of the back-propagation integral, and 3) Calculation of the total bending angle. The algorithm below assumes that the observations are arranged as in a setting occultation, i.e., the first sample is the top most sample.

Note: The mathematical notation in this section does not follow the common notation in the rest of the document.

Algorithm:

Calculation of the new coordinate system

For each sample in the occultation the angles $\varphi(t)$ and $\theta(t)$ are calculated from

$$tan\varphi(t) = \frac{z_G(t)y_L(t) - y_G(t)z_L(t)}{z_G(t)x_L(t) - x_G(t)z_L(t)}, \tag{6.120}$$

and

$$tan\theta(t) = \frac{y_G(t)x_L(t) - x_G(t)y_L(t)}{(z_G(t)x_L(t) - x_G(t)z_L(t))\,cos\varphi(t) - (y_G(t)z_L(t) - z_G(t)y_L(t))\,sin\varphi(t)}. \tag{6.121}$$

For $\varphi(t)$ and $\theta(t)$

$$-\frac{\pi}{2} < \varphi < \frac{\pi}{2} \tag{6.122}$$

$$-\frac{\pi}{2} < \theta < \frac{\pi}{2} \tag{6.123}$$

The GPS coordinates in the rotated coordinate system are be given by the transform

$$\begin{bmatrix} x_{1,G}(t) \\ y_{1,G}(t) \\ z_{1,G}(t) \end{bmatrix} = \begin{bmatrix} cos\varphi(t) & sin\varphi(t) & 0 \\ -sin\varphi(t)cos\theta(t) & cos\varphi(t)cos\theta(t) & -sin\theta(t) \\ -sin\varphi(t)sin\theta(t) & cos\varphi(t)sin\theta(t) & cos\theta(t) \end{bmatrix} \begin{bmatrix} x_G(t) \\ y_G(t) \\ z_G(t) \end{bmatrix} \tag{6.124}$$

and LEO coordinates will be given by

$$\begin{bmatrix} x_{1,L}(t) \\ y_{1,L}(t) \\ z_{1,L}(t) \end{bmatrix} = \begin{bmatrix} cos\varphi(t) & sin\varphi(t) & 0 \\ -sin\varphi(t)cos\theta(t) & cos\varphi(t)cos\theta(t) & -sin\theta(t) \\ -sin\varphi(t)sin\theta(t) & cos\varphi(t)sin\theta(t) & cos\theta(t) \end{bmatrix} \begin{bmatrix} x_L(t) \\ y_L(t) \\ z_L(t) \end{bmatrix}. \tag{6.125}$$

Then the parameters of the ellipse are calculated from

$$a_0(t) = R_{eq}, \tag{6.126}$$

and

$$b_0(t) = \frac{R_{eq}}{\sqrt{sin^2\theta(t) + \frac{1}{(1-f)^2}cos^2\theta(t)}}. \tag{6.127}$$

The candidates of the x_1 coordinate of the tangent point $x^{\mp}_{1,t}(t)$ is

$$
\begin{aligned}
x_{1,t}^{\mp}(t) &= \frac{1}{\left(z_{1,G}^2(t) + \frac{b_0^2(t)}{a_0^2(t)} x_{1,G}^2(t)\right)} \left(b_0^2(t) x_{1,G}(t)\right. \\
&\mp \left.\sqrt{b_0^4(t) x_{1,G}^2(t) + \left(z_{1,G}^2(t) + \frac{b_0^2(t)}{a_0^2(t)} x_{1,G}^2(t)\right)\left(z_{1,G}^2(t) - b_0^2(t)\right) a_0^2(t)}\right) \qquad (6.128)
\end{aligned}
$$

with corresponding $z_{1,t}^{\mp}(t)$ coordinate

$$
z_{1,t}^{\mp}(t) = b_0(t)\sqrt{1 - \frac{\left(x_{1,t}^{\mp}(t)\right)^2(t)}{a_0^2(t)}}. \qquad (6.129)
$$

The correct solution is found from

$$
\left(\left(z_{1,G}(t) - z_{1,t}^{\mp}(t)\right) + \frac{\left(x_{1,G}(t) - x_{1,t}^{\mp}(t)\right) b_0(t) x_{1,t}^{\mp}(t)}{a_0(t)\sqrt{a_0^2(t) - \left(x_{1,t}^{\mp}(t)\right)^2}} \neq 0\right)
$$

$$
\Rightarrow \mathrm{z}_{1,t}^{\mp}(t) = -z_{1,t}^{\mp}(t). \qquad (6.130)
$$

The two possible solutions from 6.128 and 6.130 are $\left(x_{1,t}^{-}(t), z_{1,t}^{-}(t)\right)$ and $\left(x_{1,t}^{+}(t), z_{1,t}^{+}(t)\right)$.
Now if

$$
\sqrt{\left(\mathrm{x}_{1,t}^{-}(t) - x_{1.L}(t)\right)^2 + \left(\mathrm{z}_{1,t}^{-}(t) - z_{1,L}(t)\right)^2} > \sqrt{\left(\mathrm{x}_{1,t}^{+}(t) - x_{1,L}(t)\right)^2 + \left(\mathrm{z}_{1,t}^{+}(t) - z_{1,L}(t)\right)^2}
$$

then

$$
\begin{aligned}
\mathrm{x}_{1,t}(t) &= x_{1,t}^{+}(t) \\
\mathrm{z}_{1,t}(t) &= z_{1,t}^{+}(t)
\end{aligned} \qquad (6.131)
$$

or

$$
\begin{aligned}
\mathrm{x}_{1,t}(t) &= x_{1,t}^{-}(t) \\
\mathrm{z}_{1,t}(t) &= z_{1,t}^{-}(t)
\end{aligned} . \qquad (6.132)
$$

The unit vector $\hat{z}(t)$ defining the z axis is now determined as

$$
\hat{z}(t) = \frac{1}{\sqrt{\left(x_{1,t}(t) - x_{1,G}(t)\right)^2 + \left(z_{1,t}(t) - z_{1,G}(t)\right)^2}} \begin{bmatrix} x_{1,t}(t) - x_{1,G}(t) \\ z_{1,t}(t) - z_{1,G}(t) \end{bmatrix}. \qquad (6.133)
$$

The rotation angle of the $\hat{z}(t)$ with respect to the $\hat{x}_1(t)$ is now given by dot product

$$
cos\nu(t) = \pm\hat{x}_1(t) \cdot \hat{z}(t), \qquad (6.134)
$$

where the positive sign must be used when $z_{1,t}(t) > z_{1,G}(t)$ and the negative sign when $z_{1,t}(t) < z_{1,G}(t)$.

The transformation matrix from $(x_1(t), z_1(t))$ coordinates to $(\xi(t), z(t))$ coordinates is then

$$\begin{bmatrix} \xi_L(t) \\ z_L(t) \end{bmatrix} = \begin{bmatrix} (x_{1,L}(t) - x_{1,t}(t))\, sin\nu(t) - (z_{1,L}(t) - z_{1,t}(t))\, cos\nu(t) \\ (x_{1,L}(t) - x_{1,t}(t))\, cos\nu(t) + (z_{1,L}(t) - z_{1,t}(t))\, sin\nu(t) \end{bmatrix}, \tag{6.135}$$

and

$$z_G(t) = (x_{1,G}(t) - x_{1,t}(t))\, cos\nu(t) + (z_{1,G}(t) - z_{1,t}(t))\, sin\nu(t). \tag{6.136}$$

For the first sample t_0 in the occultation the constant distance to the GPS is defined as

$$z_{G,k} = -z_G(t_0). \tag{6.137}$$

For all samples the corrected distance between the satellites is calculated from

$$R_{LG}(t) = \sqrt{\xi_L^2(t) + (z_L(t) + z_{G,k})^2}. \tag{6.138}$$

The center of refractivity in the (ξ, z, y_1) coordinate system is calculated for the last sample t_N in the occultation as

$$\begin{bmatrix} dr_{1,x} \\ dr_{1,y} \\ dr_{1,z} \end{bmatrix} = \begin{bmatrix} cos\varphi(t_N) & sin\varphi(t_N) & 0 \\ -sin\varphi(t_N)cos\theta(t_N) & cos\varphi(t_N)cos\theta(t_N) & -sin\theta(t_N) \\ -sin\varphi(t_N)sin\theta(t_N) & cos\varphi(t_N)sin\theta(t_N) & cos\theta(t_N) \end{bmatrix} \begin{bmatrix} dr_x \\ dr_y \\ dr_z \end{bmatrix}, \tag{6.139}$$

and

$$\begin{bmatrix} \xi_R \\ z_R \\ y_{1,R} \end{bmatrix} = \begin{bmatrix} (dr_{1,x} - x_{1,t}(t_N))\, sin\nu(t_N) - (dr_{1,z} - z_{1,t}(t_N))\, cos\nu(t_N) \\ (dr_{1,x} - x_{1,t}(t_N))\, cos\nu(t_N) + (dr_{1,z} - z_{1,t}(t_N))\, sin\nu(t_N) \\ dr_{1,y} \end{bmatrix}. \tag{6.140}$$

Calculation of the back-propagation integral

When the receiver is operating in the closed loop mode the position of the back-propagation line S shall be determined from

$$z_b = R_c sin(\alpha_{max}), \tag{6.141}$$

where

R_c = the local radius of the curvature of the Earth from Equation 6.79;

α_{max} = the maximum bending angle for the occultation derived with GO method.

The modified amplitudes and phases for each sample on both channels are calculated from

$$E_{m,i}(t) = E_i(t)/E_i(t_0), \tag{6.142}$$

and

$$\phi_{m,i}(t) = \phi_i(t) - \phi_i(t_0) + k_i\left(R_{LG}(t) - R_{LG}(t_0)\right). \tag{6.143}$$

The slope of the LEO measurement line is determined from

$$p(t) = \frac{dz_L(t)}{d\xi_L(t)}. \tag{6.144}$$

The coordinate x_{SL} along the S_L line is determined for each sample from

$$\begin{aligned} \nu_x(t) &= -arccos\left(\frac{1}{\sqrt{1+p^2(t)}}\right), \quad -\pi < \nu_x(t) < 0 \\ x_{SL}(t) &= \xi_L(t)cos(\nu_x(t)) + \left(z_L(t) - z_L(t_0)\right) sin(\nu_x(t)). \end{aligned} \tag{6.145}$$

The maximum height where the back-propagation integral is calculated is chosen user definable. The default height is 25 km.

$$\xi_{S,max} = 19.0\, km$$

The minimum calculation height is estimated from the minimum impact parameter value from GO solution as

$$\xi_{S,min} = a_{min}(t)/1.0003 - R_e. \tag{6.146}$$

The minimum calculation height shall never be negative, i.e., if $\xi_{S,min} < 0$, then $\xi_{S,min} = 0$.

The back-propagation integral is calculated for each frequency as

$$E_{0,i}(\vec{y}) = \left(\frac{k_i}{2\pi}\right)^{1/2} \int_{\xi_{L,L}}^{\xi_{L,U}} E_i(\vec{x}) \cos\varphi_{xy} \frac{e^{(-ik_i|\vec{x}-\vec{y}|-i\pi/4)}}{|\vec{x}-\vec{y}|^{1/2}} \sqrt{1+p^2} d\xi_L, \tag{6.147}$$

where

$\vec{x}$ = (ξ_L, z_L),

$\vec{y}$ = (ξ_S, z_b),

$E_i(\vec{x})$ = $E_{m,i}(\xi_L)e^{(i\phi_{m,i}(\xi_L))}$,

$$cos\varphi_{xy} = \frac{-(\xi_S-\xi_L)+(z_b-z_L)\frac{1}{p}}{\sqrt{(\xi_S-\xi_L)^2+(z_b-z_L)^2}\sqrt{1+\left(\frac{1}{p}\right)^2}}.$$

The values $E_{m,i}(\xi_l)$, $\phi_{m,i}(\xi_L)$, ξ_L, z_L, and p are derived from their time sampled series $E_{m,i}(t)$, $\phi_{m,i}(t)$, $\xi_L(t)$, $z_L(t)$, and $p(t)$ by linear interpolation between the two samples with $\xi_L(t)$ closest to the actual ξ_L.

The integration limits $\xi_{L,U}$ and $\xi_{L,L}$ are derived from finding $\xi_{L,d0}$ that is determined by

$$\frac{d\phi_{SL}}{dx_{SL}} = 0, \tag{6.148}$$

where [3]

$$\varphi_{SL}(\xi_L, \xi_S) = \phi_{m,1}(\xi_L) - k_1\sqrt{(\xi_L - \xi_S)^2 + (z_L - z_b)^2}. \tag{6.149}$$

The upper limit can now be determined by going from $\xi_L > \xi_{L,d0}$ to find $\xi_{L.U}$ for which

$$\phi_{SL}(\xi_{L,d0}, \xi_S) - \phi_{SL}(\xi_{L.U}, \xi_S) = 10\pi. \tag{6.150}$$

Similarly the lower limit is determined by going from $\xi_L < \xi_{L,d0}$ to find $\xi_{L.L}$ for which

$$\phi_{SL}(\xi_{L,d0}, \xi_S) - \phi_{SL}(\xi_{L.L}, \xi_S) = 10\pi. \tag{6.151}$$

The new value of ξ_S is now determined by

$$\xi_S = \xi_S - 0.005\,\mathrm{km}. \tag{6.152}$$

Calculation of the back-propagated bending angle

The back-propagated bending angle is calculated for all samples on both frequencies where $\xi_{L.L} < \xi_S < \xi_{L.U}$.

Before the bending angle can be calculated, phase unwrapping must be performed for the observed phase residuals. The back propagated signal can be written as

$$E_{0,i}(\xi_Z, z_b) = A_i e^{\left(i\Psi_{E,i}(\xi_S)\right)}. \tag{6.153}$$

Phase unwrapping is performed by going through the phase residual samples starting from $\Psi_{E,i}(\xi_{S,max})$ and adding 2π to the phase ambiguity number N when the phase crosses zero in the anticlockwise direction. The unwrapped phase residual for channel i can then be written as

$$\Psi_i(\xi_S) = \Psi_{E,i}(\xi_S) + 2\pi N.$$

[3]The symbol φ_{SL} in Equation 6.149 may be a typo in the reference document and should probably be ϕ_{SL}.

The total back-propagated bending angle $\alpha_{b,i}(\xi_S)$ and the corresponding impact parameter $a_{b,i}(\xi_S)$ are calculated as

$$\begin{aligned}
&\alpha_{\gamma,i}(\xi_S) = arcsin\left(-\frac{\lambda_i}{2\pi}\frac{d\Psi_i(\xi_S)}{d\xi_S}\right)\\
&a_{\xi_z,i}(\xi_S) = (z_b - z_R)sin\left(\alpha_{\gamma,i}(\xi_S)\right) + (\xi_S - \xi_R)cos\left(\alpha_{\gamma,i}(\xi_S)\right)\\
&a_i(\xi_S) = \sqrt{a_{\xi_z,i}(\xi_S)^2 + y_{1,R}^2}\\
&r_G = \sqrt{\xi_R^2 + (z_{G,k} + z_R)^2 + y_{1,R}^2}\\
&\beta = arcsin\left(\frac{-\xi_R}{r_G}\right)\\
&\gamma_i(\xi_S) = arcsin\left(\frac{a_i(\xi_S)}{r_G}\right) - \beta\\
&\alpha_{b,i}(\xi_S) = \alpha_{\gamma,i}(\xi_S) + \gamma_i(\xi_S)
\end{aligned} \quad . \tag{6.154}$$

6.2.4.3 Phase transform

Input Parameters:

1. The position vector of the GPS satellite antenna phase center $\vec{r}_{tx}\left(t_{tx}\right)$ (at the transmission time) and the position vector of the GRAS antenna phase center $\vec{r}_{rx}\left(t_{rx}\right)$ (at the reception time);
2. The instrument corrected phase residual $\rho_i\left(t\right)$, amplitude $E_i\left(t\right)$, and impact parameter a_i;
3. Center of curvature ξ_R, z_R , $y_{1,R}$;
4. Local radius of curvature $\vec{r}_c^{eci}$;
5. GPS transmission frequencies f_{L1} and f_{L2}.

Output Parameters:

1. The bending angle as a function of the impact parameter for both frequencies $\alpha_i\left(a_i\right)$.

Algorithm

The Phase Transform (PT) algorithm definition is based on **RD25** and **RD26**.

When PT processing is performed for a measurement, the “Phase Matching” bit in the WO_CHARACTERISAT flag is set.

Total bending angle α as a function of impact parameter a is calculated by differentiating the phase of the phase transformed signal $u(a)$ as

$$\alpha(a) = -\frac{d}{da}\left[Phase\left[u(a)\right]\right], \tag{6.155}$$

where

$$Phase\left[u(a)\right] = \arctan\left[\frac{Im\left[u(a)\right]}{Re\left[u(a)\right]}\right].$$

It should be noted that $u(a)$ in Equation 6.155 must be unwrapped as necessary before the phase of the transformed signal can be calculated.

In Equation 6.155 the phase transformed signal $u(a)$ is defined as

$$u(a) = \int_0^T \omega(t)\Omega(t)R(t)e^{-i\Theta(a,t)}dt, \tag{6.156}$$

where $R(t)$ is the complex signal received by GRAS

$$R(t) = E(t)e^{i\rho(t)},$$

and

$$\begin{aligned}\Theta(a,t) \quad = \quad & \frac{2\pi}{\lambda}\left[\sqrt{\left|\vec{r}_{rx}\left(t_{rx}\right)\right|^2 - a^2} + \sqrt{\left|\vec{r}_{tx}\left(t_{tx}\right)\right|^2 - a^2} + a\Gamma\left(t_{rx}\right)\right. \\ & \left. -a\arctan\left(\frac{\sqrt{\left|\vec{r}_{tx}\left(t_{tx}\right)\right|^2 - a^2}}{a}\right) - a\arctan\left(\frac{\sqrt{\left|\vec{r}_{rx}\left(t_{rx}\right)\right|^2 - a^2}}{a}\right)\right],\end{aligned}$$

where

$$\Gamma\left(t_{rx}\right) = \arccos\left[\frac{\vec{r}_{rx}\left(t_{rx}\right)\cdot\vec{r}_{tx}\left(t_{tx}\right)}{\left|\vec{r}_{rx}\left(t_{rx}\right)\right|\cdot\left|\vec{r}_{tx}\left(t_{tx}\right)\right|}\right].$$

Integral function 6.156 can be implemented as a matrix multiplication

$$\begin{bmatrix} u\left[a_0\right] \\ \vdots \\ u\left[a_F\right] \end{bmatrix} = \begin{bmatrix} e^{-i\Theta(a_0,t_0)} & \cdots & e^{-i\Theta(a_0,t_T)} \\ \vdots & \ddots & \\ e^{-i\Theta(a_F,t_0)} & & e^{-i\Theta(a_F,t_T)} \end{bmatrix} \begin{bmatrix} \omega(t_0)\Omega(t_0)R(t_0) \\ \vdots \\ \omega(t_T)\Omega(t_T)R(t_T) \end{bmatrix}, \tag{6.157}$$

where

a_1 = the smallest chosen impact parameter value;

a_F = the largest chosen impact parameter value;

t_0 = the time of the first data sample;

t_T = the time of the last data sample.

The windowing function $\omega(t)$ and amplitude normalisation function $\Omega(t)$ used in Equation 6.157 are

$$\omega(t) = a_h + b_h \cos \frac{2\pi n_s}{N_s - 1}, \tag{6.158}$$

and

$$\Omega(t) = \frac{\bar{A}_0}{\langle Amp\,[R(t)]\rangle}, \tag{6.159}$$

where

n_s = the number of the sample in the data time series;

N_s = the total number of samples;

$\bar{A}_0$ = the amplitude normalisation value;

AMP[R(t)] = the amplitude of $R(t)$, i.e., the amplitude from the measurement data.

$\langle\rangle_w$ = average over a sliding window of w samples.

The average amplitude normalisation value $\bar{A}_0$is calculated over a user selectable number m_w of samples from the beginning of the data (beginning means here the data that corresponds to the highest impact parameter value).

The impact parameter values in the calculation of Equation 6.157 are user selectable. The user shall be able to select the starting impact parameter value a_0, the impact parameter incrementation step Δa, and the end impact parameter value a_F. A regular sampling shall be assumed.

Also all other parameters of the windowing and normalisation functions are user definable. The default parameter values for the phase transform function are provided in Table 6.20.

Table 6.20: Default values for the phase transform function parameters.

Parameter	Default value	Comments
a_1	$\lvert\vec{r}_c^{\,eci}\rvert$	Local radius of curvature
a_F	$\lvert\vec{r}_c^{\,eci}\rvert + 25$km	
Δa	10 m	
m_w	1	
w	1	
a_h	0.54	Hamming window
b_h	0.46	Hamming window

The measurement data becomes very noisy at some impact parameter height near the surface. Thus, the processing with the phase transform function is stopped at the impact parameter height where the estimated phase noise level exceeds a user definable threshold level.

The phase noise estimation is performed by the Generalised Cross Validation (GCV) method. This method follows the usual spline fit approach to minimise the cost function

$$J = \frac{1}{n}\sum_{i=1}^{n}\left[f\left(t_i\right) - y_i\right]^2 + \lambda \int_{t_1}^{t_n}\left[f^m\left(t\right)\right]^2 dt, \tag{6.160}$$

where

y = the "noisy" data;

f = represents the space of the differentiable functions.

The value of the parameter λ in Equation 6.160 is important, because it determines the trade-off between the roughness of the smoothing spline and the goodness-of-fit. In the GCV method the value for the parameter λ is determined by selecting the value that minimises the generalised cross validation function

$$V\left(\lambda\right) = \frac{\frac{1}{n}\left\|\left(\mathbf{I} - \mathbf{A}\left(\lambda\right)\right)\mathbf{y}\right\|^2}{\left[\frac{1}{n}Tr\left(\mathbf{I} - \mathbf{A}\left(\lambda\right)\right)\right]^2}, \tag{6.161}$$

where

$\mathbf{I}$ = an identity matrix;

$\mathbf{A}$ = the influence matrix;

$\mathbf{y}$ = vector containing the data samples $\mathbf{y} = \left(y_1, ..., y_n\right)^T$;

n = the number of data samples.

$Tr()$ = trace of a matrix.

$\|\|$ = L^2-norm over the n-dimensional Euclidean space.

The influence matrix $\mathbf{A}$ in Equation 6.161 is solved from

$$\mathbf{g}_{n,\lambda} = \mathbf{A}(\lambda)\mathbf{y}, \tag{6.162}$$

where $\mathbf{g}_{n,\lambda} = \left(g_{n,\lambda}\left(t_1\right), ..., g_{n,\lambda}\left(t_n\right)\right)^T$, and $g_{n,\lambda}$ is the function minimising the cost function in Equation 6.160.

The phase noise level is estimated by calculating the standard deviation of the phase samples over a sliding window. The length of the window is user definable (default window length is 20 samples). The phase transform is stopped when the standard deviation of the phase data within the window exceeds a user definable threshold in comparison to the standard deviation in the previous window. The default threshold value is 10σ,i.e.,

$$\sigma_k = 10\sigma_{k-1}.$$

The ATM_MULTIPATH flag in MDR-1B is set based on the phase transform results. Currently the "Atmospheric multipath in stratosphere" and "Atmospheric multipath in troposphere" bits in ATM_MULTIPATH are defaulted to unset or zero.

6.2.4.4 Ionosphere correction

Input Parameters:

1. The bending angle as a function of the impact parameter for both frequencies $\alpha_i\,(a_i)$;
2. GPS transmission frequencies f_{L1} and f_{L2};
3.

Output Parameters:

1. Ionosphere corrected total bending angle as a function of the impact parameter $\alpha(a_1)$ [rad];
2.

Algorithm

The ionosphere correction is performed by using the algorithm specified in Section 6.2.3.6.

6.2.5 Combining level 1b products

6.2.5.1 Derivation of smoothed Level 1b products

This section has been removed.

6.2.5.2 Level 1b products quality check

Input Parameters:

1. Satellite state vectors $\vec{r}(t)$, $\vec{v}(t)$
2. Interpolation times t_{int}

Table 6.21: The list of products and the default threshold values for level 1b products quality check.

		Default threshold values		
Product	**Symbol**	**Minimum**	**Maximum**	**Quality flag**
Phase residual L1	ϕ_{lp_l1}	0 m	500 m	PHASE_L1
Phase residual L2	ϕ_{lp_l2}	0 m	500 m	PHASE_L2
Doppler shift L1	D_{atm_l1}	0 Hz	750 Hz	DOPPLER_L1
Doppler shift L2	D_{atm_l2}	0 Hz	750 Hz	DOPPLER_L2
Doppler rate L1	$\frac{D_{atm_l1}}{dt}$	0 Hz/s	25 Hz/s	DOPPLER_RATE_L1
Doppler rate L2	$\frac{D_{atm_l2}}{dt}$	0 Hz/s	25 Hz/s	DOPPLER_RATE_L2
Doppler acceleration L1	$\frac{D_{atm_l1}}{dt^2}$	0 Hz/s^2	1.5 Hz/s^2	DOPPLER_ACC_L1
Doppler acceleration L2	$\frac{D_{atm_l2}}{dt^2}$	0 Hz/s^2	1.5 Hz/s	DOPPLER_ACC_L2
Slant path TEC	TEC	$1 \cdot 10^{11}$ m^{-2}	$500 \cdot 10^{16}$m^{-2}	TEC
Slant path TEC drift	$\frac{TEC}{dt}$	$1 \cdot 10^{11}$ m^{-2}/s	$10 \cdot 10^{16}$ m^{-2}/s	TEC_DRIFT
Slant path TEC acceleration	$\frac{TEC}{dt^2}$	$1 \cdot 10^{11}$ m^{-2}/s^2	$3 \cdot 10^{16}$ m^{-2}/s^2	TEC_ACC
Bending angle L1	α_{l1}	0 rad	0.04 rad	BENDING_L1
Bending angle L2	α_{l2}	0 rad	0.04 rad	BENDING_L2
Ionosphere corrected bending angle	α	0 rad	0.04 rad	NEUTRAL_BENDING
Impact parameter L1	a_{l1}	$6378 \cdot 10^3$ m	$6478 \cdot 10^3$ m	IMPACT_L1
Impact parameter L2	a_{l2}	$6378 \cdot 10^3$ m	$6478 \cdot 10^3$ m	IMPACT_L2

Output Parameters:

1. Satellite state vectors $\vec{r}(t_k)$, $\vec{v}(t_k)$

The quality check of the level 1b products is based on comparing retrieved product to user definable threshold values. The list of checked products and the default threshold values are listed in Table 6.21. Second set of threshold values with special conditions are listed in Table 6.22.

If any of the tested parameters are outside the specified threshold value range, the respective error flag in the level 1b products is set, self explanatory information in the report of the dump processing is added, and events of user configurable severity to the CGS via the PGE interface are raised.

Quality flags that are the same for level 1a and level 1b products are listed in Table 27 in Section 4.4.2 in **AD4**. These flags are set in level 1b products based on the flags in level 1a products.

The A_FLAG, AS_FLAG, and GPS_NAV_HEALTH flags in MDR-1B are set based on the GPS constellation information provided by the GRAS GSN and in MDR-1A-EPHEMERIS.

Table 6.22: Threshold values with special conditions for level 1b quality check.

	Default threshold value			
Product	**Minimum**	**Maximum**	**Condition**	**Quality flag**
Receiver noise estimate				
L1-CA	48 dB/Hz	100 dB/Hz	$a_{l1} \geq 12$ km	L1_CA_STRAT
L1-P1	42 dB/Hz	100 dB/Hz	$a_{l2} \geq 12$ km	L1_P1_STRAT
L2-P2	35 dB/Hz	100 dB/Hz	$a_{l2} \geq 12$ km	L2_P2_STRAT
L1-CA	48 dB/Hz	100 dB/Hz	$a_{l1} < 12$ km	L1_CA_TROP
L1-P1	42 dB/Hz	100 dB/Hz	$a_{l2} < 12$ km	L1_P1_TROP
L2-P2	35 dB/Hz	100 dB/Hz	$a_{l2} < 12$ km	L2_P2_TROP

6.2.5.3 Error characteristics estimation

Input Parameters:

1. All output parameters from the level 1a and level 1b product generation functions.

Output Parameters:

1. Error estimate for the ionosphere corrected bending angle $\delta_\alpha\left(t_{rx}^{ref}\right)$;
2. Error estimate for the impact parameter $\delta_a\left(t_{rx}^{ref}\right)$;
3. Measurement error covariance matrix $\mathbf{M}_\delta$;
4. Reference measurement error covariance matrix index I_M.

The error characteristics estimation shall select an error covariance matrix index based on the characteristics of the measurement data, geolocation, and time of the measurement. While the full algorithm for the error characteristics estimation is under development, the default value for the index I_M is 0. This value shall be used in the ERROR_COVARIANCE_ID in the MDR-1B.

Other outputs from the error characteristics estimation function are set to 0 until the full algorithm is defined.

6.2.5.4 Level 1b products formatting

This function formats the GRAS Level 1b products as defined in **AD4**. There is no mathematical algorithm definition for this function.

6.3 General data processing functions

6.3.1 Interpolation functions

6.3.1.1 Satellite state vector interpolation

Input Parameters:

1. Satellite state vectors $\vec{r}(t)$, $\vec{v}(t)$
2. Interpolation times t_{int}

Output Parameters:

1. Satellite state vectors $\vec{r}(t_k)$, $\vec{v}(t_k)$

The Lagrange method with a user definable order polynomial (the default order of the polynomial is 8th) shall be used for the satellite state vector interpolation.

The equation for an nth order Lagrange polynomial is

$$f_n(x) = \frac{(x-x_1)(x-x_2)\cdots(x-x_n)}{(x_0-x_1)(x_0-x_2)\cdots(x_0-x_n)} \cdot y_0 + \frac{(x-x_0)(x-x_2)\cdots(x-x_n)}{(x_1-x_0)(x_1-x_2)\cdots(x_1-x_n)} \cdot y_1 + \cdots , \tag{6.163}$$

where x represents the time and y represents the components of the vector that is to be interpolated.

This can be expressed in generic form as

$$f_n(x) = \sum_{i=0}^{n} L_i(x) \cdot y_i, \tag{6.164}$$

where

$$L_i(x) = \prod_{\substack{j=0 \\ j \neq i}}^{n} \frac{(x-x_j)}{x_i - x_j}. \tag{6.165}$$

The algorithm must ensure that the time stamps of the original state vectors and the interpolation time t_{int} are in the same time frame.

6.3.1.2 Linear interpolation

Input Parameters:

1. Two points (x_n, y_n) and (x_{n+1}, y_{n+1}) on both sides of the interpolation point;
2. Interpolation point x_{int}.

Output Parameters:

1. Interpolated $y(x_{int})$.

Algorithm

The interpolated value y corresponding to x_{int} is calculated from

$$y(x_{int}) = y_n + \frac{y_{n+1} - y_n}{x_{n+1} - x_n}(x_{int} - x_n). \tag{6.166}$$

6.3.1.3 Bi-cubic interpolation for antenna pattern

Input Parameters:

1. Antenna characterization file in the Instrument Database;
2. Azimuth and elevation of the incidence angle (φ_g, θ_g).

Output Parameters:

1. Complex characterization of the antenna gain pattern $G(\varphi_g, \theta_g)$.

Algorithm

The bi-cubic interpolation is a fit to a cubic polynomial of two measurement points on each side of the desired point. The principle of bi-cubic interpolation is presented in Fig. 6.2. The first interpolation is performed in the "horizontal" dimension indicated by the lines 1 - 4 in the figure. The second iterations is performed in the "vertical" dimension as indicated by the line 5. The data points for interpolation from the database are selected so that the estimated azimuth and elevation of the incidence angle is the innermost azimuth and elevation angle values, i.e., the estimated incidence angle is within the innermost square of the grid.

6.3.2 Time conversion functions

6.3.2.1 UTC to MJD time format conversion

Input Parameters:

1. Time in UTC.

Output Parameters:

1. Time in MJD2000.

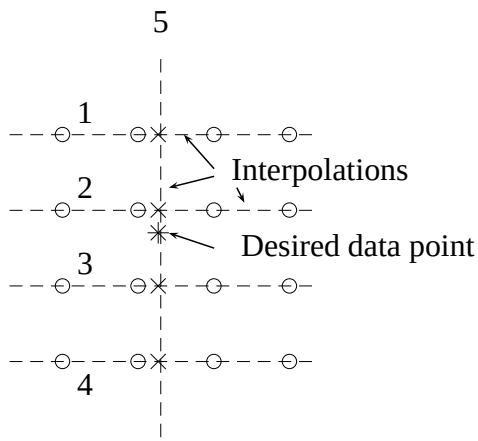

Figure 6.2: The principle of bi-cubic interpolation. The data points in the database are marked with circles and the intermediate data points after the first interpolation are marked with crosses. The final desired data point corresponding to the angles φ_g and θ_g is marked with a star.

Algorithm

The MJD2000 time format is XXXXX.YYYYYYYY, where XXXXX is the integer number of days from 00:00 1st of January 2000, and YYYYYYYY is the fraction of the day.

The UTC time is transformed to MJD2000 by

$$t[MJD2000] = (YYYY - 2000) \cdot 365 + D_{leap} + DoY + \frac{HH \cdot 3600 + mm \cdot 60 + ss + s}{24 \cdot 3600}, \tag{6.167}$$

where

$YYYY$ = year;

D_{leap} = leap day;

Doy = day of the year;

HH = hour of the day;

mm = minute of the hour;

ss = second of the minute;

s = fractions of the second.

Leap day D_{leap} shall be added to the MJD based on a leap year check showing the number of leap years between 2000 and $YYYY$. As 2000 was a leap year, the starting value of D_{leap} is 1. The algorithm calculating DoY shall check if the $YYYY$ is a leap year and take the leap day into account in the DoY value.

A user selectable option is to use MJD2000 time frame based on the UT1 time. UT1 time deviates from UTC by the amount DUT1. DUT1 shall be provided by the GRAS GSN with the EOP products. The UT1 time is derived from the UTC time by

$$UT1 = UTC + DUT1. \tag{6.168}$$

It should be noted that DUT1 is normally a constant during time periods much longer than one occultation. Thus, the conversion from UTC to UT1 does not compromise the consistency of the time stamps.

The conversion of UT1 time into MJD2000 time is performed by applying Equation 6.167.

6.3.3 Coordinate frame conversion functions

6.3.3.1 Antenna reference frame to ECI transformation

Input Parameters:

1. Unit vector in local antenna reference frame $(\hat{x}^{arf}, \hat{y}^{arf}, \hat{z}^{arf})$;
2. Metop position $(\vec{r}_{leo}^{eci})$ and velocity $(\vec{v}_{leo}^{eci})$ vectors in ECI reference frame;
3. Characterisation information in GRAS Instrument Database;
4. Metop mispointing angles $\Delta\eta$, $\Delta\xi$, $\Delta\zeta$;
5. Mean semimajor axis of the Metop orbit a_m;
6. Mean inclination of the Metop orbit i_m;
7. Angular velocity of the Earth ω_e;
8. Orbital rate of Metop ω_o.

Output Parameters:

1. Unit vector in ECI reference frame $(\hat{x}^{eci}, \hat{y}^{eci}, \hat{z}^{eci})$.

Algorithm

The coordinate frames defined onboard the Metop spacecraft are presented in Fig. 6.3 with GVA antenna reference frame as an example of the local antenna reference frame. Similar reference frame is defined locally also for GAVA and GZA.

The steps used for transforming coordinates from the local the antenna reference frame into ECI reference frame are as follows:

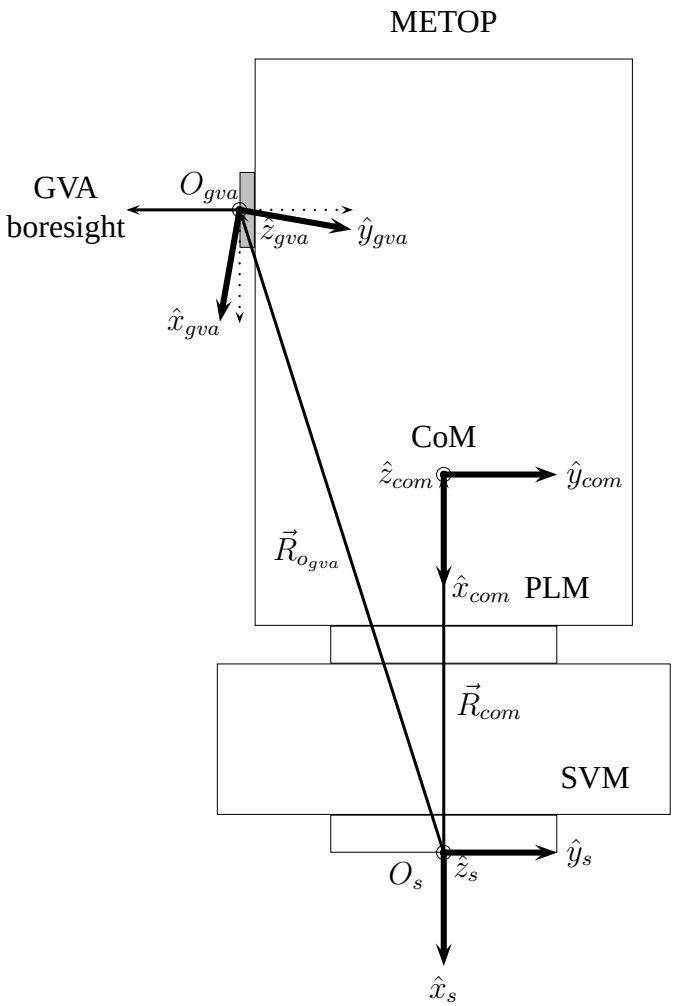

Figure 6.3: Coordinate frame definitions onboard Metop spacecraft.

1) Antenna reference frame misalignment correction

The antenna reference coordinate frame is defined for each antenna so that the origin is located at the reference point on the front of the antenna. The definition of the coordinate axes is linked to the orientation of the Spacecraft Reference (SR) frame so that the $\hat{x}_{ant}^{arf}$, $\hat{y}_{ant}^{arf}$, and $\hat{z}_{ant}^{arf}$ vectors are aligned approximately with the axis $\hat{x}_s^{srf}$, $\hat{y}_s^{srf}$, and $\hat{z}_s^{srf}$ (ant is used here to denote a GRAS antenna, i.e., GVA, GAVA, or GZA). This means that the axes in the antenna radiating surface plane are different for occultation antennas and the navigation antenna. For GVA and GAVA the $\hat{x}_{ant}^{arf}$, and $\hat{z}_{ant}^{arf}$ vectors define the plane aligned with the antenna radiating surface plane. For GZA it is defined by $\hat{x}_{ant}^{arf}$, and $\hat{y}_{ant}^{arf}$.

The differences in the directions of the $\hat{x}_{ant}^{arf}$, $\hat{y}_{ant}^{arf}$, and $\hat{z}_{ant}^{arf}$ vectors and $\hat{x}_s^{srf}$, $\hat{y}_s^{srf}$, and $\hat{z}_s^{srf}$ vectors are caused by the antenna alignment error. This error is measured after the spacecraft integration and a rotation matrix M_{ant} is provided for antenna misalignment correction.

The antenna misalignment correction is performed with the rotation

$$\begin{pmatrix} \hat{x}_{ant}^{srf} \\ \hat{y}_{ant}^{srf} \\ \hat{z}_{and}^{srf} \end{pmatrix} = \mathbf{M}_{ant} \begin{pmatrix} \hat{x}_{ant}^{arf} \\ \hat{y}_{ant}^{arf} \\ \hat{z}_{ant}^{arf} \end{pmatrix}. \tag{6.169}$$

The antenna misalignment correction matrices $\mathbf{M}_{gva}$, $\mathbf{M}_{gava}$, and $\mathbf{M}_{gza}$ are provided in the GRAS Instrument Database (GID) in the format described in **RD7**.

2) Translation from the antenna reference frame to SR

The locations of the antenna reference points are provided for each antenna in the GRAS Instrument Database (GID) in the format described in **RD7**.

The antenna reference frame is aligned with the SR frame with the translation of O_{ant} to the O_s by

$$\begin{pmatrix} \hat{x}_{s}^{srf} \\ \hat{y}_{s}^{srf} \\ \hat{z}_{s}^{srf} \end{pmatrix} = \begin{pmatrix} \hat{x}_{ant}^{srf} \\ \hat{y}_{ant}^{srf} \\ \hat{z}_{ant}^{srf} \end{pmatrix} - \vec{p}_{ant}^{srf}, \tag{6.170}$$

where

$\vec{p}_{ant}^{srf}$ = the location of the antenna reference point in the SR coordinate frame [m].

3) Translation of the origin to center of Mass (CoM)

The orbit provided by the POD is the orbit of the Metop CoM. Thus, all local orbital coordinate frames are defined as CoM as their origin. So, it is necessary to translate the origin of the coordinate frame from O_s to O_{com} as

$$\begin{pmatrix} \hat{x}_{com}^{srf} \\ \hat{y}_{com}^{srf} \\ \hat{z}_{com}^{srf} \end{pmatrix} = \begin{pmatrix} \hat{x}_{s}^{srf} \\ \hat{y}_{s}^{srf} \\ \hat{z}_{s}^{srf} \end{pmatrix} - \vec{r}_{com}^{srf}. \tag{6.171}$$

where

$\vec{r}_{com}^{srf}$ = Metop CoM position vector in SR coordinate frame provided by the spacecraft manufacturer [m].

It should be noted that the $\vec{r}_{com}^{srf}$ is changing slowly during the mission life time due to the consumption of the spacecraft fuel. So, its correct value has to be requested via the PGE.

4) Rotation from SR to the Local Relative Yaw Steering Orbital Reference frame (YSOR)

After step 3) the coordinate frame is now perfectly aligned with the SR frame and fixed to the body of the spacecraft. The next step is to rotate the coordinate frame so that it is aligned with the Local Relative Yaw Steering Orbital Reference Frame (YSOR) frame.

The Attitude and Orbit Control System (AOCS) tries to keep the spacecraft perfectly aligned with the YSOR frame when the spacecraft is in Yaw Steering Mode (YSM). In this situation the coordinate frames would be aligned so that $\hat{T}'||-\hat{x}_{com}$, $\hat{R}'||-\hat{y}_{com}$, and $\hat{L}'||\hat{z}_{com}$. In reality the alignment is not perfect. The alignment error is characterized as the spacecraft mispointing angles $\Delta\eta$, $\Delta\xi$, and $\Delta\zeta$, corresponding to the roll, pitch, and yaw mispointing respectively. The spacecraft mispointing angles are obtained via the PGE. If mispointing angles are not available, the ATTITUDE_MISSING flag is set in the corresponding MDRs.

The correction for the mispointing is calculated by Euler angle rotation as

$$\begin{pmatrix} \hat{T}' \\ \hat{R}' \\ \hat{L}' \end{pmatrix} = (\mathbf{R_z}(\Delta\zeta)\mathbf{R_x}(-\Delta\xi)\mathbf{R_y}(-\Delta\eta))^{-1} \begin{pmatrix} \hat{x}_{com}^{srf} \\ \hat{y}_{com}^{srf} \\ \hat{z}_{com}^{srf} \end{pmatrix}, \tag{6.172}$$

where

$$\mathbf{R_x}(w) = \begin{pmatrix} 1 & 0 & 0 \\ 0 & \cos w & \sin w \\ 0 & -\sin w & \cos w \end{pmatrix},$$

$$\mathbf{R}_y(w) = \begin{pmatrix} \cos w & 0 & -\sin w \\ 0 & 1 & 0 \\ \sin w & 0 & \cos w \end{pmatrix},$$

$$\mathbf{R_z}(w) = \begin{pmatrix} \cos w & \sin w & 0 \\ -\sin w & \cos w & 0 \\ 0 & 0 & 1 \end{pmatrix}.$$

5) Rotation from YSOR to the Local Relative Orbital Reference frame (LROR)

The LROR and the YSOR coordinate frames are not aligned as $\hat{R}_1$is in general not parallel with $\hat{R}'$. The alignment of the coordinate frames is performed with a similar Euler rotation as in step 4) by

$$\begin{pmatrix} \hat{T}_1 \\ \hat{R}_1 \\ \hat{L}_1 \end{pmatrix} = (\mathbf{R_z}(\zeta)\mathbf{R_x}(-\xi)\mathbf{R_y}(-\eta))^{-1} \begin{pmatrix} \hat{T}' \\ \hat{R}' \\ \hat{L}' \end{pmatrix}. \tag{6.173}$$

The roll angle ζ, pitch angle ξ, and yaw angle η depend on the Metop orbit parameters and orbital position as

$$\eta = C_y \sin(\theta_{tl}), \tag{6.174}$$

$$\xi = C_x \sin(2\theta_{tl}), \tag{6.175}$$

$$\zeta = C_z \cos(\theta_{tl}) \left(1 - \frac{[C_z \cos(\theta_{tl})]^2}{3}\right), \tag{6.176}$$

where

$$\theta_{tl} = \omega_p + M_m, \tag{6.177}$$

where

ω_p = the osculating argument of perigee;

M_m = the mean anomaly.

ω_p and M_m in Equation 6.177 are calculated from the Metop position and velocity vectors provided by the NRT POD.

The AOCS rotation amplitudes C_x, C_y, and C_z are functions of the Metop orbit and are given by

$$C_x = -e_e^2 \left(\frac{a_e}{a_m}\right) \frac{\sin^2(i_m)}{2}, \tag{6.178}$$

$$C_y = -(e_e)^2 \left(\frac{a_e}{a_m}\right) sin(i_m)cos(i_m), \tag{6.179}$$

$$C_z = \frac{k \cos(i_m - 90)}{i_m + k \sin(i_m - 90)}, \tag{6.180}$$

where

a_m = mean semi-major axis of Metop orbit;

i_m = mean inclination of the Metop orbit;

a_e = semi-major axis of the reference ellipsoid;

e_e = eccentricity of the reference ellipsoid.

Table 6.23: WGS84 reference ellipsoid parameters.

Parameter	Value
a_e	6378 137 m
$1/f$	298.257223563
e_e	$= \sqrt{1-(1-f)^2}$ =0.08181919

The ratio k is

$$k = \frac{\omega_e}{\omega_o}, \tag{6.181}$$

where

ω_e = angular velocity of the Earth [rad/s];

ω_o = orbital rate of Metop [rad/s].

The parameters of the WGS84 reference ellipsoid are listed in Table 6.23

6) Rotation to the Local Orbital Reference (LOR) frame

The LROR reference frame is inconvenient for GRAS data processing as the L_1axis is defined to be parallel to the local normal of the Earth's reference ellipsoid (WGS84) directed upward and crossing the spacecraft CoM. This means that the L_1axis is parallel to the Metop position vector $\vec{r}_{leo}^{eci}$ only in special cases (see Fig. 6.4). Rotation of the LROR coordinate frame to the LOR frame is not trivial because the direction of the $\vec{r'}_{leo}^{eci}$vector and the length of the Δz^{eci} vary depending of the Metop orbital position.

The rotation matrix for the coordinate transform is derived using the definition of the Metop LOR frame and the $\vec{r}_{leo}^{eci}$ and the $\vec{v}_{leo}^{eci}$ vectors in ECI frame.

Two slightly different methods for the derivation of the geodetic coordinate frame quantity Δz^{eci} can be defined depending on the required accuracy:

(1) For the incidence angle estimation in the level 1a processing Δz can be approximated as

$$\Delta z = N e_e^2 \sin\left[\varphi'_g + f \sin\left(2\varphi'_g\right)\right], \tag{6.182}$$

where

N = an auxiliary quantity illustrated in Figure 6.4;

e_e = eccentricity of the reference ellipsoid;

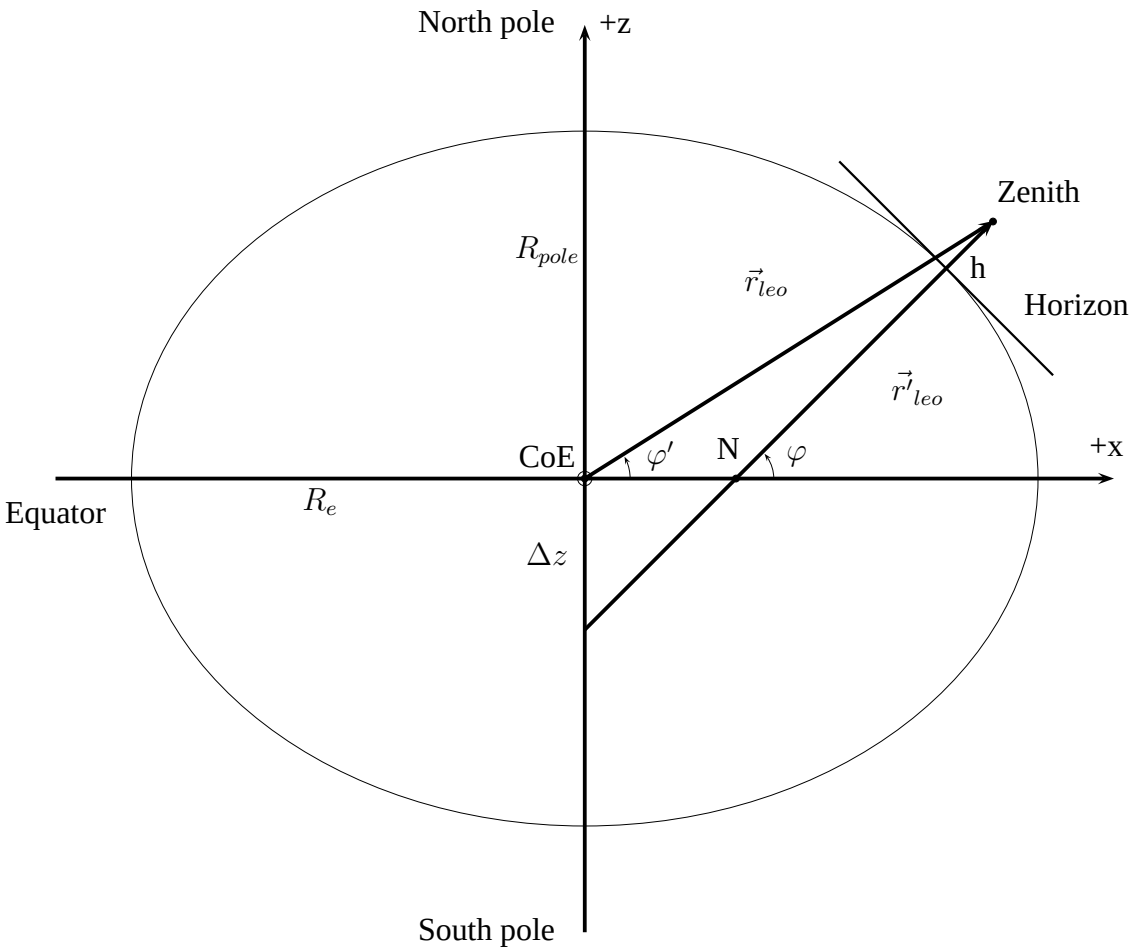

Figure 6.4: Geometry of the geodetic and geocentric coordinate frames.

φ'_g = the geocentric latitude;

f = flattening of the reference ellipsoid.

The geocentric latitude is calculated from the Metop coordinates in ECI frame as

$$\varphi'_g = arctan\left(\frac{z}{\sqrt{x^2+y^2}}\right), \tag{6.183}$$

where x, y, and z are the Metop CoM coordinates in ECI coordinate frame.

Quantity N can be calculated as

$$N = \frac{a_e}{\sqrt{1-e_e^2\sin^2\varphi}},$$

where $\varphi$is approximated from

$$\varphi = \varphi' + f \sin(2\varphi').$$

(2) In the level 1b processing the full iterative algorithm defined in Section 6.3.3.3 has to be used for estimating Δz.

The Metop geodetic position vector $\vec{r'}_{leo}^{eci}$ can now be defined as a vector sum

$$\begin{aligned} \vec{r'}_{leo}^{eci} &= \vec{r}_{leo}^{eci} - \Delta z \hat{z}^{eci}, \\ &= x\hat{x}^{eci} + y\hat{y}^{eci} + (z - \Delta z)\hat{z}^{eci}, \end{aligned} \tag{6.184}$$

where $\hat{x}^{eci}$, $\hat{y}^{eci}$, and $\hat{z}^{eci}$ is a unit vectors defining the ECI coordinate frame.

The rotation matrix $\mathbf{M}$ from ECI frame to LROR frame can be derived by applying Equation 6.184 and the Metop velocity vector $\vec{v}_{leo}^{eci}$ to the definitions of the LROR frame as in **AD7.**

The unit vector $\hat{L}_1$can be expressed using the definition of the LROR frame as

$$\begin{aligned} \hat{L}_1 &= \frac{\vec{r'}_{leo}^{eci}}{\left|\vec{r'}_{leo}^{eci}\right|} \\ &= \frac{x\hat{x}^{eci} + y\hat{y}^{eci} + (z - \Delta z)\hat{z}^{eci}}{\sqrt{x^2 + y^2 + (z - \Delta z)^2}} \\ &= \frac{x}{r'_{leo}}\hat{x}^{eci} + \frac{y}{r'_{leo}}\hat{y}^{eci} + \frac{(z - \Delta z)}{r'_{leo}}\hat{z}^{eci} \\ &= M_{31}\hat{x}^{eci} + M_{32}\hat{y}^{eci} + M_{33}\hat{z}^{eci}, \end{aligned} \tag{6.185}$$

where

r'_{leo} = $\left|\vec{r'}_{leo}^{eci}\right|$;

(x, y, z) = Metop position in the ECI frame [m].

The unit vector $\vec{T}_1$ perpendicular to the plane containing $\hat{L}_1$ and $\vec{v}_{leo}^{eci}$ is can be derived with the cross product

$$\begin{aligned} \vec{T}_1 &= \vec{v}_{leo}^{eci} \times \hat{L}_1 \\ &= \left(v_{leox}\hat{x}^{eci} + v_{leoy}\hat{y}^{eci} + v_{leoz}\hat{z}^{eci}\right) \times \hat{L}_1 \\ &= \left(v_{leoy}\frac{z - \Delta z}{r'_{leo}} - v_{leoz}\frac{y}{r'_{leo}}\right)\hat{x}^{eci} + \left(v_{leoz}\frac{y}{r'_{leo}} - v_{leox}\frac{z - \Delta z}{r'_{leo}}\right)\hat{y}^{eci} + \left(v_{leox}\frac{y}{r'_{leo}} - v_{leoy}\frac{x}{r'_{leo}}\right)\hat{z}^{eci} \\ &= \left(v_{leoy}M_{33} - v_{leoz}M_{32}\right)\hat{x}^{eci} + \left(v_{leoz}M_{31} - v_{leox}M_{33}\right)\hat{y}^{eci} + \left(v_{leox}M_{32} - v_{leoy}M_{31}\right)\hat{z}^{eci}, \end{aligned} \tag{6.186}$$

where

(v_x, v_y, v_z) = Metop velocity in the ECI frame [m/s].

The unit vector $\hat{T}_1$ is then

$$\begin{aligned}
\hat{T}_1 &= \frac{\vec{T}_1}{\left|\vec{T}_1\right|} \\
&= \left(\frac{v_{leoy}\frac{z-\Delta z}{r'_{leo}} - v_{leoz}\frac{y}{r'_{leo}}}{T_1}\right)\hat{x}^{eci} + \left(\frac{v_{leoz}\frac{y}{r'_{leo}} - v_{leox}\frac{z-\Delta z}{r'_{leo}}}{T_1}\right)\hat{y}^{eci} + \left(\frac{v_{leox}\frac{y}{r'_{leo}} - v_{leoy}\frac{x}{r'_{leo}}}{T_1}\right)\hat{z}^{eci} \\
&= M_{11}\hat{x}^{eci} + M_{12}\hat{y}^{eci} + M_{13}\hat{z}^{eci}, \qquad (6.187)
\end{aligned}$$

where

$$T_1 = \sqrt{\left(v_y\frac{z-\Delta z}{r'_{leo}} - v_z\frac{y}{r'_{leo}}\right)^2 + \left(v_z\frac{y}{r'_{leo}} - v_x\frac{z-\Delta z}{r'_{leo}}\right)^2 + \left(v_x\frac{y}{r'_{leo}} - v_y\frac{x}{r'_{leo}}\right)^2}. \qquad (6.188)$$

The unit vector $\hat{R}_1$ completing a right-hand system is

$$\begin{aligned}
\hat{R}_1 &= \hat{L}_1 \times \hat{T}_1 \\
&= \left(\frac{y}{r'_{leo}}\frac{v_{leox}\frac{y}{r'_{leo}} - v_{leoy}\frac{x}{r'_{leo}}}{T_1} - \frac{z-\Delta z}{r'_{leo}}\frac{v_{leoz}\frac{y}{r'_{leo}} - v_{leox}\frac{z-\Delta z}{r'_{leo}}}{T_1}\right)\hat{x}^{eci} \\
&\quad + \left(\frac{z-\Delta z}{r'_{leo}}\frac{v_{leoy}\frac{z-\Delta z}{r'_{leo}} - v_{leoz}\frac{y}{r'_{leo}}}{T_1} - \frac{x}{r'_{leo}}\frac{v_{leox}\frac{y}{r'_{leo}} - v_{leoy}\frac{x}{r'_{leo}}}{T_1}\right)\hat{y}^{eci} \\
&\quad + \left(\frac{x}{r'_{leo}}\frac{v_{leoz}\frac{y}{r'_{leo}} - v_{leox}\frac{z-\Delta z}{r'_{leo}}}{T_1} - \frac{y}{r'_{leo}}\frac{v_{leoy}\frac{z-\Delta z}{r'_{leo}} - v_{leoz}\frac{y}{r'_{leo}}}{T_1}\right)\hat{z}^{eci} \\
&= (M_{32}M_{13} - M_{33}M_{12})\,\hat{x}^{eci} + (M_{33}M_{11} - M_{31}M_{13})\,\hat{y}^{eci} + (M_{31}M_{12} - M_{32}M_{11})\,\hat{z}^{eci} \\
&= M_{21}\hat{x}^{eci} + M_{22}\hat{y}^{eci} + M_{23}\hat{z}^{eci}. \qquad (6.189)
\end{aligned}$$

The rotation of the coordinate frame can now be written as

$$\begin{pmatrix} \hat{T}_1 \\ \hat{R}_1 \\ \hat{L}_1 \end{pmatrix} = \mathbf{M}\begin{pmatrix} \hat{x}^{eci} \\ \hat{y}^{eci} \\ \hat{z}^{eci} \end{pmatrix}, \qquad (6.190)$$

where the elements of the matrix $\mathbf{M}$ are defined in Equations 6.187, 6.189, and 6.185.

The rotation matrix $\mathbf{M}$ aligns directly the orientation of the LROR frame and the ECI frame without using Local Orbital Reference frame (LOR) as an intermediate step.

Taking into account the translation of the origin of the coordinate frame from Metop CoM to center of the ECI frame the final coordinate transform step can be written as

$$\begin{pmatrix} \hat{x}_{ant}^{eci} \\ \hat{y}_{ant}^{eci} \\ \hat{z}_{ant}^{eci} \end{pmatrix} = \mathbf{M}^{-1} \begin{pmatrix} \hat{T}_1 \\ \hat{R}_1 \\ \hat{L}_1 \end{pmatrix} + \vec{r}_{leo.}^{eci} \tag{6.191}$$

6.3.3.2 WGS84 to ITRF97 coordinate transform

Input Parameters:

1. Position vector in WGS84 coordinates $\vec{r}^{wgs84}$

Output Parameters:

1. Position vector in ITRF97 coordinates $\vec{r}^{itrf97}$

Algorithm

The WGS84 coordinates are transformed to ITRF97 frame using a Helmert transform

$$\vec{r}^{itrf} = \mathbf{M_h}^{-1}\vec{r}^{wgs84} - \mathbf{M_h}^{-1}\mathbf{T_h}. \tag{6.192}$$

The matrices $\mathbf{M_h}$ and $\mathbf{T_h}$ in Equation 6.192 are

$$\mathbf{M_h} = \begin{pmatrix} +D & -R_3 & +R_2 \\ +R_3 & +D & -R_1 \\ -R_2 & +R_1 & +D \end{pmatrix}, \tag{6.193}$$

and

$$\mathbf{T_h} = \begin{pmatrix} T_1 \\ T_2 \\ T_3 \end{pmatrix},$$

where

T_1 = +1 [cm];

T_2 = -1 [cm];

T_3 = -2 [cm];

D = +0.3·10^{-9};

R_1 = +0.6 [mas];

R_2 = +1.2 [mas];

R_3 = +0.7 [mas].

6.3.3.3 Derivation of geodetic coordinates

Input Parameters:

1. Geocentric Cartesian ECEF coordinates (x, y, z);
2. Reference ellipsoid semimajor axis $a_e$and flattening f.

Output Parameters:

1. Δz;
2. N;
3. Geodetic longitude λ_g;
4. Geodetic latitude φ_g;
5. Geodetic height above the reference ellipsoid h_g.

Algorithm

The first task is to calculate Δz. This can be done using iteration **[RD15]** and geometrical definition of Δz as

$$\Delta z = z - (N + h) \sin \varphi_g = N e_e^2 \sin \varphi_g, \tag{6.194}$$

where the eccentricity of the reference ellipsoid e_e is

$$e_e = \sqrt{1 - (1 - f)^2}. \tag{6.195}$$

The Earth flattening ratio f depend on the used Earth model. The parameters for the default Earth model (WGS84) ellipsoid are provided in Table 6.23.

At the start of the iteration the Δz is set to

$$\Delta z = e_e^2 z, \tag{6.196}$$

where z is the z coordinate of the Metop position in ECI frame.

The improved values are calculated from the equations

$$\sin\varphi_g = \frac{z+\Delta z}{\sqrt{x^2+y^2+(z+\Delta z)^2}}, \tag{6.197}$$

$$N = \frac{a_e}{\sqrt{1-e_e^2\sin^2\varphi_g}}, \tag{6.198}$$

$$\Delta z = N e_e^2 \sin\varphi_g, \tag{6.199}$$

where $a_e$is the semimajor axis of the reference ellipsoid.

The iteration is repeated until the Δz improvement is less than a user definable criteria (default criteria = 1 cm).

The geodetic longitude and latitude and the height above the reference ellipsoid are calculated from

$$\lambda_g = \arctan 2\left(y, x\right), \tag{6.200}$$

$$\varphi_g = \arctan\left(\frac{z+\Delta z}{\sqrt{x^2+y^2}}\right), \tag{6.201}$$

and

$$h_g = \sqrt{x^2+y^2+(z+\Delta z)^2} - N. \tag{6.202}$$

6.3.3.4 ECEF to ECI coordinate transform

Input Parameter:

1. Coordinates in ECEF frame.

Output Parameter:

1. Coordinates in ECI frame.

The baseline ECEF to ECI coordinate transform algorithm is defined e.g. in Equation 6.2.1 of **RD15**. The terms for Equation 6.2.1 in **RD15** are defined in Section 5 of the same book.

Two additional corrections that are not included into the algorithm specified in **RD15** must be taken into account when fiducial station coordinates provided e.g. by the GSN in ECEF frame are transformed into ECI frame:

1. A correction for the short-period tidal variations shall be applied to the Earth Orientation Parameters by using the R. Ray's oceanic tide model. The mathematical formulation of the Ray's model is provided in **RD27**.
2. Solid Earth Tide correction shall be applied to the ECEF coordinates as user selectable options. The correction shall include both the Dynamic and Permanent Tide. The user shall be able to toggle either correction on and off independently without restarting the PPF software. The mathematical formulation for the Solid Earth Tide model is provided in **RD28**.

6.3.4 Fiducial station incidence angle determination

Input Parameters:

1. GPS antenna phase center position vector in ECI frame $\vec{r}_{tx}^{eci}$;
2. Fiducial station antenna phase center position vector in ITRF coordinate frame $\vec{r}_{fs}^{itrf}$;
3. Earth model identification (e.g. WGS84).

Output Parameters:

1. Elevation angle of the incoming ray ε_{fs}^{eci};
2. Azimuth angle of the incoming ray θ_{fs}^{eci};
3. Geodetic coordinates of the fiducial station λ_{g_fs}, φ_{g_fs}, h_{g_fs}.

Algorithm

The estimation of the incidence angle of the incoming ray at the fiducial station is started by defining a unit vector normal to the ellipsoid surface at the coordinates of the fiducial station. The geodetic position vector of the fiducial station is derived by

$$\begin{aligned} \vec{r'}_{fs}^{ecef} &= \vec{r}_{fs}^{ecef} - \Delta z \hat{z}^{ecef}, \\ &= x_{fs}\hat{x}^{ecef} + y_{fs}\hat{y}^{ecef} + (z_{fs} + \Delta z)\hat{z}^{ecef}, \end{aligned} \tag{6.203}$$

where $\hat{x}^{ecef}$, $\hat{y}^{ecef}$, and $\hat{z}^{ecef}$ is a unit vectors defining the ECEF coordinate frame.

The parameter Δz is derived using the iterative algorithm described in Section 6.3.3.3. This algorithm will also produce the geodetic latitude, longitude, and height of the antenna phase center.

The unit vector normal to the ellipsoid surface is now

$$\hat{n}_s^{ecef} = \frac{x_{fs}\hat{x}^{ecef} + y_{fs}\hat{y}^{ecef} + (z_{fs} + \Delta z)\hat{z}^{ecef}}{\sqrt{x_{fs}^2 + y_{fs}^2 + (z_{fs} + \Delta z)^2}}. \tag{6.204}$$

The unit vector $\hat{n}_s^{ecef}$ and the position vector of the fiducial station $\vec{r}_{fs}^{eci}$ are transformed from the ECEF coordinate frame to ECI frame as specified in Section 6.3.3.4.

The vector pointing from the phase center of the fiducial station antenna to the phase center of the GPS antenna is

$$\vec{r}_{ray}^{eci} = \vec{r}_{tx}^{eci} - \vec{r}_{fs}^{eci}. \tag{6.205}$$

The elevation angle ε_{fs}^{eci} of the GPS satellite for the fiducial station is then

$$\varepsilon_{fs}^{eci} = \frac{\pi}{2} - \arccos\left(\frac{\vec{r}_{ray}^{eci} \cdot \hat{n}_s^{eci}}{\left|\vec{r}_{ray}^{eci}\right|}\right). \tag{6.206}$$

The azimuth angle θ_{fs}^{eci} of the GPS satellite from the local geodetic north is

$$\theta_{fs}^{eci} = \arctan 2\left(\vec{r}_{ray}^{eci} \cdot \hat{y}_{local}^{eci}, \vec{r}_{ray}^{eci} \cdot \hat{x}_{local}^{eci}\right), \tag{6.207}$$

where

$$\hat{y}_{local}^{eci} = \hat{z}^{eci} \times \hat{n}_s^{eci}, \tag{6.208}$$

and

$$\hat{x}_{local}^{eci} = \hat{n}_s^{eci} \times \hat{y}_{local}^{eci}. \tag{6.209}$$

It should be noted that this function can not be used for elevation angles below $20°$ as it does not take into account the bending of the ray path in the atmosphere.

6.3.5 Atmosphere models

6.3.5.1 Neutral atmosphere delay mapping function

Input Parameter:

1. Time of the measurement $t_{rx_fs}^{ref}$;
2. Elevation of the measured GPS satellite $\varepsilon\left(t_{rx_fs}^{ref}\right)$;
3. Latitude of the fiducial station φ_{fs};
4. Height of the fiducial station above sea level h_{fs}.

Output Parameter:

1. Hydrostatic mapping function $m_h\left(t^{ref}_{rx_fs}\right)$;
2. Wet mapping function $m_w\left(t^{ref}_{rx_fs}\right)$.

The Niell mapping function is used in the GRAS data processing algorithm [**RD16**].
The hydrostatic (dry atmosphere) mapping function is derived from

$$m_h(\varepsilon) = m_{h1}(\varepsilon) + \Delta m(\varepsilon), \tag{6.210}$$

where

$$m_{h1}(\varepsilon) = \frac{\left(1 + \frac{a}{1+\frac{b}{1+c}}\right)}{\left(sin(\varepsilon) + \frac{a}{sin(\varepsilon)+\frac{b}{sin(\varepsilon)+c}}\right)}, \tag{6.211}$$

and

$$\Delta m(\varepsilon) = \left(\frac{1}{sin(\varepsilon)} - \frac{\left(1 + \frac{a_{ht}}{1+\frac{b_{ht}}{1+c_{ht}}}\right)}{\left(sin(\varepsilon) + \frac{a_{ht}}{sin(\varepsilon)+\frac{b_{ht}}{sin(\varepsilon)+c_{ht}}}\right)}\right) \cdot h_{fs.} \tag{6.212}$$

The coefficients a,b, and c for the Equations 6.211 and 6.212 are derived from

$$a(\varphi_i, t^{dyo}_{rx_fs}) = a_{avg}\left(\varphi_{fs}\right) + a_{amp}\left(\varphi_{fs}\right)\cos\left(2\pi\frac{t^{doy}_{rx_fs} - T_0}{365.25}\right), \tag{6.213}$$

$$b(\varphi_i, t^{dyo}_{rx_fs}) = b_{avg}\left(\varphi_{fs}\right) + b_{amp}\left(\varphi_{fs}\right)\cos\left(2\pi\frac{t^{doy}_{rx_fs} - T_0}{365.25}\right), \tag{6.214}$$

and

$$c(\varphi_i, t^{dyo}_{rx_fs}) = c_{avg}\left(\varphi_{fs}\right) + c_{amp}\left(\varphi_{fs}\right)\cos\left(2\pi\frac{t^{doy}_{rx_fs} - T_0}{365.25}\right), \tag{6.215}$$

where

φ_i = latitude;

$t^{dyo}_{rx_fs}$ = the time of the measurement as the day of the year from 1st of January, 00:00 hrs;

Table 6.24: Coefficients for the hydrostatic mapping function.

	Latitude (φ_i)				
	15°	30°	45°	60°	75°
	Average				
a_{avg}	$1.2769934 \cdot 10^{-3}$	$1.2683230 \cdot 10^{-3}$	$1.2465397 \cdot 10^{-3}$	$1.2196049 \cdot 10^{-3}$	$1.2045996 \cdot 10^{-3}$
b_{avg}	$2.9153695 \cdot 10^{-3}$	$2.9152299 \cdot 10^{-3}$	$2.9288445 \cdot 10^{-3}$	$2.9022565 \cdot 10^{-3}$	$2.9024912 \cdot 10^{-3}$
c_{avg}	$62.610505 \cdot 10^{-3}$	$62.837393 \cdot 10^{-3}$	$63.721774 \cdot 10^{-3}$	$63.824265 \cdot 10^{-3}$	$64.258455 \cdot 10^{-3}$
	Amplitude				
a_{amp}	0.0	$1.2709626 \cdot 10^{-5}$	$2.6523662 \cdot 10^{-5}$	$3.4000452 \cdot 10^{-5}$	$4.1202191 \cdot 10^{-5}$
b_{amp}	0.0	$2.1414979 \cdot 10^{-5}$	$3.0160779 \cdot 10^{-5}$	$7.2562722 \cdot 10^{-5}$	$11.723375 \cdot 10^{-5}$
c_{amp}	0.0	$9.0128400 \cdot 10^{-5}$	$4.3497037 \cdot 10^{-5}$	$84.795348 \cdot 10^{-5}$	$170.37206 \cdot 10^{-5}$
	Height correction				
a_{ht}	$2.53 \cdot 10^{-5}$				
b_{ht}	$5.49 \cdot 10^{-3}$				
c_{ht}	$1.14 \cdot 10^{-3}$				

Table 6.25: Coefficients for the wet mapping function.

	Latitude (φ_i)				
	15°	30°	45°	60°	75°
a	$5.8021897 \cdot 10^{-4}$	$5.6794847 \cdot 10^{-4}$	$5.8118019 \cdot 10^{-4}$	$5.9727542 \cdot 10^{-4}$	$6.1641693 \cdot 10^{-4}$
b	$1.4275268 \cdot 10^{-3}$	$1.5138625 \cdot 10^{-3}$	$1.4572752 \cdot 10^{-3}$	$1.5007428 \cdot 10^{-3}$	$1.7599082 \cdot 10^{-3}$
c	$4.3472961 \cdot 10^{-2}$	$4.6729510 \cdot 10^{-2}$	$4.3908931 \cdot 10^{-2}$	$4.4626982 \cdot 10^{-2}$	$5.4736038 \cdot 10^{-2}$

T_0 = 28.

The parameters for the Equations 6.213, 6.214, and 6.215 are given in Table 6.24. The value of $a(\varphi_{fs}, t^{dyo}_{rx_fs})$ is obtained by interpolating linearly between the two nearest $a(\varphi_i, t^{dyo}_{rx_fs})$. Similar procedure is applied to get $b(\varphi_{fs}, t^{dyo}_{rx_fs})$ and $c(\varphi_{fs}, t^{dyo}_{rx_fs})$.

The wet mapping function is

$$m_w(\varepsilon, \varphi_{fs}) = \frac{\left(1 + \frac{a}{1+\frac{b}{1+c}}\right)}{\left(sin(\varepsilon) + \frac{a}{sin(\varepsilon)+\frac{b}{sin(\varepsilon)+c}}\right)}, \tag{6.216}$$

For the wet mapping function the coefficients a, b, and c are provided directly in Table 6.25. The value of $m_w(\varepsilon, \varphi_{fs})$ is obtained by interpolating linearly between the two nearest $m_w(\varepsilon, \varphi_i)$.

6.3.5.2 Hydrostatic delay model

Input Parameter:

1. Surface pressure at the fiducial station P_{s_fs} or pressure at the geodetic surface level at the station location P_0;
2. Latitude of the fiducial station φ_{fs};
3. Geodetic height of the fiducial station h_{fs}.

Output Parameter:

1. Zenith hydrostatic delay estimate ΔL_h.

The ZHD (Zenith Hydrostatic Delay) is estimated from the model [**RD17**]

$$\Delta L_h = \frac{2.2779 P_{s_fs}}{(1 - 0.00266 \cos 2\varphi_{fs} - 0.00028 h_{fs})} \cdot 10^{-3}. \tag{6.217}$$

If pressure measurements at the station are not available, NWP forecast pressure at the time of the measurement and at the geodetic coordinates of the station shall be requested via PGE. If NWP forecast data is used in the processing, the VIADR-1B-TZD shall be updated to include the same information.

6.3.5.3 Wet delay model

Input Parameter:

1. Surface partial pressure of the water vapor at the fiducial station e_{s_fs};
2. Surface temperature the fiducial station T_{s_fs};
3. Latitude of the fiducial station φ_{fs};
4. Geodetic height of the fiducial station h_{fs}.

Output Parameter:

1. Zenith wet delay estimate ΔL_w.

The ZHD (Zenith Hydrostatic Delay) is estimated from the model [**RD1**8]

$$\Delta L_w = \frac{10^{-6} k_3' R_d}{g_m (\lambda_w + 1) - \beta_T R_d} \cdot \frac{e_{s_fs}}{T_{s_fs}}, \tag{6.218}$$

where

k_3' = $3.82 \cdot 10^5$ [K^{2}mbar^{-1}] [**RD17**];

R_d = the gas constant for dry air = 2.87 [JK^{-1}kg^{-1}];

g_m = the gravity acceleration at the mass centre of a vertical column of the atmosphere = $9.784\,(1 - 0.00266\cos 2\varphi_{fs} - 0.00028h_{fs})$ [ms^{-2}] [**RD19**];

λ_w = the water vapor lapse rate = 3;

β_T = the temperature lapse rate = 6.2.

If partial pressure of the water vapor and temperature measurements at the station are not available, NWP forecast parameters at the time of the measurement and at the geodetic coordinates of the station shall be requested via PGE. If NWP forecast data is used in the processing, the VIADR-1B-TZD shall be updated to include the same information.

6.3.6 Filtering functions

6.3.6.1 Adaptive low-pass filter

Input Parameters:

1. Time series of non-filtered data samples $x(t)$;
2. SLTH values corresponding to the data samples $SLTH(t)$;
3. Filtering parameters $B(t)$ and $L(t)$;

Output Parameters:

1. Time series of filtered data samples $y(t)$;

Algorithm

A low pass filter implemented as Sinc function truncated by a Blackman-Harris window can be written as

$$y(t) = \frac{\int\limits_{-L(t)/2}^{L(t)/2} h\left(s; B(t), L(t)\right) x\left(t - s\right) ds}{\int_{-L(t)/2}^{L(t)/2} h\left(s; B(t), L(t)\right) ds}, \tag{6.219}$$

where

$$
\begin{aligned}
h\left(s; B(t), L(t)\right) &= \left[H\left(s+\frac{L(t)}{2}\right) - H\left(s-\frac{L(t)}{2}\right)\right] \\
&\cdot \left[a_{bh} - b_{bh}\cos\left(2\pi\left(\frac{s}{L(t)}+\frac{1}{2}\right)\right) + c_{bh}\cos\left(4\pi\left(\frac{s}{L(t)}+\frac{1}{2}\right)\right)\right] \\
&\cdot \left[\frac{\sin\left(2\pi B(t)s\right)}{\pi s}\right],
\end{aligned}
$$

where

$$
H(x) = \begin{cases} 1 \,\forall\, x > 0 \\ \frac{1}{2} \,\forall\, x = 0 \\ 0 \,\forall\, x < 0 \end{cases} .
$$

The windowing function for the filter is selected by the coefficients a,b, and c. For Blackman-Harris window the coefficients are $a_{bh} = 0.42$, $b_{bh} = 0.5$, and $c_{bh} = 0.08$.

The parameters $B(t)$ and $L(t)$ define the filter bandwidth and attenuation in the passband and in the stopband. $B(t)$ and $L(t)$ are nth order user definable polynomials to allow adaptation of the filter bandwidth as a function of time. The user provides the $B(t)$ and $L(t)$ values over specific SLTH ranges (see e.g. Table 5.3) together with a polynomial order n. The filtering function shall perform a polynomial fit to generate $B(SLTH)$ and $L(SLTH)$. It should be noted that $B(t)$ and $L(t)$ do not have to be continuous. The user specified number of B and L values must be compliant with the order of the polynomial so that the polynomial fit is feasible.

A user definable option is to apply the low-pass filter for any input data including the products from GRAS GSN and GRAS/Metop NRT POD. The filtering parameters are user definable separately for each input data.

6.3.7 Pseudorange calculations

6.3.7.1 C/A code pseudorange

The mathematical formulation of the C/A code pseudorange derivation has been removed.

6.3.7.2 P code pseudorange

The mathematical formulation of the P code pseudorange derivation has been removed.

6.4 Occultation Table Generation

Input Parameters:

1. Metop CoM position vector $\vec{r}_{leo}\left(t^{mjd}\right)$;
2. Metop CoM velocity vector $\vec{v}^{eci}_{leo}\left(t^{mjd}\right)$;
3. GPS CoM position vector $\vec{r}_{gps}\left(t^{mjd}\right)$.

Table 6.26: Default parameters for occultation table generation.

Parameter	Default value	Range
Metop orbit arc length	36 h	0 - 48 h
GPS orbit arc length	36 h	0 - 48 h
Position vector sampling interval	10 s	1 - 60 s
Occultation table generation time	11:00	00:00 - 24:00
Occultation table dissemination time	11:30	00:00 - 24:00
SLTH measurement start for geolocation	80 km	-60 - 80 km
SLTH measurement end for geolocation	-60 km	-60 - 80 km

Output Parameters:

1. Occultation table as defined in **AD4**.

The purpose of the occultation table generation function is to predict and name all measurements that GRAS theoretically would be able to measure for a user definable time period. These measurements include rising and setting occultations, and all navigation measurements by GZA. This information is sent to the GRAS GSN for optimizing the data flow from GSN to EPS CGS.

Algorithm

The baseline assumption is that the occultation generation function requests predicted Metop position and velocity vectors from an orbit propagation function for a defined orbit arc length and with a defined sampling interval. The default values and value ranges for these parameters are listed in Table 6.26. All parameters are user definable.

The orbit propagation function generates the Metop position and velocity vector samples and the corresponding time stamps as

$$\left\{ \left(\vec{r}_{leo}^{eci}(i), \vec{v}_{leo}^{eci}(i), t_{epoch}^{mjd}(i) \right) ;\ i : 1 \rightarrow N \right\},$$

where

$t_{epoch}^{mjd}(i)$ = the epoch of the position and velocity vector sample i in MJD2000 time frame [s].

The NRT GPS position vectors provided by the GRAS GSN are used in the occultation table generation. The sampling interval of the GPS position vectors in the GSN products is normally much longer than the sampling interval defined in Table 6.26. The GPS position vectors shall be interpolated to the epochs of the Metop position and velocity vectors using the Lagrange interpolation algorithm described in Section 6.3.1.1 extending the set of vector samples to

$$\left\{ \left(\vec{r}_{leo}^{eci}(i), \vec{v}_{leo}^{eci}(i), \vec{r}_{gps_k}^{eci}(i), t_{epoch}^{mjd}(i) \right) ;\ i : 1 \rightarrow N,\ k : 1 - 32 \right\},$$

where index k denotes the PRN numbers of the operational GPS satellites.

The occultation table generation is based on the determination of the incidence angle of the ray from each GPS satellite to the GRAS occultation and navigation antennas.

The unit vectors normal to each GRAS antenna radiating surface plane can be approximated by ignoring antenna misalignment and Metop mispointing, and by positioning the antennas at the Metop CoM as

$$\hat{n}^{eci}_{gva} = \frac{\vec{v}^{eci}_{leo}}{|\vec{v}^{eci}_{leo}|}, \tag{6.220}$$

$$\hat{n}^{eci}_{gava} = \frac{-\vec{v}^{eci}_{leo}}{|\vec{v}^{eci}_{leo}|}, \tag{6.221}$$

$$\hat{n}^{eci}_{gza} = \frac{\vec{r}^{eci}_{leo}}{|\vec{r}^{eci}_{leo}|}. \tag{6.222}$$

A unit vector anti-parallel to the incoming ray (ignoring the bending of the ray path in the atmosphere) is derived from

$$\hat{r}^{eci}_{apx_k} = \frac{\vec{r}^{eci}_{gps_k} - \vec{r}^{eci}_{leo}}{\left|\vec{r}^{eci}_{gps_}k - \vec{r}^{eci}_{leo}\right|}.$$

The elevation $\theta^{eci}_{gps_k}$ and azimuth $\varphi^{eci}_{gps_k}$ angles of the incoming ray can now be derived from

$$\theta^{eci}_{gps_k} = \arccos\left(\frac{\hat{r}^{eci}_{apx_k} \cdot \hat{n}_{gza}}{\left|\hat{r}^{eci}_{apx_k}\right| \left|\hat{n}_{gza}\right|}\right), \tag{6.223}$$

$$\varphi^{eci}_{gps_k} = \arctan\left(\frac{\hat{r}^{eci}_{apx_k} \cdot (\hat{n}_{gva} \times \hat{n}_{gza})}{\hat{r}^{eci}_{apx_k} \cdot \hat{n}_{gva}}\right). \tag{6.224}$$

Because of the definition of the coordinate system, the derived azimuth and elevation angles are the same for each GRAS antenna. This is taken into account in the definition of the field of view for each antenna and thus an incoming ray can only be visible as a maximum for one antenna at a time.

By using Equations 6.223 and 6.224 for for each GPS satellite for each epoch the set of samples for each satellite state vector epoch can be expanded to

$$\left\{\left(\vec{r}^{eci}_{leo}(i), \vec{v}^{eci}_{leo}(i), \vec{r}^{eci}_{gps_k}(i), \theta^{eci}_{gps_k}(i), \varphi^{eci}_{gps_k}(i), t^{mjd}_{epoch}(i)\right);\ i : 1 \rightarrow N,\ k : 1 - 32\right\}.$$

The start and end epochs of the occultation and navigation measurements can be identified from the total set of samples by identifying the epochs when the elevation and azimuth angles of the incoming rays enter and leave the “occultation windows” defined for each GRAS antenna in Table 6.27. The accuracy of the occultation measurement start and end epoch estimation is improved by

Table 6.27: Measurement start and end determination parameters for each GRAS antenna.

Antenna	Elevation	Azimuth	SLTH height
GVA	-23° - -26°	45° - -45°	-40 - 80 km
GAVA	-23° - -26°	135° - 180°, -135° - -180°	-40 - 80 km
GZA	20° - 90°	0° - 360°	NA

determining when the predicted SLTH exceeds the specified height range. All parameters in Table 6.27 are used definable.

The geolocation is determined at the epoch when the SLTH reaches the values specified in the fields "SLTH measurement start" and "SLTH measurement end" in Table 6.26. It is important to note that the start and end SLTH values are specified for setting occultations. For the rising occultations the values have to be swapped. The determined geodetic coordinates are to be written into the fields PRED_START_LAT, PRED_START_LONG and PRED_END_LAT, PRED_END_LONG in the occultation table.

Because the bending angle of the ray is not known at the time of the occultation table generation, the geodetic coordinates of the measurement must be derived by using a straight line between the satellites and the SLTH. SLTH is the shortest distance between a reference ellipsoid surface and the straight line between the occulting GPS satellite and the Metop. The ECI coordinates of this point can be determined by expanding or contracting the reference ellipsoid so that it has exactly one common point with the straight line. At this point the straight line is tangent to the ellipsoid surface. The geodetic height of the common point from the surface of the reference ellipsoid is the SLTH value.

The position vector of the tangent point can be calculated from

$$\vec{r}^{eci}_{tan_pred} = \vec{r}^{eci}_{gps} + \frac{-\beta_e}{2\alpha_e}\left(\vec{r}^{eci}_{leo} - \vec{r}^{eci}_{gps}\right), \tag{6.225}$$

where

$$\beta_e = \frac{1}{\left|\vec{r}^{eci}_{leo} - \vec{r}^{eci}_{gps}\right|}\left[2a_1\left(a_2 - a_1\right) + 2b_1\left(b_2 - b_1\right) + \frac{2c_1\left(c_2 - c_1\right)}{\left(1-f\right)^2}\right],$$

and

$$\alpha_e = \frac{1}{\left|\vec{r}^{eci}_{leo} - \vec{r}^{eci}_{gps}\right|}\left[\left(a_2 - a_1\right)^2 + \left(b_2 - b_1\right)^2 + \frac{\left(c_2 - c_1\right)^2}{\left(1-f\right)^2}\right],$$

and

$\vec{r}^{eci}_{leo}$ = the position vector of the Metop satellite CoM in ECI frame;

$\vec{r}^{eci}_{gps}$ = the position vector of the occulting GPS satellite CoM in ECI frame;

a_1, b_1, c_1 = the components of the $\vec{r}_{gps}^{eci}$ as $\vec{r}_{gps}^{eci} = a_1\hat{x}^{eci} + b_1\hat{y}^{eci} + c_1\hat{z}^{eci}$;

a_2, b_2, c_2 = the components of the $\vec{r}_{leo}^{eci}$ as $\vec{r}_{leo}^{eci} = a_2\hat{x}^{eci} + b_2\hat{y}^{eci} + c_2\hat{z}^{eci}$.

The semi-major axis of the ellipsoid that corresponds to the determined geolocation can be derived from using α_e and β_e as

$$a'_e = \sqrt{\gamma_e - \frac{\beta_e^2}{4\alpha_e}}, \tag{6.226}$$

where

$$\gamma_e = a_1^2 + b_1^2 + \frac{c_1^2}{(1-f)^2},$$

The coordinates given by Equation 6.225 must be transformed to ECEF coordinate frame before they can be converted to latitude, longitude and geodetic height. The geodetic coordinate derivation is specified in Section 6.3.3.3. The geodetic height from the geodetic coordinate derivation is the SLTH value.

The output data from the occultation table generation function is specified in the VIADR-1A-OCCULTATION TABLE record in **AD4**.

Appendinx A: GRAS/Metop Precise Orbit Determination with Square Root Information Filter

A.1 SRIF ALGORITHM DESCRIPTION

A.1.1 Introduction

The Square Root Information Filter (SRIF) is a sequential estimator that incorporates a dynamical model in an orbital propagator together with a measurement simulator to adjust an orbit to a set of measurements that are sequentially incorporated into the filter (one by one or in batches).

SRIF has some advantages with respect to other sequential filters (e.g. Kalman) from the computational estability point of view at the same time that allows the resolution of non-lineatities in the dynamical equations in a similar manner as a least-squares algorithm does.

The following sections describe the basic principles of he SRIF algorithms and provide the algorithms to implement a software package to solve the precise orbit determination problem of Metop using SRIF.

To minimise the amount of ancillary information provided in this document, it is assumed that the basic principles of orbit determination are known (refer to **[RD22]**).

A.1.2 Linearised Dynamical Problem

The problem to be solved corresponds to the state transition linearised equation

$$\begin{bmatrix} p \\ x \\ y \end{bmatrix}_{k+1} = \begin{bmatrix} M & 0 & 0 \\ V_p & V_x & V_y \\ 0 & 0 & I \end{bmatrix} \begin{bmatrix} p \\ x \\ y \end{bmatrix}_k + \begin{bmatrix} w_i \\ 0 \\ 0 \end{bmatrix} \qquad (A.1.2\text{-}1)$$

where p, x and y are the correlated process noise, state vector and bias arrays with sizes n_p, n_x *and* n_y respectively.

The sub-matrices V_p, V_x *and* V_y are the transition matrices for x with respect to p, x and y respectively. This formulation is generic and corresponds to the state transition between two consecutive times t_k and t_{k+1} that can be represented by the mentioned variables and transition matrices.

The transition matrices contain the partial derivatives of the estimated parameter x_i with respect to the corresponding variables at t_k.

$$\left(v_{i,j}\right)_p = \frac{\partial x_i}{\partial p_j}$$
$$\left(v_{i,j}\right)_x = \frac{\partial x_i}{\partial x_j}$$
$$\left(v_{i,j}\right)_y = \frac{\partial x_i}{\partial y_j} \qquad (A.1.2\text{-}2)$$

The matrix *M* the transition matrix of *p*. It is diagonal and in the particular case of Exponentially Correlated Random Variables (ECRV, **[RD24]** page 152) each element takes the form

$$m_i = e^{-\frac{\Delta t}{t_i}} \quad \Leftarrow \quad \left(p_i\right)_{k+1} = \left(p_i\right)_k e^{-\frac{\Delta t}{t_i}} + w_i \qquad (A.1.2\text{-}3)$$

where t_i is the correlation time for the *i*-th variable.

The vector w_i is the white noise associated to the correlated variables in *p*.

The sub-matrix I is the unit matrix

A.1.3 Linearised Data Equation

The dynamical system described above is observed by a set of observations whose data equation is linearly expressed as (sub-indices between parentheses indicate matrix or array sizing)

$$z_{(m)} = A_{(m\times n)} \cdot x_{(n)} + n_{(m)} \qquad (A.1.3\text{-}1)$$

This equation represents a set of *m* observations in the array z with associated observation errors in array n used to estimate a set of n parameters contained in x through the $m\times n$ matrix of observation partials A.

A.1.3.1 Normalisation

The *m*-sized vector of observation errors ν is assumed to have zero mean and unit covariance; i.e. the initial data equation is normalised (weighted) with the observation covariance. This is accomplished by the use of the observation covariance matrix Q_0.

$$Q_0 = \begin{bmatrix} s_{11}^2 & s_{12} & \cdots & s_{1m} \\ s_{21} & s_{22}^2 & \cdots & s_{2m} \\ \vdots & \vdots & \ddots & \vdots \\ s_{m1} & s_{m2} & \cdots & s_{mm}^2 \end{bmatrix} \qquad (A.1.3\text{-}2)$$

The relationships between z, n and A with their corresponding de-normalised Y, e and F versions are the following

$$z = \Lambda_0^{-1} \cdot Y \qquad (A.1.3\text{-}3)$$
$$n = \Lambda_0^{-1} \cdot e$$
$$A = \Lambda_0^{-1} \cdot F$$

being Λ_0 lower triangular given by $\Lambda_0 \cdot \Lambda_0^T = Q_0$

This allows assigning to each observation its right importance in comparison to the total data set at the same time that allows mixing observations of different nature (e.g. range and Doppler)

If the observations are not correlated then Q_0 is diagonal and the expressions above are simplified with

$$Q_0 = \begin{bmatrix} s_{11}^2 & 0 & \cdots & 0 \\ 0 & s_{22}^2 & \cdots & 0 \\ \vdots & \vdots & \ddots & \vdots \\ 0 & 0 & \cdots & s_{mm}^2 \end{bmatrix} \Rightarrow \Lambda_0^{-1} = \begin{bmatrix} \frac{1}{s_{11}} & 0 & \cdots & 0 \\ 0 & \frac{1}{s_{22}} & \cdots & 0 \\ \vdots & \vdots & \ddots & \vdots \\ 0 & 0 & \cdots & \frac{1}{s_{mm}} \end{bmatrix} \qquad (A.1.3\text{-}4)$$

The knowledge of Q_0 does not permit in general the implementation of the full matrix. The non-correlation between measurements is questionable in general since some of the items (e.g. the receiver clock offset) that contribute in the observation are correlated between consecutive epoch and also across measurements coming from different emitter. However, it is in general not possible to establish a-priori the levels for these correlations to build the full Q_0. In practice, the use of a diagonal Q_0 suffices the need of providing a-priori information on the measurements and also the relative weighting of the observations with respect to the dynamics.

A.1.3.2 Data Equation Interpretation

In the data equation, z and x represent incremental values with respect to a reference usually taken to be the initial one. This means that x is the increment to apply to the initial estimate of the extended state vector x_0 to obtain its updated estimated value x_e and z represents the computed observation residual between the measured observation y_{real} and the one computed from the observation models y

$$z = \Lambda_0^{-1} \cdot Y = \Lambda_0^{-1} \cdot (y_{real} - y) \qquad (A.1.3\text{-}5)$$

$$x = x_e - x_0$$

The matrix of observation partials is defined as

$$F_{(m\times n)} = \begin{bmatrix} \frac{\partial y_1}{\partial x_1} & \frac{\partial y_1}{\partial x_2} & \cdots & \frac{\partial y_1}{\partial x_n} \\ \frac{\partial y_2}{\partial x_1} & \frac{\partial y_2}{\partial x_2} & \cdots & \frac{\partial y_2}{\partial x_n} \\ \vdots & \vdots & \ddots & \vdots \\ \frac{\partial y_m}{\partial x_1} & \frac{\partial y_m}{\partial x_2} & \cdots & \frac{\partial y_m}{\partial x_n} \end{bmatrix}_{x=x_0} \qquad (A.1.3\text{-}6)$$

In the general case one intends to minimise some magnitude associated to the observation error. For instance one could chose x to minimise the square sum of the weighted observation errors J

$$J = \sum_{j=1}^{m} n_j^2 = n^T \cdot n = e^T \cdot Q_0^{-1} \cdot e \qquad (A.1.3\text{-}7)$$

A.1.4 The SRIF Information Matrix

The principle of the SRIF algorithm is based on the implementation of the following information array

$$\begin{bmatrix} \tilde{R}_{(n\times n)} & \tilde{z}_{(n)} \\ A_{(m\times n)} & z_{(m)} \end{bmatrix}_{(n+m)\times(n+1)} \qquad (A.1.4\text{-}1)$$

This matrix contains the information of an arbitrary (processing-wise speaking) previous state in terms of covariance and observations $\begin{bmatrix}\tilde{R} & \tilde{z}\end{bmatrix}$ and the information added by a set of m new observations through the $\begin{bmatrix}A & z\end{bmatrix}$ part of the array.

The relationship between $\begin{bmatrix}\tilde{R} & \tilde{z}\end{bmatrix}$ and the parameter estimation vector is given by

$$\tilde{z} = \tilde{R} \cdot x + \tilde{n} \qquad (A.1.4\text{-}2)$$

which has the form of a data equation for some n fictitious observations $\tilde{z}$ with associated noise $\tilde{n}$

From the practical point of view one has a state k (at time t_k) represented by $\begin{bmatrix}\tilde{R} & \tilde{z}\end{bmatrix}_k$ that is updated with a set of new observations represented by $\begin{bmatrix}A & z\end{bmatrix}_k$. This new set of observations is incorporated into the process by the adequate orthogonal transformation T to obtain the the updated information array $\begin{bmatrix}\hat{R} & \hat{z}\end{bmatrix}_k$, still at t_k, and the residuals e_k of the incorporated observations. The updated information array $\begin{bmatrix}\hat{R} & \hat{z}\end{bmatrix}_k$ is then propagated to the next state k, at t_{k+1} also by means of orthogonal transformation (see 3.5.3) This updated value of the

observation array $\begin{bmatrix}\tilde{R} & \tilde{z}\end{bmatrix}_{k+1}$ can be used to initialise state *k+1*. All this process can be summarised as follows:

$$\begin{bmatrix}\tilde{R} & \tilde{z}\\ A & z\end{bmatrix}_k \xrightarrow{T} \begin{bmatrix}\hat{R} & \hat{z}\\ 0 & e\end{bmatrix}_k \left\langle \begin{matrix}\begin{bmatrix}\hat{R} & \hat{z}\end{bmatrix}_k \xrightarrow{T} \begin{bmatrix}\tilde{R} & \tilde{z}\end{bmatrix}_{k+1}\\ e_k \\ \\ \begin{bmatrix}A & z\end{bmatrix}_{k+1}\end{matrix}\right\rangle \longrightarrow \begin{bmatrix}\tilde{R} & \tilde{z}\\ A & z\end{bmatrix}_{k+1} \qquad (A.1.4\text{-}3)$$

This can be used to sequentially process any number of sets of an arbitrary number of *m* observations just by feeding as initial information array with the one resulting from the process and combining it with any new set of observations.

The estimates of the state vector at *k* and *k+1* can then be directly obtained from

$$x_k = \hat{R}^{-1} \cdot \hat{z}_k \qquad (A.1.4\text{-}4)$$
$$x_{k+1} = \tilde{R}^{-1} \cdot \tilde{z}_{k+1}$$

A.1.5 SRIF Algorithm Computation Method

A.1.5.1 Initialisation

In the first step of the SRIF processing one needs to provide initial values R_0 and x_0.

The initialisation of the algorithm can be accomplished easily by means of the initial parameter covariance, i.e.

$$P_0^{-1} = R_0 \cdot R_0^T \quad \Leftrightarrow \quad R_0 = \sqrt{P_0^{-1}} \qquad (A.1.5\text{-}1)$$

where R_0 is lower triangular.

In the common case of initial diagonal covariance matrix (this is the usual situation as no a-priori knowledge of the correlation between the different estimated parameters is in general available) this factorisation becomes

$$R_0 = \sqrt{P_0^{-1}} \quad \Rightarrow \quad \begin{cases} r_{ij} = s_{ij}^{-1} & i = j \\ 0 & i \neq j \end{cases} \qquad (A.1.5\text{-}2)$$

In either case, the initial value of the information array becomes

$$\begin{bmatrix}\tilde{R}_0 & \tilde{z}_0\end{bmatrix} = \begin{bmatrix}R_0 & R_0 \cdot x_0\end{bmatrix} \qquad (A.1.5\text{-}3)$$

In the successive addition of new observations the new R is part of the result of the processing itself.

A.1.5.2 Array Updating

Once the algorithm has been initialised it is necessary to define the mechanism that allows incorporating a batch of new observations and lets the filter step to the following state. As identified above this is accomplished by means of an orthogonal transformation T that converts the information array augmented with the new observations into an equivalent matrix in which the contribution of the observation partials A is nullified. For convenience, it is useful to select such an orthogonal transformation such that it not only nullifies A but that also the resulting matrix $\hat{R}$ is triangular

$$\begin{bmatrix} \tilde{R} \\ A \end{bmatrix} \xrightarrow{T} \begin{bmatrix} \hat{R} \\ 0 \end{bmatrix} \qquad (A.1.5\text{-}4)$$

The transformation has to be applied not only to the information matrix but also to the observations vector in order to be able to obtain the new estimated parameters and the residuals. The complete transformation equation becomes then

$$\begin{bmatrix} \tilde{R} & \tilde{z} \\ A & z \end{bmatrix} = \begin{bmatrix} \tilde{r}_{11} & \tilde{r}_{12} & \cdots & \tilde{r}_{1n} & \tilde{z}_1 \\ \tilde{r}_{21} & \tilde{r}_{22} & \cdots & \tilde{r}_{2n} & \tilde{z}_1 \\ \vdots & \vdots & \ddots & \vdots & \vdots \\ \tilde{r}_{n1} & \tilde{r}_{n2} & \cdots & \tilde{r}_{nn} & \tilde{z}_{n1} \\ a_{11} & a_{12} & \cdots & a_{1n} & z_1 \\ a_{21} & a_{22} & \cdots & a_{2n} & z \\ \vdots & \vdots & \ddots & \vdots & \vdots \\ a_{m1} & a_{m2} & \cdots & a_{mn} & z_{n1} \end{bmatrix} \xrightarrow{T} \begin{bmatrix} \hat{r}_{11} & \hat{r}_{12} & \cdots & \hat{r}_{1n} & \hat{z}_1 \\ 0 & \hat{r}_{22} & \cdots & \hat{r}_{2n} & \hat{z}_2 \\ \vdots & \vdots & \ddots & \vdots & \vdots \\ 0 & 0 & \cdots & \hat{r}_{nn} & \hat{z}_n \\ 0 & 0 & \cdots & 0 & e_1 \\ 0 & 0 & \cdots & 0 & e_2 \\ \vdots & \vdots & \ddots & \vdots & \vdots \\ 0 & 0 & \cdots & 0 & e_m \end{bmatrix} = \begin{bmatrix} \hat{R} & \hat{z} \\ 0 & e \end{bmatrix} \qquad (A.1.5\text{-}5)$$

This orthogonal transformation can be obtained by means of a Householder transformation matrix (see 3.6 below).

In each filtering step the solution of the estimated parameters and the covariance matrix is obtained with a back substitution method from the equations

$$\hat{R} \cdot x = \hat{z} \qquad (A.1.5\text{-}6)$$

$$P = \left(\hat{R} \cdot \hat{R}^T\right)^{-1} = \hat{R}^{-1} \cdot \hat{R}^{-T}$$

From the implementation point of view, it is interesting to separate the information array into two arrays $[\tilde{S}]$ and $[\tilde{R}_y \quad \tilde{z}_y]$ in the following way

$$[\tilde{R} \quad \tilde{z}] = \begin{bmatrix} \tilde{S} \\ \tilde{R}_y \quad \tilde{z}_y \end{bmatrix} = \begin{bmatrix} \tilde{S}_p & \tilde{S}_x & \tilde{S}_y & \tilde{S}_z \\ 0 & 0 & \tilde{R}_y & \tilde{z}_y \end{bmatrix} = \begin{bmatrix} \tilde{R}_p & \tilde{R}_{px} & \tilde{R}_{py} & \tilde{z}_p \\ \tilde{R}_{xp} & \tilde{R}_x & \tilde{R}_{xp} & \tilde{z}_x \\ 0 & 0 & \tilde{R}_y & \tilde{z}_y \end{bmatrix} \qquad (A.1.5\text{-}7)$$

The processing of the observations is better performed in two steps that take into account the adopted partitioning of the information array.

The first step consists in solving the $\tilde{S}$ array disregarding the bias part $\lfloor \tilde{R}_y \quad \tilde{z}_y \rfloor$

$$\begin{bmatrix} \tilde{S}_p & \tilde{S}_x & \tilde{S}_y & \tilde{S}_z \\ A_p & A_x & A_y & z \end{bmatrix} \xrightarrow{T} \begin{bmatrix} \hat{S}_p & \hat{S}_x & \hat{S}_y & \hat{S}_z \\ 0 & 0 & \hat{A}_y & \hat{z} \end{bmatrix} \qquad (A.1.5\text{-}8)$$

with

$$\hat{S}_p = \begin{bmatrix} \hat{R}_p \\ 0 \end{bmatrix} \qquad (A.1.5\text{-}9)$$

being $\hat{R}_p$ upper triangular

$$\hat{S}_x = \begin{bmatrix} \hat{R}_{px} \\ \hat{R}_x \end{bmatrix} \qquad (A.1.5\text{-}10)$$

being $\hat{R}_x$ upper triangular

The second step solves $\lfloor \tilde{R}_y \quad \tilde{z}_y \rfloor$ using information from the first step

$$\begin{bmatrix} \tilde{R}_y & \tilde{z}_y \\ \hat{A}_y & \hat{z} \end{bmatrix} \xrightarrow{T} \begin{bmatrix} \hat{R}_y & \hat{z}_y \\ 0 & e \end{bmatrix} \qquad (A.1.5\text{-}11)$$

being $\hat{R}_y$ upper triangular

A.1.5.3 Propagation

Once the set of observations have been used to update the information array at state k it is necessary to propagate it to the state $k+1$ (e.g. identified by the time of the last processed observation). This allows to sequentially process the next batches of observations. The propagation is also performed in two steps taking advantage of the array decomposition adopted during the update phase. Additionally to all the elements involved in the update phase, propagation requires the knowledge of the transition matrices M, V_p, V_x and V_y and the covariance Q_0 of the noises w_k associated to the correlated variables in p.

The first step propagates the $\hat{S}$ array disregarding the bias part $\lfloor \hat{R}_y \quad \hat{z}_y \rfloor$. For this purpose the augmented information array $\hat{S}_A$ at k is formed

$$S_A = \begin{bmatrix} -R_w \cdot M & R_w & 0 & 0 & z_w \\ \hat{S}_p - S_x^d \cdot V_p & 0 & S_x^d & \hat{S}_y - S_x^d \cdot V_y & \hat{S}_z \end{bmatrix}_{(2n_p+n_x+n_y+1)\times(2n_p+n_x)} \qquad (A.1.5\text{-}12)$$

with

$$S_x^d = \hat{S}_p V_x^{-1} \qquad (A.1.5\text{-}13)$$
$$R_w^{-1} \cdot \left(R_w^{-1}\right)^T = Q$$
$$z_w = R_w \cdot w_k$$

The appropriate Householder transformation is then applied to obtain the propagated state at $k+1$

$$\begin{bmatrix} -R_w \cdot M & R_w & 0 & 0 & z_w \\ \hat{S}_p - S_x^d \cdot V_p & 0 & S_x^d & \hat{S}_y - S_x^d \cdot V_y & \hat{S}_z \end{bmatrix}_k \xrightarrow{T} \begin{bmatrix} R_p^* & R_{pp}^* & R_{px}^* & R_{py}^* & z_p^* \\ 0 & \tilde{S}_p & \tilde{S}_x & \tilde{S}_y & \tilde{S}_z \end{bmatrix}_{k+1} \qquad (A.1.5\text{-}14)$$

with R_p^* upper triangular and

$$\tilde{S}_p = \begin{bmatrix} \tilde{R}_p \\ \tilde{R}_{xp} \end{bmatrix}; \qquad \tilde{S}_x = \begin{bmatrix} \tilde{R}_{px} \\ \tilde{R}_x \end{bmatrix}; \qquad \tilde{S}_y = \begin{bmatrix} \tilde{R}_{py} \\ \tilde{R}_{xy} \end{bmatrix}; \qquad \tilde{S}_z = \begin{bmatrix} \tilde{z}_p \\ \tilde{z}_x \end{bmatrix} \qquad (A.1.5\text{-}15)$$

The propagation of the $\left[\hat{R}_y \quad \hat{z}_y\right]$ to the state k is quite simple and represented by

$$\left[\tilde{R}_y \quad \tilde{z}_y\right]_{k+1} = \left[\hat{R}_y \quad \hat{z}_y\right]_k \qquad (A.1.5\text{-}16)$$

A.1.5.4 Partitioned Estimates and Covariance

A convenient way of computing the new values of the estimates and the covariance makes use of the partitioned information array described above. Using this method the following computations are possible

1. *Computed estimates* of p and x as if the y biases did not exist

$$\begin{bmatrix} \hat{p} \\ \hat{x} \end{bmatrix}_k^c = \left[\hat{S}_p \;\; \hat{S}_x\right]^{-1} \hat{S}_z \qquad (A.1.5\text{-}17)$$

2. *Biases estimate*

$$\hat{y}_k = \hat{R}_y^{-1} \cdot \hat{z}_y \qquad (A.1.5\text{-}18)$$

3. *Sensitivity*

$$S_e = -\left[\hat{S}_p \;\; \hat{S}_x\right]^{-1} \hat{S}_y \qquad (A.1.5\text{-}19)$$

4. *Estimates* of p and x

$$\begin{bmatrix} \hat{p} \\ \hat{x} \end{bmatrix}_k = \begin{bmatrix} \hat{p} \\ \hat{x} \end{bmatrix}_k^c + S_e \cdot \hat{y}_k \qquad (A.1.5\text{-}20)$$

5. *Computed covariance* of p and x as if the y biases did not exist

$$P_{p,x}^c = \left[\hat{S}_p \;\; \hat{S}_x\right]^{-1} \cdot \left(\left[\hat{S}_p \;\; \hat{S}_x\right]^{-1}\right)^T \qquad (A.1.5\text{-}21)$$

6. *Biases covariance*

$$P_y = \hat{R}_y^{-1} \cdot \left(\hat{R}_y^{-1}\right)^T \qquad (A.1.5\text{-}22)$$

7. *Covariance* of p and x

$$P_{p,x} = P_{p,x}^c + \left(S_e \cdot \hat{R}_y^{-1}\right) \cdot \left(S_e \cdot \hat{R}_y^{-1}\right)^T \qquad (A.1.5\text{-}23)$$

A.1.6 Householder Transformation

A.1.6.1 Mathematical Theory

This transformation will allow the conversion of a matrix into an upper triangular one. This will simplify the solving of any system of linear equations by means of a back substitution procedure (avoiding the need of the matrix inversion).

The main idea behind the transformation is the geometric reflection of a vector with respect to a plane. Let w be the vector that defines the plane orientation, y the vector to be reflected, and y_r the result of the reflection. y and y_r can be expressed analytically as:

$$\begin{aligned} y &= (y^T \cdot w)w + v \\ y_r &= -(y^T \cdot w)w + v \end{aligned} \qquad (A.1.6\text{-}1)$$

Subtracting both equations (to eliminate v):

$$y_r = y - 2(y^T w)w \qquad (A.1.6\text{-}2)$$

The above equation can be rearranged to obtain:

$$y_r = y - 2(w \cdot w^T)y = (I - 2w \cdot w^T)y \qquad (A.1.6\text{-}3)$$

Hence, the matrix T that defines the Householder transformation is:

$$T = I - 2w \cdot w^T \qquad (A.1.6\text{-}4)$$

This matrix has important properties, namely it is orthogonal and idempotent:

$$T^2 = (I - 2w \cdot w^T) \cdot (I - 2w \cdot w^T) = \qquad (A.1.6\text{-}5)$$
$$I - 4w \cdot w^T + 4w \cdot (w^T w) \cdot w^T = I$$

Therefore $T = T^{-1}$, taking into account $T = T^T$ (symmetry), $T = T^{-T}$, proving orthogonality.

The transformation performed by T can be expressed as:

$$T \cdot y = y - gw \qquad (A.1.6\text{-}6)$$

where

$$g = 2\frac{y^T \cdot w}{w^T \cdot w} \qquad (A.1.6\text{-}7)$$

Using this last expression requires an order of computation less than direct calculation of T, and this form will be the one used in the SRIF algorithm.

As it has been mentioned above, this transformation is used to obtain upper triangular matrices. To achieve this goal it is enough to choose y_r lying on $(s, 0, \ldots, 0)$ Then, the vector w should be:

$$w = \frac{1}{g}(y - s \cdot e) \qquad (A.1.6\text{-}8)$$
$$e = (1, 0, \ldots, 0)$$

Then it is possible to obtain zeroes below the first element of the transformed vector y with the following approach

$$s = -\mathrm{sgn}(y_1)(y^T \cdot y)^{1/2} \qquad (A.1.6\text{-}9)$$
$$u_1 = y_1 - s$$
$$u_j = y_j \quad , \quad j > 1$$

with the transformation be written as

$$T \cdot y = s \cdot e \qquad (A.1.6\text{-}10)$$

A.1.6.2 Application to SRIF

The basic objective of applying the Householder transformation to the SRIF information matrix is to obtain an upper triangular matrix from which the new values of the state vector estimate and its associated covariance matrix can be calculated. Mathematically this can be expressed as

$$\tilde{H} = \begin{bmatrix} \tilde{R}_{(n\times n)} & \tilde{z}_{(n)} \\ A_{(m\times n)} & z_{(m)} \end{bmatrix}_{(n+m)\times(n+1)} \xrightarrow{T} \begin{bmatrix} \hat{R}_{(n\times n)} & \hat{z}_{(n)} \\ 0 & e_{(m)} \end{bmatrix}_{(n+m)\times(n+1)} = \hat{H} \qquad (A.1.6\text{-}11)$$

The formulation for the Householder transformation that accomplishes this task is

$$
\left.
\begin{array}{l}
\hat{R}_{i,i} = -\mathrm{sgn}(\tilde{R}_{i,i}) \cdot \sqrt{\sum_{j=i}^{n} \tilde{R}_{j,i}^2 + \sum_{j=i}^{m} A_{j,i}^2} \\
u_i = \tilde{H}_{i,i} - \hat{R}_{i,i} \\
u_j = \tilde{H}_{j,i} \;\; , \;\; j = i+1,\ldots,n \\
u_{n+j} = A_{j,i} \;\; , \;\; j = i,\ldots,m \\
b = \dfrac{1}{\hat{R}_{i,i} \cdot u_i} \\
\left.
\begin{array}{l}
g = b \cdot \left(\sum_{k=i}^{n} u_k \cdot \tilde{R}_{k,j} + \sum_{k=i}^{m} u_{n+k} \cdot A_{k,j} \right) \\
\hat{R}_{k,j} = \tilde{R}_{k,j} + g \cdot u_k \;\; , \;\; k = i,\ldots,n \\
A_{k,j} = 0 \;\; , \;\; k = 1,m
\end{array}
\right\} j = i+1,\ldots,n+1
\end{array}
\right\} i = 1,\ldots,n
\qquad (A.1.6\text{-}12)
$$

Computationally is better to express the algorithm as a function of the overall matrices H

$$
\left.
\begin{array}{l}
\hat{H}_{i,i} = -\mathrm{sgn}(\tilde{H}_{i,i}) \cdot \sqrt{\sum_{j=i}^{n+m} \tilde{H}_{j,i}^2} \\
u_i = \tilde{H}_{i,i} - \hat{H}_{i,i} \\
u_j = \tilde{H}_{j,i} \;\; , \;\; j = i+1,\ldots,n+m \\
b = \dfrac{1}{\hat{H}_{i,i} \cdot u_i} \\
\left.
\begin{array}{l}
g = b \cdot \sum_{k=i}^{n+m} u_k \cdot \tilde{H}_{k,j} \\
\hat{H}_{k,j} = \tilde{H}_{k,j} + g \cdot u_k \;\; , \;\; k = i,\ldots,n+m
\end{array}
\right\} j = i+1,\ldots,n+1
\end{array}
\right\} i = 1,\ldots,n
\qquad (A.1.6\text{-}13)
$$

A.1.7 Non-linear Formulation

Since the estimation problem has been linearised to be solved, the solution of situations in which the estimate deviates from the real solution more than the target accuracy is not possible with the formulation described above. In this situation the obtained estimate does not lead to the minimum quadratic summation of observation errors. To overcome this problem one can iterate the estimated solution by means of the linear formulation until the minimum quadratic summation of observation errors has been reached with a certain convergence criterion. The following describes the mechanisms that allow the implementation of such iterative algorithm

One starts with the information matrix that represents the system state at certain point and a new set of observations to be processed to obtain the state at the new point. As seen before the objective of the linearisation is to obtain a new information matrix that in turn allows the

computation of a set of improved estimated parameters. This is accomplished by means of an orthogonal transformation whose basic reference equation is

$$\begin{bmatrix} \tilde{R}_0 & \tilde{z}_0 \\ A & z \end{bmatrix} \xrightarrow{T} \begin{bmatrix} \hat{R} & \hat{z} \\ 0 & e \end{bmatrix} \qquad (A.1.7\text{-}1)$$

The iterative process consists in feeding the new estimate $\hat{z}$ into the initial information array to obtain a better estimate of $\hat{z}$. The algorithm can be represented as follows

$$\begin{bmatrix} \tilde{R}_i & \tilde{z}_i \\ A_i & z_i \end{bmatrix} \xrightarrow{T} \begin{bmatrix} \hat{R}_i & \hat{z}_i \\ 0 & e_i \end{bmatrix} \longrightarrow x_i = \hat{R}_i^{-1} \cdot \hat{z}_i$$

Compute new A_i and z_i (i = i + 1)

In this approach the elements sub-indexed with i are calculated every iteration. $\hat{R}_i$, $\hat{z}_i$ and e_i are computed as part of the SRIF algorithm itself (by means of the orthogonal transformation) while A_i and z_i have to be recomputed every iteration based on the new estimate $\hat{z}_i$ (e.g. recalculation of the observations z_i and the observation partials A_i based on the orbit propagation with the just estimated state x_i). The information matrix at the beginning of the iterative process $\tilde{R}_i$ remains the same from one iteration to the next.

The iterative process can be stopped when the convergence criterion defined by a given ε value is fulfilled. For instance

$$\left| \, \| e_{i+1} \| - \| e_i \| \, \right| = \left| \, e_{i+1}^T \cdot e_{i+1} - e_i^T \cdot e_i \, \right| < e \qquad (A.1.7\text{-}2)$$

A.2 ORBIT DETERMINATION WITH SRIF

A.2.1 Algorithm Description

The target of this document was identified in the introduction to describe the implementation of a Square Root Information Filter (SRIF) for orbit determination purposes. The previous chapters described the generalities of the SRIF algorithms. The following paragraphs intend to bring SRIF into the orbit determination context in which three main elements are involved:

- Orbit propagation that provides the dynamic behaviour of the system. This includes both the propagation of the satellite state vector and the variational partials (it is assumed that observation partials are computed analytically)

- Observation processing that allows connecting the real world with the scenario defined by the dynamics through the orbit propagation

- Parameter estimation that permits the tuning of dynamical model parameters and observation modelling parameters in order to obtain the best possible orbit within the target accuracy and provide values for the tuned coefficients.

The implementation of SRIF as filtering algorithm has no impact in the observation processing part since the computation of observations and their partials depends only on the state vector at the observation time. The main impact resides in the orbit propagation and of course in the parameter estimation whose core is the SRIF algorithm itself.

The orbit propagation scheme relays on the use of a numerical integrator that can be either a single-step method (e.g. Runge-Kutta) or a multi-step method (e.g. Adams-Bashforth). Multi-step methods require a single-step method in order to be initialised. The use of SRIF requires that estimate of the initial state vector is updated every time a batch of observations is processed. If a multi-step method is used to propagate the state vector and variational partials, it will have to be reinitialised every time the filtering sequence is executed. The problem has to be analysed on a case by case basis to determine whether the use of multi-step methods is useful at all. In the case when the number of integration steps between consecutive calls to the SRIF algorithm is large one can consider the possibility of implementing such a method, otherwise one may spend all the processing sequence inside the initialisation method.

The sequential processing of observation for orbit determination with SRIF responds to the following sequence of activities:

1. Initialise the orbit propagation with the initial extended state vector (orbit state vector plus initial values of variational partials)

2. Initialise the SRIF algorithm as explained in 3.5 (i.e. provide initial values for $\tilde{R}$ and $\tilde{z}$)

3. Collect the observations to be processed together in one go

4. Propagate the extended state vector at least to the time of the last observation (with the NAPEOS propagator implementation, this orbit integration takes up to the integration step after the last observation time and then the state vector at each observation epoch are interpolated from a table)

5. Process each of the observations and compute the observation differences z and the observation partials A arrays

6. Perform the SRIF filtering to obtain observation residuals e, the triangular information matrix $\hat{R}$ and new values for the extended state vector from $\hat{R} \cdot x = \hat{z}$.

7. If a non-linear approach is being undertaken repeat the sequence from step 1 substituting the initial value of the extended state vector with the just estimated one. Repeat this procedure until certain convergence criterion is fulfilled.

8. Map the estimated state vector to the epoch of the last processed observation and reinitialise the propagator with the extended state vector at that point. This includes the propagation of the information arrays from state *k* to state *k+1* (i.e. obtain $\left[\tilde{R} \quad \tilde{z}\right]_{k+1}$ from $\left[\hat{R} \quad \hat{z}\right]_k$)

9. Come back to step 2 to process each new set of observations. This is performed substituting the initial information array by the final one obtained in the processing of the previous set of observations.

A.2.2 Observation Modelling

For the purpose of this document only GPS like observations are considered. Only estimation aspects are considered while the detailed modelling of the observation simulation is outside the scope of the study.

GPS measurement: Measurement for the count of times between two time marks from clocks aboard of two satellites or one aboard a satellite and another at a ground station. The signal is emitted by a GPS satellite (*e*) and then captured by a GPS receiver (*r*). The distance measure can be done in terms of travel time by clock mark differencing (pseudo-range) or by the count of carrier phase cycles between emission and reception (carrier phase). The equation for these type of observations is

$$r = |\vec{x}_e - \vec{x}_r| - \frac{(\vec{x}_e - \vec{x}_r)\cdot\vec{v}_e}{c} + \Delta r + c\Delta T_{tro} \pm c\Delta T_{ion} + c\Delta T_r - c\Delta T_e + c\Delta T_{rel} + \Delta r_e^{COM} + \Delta r_r^{COM} \qquad (A.2.2\text{-}1)$$

with

$\lvert\vec{x}_e - \vec{x}_r\rvert - \frac{(\vec{x}_e - \vec{x}_r)\cdot\vec{v}_e}{c}$	$\Rightarrow$	geometrical measurement (m)
Δr	$\Rightarrow$	measurement bias including phase ambiguity (m)
ΔT_{tro}	$\Rightarrow$	troposphere refraction delay (s)
ΔT_{ion}	$\Rightarrow$	ionosphere refraction delay (s)
		+ pseudo-range
		– carrier phase
ΔT_r	$\Rightarrow$	receiver clock error (s)
ΔT_e	$\Rightarrow$	emitter clock error (s)
ΔT_{rel}	$\Rightarrow$	relativistic correction (s)
Δr_e^{COM}	$\Rightarrow$	emitter centre of mass correction (m)
Δr_r^{COM}	$\Rightarrow$	receiver centre of mass correction (m)

and all magnitudes are computed at the observation time.

In the Metop POD some simplifications can be performed with respect to this general formulation

$$r = |\vec{x}_e - \vec{x}_r| - \frac{(\vec{x}_e - \vec{x}_r)\cdot\vec{v}_e}{c} + \Delta r + c\Delta T_r - c\Delta T_e + c\Delta T_{rel} + \Delta r_e^{COM} + \Delta r_r^{COM} \qquad (A.2.2\text{-}2)$$

where it has been taken into account that no tropospheric effects need be considered at the Metop altitude and that the ionospheric free combination is used as input to the orbit determination filter.

The generation of the ionospheric-free combination is performed with the following formula

$$P_0 = \frac{f_1^2}{f_1^2 - f_2^2} P_1 - \frac{f_2^2}{f_1^2 - f_2^2} P_2 \qquad (A.2.2\text{-}3)$$

where P stand for either code or phase observations (see **[RD22]** GRASPOD study TN-01 section 6.1.3.3 for details)

A.2.2.1 Pseudo-range Generation Algorithm

The data delivered by the GRAS receiver does include direct pseudo-range information in the code data as part of the telemetry delivered by the satellite. Instead of pseudo-range from the C/A code, C/A code phase samples are contained in the tracking data for navigation.

The C/A code phase contains and integer number of 299729.384 m ambiguity (associated to a sampling rate at 1ms intervals with a speed of light of 299729.384 km/s) that prevents the direct use of such measurements as input for orbit determination purposes. This ambiguity corresponds to the repetition of the 1024 chip rate at the speed of light.

In the assumption that this ambiguity is the only difference between the pseudo-range and the code phase, one can derive the pseudo-range from the code phase as far as that integer number can be computed accurately. In this circumstances, the relationship between the pseudo-range and the code phase is given by

$$P_{C/A} = \Phi_{C/A} + N \cdot \Lambda \qquad (A.2.2\text{-}4)$$

where

$P_{C/A}$	pseudo range associated to the C/A code
$\Phi_{C/A}$	C/A code phase,
Λ	300 km ambiguity associated to the 1024 Hz chip rate of the C/A code and
N	integer quantity to be calculated.

The measured value of $\Phi_{C/A}$ in *(4.2-4)* is derived in metres from

$$\Phi_{C/A} = \frac{CC + \frac{CP}{2^{16}}}{1023 \cdot 10^3} c \qquad (A.2.2\text{-}5)$$

where CC and CP are the code phase constituents contained in the telemetry packets.

$P_{C/A}$ can be computed from *(4.2-2)* where substituting *(4.2-4)* leads to

$$N = \text{nint}\left(\frac{|\vec{x}_e - \vec{x}_r| - \frac{(\vec{x}_e - \vec{x}_r)\cdot \vec{v}_e}{c} + \Delta r + c\Delta T_r - c\Delta T_e + c\Delta T_{rel} + \Delta r_e^{COM} + \Delta r_r^{COM} - \Phi_{C/A}}{\Lambda} \right) \qquad (A.2.2\text{-}6)$$

where the mathematical function **nint** returns the nearest integer to the expression between parentheses and orbital positions and velocities are computed at reception time (UTC associated to the evolution of the IMT scale).

The feasibility of this equation depends on the ability to determine the numerator of the expression about with an accuracy better than 0.5Λ (in practice with an accuracy much better that 0.5Λ). In this situation once can compute N without integer uncertainty. The following typical order of magnitude and accuracies are expected for each of the terms in the numerator:

Item	Magnitude (m)	Accuracy (m)	Comment
$\lvert \vec{x}_e - \vec{x}_r \rvert$	$2 \cdot 10^7$	< 10	From GSN and GRAS POD solutions
$\frac{(\vec{x}_e - \vec{x}_r)\cdot \vec{v}_e}{c}$	10^{-1}	< 1	From GSN and GRAS POD solutions
Δr	< 1	< 1	Predicted from GRAS POD solution
$c\Delta T_e$	Variable	3.0	Clock predicted from GRAS GSN solution ($1ms \pm 10ns$)
$c\Delta T_r$	Variable	3.0	Clock predicted from GRAS POD solution ($1ms \pm 10ns$)
$c\Delta T_{rel}$	< 1	0	Deterministic correction
Δr_e^{COM}	1	0.01	Deterministic correction
Δr_r^{COM}	1	0.01	Deterministic correction

Table 2.2-1: Magnitudes and errors in pseudo-range computation

From the magnitudes in this table some are just inputs to the GRAS POD (i.e. the GPS constellation positions, velocities and clock offsets), some require a-priori knowledge of the Metop precise orbit (i.e. Metop position and velocity, receiver clock offset and measurement bias) and some are deterministic from a model (centre of mass corrections and relativistic effects).

In order to simplify the pseudo-range calculation one can neglect all those terms whose overall contribution to the theoretical pseudo-range computation is small compared to Λ. In this way, one can compute the pseudo-range with an accuracy better than 10 meters according to the equation

$$r = |\vec{x}_e - \vec{x}_r| - \frac{(\vec{x}_e - \vec{x}_r)\cdot\vec{v}_e}{c} + c\Delta T_r - c\Delta T_e \qquad (A.2.2\text{-}7)$$

The equation for the estimation of the code phase ambiguity becomes then

$$N = \mathrm{nint}\left(\frac{|\vec{x}_e - \vec{x}_r| - \frac{(\vec{x}_e - \vec{x}_r)\cdot\vec{v}_e}{c} + c\Delta T_r - c\Delta T_e - \Phi_{C/A}}{\Lambda}\right) \qquad (A.2.2\text{-}8)$$

where $\vec{x}_e$, $\vec{v}_e$ and ΔT_e are inputs coming from the GSN POD constellation solution, Λ is the constant value of one ambiguity cycle ($\Lambda = 292.766\ km$) and $\Phi_{C/A}$ is provided by Level 1a as the navigation measurement.

The values for $\vec{x}_r$ and ΔT_r can be obtained from two sources

- From the previous POD processing step taken from the prediction of Metop orbit and clock. For the purpose of the pseudo-range computation the accuracy can be considered the same as the POD itself.
- From the navigation solution. This is used for initialisation of the processing in case that no previous GRAS POD step is available (system initialisation or reset after GRAS instrument switch-off/switch-on)

A.2.3 Parameter Estimation

This section deals with the identification of estimated parameters as part of the orbit determination and their mapping to the different information arrays that conform the SRIF algorithm.

As first step one must identify the different variables involved in the orbit determination process and then map them in one of the three categories envisaged by SRIF. Depending of the type of process noise associated to the parameter being estimated and its type of variation in the evolution of its estimation, each parameter can be categorised as

- Bias (y): slowly varying parameter (characteristic time is infinity with respect to data processing) and the associated process noise is represented by white noise.
- Correlated (p): exponentially correlated variation of the parameter and the associated process noise is represented by an exponentially correlated random variable ECRV (coloured noise).
- State (x): dynamical estimated parameter with variation directly associated to the estimation process and the associated process noise is represented by white noise.

For the purpose of generality one should include all parameters that are potentially subject to be considered as part of the orbit determination although in some cases one could drop some of them depending on accuracy requirements. The following table summarises the list of estimated parameters and the initial foreseen mapping into the SRIF categories for a generic orbit determination scenario (not particularised to the GRAS POD problem).

Name	Association	Variations	SRIF		
			p	*x*	*y*
State Vector	Satellite	✓		✓	
Solar Radiation Coefficient	Satellite	✓	✓		
Aerodynamic Coefficient	Satellite	✓	✓		
Albedo Coefficient	Satellite	✓	✓		
Infrared Coefficient	Satellite	✓	✓		
Empirical Acceleration	Satellite	✓			✓
Satellite Clock Bias (*)	Satellite		✓		✓
Satellite Transponder Delay	Satellite				✓
Atmospheric Scale Factor	Satellite/Station Satellite/Satellite		✓		
Station Position	Station			✓	
Station Clock Bias	Station				✓
Station Clock Drift	Station				✓
Measurement Bias	Satellite/Station Satellite/Satellite				✓
Earth Orientation Parameter	Global		✓		
Length of the Day	Global		✓		
GPS Clock Bias (*)	Satellite/Station Satellite/Satellite		✓		✓

(*) Depending on the approach, the satellite clock bias may be a pure offset estimated epoch-wise, a polynomial adjustment of the clock evolution, an exponentially correlated random variable or a combination of the last two.

In the particular case of the Metop orbit determination, the table above reduces to the following one

Name	Association	Variations	SRIF		
			p	*x*	*y*
State Vector	Satellite	✓		✓	
Solar Radiation Coefficient	Satellite	✓	✓		
Aerodynamic Coefficient	Satellite	✓	✓		
Empirical Acceleration	Satellite	✓			✓
Satellite Clock Bias (*)	Satellite		✓		✓
Measurement Bias	Satellite/Satellite				✓

(*) Depending on the approach, the satellite clock bias may be a pure offset estimated epoch-wise, a polynomial adjustment of the clock evolution, an exponentially correlated random variable or a combination of the last two.

A.2.3.1 Observation Partials

For the update of the SRIF state with a set of observations one must compute the matrix A which contains the partial derivatives of each individual observation with respect to the estimated parameters. The general expression for the element *i,j* in the matrix A is

$$A = [a_{ij}] = \frac{\partial f_i}{\partial b_j} \qquad (A.2.3\text{-}1)$$

where f_i represents the function that generates the simulation of observation i and b_j represent any of the estimated parameters.

In the particular case when the estimated parameter is the state vector or one of the unknowns in the force models, the partials above cannot be computed directly and the following expanded equation has to be used

$$\frac{\partial f_i}{\partial b_j} = \frac{\partial f_i}{\partial x}\frac{\partial x}{\partial b_i} + \frac{\partial f_i}{\partial y}\frac{\partial y}{\partial b_i} + \frac{\partial f_i}{\partial z}\frac{\partial z}{\partial b_i} + \frac{\partial f_i}{\partial v_x}\frac{\partial v_x}{\partial b_i} + \frac{\partial f_i}{\partial v_y}\frac{\partial v_y}{\partial b_i} + \frac{\partial f_i}{\partial v_z}\frac{\partial v_z}{\partial b_i} \qquad (A.2.3\text{-}2)$$

where (x, y, z, v_x, v_y, v_z) are the components of the satellite state vector whose partial derivatives with respect to the estimated parameters have to be calculated by integration of the variational equations. The partial of the computed observation with respect to the satellite state vector can be directly computed from the simulation model.

In the following sections, the partial derivatives of the elements that are to be estimated as part of the SRIF process are provided. No numerical derivation (except for the atmospheric density with respect to orbital height) is expected and all partial derivatives are to be computed from their

analytical expressions derived either from the dynamic or from the observation equations as appropriate.

A.2.3.2 Observation Partials for GPS Measurements

The starting point is the equation that simulates the observation for the specific Metop POD problem (see A.2.2).

$$r = |\vec{x}_e - \vec{x}_r| - \frac{(\vec{x}_e - \vec{x}_r)\cdot \vec{v}_e}{c} + \Delta r + c\Delta T_r - c\Delta T_e + c\Delta T_{rel} + \Delta r_e^{COM} + \Delta r_r^{COM} \qquad (A.2.3\text{-}3)$$

2.3.2.1 Receiver Partials

Partial derivative of the observation with respect to the **receiver position** (satellite centre of mass) at observation epoch

$$\frac{\partial r}{\partial \vec{x}_r} = -\frac{\vec{x}_e - \vec{x}_r}{|\vec{x}_e - \vec{x}_r|} + \frac{\vec{v}_e}{c} \qquad (A.2.3\text{-}4)$$

where $\frac{\partial r}{\partial \vec{x}_r}$ represents a three dimensional vector, i.e. one component for each partial derivative with respect to each of the satellite position components.

Partial derivatives of the observation with respect to the **receiver clock bias** and **receiver clock drift** at observation epoch

$$\frac{\partial r}{\partial \Delta T_r} = c \qquad (A.2.3\text{-}5)$$

$$\frac{\partial r}{\partial \Delta \dot{T}_r} = ct$$

The final implementation of this partial derivatives depends on the selected clock model. This is discussed in 4.7

2.3.2.2 Dynamic Partials

Partial derivatives of the observation with respect to the solar radiation pressure coefficient C_R at observation epoch

$$\frac{\partial r}{\partial C_R} = \frac{\partial r}{\partial \vec{x}_r}\cdot\frac{\partial \vec{x}_r}{\partial C_R} = \left[-\frac{\vec{x}_e}{|\vec{x}_e - \vec{x}_r|} + \frac{\vec{v}_e}{c}\right]\cdot\frac{\partial \vec{x}_r}{\partial C_R} \qquad (A.2.3\text{-}6)$$

Partial derivatives of the observation with respect to the aerodynamic drag coefficient C_D at observation epoch

$$\frac{\partial r}{\partial C_D} = \frac{\partial r}{\partial \vec{x}_r} \cdot \frac{\partial \vec{x}_r}{\partial C_D} = \left[-\frac{\vec{x}_e}{|\vec{x}_e - \vec{x}_r|} + \frac{\vec{v}_e}{c} \right] \cdot \frac{\partial \vec{x}_r}{\partial C_D} \qquad (A.2.3\text{-}7)$$

Partial derivatives of the observation with respect to initial state vector $\vec{x}_{r0}$ at observation epoch

$$\frac{\partial r}{\partial \vec{x}_{r0}} = \frac{\partial r}{\partial \vec{x}_r} \cdot \frac{\partial \vec{x}_r}{\partial \vec{x}_{r0}} = \frac{\partial \vec{x}_r}{\partial \vec{x}_{r0}} \left[-\frac{\vec{x}_e}{|\vec{x}_e - \vec{x}_r|} + \frac{\vec{v}_e}{c} \right] \qquad (A.2.3\text{-}8)$$

where $\frac{\partial r}{\partial \vec{x}_{r0}}$ represents a three dimensional vector, i.e. one component for each partial derivative with respect to each of the satellite position components and $\frac{\partial \vec{x}_r}{\partial \vec{x}_{r0}}$ is a symmetric square matrix of dimension and rank three (the transition matrix)

A.2.3.3 Variational Equations

To complete the computation of the partial derivatives of the observations with respect to the dynamical model parameters one need to integrate the variational equations that yield the missing terms $\frac{\partial \vec{x}_r}{\partial \vec{x}_{r0}}$, $\frac{\partial \vec{x}_r}{\partial C_R}$ and $\frac{\partial \vec{x}_r}{\partial C_D}$

The variational equations respond to the second order differential equation

$$\ddot{X}_m = D_1 \cdot X_m + D_2 \cdot \dot{X}_m + A_f \qquad (A.2.3\text{-}9)$$

where the variable being integrated X_m is a matrix containing

$$X_m = \begin{bmatrix} \frac{\partial x}{\partial x_0} & \frac{\partial x}{\partial y_0} & \frac{\partial x}{\partial z_0} & \frac{\partial x}{\partial \dot{x}_0} & \frac{\partial x}{\partial \dot{y}_0} & \frac{\partial x}{\partial \dot{z}_0} & \frac{\partial x}{\partial C_R} & \frac{\partial x}{\partial C_D} \\ \frac{\partial y}{\partial x_0} & \frac{\partial y}{\partial y_0} & \frac{\partial y}{\partial z_0} & \frac{\partial y}{\partial \dot{x}_0} & \frac{\partial y}{\partial \dot{y}_0} & \frac{\partial y}{\partial \dot{z}_0} & \frac{\partial y}{\partial C_R} & \frac{\partial y}{\partial C_D} \\ \frac{\partial z}{\partial x_0} & \frac{\partial z}{\partial y_0} & \frac{\partial z}{\partial z_0} & \frac{\partial z}{\partial \dot{x}_0} & \frac{\partial z}{\partial \dot{y}_0} & \frac{\partial z}{\partial \dot{z}_0} & \frac{\partial z}{\partial C_R} & \frac{\partial z}{\partial C_D} \end{bmatrix} \qquad (A.2.3\text{-}10)$$

with the initial conditions

$$X_m^0 = \begin{bmatrix} 1 & 0 & 0 & 0 & 0 & 0 & 0 & 0 \\ 0 & 1 & 0 & 0 & 0 & 0 & 0 & 0 \\ 0 & 0 & 1 & 0 & 0 & 0 & 0 & 0 \end{bmatrix}, \quad \dot{X}_m^0 = \begin{bmatrix} 0 & 0 & 0 & 1 & 0 & 0 & 0 & 0 \\ 0 & 0 & 0 & 0 & 1 & 0 & 0 & 0 \\ 0 & 0 & 0 & 0 & 0 & 1 & 0 & 0 \end{bmatrix} \qquad (A.2.3\text{-}11)$$

The coefficients of the differential equations are obtained from

$$D_1 = \begin{bmatrix} \frac{\partial a_x}{\partial x} & \frac{\partial a_x}{\partial y} & \frac{\partial a_x}{\partial z} \\ \frac{\partial a_y}{\partial x} & \frac{\partial a_y}{\partial y} & \frac{\partial a_y}{\partial z} \\ \frac{\partial a_z}{\partial x} & \frac{\partial a_z}{\partial y} & \frac{\partial a_z}{\partial z} \end{bmatrix} D_2 = \begin{bmatrix} \frac{\partial a_x}{\partial \dot{x}} & \frac{\partial a_x}{\partial \dot{y}} & \frac{\partial a_x}{\partial \dot{z}} \\ \frac{\partial a_y}{\partial \dot{x}} & \frac{\partial a_y}{\partial \dot{y}} & \frac{\partial a_y}{\partial \dot{z}} \\ \frac{\partial a_z}{\partial \dot{x}} & \frac{\partial a_z}{\partial \dot{y}} & \frac{\partial a_z}{\partial \dot{z}} \end{bmatrix} \qquad (A.2.3\text{-}12)$$

that are the partial derivatives of the acceleration with respect to position and velocity at the integration epoch, and

$$A_f = \begin{bmatrix} 0 & 0 & 0 & 0 & 0 & 0 & \frac{\partial a_x}{\partial C_R} & \frac{\partial a_x}{\partial C_D} \\ 0 & 0 & 0 & 0 & 0 & 0 & \frac{\partial a_y}{\partial C_R} & \frac{\partial a_y}{\partial C_D} \\ 0 & 0 & 0 & 0 & 0 & 0 & \frac{\partial a_z}{\partial C_R} & \frac{\partial a_z}{\partial C_D} \end{bmatrix} \qquad (A.2.3\text{-}13)$$

that are the partial derivatives of the acceleration with respect to the model parameters at epoch.

This formulation can be expressed also a first order differential equation

$$\dot{Y} = \hat{D}Y + \hat{A}_f \qquad (A.2.3\text{-}14)$$

where

$$Y = \begin{bmatrix} X \\ \dot{X} \end{bmatrix} \qquad \hat{D} = \begin{bmatrix} 0 & I \\ D_1 & D_2 \end{bmatrix} \qquad \hat{A}_f = \begin{bmatrix} 0 \\ A_f \end{bmatrix} \qquad (A.2.3\text{-}15)$$

with the initial condition

$$Y_0 = \begin{bmatrix} 1 & 0 & 0 & 0 & 0 & 0 & \dots & 0 & 0 \\ 0 & 1 & 0 & 0 & 0 & 0 & \dots & 0 & 0 \\ 0 & 0 & 1 & 0 & 0 & 0 & \dots & 0 & 0 \\ 0 & 0 & 0 & 1 & 0 & 0 & \dots & 0 & 0 \\ 0 & 0 & 0 & 0 & 1 & 0 & \dots & 0 & 0 \\ 0 & 0 & 0 & 0 & 0 & 1 & \dots & 0 & 0 \end{bmatrix} \qquad (A.2.3\text{-}16)$$

A.2.4 Functional Decomposition

The following figure describes the high level decomposition of the GRAS POD subsystem:

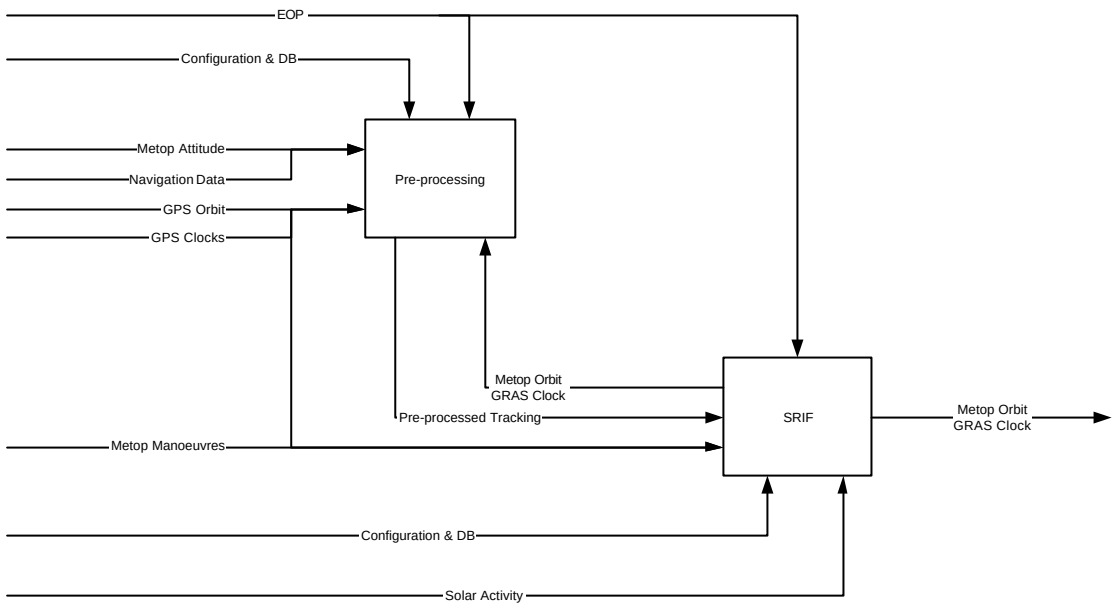

Figure 2.4-1: GRAS POD Functional Decomposition

A.2.4.1 Processing

Two main functions can be identified within the GRAS POD

- Pre-processing: in charge of the reformatting of the input data and the implementation of corrections that do not depend on the precise Metop orbit and clock.. The corrections are implemented on the basis of predicted Metop orbits generated by the SRIF component. These are
  - Navigation data ingestion and reformatting
  - Centre of mass correction
  - Generation of ionospheric free combinations
  - GPS clock correction
  - Generation of pseudo-range from C/A code phase (see A.2.2.1 for algorithm)
- SIRF: this is the precise orbit determination process itself. Ingests the pre-processed navigation data and generates precise Metop orbit and precise GRAS clock offsets. The generated precise orbits are propagated into the near future to be fed back to the pre-processor .

A.2.4.2 Inputs

From the functional point of view the following main inputs are required for the GRAS POD processing:

- Navigation data: contains the phase and C/A code phase data used for the estimation of the precise Metop orbit and the precise GRAS clock offsets. Time stamping of this data is expected at instrument sensing

time in UTC_{GRAS}. This UTC_{GRAS} is in reality the instrument time (IMT) correlated to UTC through the navigation solution. Expected data rate is 1 Hz. Only used in pre-processing.

- Metop Attitude: information about the true Metop attitude if available. As this may not be the case in near-real time the predicted attitude is expected, either as absolute attitude or as offsets (depointings) with respect to the nominal attitude. Only yaw steering mode is supported. Only used in pre-processing.

- Metop manoeuvres: only used to propagate the orbit across them. No calibration is intended. Only used in SRIF.

- GPS orbits: Orbit file with position and velocity of the GPS constellation. Used both by the pre-processor and SRIF.

- GPS clocks: information about the evolution of the GPS constellation on-board clocks. Interpolated to the observation epochs to correct the GRAS measurements. Only used in pre-processing.

Additionally the following ancillary data flows are identified:

- EOP: history file with the Earth Orientation Parameters needed to compute the transformation between the Earth fixed frame (ITRF-XX) and inertial reference frame (J2000.0).

- Solar activity: history file with the daily values of solar activity (f10.7) and geomagnetic index (a_p) required to compute the atmospheric density.

- Configuration and DB: this dataset hold all the configuration of the POD processing which is static and also the context data required to maintain the execution between consecutive runs. This dataset is built based on the NAPEOS philosophy as this navigation package is the basis of the POD implementation. The main contents of this dataset is

    - Databases: holding information about the Metop satellite, the GRAS instrument, the active GPS constellation, etc. Only contains POD specific items.

    - Configuration files: oriented to the tuning of the POD process. Include data weighting, statistical parameters of the SRIF filtering, data window configuration, estimation parameter selection, etc.

    - Context data: containing basically the information array of the SRIF process and the associated data that permits the execution of the consecutive orbit determination steps and the monitoring of the performance of the process.

A.2.4.3 Outputs

From the functional point of view the following outputs are provided by the GRAS POD processing:

- Precise Metop orbit: sequence of state vectors in the J2000.0 reference frame at 1 minute intervals (interpolation at intermediate epochs to be performed by a 8th order polynomial interpolator).

- Precise GRAS clock offsets: either a sequence of individual offsets at one second rate to be linearly interpolated or as a set of coefficients of a polynomial that can be directly substituted with UTC to obtain the specific offset at a given epoch. The given values represent the offsets of the GRAS instrument clock with respect to the time coordinate frame fixed by the GSN (UTC_{GSN}) as part of the GPS constellation orbit determination (UTC_{GSN} is close to true UTC but it is not true UTC. It is

extremely important not to introduce any external reference time to maintain consistency in the processing).

A.2.5 Interfaces

The following table summarises the interfaces for the GRAS POD. In this table each interface element is labelled with the identification of the source of the interface (i.e. Level 1a internal, external, context data)

Interface	Description	Format	Source
Navigation Data	Tracking data from the GRAS receiver pre-processed by the Level 1a processor	NTDF	Internal (*)
EOP	Earth Orientation Parameters	NAPEOS	External
Solar Activity	Solar Activity and Geomagnetic Activity indices	NAPEOS	External
GPS Orbit	GPS constellation orbitographic information	SP3 (**)	External
GPS Clocks	GPS constellation clock offsets	NAPEOS	External
Metop Attitude	~~TBD. It may disappear if replaced by n~~Nominal attitude.	NAPEOS	External
Metop Manoeuvres	Implemented manoeuvre times~~ and ΔV~~.	NAPEOS	External
SRIF	Context information to provide the POD execution with the state from the previous execution	NAPEOS	Context

(*) This interface is internal with respect to the Level 1a processing as the POD is encapsulated in it. If the interface is regarded with the POD isolated, this interface is external (POD detached from Level-1a). NTDF is the Napeos Tracking Data Format supported by the intended software infrastructure for the implementation of the GRAS POD.

(**) SP3 with velocity

The behaviour of the identified interface types is as follows

- **External**: the data is expected from the PGF to be available before each execution of the processor. This includes update of the contents of the files to contain the appropriate up to date information relating GPS constellation (e.g. SP3) status and geophysical information (e.g. EOP)

- **Internal**: the GRAS PPF manages this data internally to make it available to the POD

- **Context**: the POD is responsible for the generation of its context data to be made available to the PPF, which in turn makes it available to the PGF. The PGF is responsible for make this data available to the PPF in the next processor execution.

~~The implementation details for these interfaces in terms of format and data contents is to be defined in TBD.~~

Additionally there are number of static interface files required for the execution of the POD. These files contain the information defining the static geophysical behaviour of the models implemented in the POD. These are:

Interface	Description	Type
Geopotential	Expansion in spherical harmonics of the Earth gravitational potential	Static
JPL ephemeris	Development Ephemeris (DE) for the positioning of the solar system bodies delivered by JPL	Static
Nutation	IAU1980 nutation series	Static
Precession	IAU1976 precession coefficients	Static
Earth Rotation	Aoki model for Earth rotation	Static
Ocean Tide	Series expansion for ocean tide modelling	Static
Solid tide	Series expansion for solid tide modelling	Static
Physical constants database	Database with the basic physical definitions	NAPEOS
Satellite database	Description of the configured satellites for POD (includes GPS constellation)	NAPEOS
Transponder database	Description of the configured transponder aboard the different configured satellites (include GPS constellation)	NAPEOS
POD steering	Steering configuration files for the POD process	NAPEOS

The behaviour of the described interfaces is as follows

- **Static**: the file does not change in the course of the mission lifetime
- **NAPEOS**: access to the configuration of the POD that may change under certain circumstances (e.g. satellite database updated when a new GPS satellite is launched or de-orbited)

The handling on these files is to be defined based on the constraints that may appear from the PGF.

A.2.6 Orbit Determination

A.2.6.1 Algorithms

Except for the SRIF specific elements described in the former part of this document, the orbit determination algorithms are fully described in **[RD22]** (GRASPOD TN-01). The validity of these algorithms is demonstrated in **[RD22]** and **[RD23]** and therefore no further details are to be given in this technical note.

A.2.6.2 Performance

The main driver in the implementation of a sequential filter for orbit determination is to cop with the real time requirements imposed to the processing. In the GRAS POD case these requirements are not real time strictly speaking but the concept of near real time (NRT) imposes constraints to the processing for which the sequential implementation is more suitable.

In the assumption that the amount of data to be process each time that the POD is launched is of the order of 10 minutes (time span measured in terms of the evolution of orbital data) one can directly refer to the result of the POD to analyse the amount processing required in the SRIF implementation.

In terms of data processing the amount of computation is identical since the models implemented in BAHN-V7 are the same as those intended in SRIF (except for the clock model). The different way in which the estimation process is implemented in SRIF with respect to BAHN-7 does not represent a major computational overhead. Even if the formulation may lead to the conclusion that several matrix operations are to be performed, these are to certain extent the same as those implemented in the least squares process, as the same matrices have to be computed to generate at the end something similar to the normal matrix. In the least squares case this matrix is inverted and in the SRIF case transformed by means of Housholder operations. One advantage of the SRIF with respect to the least squares is that the sequential filtering solves for the next state in one iteration while the least squares requires various iterations to converge to the final solution. The SRIF could be complicated if there is need to solve for non-linearities before putting the data through the filter but still in this case only one or two iterations can be expected.

With this rationale in mind one can only expect that the SRIF performs as least a good as the least squares in the processing of 10 minute arcs. As reference the following figure (taken from the performance analysis in the GRASPOD study TN-01) shows the maximum expected CPU times for the processing of one step of POD with SIRF.

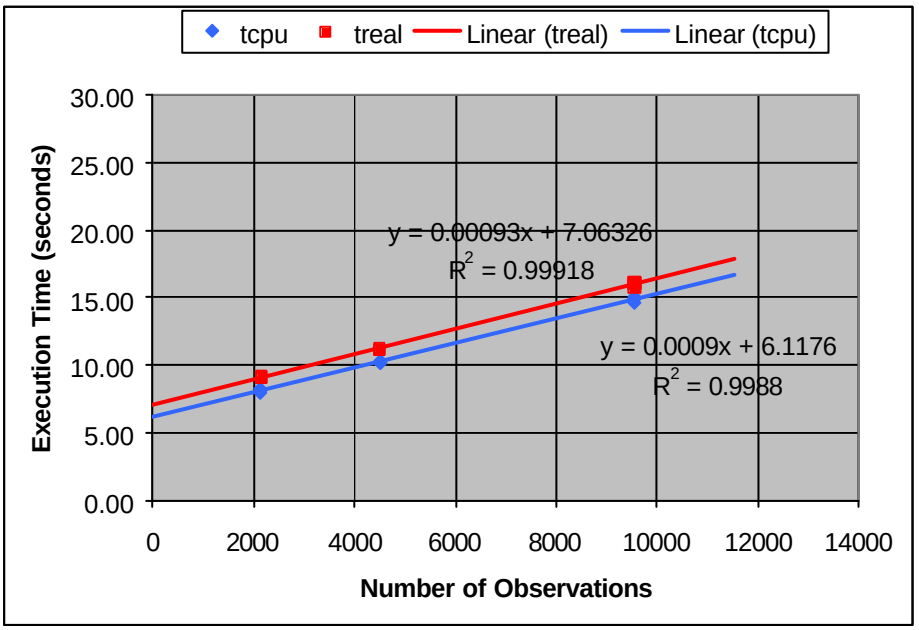

Figure 2.6-1: CPU consumption with LSM (from GRASPOD TN-01)

The computed CPU times take into account an average visibility of 6-7 satellites at each epoch and a data rate of one data epoch per second (6-7 simultaneous observations in pseudo-range and carrier phase). This leads to a level of processing of around 8000 observations per 10 minute arc. The corresponding processing time is in the order of 15 seconds, which is expected to be the upper limit for the SRIF implementation assuming the same conditions as for the LSM.

A.2.6.3 Data Rates

The expected data rate at the different interface points depends on the rate of change of the data in each of the interfaces (e.g. daily or half-daily variation for EOP) and the system constraints in terms of data availability at the interface points.

The SRIF algorithm has no limitations in the way in which the data has to be ingested. This is particularly relevant for the navigation data, which is the source of the orbit determination evolution. SRIF can take one measurement (set of simultaneous GRAS observations at the same epoch) at a time and update the state vector at the observation epoch or process a batch of measurements over a time window and update the state vector at the end of the window epoch or at any intermediate epoch. Here state vector means extended state vector, this is position and velocity and any other parameter being estimated as part of the SRIF process.

The limitations in this approach comes from the observability of the parameters that require a minimum amount of data for the estimation. In this case, the dataflow at the interface points has to be controlled in such a way that enough data is accumulated before the POD process is launched. This is the case for the clock estimation in which a certain window may be required to permit adequate estimation of the clock bias and its drift by filtering the noise introduced by the measurements (see 4.7.3).

Looking at the results of the GRASPOD study and at the simulation in 4.7.3 below, one can expect to process data arcs covering some 10 minutes of navigation data. This minimises the number of execution of the POD process whilst respecting the timelines constraint. Simultaneously this window permits filtering the signal noises of the order of the nano-second that hide the true behaviour of the clock (see Figure 2.7-6~~Figure 2.7-6~~)

A very important issue in this windowing scheme is the need for strict sequential processing. As demonstrated in the GRASPOD study (see **[RD23]** GRASPOD final report) isolated 10 minute data arcs do not suffice to meet the target accuracy requirements. The only way to guarantee that target accuracy is met is by processing at least one orbital revolution of data in the case of LSM. In SRIF this is accomplished by transferring the information between consecutive 10 minute arcs in the SRIF information matrix before accumulating the information provided by the new observations in the current 10 minutes arc (refer to A.2.3). **The SRIF process shall be strictly sequential with respect to orbit time.**

A.2.7 Clock Estimation Algorithms

A.2.7.1 Introduction

This section aims to the selection of the clock model algorithm that allows the precise estimation of the GRAS clock offsets. It has been decomposed in to parts:

- The first one (A.2.7.2 Clock Model Simulation) dedicated to possible simulation scenarios to understand the clock behaviour and to provide the models that later on will allow the validation of the implementation with simulated data.

- The second one (A.2.7.3 Clock model for estimation) which decides the model for the implementation of the clock observation model based on an analysis of the behaviour of the estimation with respect to measurement noise and clock stability.

A.2.7.2 Clock Model Simulation

The main purpose of the inclusion of a clock model in the GRAS POD process is to allow the stable estimation of the clock behaviour minimising the impact of external errors in the final computed clock offset values. If the process is implemented properly, the resulting non-modelled errors will go to the observations residuals and neither to the clock nor to the orbit.

The only information available about the clock behaviour is related to its short and long term stabilities based on the Allen deviation provided by the clock manufacturer. According to this information it is guaranteed that the Allan deviation is below the 10^{-12} seconds level for any integration interval between 1 second and 100 seconds.

In the frame of the SRIF algorithm, a number of clock parameters are to be computed at each estimation step. The characteristic time of the SRIF filter update is 10 minutes as the basis for SRIF filtering. This value can be considered as the basis for the processing although other filtering time steps can be regarded by system configuration. This filtering step has been selected based on the expected data rate delivered to the GRAS processor.

2.7.2.1 Two-state white noise model

The first model proposed to represent the GRAS clock is described by a two state polynomial process driven by white noise. The generic formulation for such model responds to the differential equation

$$\frac{\mathrm{d}}{\mathrm{d}t}\vec{x}(t) = F\vec{x}(t) + \vec{w}(t) \qquad \textit{(A.2.7-1)}$$

where

$$x(t) = \begin{bmatrix} a(t) \\ b(t) \end{bmatrix} \qquad F = \begin{bmatrix} 0 & 1 \\ 0 & 0 \end{bmatrix} \qquad \vec{w}(t) = \begin{bmatrix} w_a(t) \\ w_b(t) \end{bmatrix} \qquad \textit{(A.2.7-2)}$$

being $a(t)$ and $b(t)$ the time dependent coefficients of the polynomial representing the evolution of the clock (initial bias and drift respectively). w_a and w_b are uncorrelated white noises (associated to $a(t)$ and $b(t)$ respectively) with variance rates $q_a(t)$ and $q_b(t)$; this is

$$\mathrm{E}\left[\int_t^{t+dt} w_j(u)du\right]^2 = \int_t^{t+dt} q_j(u)du = dt\, q_j(t) \qquad (A.2.7\text{-}3)$$

This formulation can also be expressed in discrete form more suitable for the type of processing to be performed in the frame of the GRAS POD

$$\vec{x}_k = \Phi(dt)\vec{x}_{k-1} + \vec{w}_k \qquad (A.2.7\text{-}4)$$

where

$$\Phi(t) = \begin{bmatrix} 1 & dt \\ 0 & 1 \end{bmatrix} \qquad (A.2.7\text{-}5)$$

with $dt = t_k - t_{k-1}$. The subindex k corresponds to the variable value at t_k and the corresponding time process noise covariance for this discrete formulation is

$$Q_k = \mathrm{E}\left[w_k w_k^T\right] = \begin{bmatrix} q_a dt + \dfrac{q_b dt^3}{3} & \dfrac{q_b dt^2}{2} \\ \dfrac{q_b dt^2}{2} & q_b dt \end{bmatrix} \qquad (A.2.7\text{-}6)$$

2.7.2.2 Two-state coloured noise model

The second model proposed to represent the GRAS clock is described by a two state polynomial process driven by coloured noise (i.e. exponentially correlated random signal). The generic formulation for such model is the summation of a deterministic part that responds to the differential equation

$$\frac{\mathrm{d}}{\mathrm{d}t}\vec{x}(t) = F\vec{x}(t) + \frac{\mathrm{d}}{\mathrm{d}t}\vec{p}(t) \qquad (A.2.7\text{-}7)$$

where

$$x(t) = \begin{bmatrix} a(t) \\ b(t) \end{bmatrix} \qquad F = \begin{bmatrix} 0 & 1 \\ 0 & 0 \end{bmatrix} \qquad \vec{p}(t) = \begin{bmatrix} p_a(t) \\ 0 \end{bmatrix} \qquad (A.2.7\text{-}8)$$

being $a(t)$ and $b(t)$ the time dependent coefficients of the polynomial representing the evolution of the clock (initial bias and drift respectively) and $p_a(t)$ the exponentially correlated random variable (ECRV or coloured noise) associated to the clock behaviour, which responds to the differential equation

$$\frac{\mathrm{d}}{\mathrm{d}t}p(t) = -\frac{1}{t}p(t) + w(t) \qquad (A.2.7\text{-}9)$$

where t is the time constant that characterises the ECRV behaviour and $w(t)$ is white process noise with variance rate $q(t)$, this is

$$\mathrm{E}\left[\int_t^{t+dt} w(u)du\right]^2 = \int_t^{t+dt} q(u)du = dt\,q(t) \qquad (A.2.7\text{-}10)$$

This formulation can also be expressed in discrete form more suitable for the type of processing to be performed in the frame of the GRAS POD

$$\vec{x}(t_k) = \Phi(dt)\vec{x}(t_{k-1}) + \vec{p}(k) \qquad (A.2.7\text{-}11)$$

where

$$\Phi(dt) = \begin{bmatrix} 1 & dt \\ 0 & 1 \end{bmatrix} \qquad p_k = p_{k-1}\,\mathrm{e}^{-\frac{dt}{t}} + w_k \qquad (A.2.7\text{-}12)$$

with $dt = t_k - t_{k-1}$. The subindex k corresponds to the variable value at t_k and the corresponding time process noise covariance for this discrete formulation is

$$Q_k = \mathrm{E}\left[w_k^2\right] = \left(1 - \mathrm{e}^{-\frac{dt}{t}}\right)q \qquad (A.2.7\text{-}13)$$

A.2.7.3 Clock model for estimation

Either of the two proposed models are based on the estimation of two separate items: the trend of the clock with long characteristic variation times (basically bias and drift) and the short term variation around the long term evolution. While the first part of the estimation accounts for the constant deviation in frequency of the oscillator with respect to the ideal clock, the second part intends to represent the short periodic effects.

As can be seen from the simulation models proposed above, there is always a stochastic part based on noise. This part cannot be estimated by definition of noise. The idea when proposing a model for estimation is to provide a formulation that can simultaneously represent the behaviour of the clock with the maximum fidelity filtering the noise to the level of fulfilment of the requirements.

2.7.3.1 Measurement noise and observability

The two proposed models contain the elements to simulate the clock in the absence of any other external perturbation. The actual observation of the clock is performed through the measurements provided by the receiver, in which the clock is contaminated by other error sources which have the main effect in the observability of the short term evolution of the clock

and in the ground value (bias). The following figure represent a simulation of a clock before and after superimposing measurement noise with 1ns RMS.

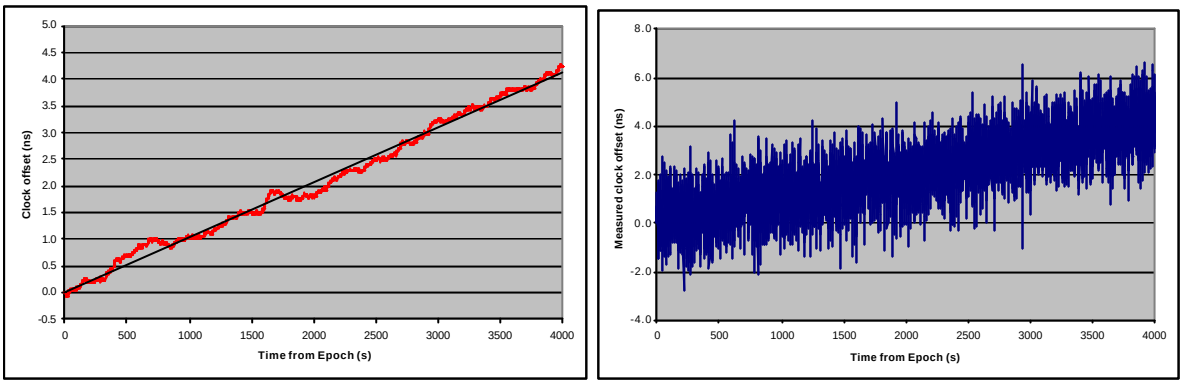

Figure 2.7-1: Actual and Measured Snap-shot Clock

Depending on the target accuracy to be obtained the final approach in the clock estimation can be as simple as determining the least squares linear fit or a more sophisticated method may be needed to try to follow the clock trend around the linear trend. Of course the observation of the short term behaviour of the clock around the linear trend is complicated by the measurement noise, and the final level of accuracy that can be obtained proportionally reduced or totally cancelled.

2.7.3.2 Characteristic Times

In he estimation of any parameter (including the clock) as part of the orbit determination process one must take into account the typical variations of the related perturbations and the characteristic time of variation of the parameters themselves. If one intends to estimate a clock bias and a drift with just a linear model for a whole orbital revolution, it is very likely that one cycle per revolution effects could be left behind and the final solution could be corrupted.

Characteristic variation means characteristic time for a repetition of the changes of a certain magnitude and also the amplitude of variation of such magnitude. The interesting situation appears only when both of them are in the range of effect in the measures parameters. Changes in amplitude below the required accuracy are uninteresting (even if observable) and so are changes that happen at a rate that cannot be observed (e.g. white noise).

In the particular case of the GRAS POD the characteristic time is driven by the length of the occultations (100 seconds), the orbital period (102 minutes) and the data delivery rate (10 minutes). Additionally one can tune the system to process the data at different rates or within different windows in such a way that effects that are long or short term with respect to that forced characteristic time are filtered (i.e. tune the system to behave as a band-pass filter). As an example, one can process the 10 minutes of available data in slots of 1 minute to avoid having to take into account effects that have one cycle per revolution effect (e.g. thermal effects) which could probably have an impact if the whole batch of 10 minutes is processed altogether.

The following scheme represents a clock whose characteristic time of short term variation is of the order of 10 seconds and without measurement noise added. This clock is estimated using models with characteristic time windows of 10, 50, 100 and 500 seconds. While the following of

the estimation is almost perfect for the 10 seconds window scheme, the selection of any other window filters out the short term evolution . The 500 seconds window cannot even follow the mid term evolution.

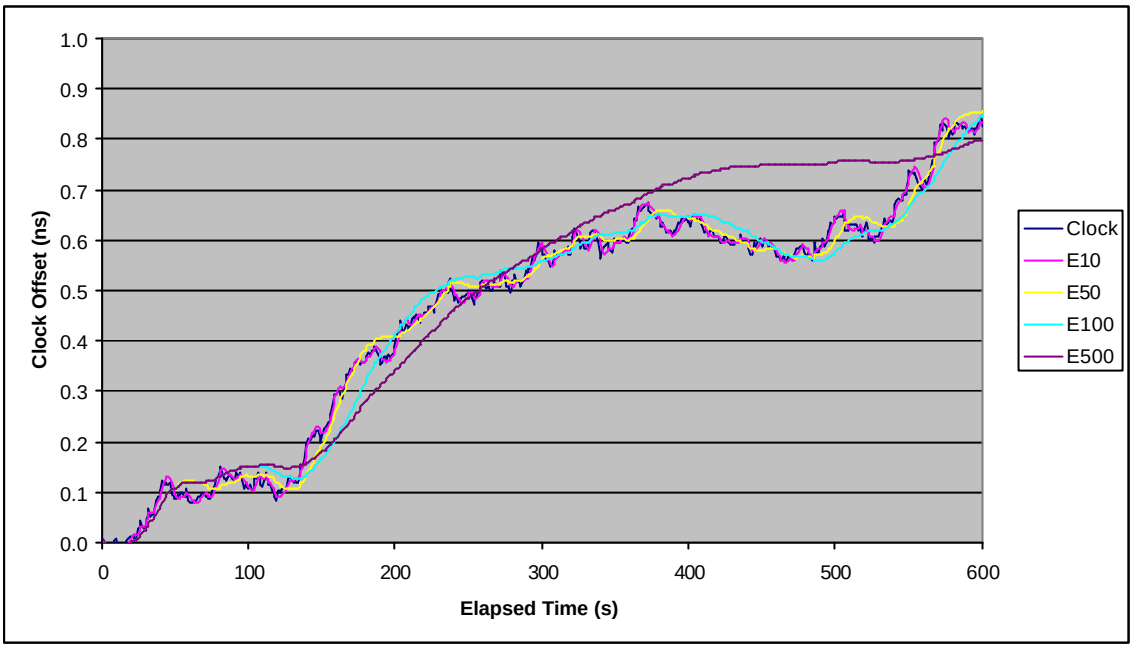

Figure 2.7-2: Estimation windowing scheme (without measurement noise)

The situation is drastically complicated in the presence of measurement noise. The following figure represents a case in which white noise with 0.5 ns RMS has been added to the clock estimates (snap-shot solutions represented by dots in the figure). In this situation, the actual signal of the clock cannot be recovered because it is masked by the much higher noise introduced by the measurements. The noise can only be filtered by increasing the size of the window. A compromise between signal loss and noise reduction must be found. Still any of the filtered solutions would produce better results than the uncorrelated snap-shot solution.

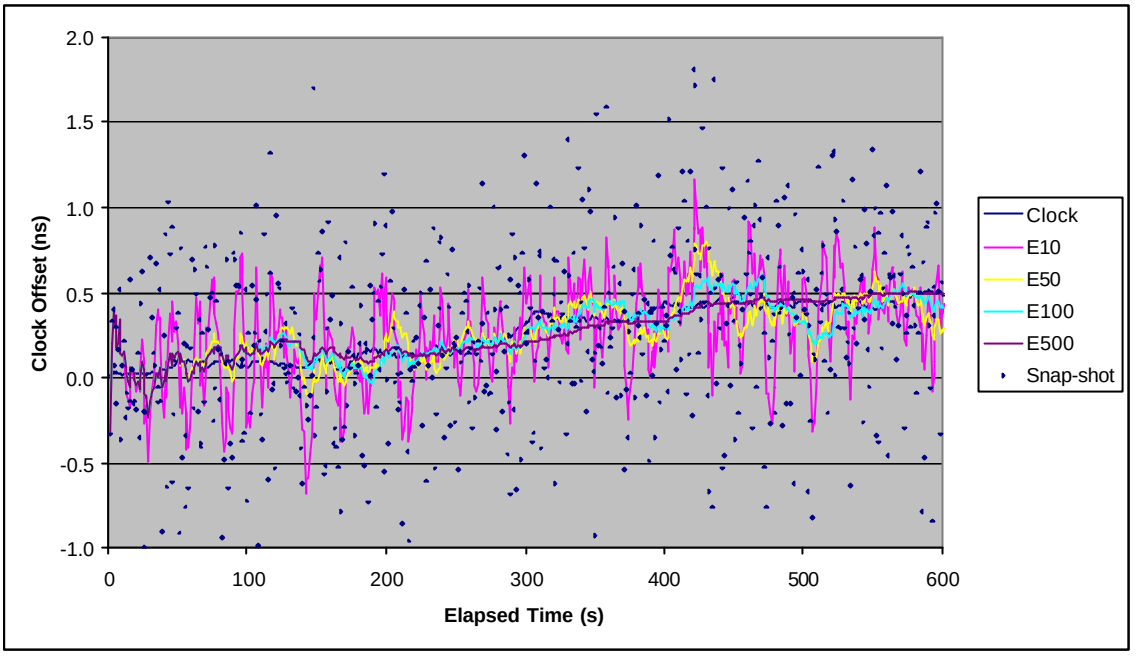

Figure 2.7-3: Estimation windowing scheme (with measurement noise)

2.7.3.3 Proposed Clock Observation Model for Estimation

The clock observation model to be applied is a direct consequence of the consideration provided above.

For robustness considerations, the model should be the simplest possible one that permits reaching the prescribed level of accuracy.

Since the highest frequency noises cannot be reproduced in estimation (in particular white noise), the model has to be chosen in such way that these variations be filtered to the level in which there is no accuracy degradation. With the target requirement of 0.5 ns RMS (equivalent to 1 ns at 2-sigma) the model should be able to follow any frequency that has a variation higher than that level. This can be tested by verifying that the differences between the real clock and the estimated clock is statistically better than those 0.5 ns RMS

Both of the models proposed above permit the selection of the adequate windowing level in such a way that the clock path can be followed.

In the case of the model driven by white noise one can estimate the initial bias and drift inside each independent window to estimate the best fit of the clock to the model based on the observations. In the SRIF scenario this can be managed by estimating the clock bias and drift within the bias section (this is the y part of the matrix) and then manipulating the information matrix between successive steps to obtain the adequate behaviour in the correlation between successive estimation steps.

In the case of the model driven by an ECRV the clock bias and drift are estimated as biases in the SRIF sense (this is the y part of the matrix). These biases represent the overall linear trend of the clock while the local behaviour at intermediate and high frequencies is obtained through

the estimation of an ECRV (this is the p part of the matrix) with the adequate characteristic time value t selected in such a way that the right high frequencies are filtered.

In either of the two cases, **the proposed model for estimation is the following**

$$\Delta t_{GRAS} = a(t) + b(t)t + p(t) \qquad (A.2.7\text{-}14)$$

where the parameters to be estimated are $a(t)$, $b(t)$ and optionally (if the ECRV driven model is used) $p(t)$.

If the clock behaviour is as good as the manufacturer indicates in the specification the term $p(t)$ may be omitted in the clock estimation processing. However, the inclusion of this term in the implementation leaves the possibility to account for unexpected behaviours with minimum implementation and validation penalty.

2.7.3.4 Estimation clock model simulation

As preliminary simulation of this process, a rolling average mechanism has been implemented on top of simulated clock data with constant Allen variance of 10^{-12} s in the range 1 to 100 seconds. Even if not completely equivalent to the final implementation, this rolling average mechanism will serve the purpose of illustrating the overall behaviour of the estimation process.

The following figure shows the overall behaviour of such clock for an interval of one hour, before and after adding measurement noise of 0.5 ns RMS

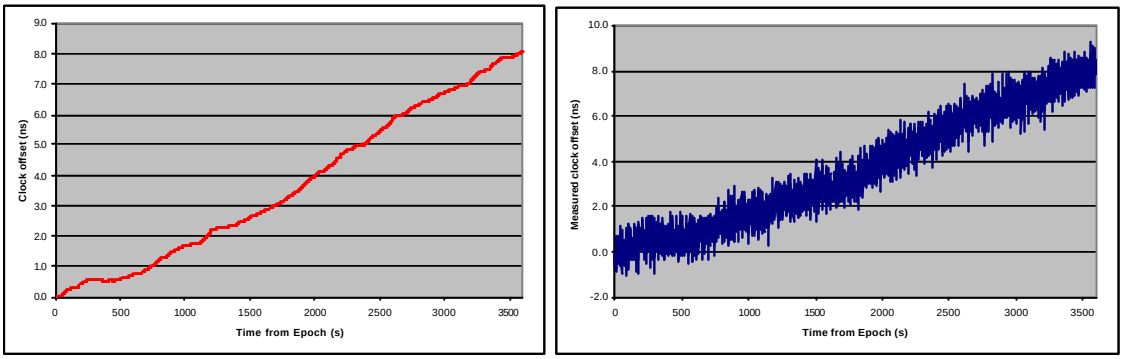

Figure 2.7-4: GRAS Clock Simulation

The estimation of the ideal clock does not present any problem as shown in 2.7.3.2. In this particular case not even if selecting wide windows of 500 seconds as shown in the following figure. This has to do with the stability of the clock in the short and medium term.

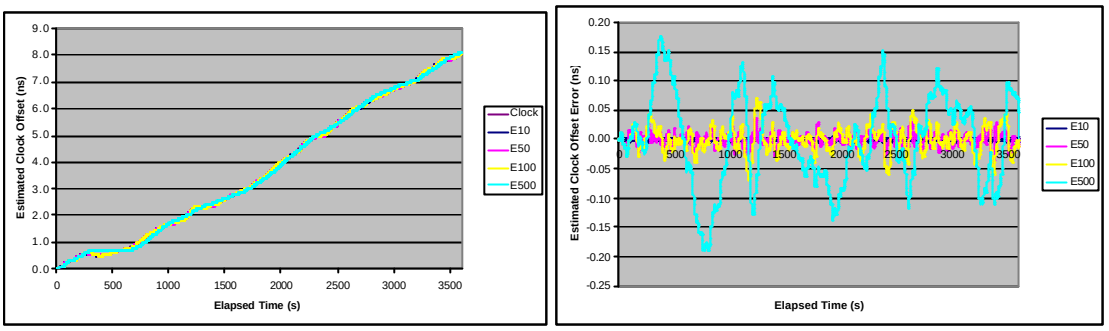

Figure 2.7-5: GRAS Clock Estimation Example (without measurement noise)

The statistical summary of the clock estimation shown in these figures is

Window Size (s)	Error RMS (ns)
10	0.001693
50	0.011026
100	0.021667
500	0.077274

Table 2.7-1: GRAS Clock Estimation Statistics (without measurement noise)

The same example can then be repeated in the presence of measurement noise (see following figures). For the purpose of this example, this noise is introduced not directly as noise in the measurements but as the effect in the uncorrelated estimation of the individual clocks at 1Hz. This corresponds to the snap-shot clock estimation.

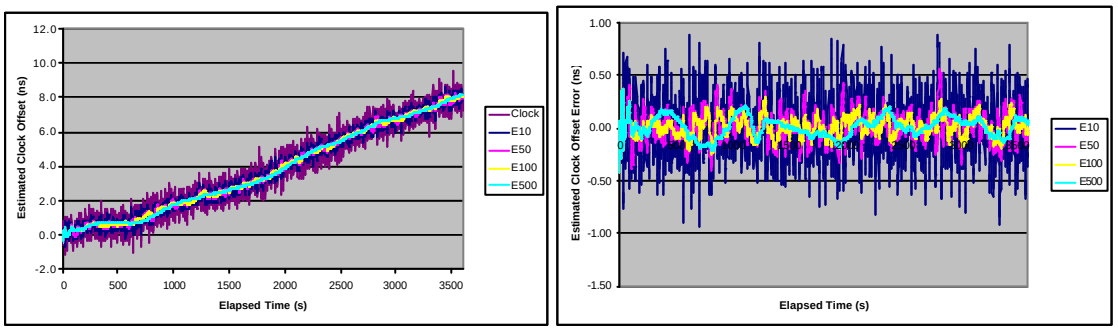

Figure 2.7-6: GRAS Clock Estimation Example (0.5 ns RMS measurement noise)

The statistical summary of the clock estimation shown in these figures is

Window Size (s)	Error RMS (ns)
10	0.271595
50	0.137283
100	0.093985
500	0.095423

Table 2.7-2: GRAS Clock Estimation Statistics (0.5 ns RMS measurement noise)

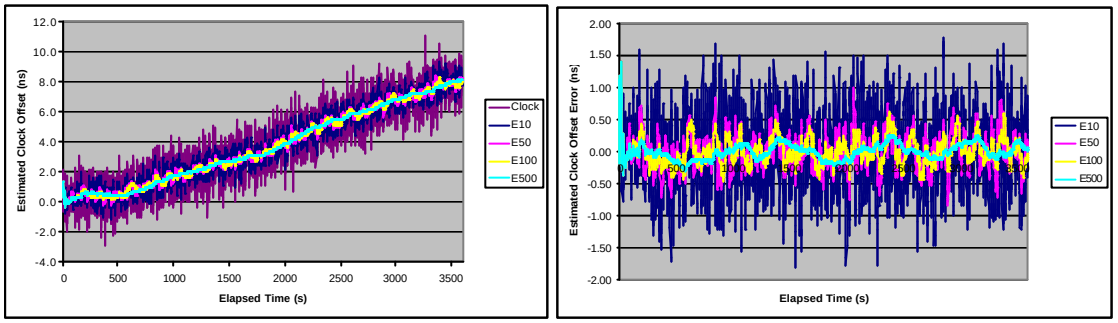

Figure 2.7-7: GRAS Clock Estimation Example (1.0 ns RMS measurement noise)

The statistical summary of the clock estimation shown in these figures is

Window Size (s)	Error RMS (ns)
10	0.564661
50	0.272619
100	0.200439
500	0.125032

Table 2.7-3: GRAS Clock Estimation Statistics (1.0 ns RMS measurement noise)